

UNIVERSITY OF GRANADA
DEPARTMENT OF CHEMICAL ENGINEERING



**APPLICATION OF ION EXCHANGE TECHNOLOGY TO
OLIVE MILL WASTEWATER TREATMENT**

Ph.D. THESIS 2015

María Dolores Víctor Ortega

Supervisors

Dr. Antonio Martínez Férez
Dr. Javier Miguel Ochando Pulido

UNIVERSIDAD DE GRANADA
DEPARTAMENTO DE INGENIERÍA QUÍMICA



**APLICACIÓN DE LA TECNOLOGÍA DE INTERCAMBIO
IÓNICO A LA DEPURACIÓN DE AGUAS RESIDUALES DE
LA INDUSTRIA OLEÍCOLA**

TESIS DOCTORAL 2015

María Dolores Víctor Ortega

Directores

Dr. Antonio Martínez Férez
Dr. Javier Miguel Ochando Pulido

Editor: Universidad de Granada.Tesis Doctorales
Autora: María Dolores Víctor Ortega
ISBN: 978-84-9125-324-2
URI: <http://hdl.handle.net/10481/41121>

**APPLICATION OF ION EXCHANGE TECHNOLOGY TO
OLIVE MILL WASTEWATER TREATMENT**

**APLICACIÓN DE LA TECNOLOGÍA DE INTERCAMBIO IÓNICO A LA
DEPURACIÓN DE AGUAS RESIDUALES DE LA INDUSTRIA OELÍCOLA**

Por:

MARÍA DOLORES VÍCTOR ORTEGA

Memoria presentada para la obtención del grado Internacional de Doctor por
la Universidad de Granada

PROGRAMA DE DOCTORADO EN QUÍMICA

Granada, octubre 2015

Los Directores de la Tesis:

Prof. Dr. Antonio Martínez Férez
Profesor Titular del Departamento de
Ingeniería Química

Dr. Javier Miguel Ochando Pulido
Personal Investigador Postdoctoral del
Departamento de Ingeniería Química

La doctoranda María Dolores Víctor Ortega y los directores de la tesis Antonio Martínez Férez y Javier Miguel Ochando Pulido, garantizamos, al firmar esta tesis doctoral, que el trabajo ha sido realizado por la doctoranda bajo la dirección de los directores de la tesis y hasta donde nuestro conocimiento alcanza, en la realización del trabajo, se han respetado los derechos de otros autores a ser citados, cuando se han utilizado sus resultados o publicaciones.

Granada, 30 de octubre de 2015.

Director/es de la Tesis

Doctoranda

Fdo.: Antonio Martínez Férez

Fdo.: María Dolores Víctor Ortega

Fdo: Javier Miguel Ochando Pulido

Contents

I Introduction	1
1 Background	3
1.1 Olive oil production process.....	3
1.2 Olive mill wastewater: a key current environmental issue.....	5
1.3 Technologies for olive mill wastewater purification.....	6
1.3.1 Fenton-like secondary treatment of OMW-2.....	7
1.3.2 Characterization of OMW-2 exiting the secondary treatment.....	10
1.4 Ion exchange technology for water purification.....	13
1.4.1 Heavy metals removal through ion exchange.....	14
1.4.2 Anionic pollutants removal through ion exchange.....	15
1.5 References.....	17
2 Justification and Objectives	23
2.1 Justification.....	23
2.2 Structure of the thesis.....	25
3 Experimental details	29
3.1 Ion exchange resins.....	29
3.2 Ion exchange equipment.....	30
3.3 Analytical methods.....	31
3.4 Recirculation and continuous mode experiments.....	32
3.4.1 Recirculation-mode experiments.....	32
3.4.2 Continuous-mode experiments.....	33
3.5 References.....	34
II Results	35
4 Ion exchange as an efficient pretreatment system for reduction of membrane fouling in the purification of model OMW	37
4.1 Introduction.....	38
4.2 Experimental.....	41
4.2.1 OMW treatment.....	41
4.2.2 Ion exchange process.....	43
4.2.3 Analytical methods.....	46

4.3 Results and discussion.....	47
4.3.1 Characterization of OMWST.....	47
4.3.2 Resins disposition.....	48
4.3.3 Effect of temperature.....	51
4.3.4 Regeneration and industrial application.....	56
4.4 Conclusions.....	57
4.5 References.....	58
5 Final purification of synthetic olive oil mill wastewater treated by chemical oxidation using ion exchange: study of operating parameters	63
5.1 Introduction.....	64
5.2 Materials and methods.....	67
5.2.1 Model water solutions.....	67
5.2.2 Ion exchange system.....	68
5.2.3 IE resins conditioning and regeneration.....	69
5.2.4 Recirculation mode IE experiments.....	69
5.2.5 Analytical methods.....	70
5.3 Results and discussion.....	71
5.3.1 Effect of recirculation time.....	71
5.3.2 Effect of temperature.....	72
5.3.3 Effect of flow rate.....	75
5.3.4 IE potential for the reuse of the final treated water in the olive-oil process.....	77
5.4 Conclusions.....	77
5.5 References.....	78
6 Impacts of integrated strong-acid cation exchange and weak-base anion exchange process for successful removal of saline toxicity from model olive mill wastewater	83
6.1 Introduction.....	84
6.2 Experimental section.....	88
6.2.1 IE equipment and resins.....	88
6.2.2 Operating conditions in semi-batch IE experiments.....	90
6.2.3 IE equilibrium experiments.....	90
6.2.4 Continuous IE experiments.....	91
6.2.5 Analytical methods.....	92
6.3 Results and discussion.....	92
6.3.1 Effect of pH.....	92
6.3.2 Effect of initial concentration.....	94
6.3.3 Equilibrium isotherms.....	95

6.3.4	Continuous IE process.....	98
6.4	Conclusions.....	100
6.5	References.....	101
7	Thermodynamic and kinetic studies on iron removal by means of a novel strong-acid cation exchange resin for olive mill effluent reclamation	107
7.1	Introduction.....	108
7.2	Experimental.....	110
7.2.1	Materials.....	110
7.2.2	Ion exchange equipment.....	111
7.2.3	Iron ion exchange experiments.....	112
7.2.4	Procedures.....	112
7.3	Results and discussion.....	113
7.3.1	Effect of feedstream concentration.....	113
7.3.2	Equilibrium isotherms.....	114
7.3.3	IE kinetics.....	118
7.4	Conclusions.....	123
7.5	References.....	124
8	Iron removal and reuse from Fenton-like pretreated olive mill wastewater with novel strong-acid cation exchange resin fixed-bed column	129
8.1	Introduction.....	130
8.2	Methods and materials.....	132
8.2.1	Ion exchange resin.....	132
8.2.2	Ion exchange bench-scale plant.....	132
8.2.3	Analytical methods.....	133
8.2.4	Inlet pH impact.....	133
8.2.5	Fixed-bed column studies.....	134
8.2.6	IE process modelling: breakthrough curves.....	135
8.2.7	Regeneration and reuse of the ion exchange resin.....	137
8.3	Results and discussion.....	138
8.3.1	Effect of inlet pH.....	138
8.3.2	Breakthrough curve experiments.....	139
8.3.3	Regeneration and industrial application.....	145
8.4	Conclusions.....	147
8.5	References.....	148
9	Phenols removal from industrial effluents through novel polymeric resins: kinetics and equilibrium studies	153
9.1	Introduction.....	154

9.2 Experimental.....	156
9.2.1 Materials.....	156
9.2.2 Ion exchange equipment.....	157
9.2.3 Equilibrium experiments.....	157
9.2.4 Procedures.....	158
9.3 Results and discussion.....	159
9.3.1 Effect of recirculation time and initial concentration.....	159
9.3.2 Equilibrium isotherms.....	161
9.3.3 Kinetic characterization.....	166
9.3.4 Gibbs free energy.....	171
9.4 Conclusions.....	173
9.5 References.....	174
10 Performance and modelling of continuous ion exchange processes for phenols recovery from olive mill wastewater	179
10.1 Introduction.....	180
10.2 Methods and materials.....	183
10.2.1 Materials.....	183
10.2.2 Analytical methods.....	184
10.2.3 Initial pH study experiments.....	184
10.2.4 Continuous-mode IE studies.....	185
10.2.5 Breakthrough curves modelling.....	187
10.2.6 Resins regeneration and phenols recovery.....	189
10.3 Results and discussion.....	189
10.3.1 Effect of initial pH.....	189
10.3.2 Breakthrough curve studies.....	190
10.3.3 Phenols recovery.....	198
10.4 Conclusions.....	199
10.5 References.....	200
11 Ion exchange system for the final purification of olive mill wastewater: performance of model vs. real effluent treatment	205
11.1 Introduction.....	206
11.2 Experimental section.....	208
11.2.1 Model water solutions.....	208
11.2.2 Real OMW samples.....	208
11.2.3 Ion exchange process.....	209
11.2.4 Recirculation and continuous IE experiments.....	210
11.2.5 Analytical methods.....	211

11.3	Results and discussion.....	212
11.3.1	Recirculation mode experiments.....	212
11.3.2	Continuous mode experiments.....	215
11.4	Conclusions.....	217
11.5	References.....	218
12	Experimental design for optimization of olive mill wastewater final purification with Dowex Marathon C and Amberlite IRA-67 ion exchange resins	223
12.1	Introduction.....	224
12.2	Experimental section.....	227
12.2.1	Materials.....	227
12.2.2	Ion exchange equipment.....	228
12.2.3	Recirculation IE experiments.....	229
12.2.4	Experimental design and optimization of IE operating parameters....	230
12.2.5	Analytical methods.....	231
12.3	Results and discussion.....	232
12.3.1	Resins disposition study.....	232
12.3.2	Optimization study.....	234
12.3.3	Effect of IE resins dosages.....	239
12.3.4	Industrial application of continuous IE process.....	240
12.4	Conclusions.....	242
12.5	References.....	242
13	Comparison and optimization of different ion exchange resins combinations for final treatment of olive mill effluent	249
13.1	Introduction.....	250
13.2	Experimental section.....	252
13.2.1	Materials.....	252
13.2.2	Ion exchange equipment.....	254
13.2.3	Recirculation IE experiments.....	255
13.2.4	Experimental design and optimization of IE operating parameters....	256
13.2.5	Analytical procedures.....	257
13.3	Results and discussion.....	258
13.3.1	Resins disposition studies.....	258
13.3.2	IE process optimization.....	264
13.3.3	Continuous IE processes.....	265
13.4	Conclusions.....	267
13.5	References.....	268

14 Impacts of main parameters on the regeneration process efficiency of several ion exchange resins after final purification of olive mill effluent	273
14.1 Introduction.....	274
14.2 Methods and materials.....	276
14.2.1 Ion exchange resins and equipment.....	276
14.2.2 Chemicals.....	278
14.2.3 Regeneration experiments.....	278
14.2.4 Analytical methods.....	279
14.3 Results and discussion.....	280
14.3.1 Nature of regenerant solutions.....	280
14.3.2 Regenerant solutions concentration.....	283
14.3.3 Effect of temperature.....	285
14.3.4 Effect of flow rate.....	286
14.4 Conclusions.....	288
14.5 References.....	288
III Summary and Conclusions	291
15 Conclusions	293
16 Resumen	299
16.1 Antecedentes.....	299
16.2 Justificación y objetivos.....	303
16.3 Conclusiones.....	308

PART I

INTRODUCTION

CHAPTER 1

BACKGROUND

In this chapter an overview of the state-of-the-art in the field of olive mill wastewater treatment as well as ion exchange technology is given, with special focus on the main advantages this technique presents with respect to the commonly used wastewater treatment technologies, such as membrane systems.

1.1 Olive oil production process

In the last years, olive oil industry has become one of the main engines of the economy of the Mediterranean basin countries, of which Spain, Italy and Greece cope with the highest total world production. Other countries with an important annual olive oil yield are Syria and the Northern African countries - Algeria, Turkey, Morocco, Tunisia, Libya, Lebanon - as well as Portugal, France, Serbia and Montenegro, Macedonia, Cyprus, Egypt, Israel and Jordan (Figure 1.1).

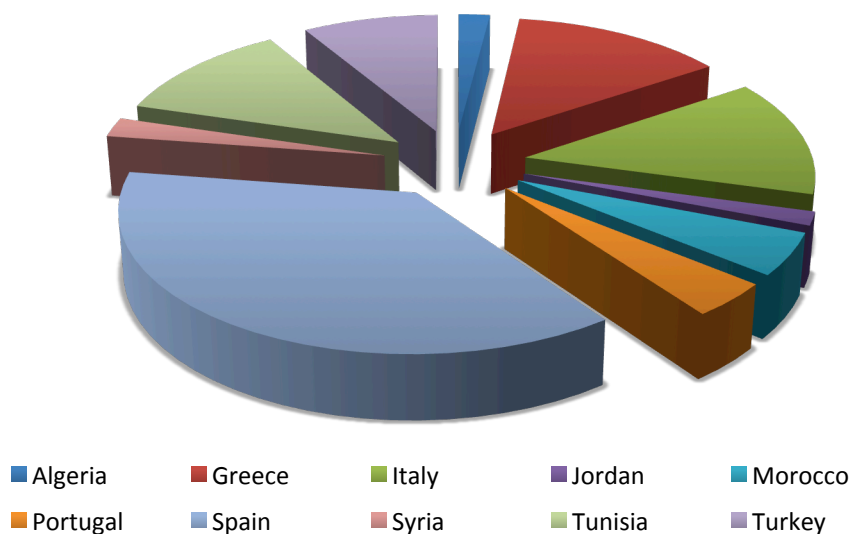


Figure 1.1. Olive oil sector worldwide (International Olive Oil Council, IOOC 2014).

Olive oil can be obtained in two main ways in olive mills, depending on the technology of the facilities: by means of the traditional system, which is of limited use in some olive mills protected as equity, or by modern systems born in virtue of the evolution of the sector making possible the continuous production of olive oil. In this case, we can distinguish between the

three-phase and the two-phase extraction procedures, of which the former has been substituted by the latter over time in some countries because of environmental concerns. The following figure (Figure 1.2) shows the operational flow diagram for the olive oil extraction of the three different processes.

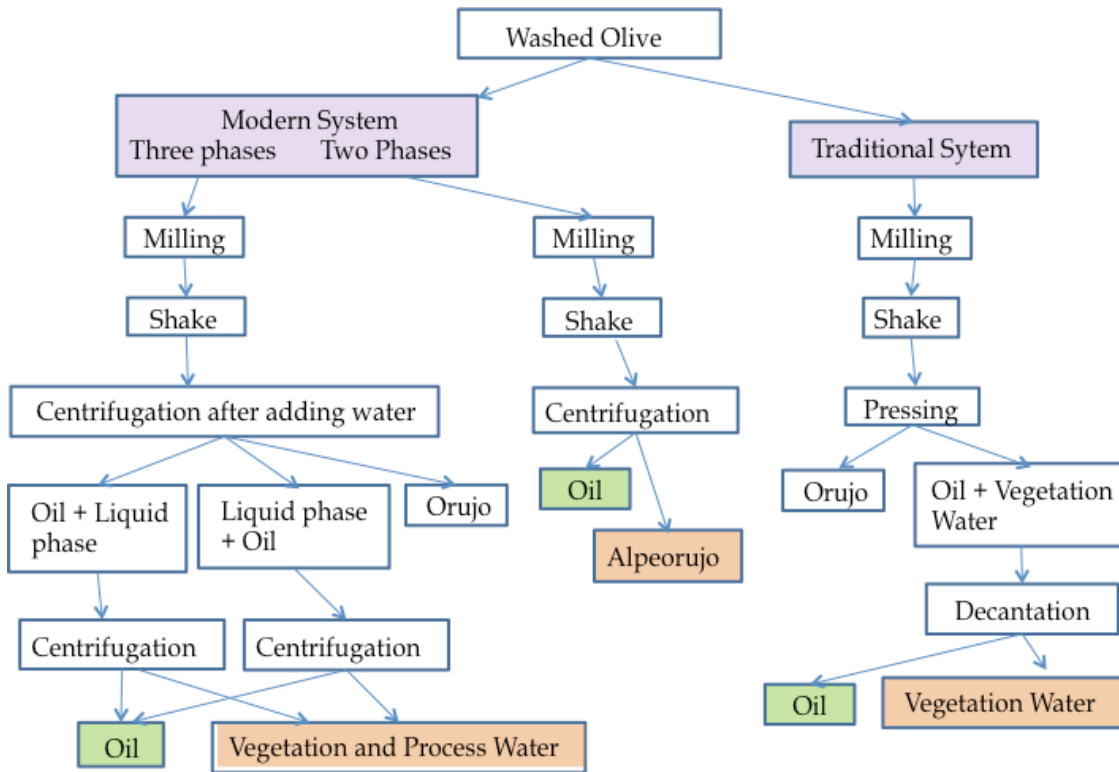


Figure 1.2. Flow diagram of the three olive oil extraction processes.

Experience with the two olive oil extraction processes shows that the two-phase system has some advantages, i.e., better retention of polyphenols because no water is added and there is less loss of oil if the system is operated properly.

The two-phase system produces the greatest weight of solid waste because it has the highest moisture content. It also produces the least amount of wastewater with the lowest Biological Oxygen Demand (BOD). The polyphenol content of the oil is lowest in the 3-phase system because of the addition of water during the centrifugation process.

The quality of the oil produced by the two-phase system is higher than the quality of the three-phase oil. This is due to the higher concentration of polyphenols and o-diphenols which occurs with the new system, which gives more stability during storage, thus quality being similar to

that obtained by classical means of pressure on the appearance of content in polyphenols (AMA, 1994).

1.2 Olive mill wastewater: a key current environmental issue

As aforementioned, virgin olive oil has been produced using pressure for solid-liquid separation since ancient times. However, this system has been substituted progressively by processes based on olive pomace centrifugation, which have become widespread during the last decades. These include two-phase and three-phase centrifugation systems. As a consequence, the amount of effluents derived from the olive oil industry has risen up sharply, which consist of olive vegetation wastewater (OVW) and olives washing wastewater (OWW), together called olive mill wastewater (OMW) (Hanafia et al., 2011). Figure 1.3 shows artificial lagoons, which are used for storage of both olive mill effluents.



Figure 1.3. Artificial lagoons for storage and natural evaporation of OWW (left photograph) and OMW (right photograph).

This environmental problem concerns especially the Mediterranean countries, which cope with 97 % of the worldwide olive oil production, while European Union (EU) countries produce 84 %, but olives are also cultivated outside the Mediterranean area, in the Middle East, the USA, Argentina and Australia. In Spain, the main olive oil producer worldwide, there are more than 1700 olive oil factories, which produce more than 1,700,000 tons of olive oil during the 2013/2014 campaign. Olives and olive oil production grows year by year, and so does OMW. An olive oil factory can produce 10-15 m³/day of OMW. This wastewater is a heavy polluted liquid stream characterized by a low pH value, black colour, very high chemical oxygen demand (COD) and a high concentration of microbial growth inhibiting compounds, such as phenolic compounds and tannins (Fezzani and Cheikh, 2010). Also inorganic compounds such as chloride, sulphate and phosphoric salts of potassium, calcium, iron, magnesium, sodium,

copper and traces of other elements are present in OMW (Di Giovacchino, 1985; Voreadou, 1989). Environmental problems in relation to OMW disposal such as soil pollution, water body pollution, underground leakage and odour are commonly encountered.

OMW must be treated before its disposal according to the present-day European environmental rules. This constitutes a high cost for the olive oil manufacturer. In addition, decentralization and small size of most olive oil production factories impede a centralized treatment for OMW and makes it necessary to find a feasible and flexible solution for the small plants.

Besides, OMW composition is not constant and varies greatly depending on several factors such as climatic and cultivation parameters and the milling method applied for the olive oil production. This results in a high cost for its disposal and a huge amount of potable water consumption.

1.3 Technologies for olive mill wastewater purification

A plethora of management practices for the reclamation of OMW have been proposed so far, having led to different results. Conventional treatments include lagooning or natural evaporation (Annesini and Gironi, 1991), thermal concentration (Paraskeva and Diamadopoulos, 2006), composting (Bouranis et al., 1995; Cegarra et al., 1996; Papadimitriou et al., 1997), treatments with lime (Aktas et al., 2001), treatments with clay (Al-Malah et al., 2000), physico-chemical procedures such as coagulation-flocculation (Martínez-Nieto et al., 2011b; Sarika et al., 2005; Stoller, 2009) and electrocoagulation (Inan et al., 2004; Tezcan et al., 2006), and biological treatments (Ammary, 2005; Fountoulakis et al., 2002; Garrido et al., 2002; Hodaifa et al., 2008; Marques, 2001). Biological management of OMW is a hard task and right now not applied on a large scale due to seasonality and resistance of OMW to biological degradation.

Within this context, chemical remediation strategies are required for the depuration of these bio-refractory wastewaters (Niaounakis and Halvadakis, 2006; Paraskeva and Diamadopoulos, 2006). These treatments are known as ‘advanced oxidation processes’ (AOPs), including ozonation (de Heredia and Garcia, 2005), Fenton’s reagent (Martínez-Nieto et al., 2011a), photocatalysis (De Caprariis et al., 2012; Sacco et al., 2012; Stoller and Bravi, 2010) as well as electrochemical (Cañizares et al., 2006; Papastefanakis et al., 2010; Tezcan et al., 2008) and hybrid processes (Grafias et al., 2010; Khoufi et al. 2006; Lafi et al., 2009; Rizzo et al., 2008).

Among them, Fenton’s process and TiO₂ photocatalysis offer a series of advantages that make them cost-effective and technically attractive (Cañizares et al., 2009). However, Fenton’s

process appears to be the most economically advantageous since it may be conducted at ambient temperature and pressure conditions, and also due its equipment simplicity and operational ease. Oxidation of many organic substances with H_2O_2 can be improved by adding a catalyst (Fe^{2+} or more rarely Cu^{2+} or other transition metal ions) to activate the H_2O_2 molecule, leading to the formation of hydroperoxyl ($\text{HO}_2\cdot$) and hydroxyl radicals ($\text{HO}\cdot$), which are the true oxidant species. Nevertheless, the main drawback of these processes relies on the cost of the reactants (H_2O_2 and Fe^{2+} ions). For this reason, Martínez Nieto et al. (2011a) introduced in former works on a lab scale several methods in order to use the cheaper Fe^{3+} salts rather than Fe^{2+} salts, examining the performance of several catalysts including Mohr salt ($\text{Fe}(\text{SO}_4)_2(\text{NH}_4)_2 \cdot 6\text{H}_2\text{O}$), ferric perchlorate and ferric chloride.

On the other hand, OMW are also known to have significant saline toxicity levels, exhibiting high electroconductivity (EC) values. Conventional physicochemical treatments cannot abate the high concentration of dissolved monovalent and divalent ions present in these effluents, and thus it is necessary to resort to advanced separation technologies in order to attempt complete depuration of OMW.

As olive oil two-phase production process is the most commonly used nowadays, we will focus on the treatment of the wastewater coming from this production system (OMW-2)

1.3.1 Fenton-like secondary treatment of OMW-2

Best operating conditions found on lab scale experiments (Martínez Nieto et al., 2011a) suggested working at ambient temperature, without pH control, agitation speed 60 rpm, oxidizing agent concentration $[\text{H}_2\text{O}_2]$ equal to 5 % (w/v) and $[\text{FeCl}_3]/[\text{H}_2\text{O}_2]$ ratio between 0.01 % - 0.04 % (w/w).

After the preliminary lab-scale study, OMW-2 was subjected to a secondary treatment on a pilot scale, consisting firstly in a Fenton-like chemical oxidation process. For the scale-up of the process, OWW and OMW-2 (Table 1.1) were mixed in 1:1 (v/v) proportion in order to stabilize the mean value of the organic concentration of the effluent stream entering the treatment system (OMW-2), thus avoiding sensible fluctuations in the COD parameter. In this stage, the OMW-2 stream was pumped into a stirred reactor tank in which an oxidizing agent (hydrogen peroxide, H_2O_2) and a catalyst (ferric chloride, FeCl_3) were added (Hodaifa et al., 2013).

In sum, the proposed secondary treatment comprised sequentially Fenton-like advanced chemical oxidation, flocculation-sedimentation and finally filtration through gravel and olive

stones (Hodaifa et al., 2013). The flow diagram of the secondary treatment process is depicted in Figure 1.4, and a photograph of the pilot plant is shown in Figure 1.5.

Table 1.1. Physicochemical characterization of raw olive mill effluents.

Parameter	OMW-P	OMW-3	OMET-2	OMW-2	OWW
pH	4.5	5.4	7.2	4.9	6.3
Moisture, %	93.0	93.4	99.4	99.3	99.7
Total solids, %	12.0	6.6	0.59	0.6	0.27
Organic substances, %	10.5	5.8	0.39	0.49	0.10
Ashes, %	1.5	0.9	0.21	0.11	0.17
BOD ₅ , mg O ₂ ·L ⁻¹	90.0	42.0	0.29	0.79	0.50
COD, mg O ₂ ·L ⁻¹	180.0	151.4	7.1	7.8	0.8
Total phenols, mg·L ⁻¹	2,400	921.0	86.0	157.0	4.0
EC, mS·cm ⁻¹	9.0	7.9	1.9	1.3	0.9

OWW: olives washing wastewater; OMW-P, OMW-3 and OMW-2: olive mill wastewater from batch press process as well as three-phase and two-phase continuous extraction procedures, respectively; OMET-2: mixture of all effluents produced in the olive mill, including OWW, OMW and from other activities at the facility (e.g., cleaning and sanitation); COD: chemical oxygen demand; BOD₅: biological oxygen demand; EC: conductivity.

The pilot plant was located on the premises of the Department of Chemical Engineering at the University of Granada (Figure 1.5).

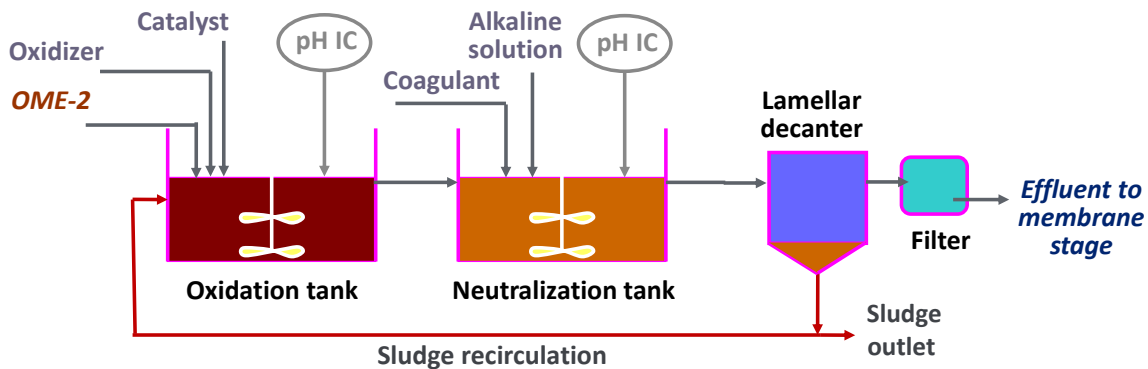


Figure 1.4. Flow diagram of the Fenton-like secondary treatment of OMW-2 on a pilot scale.

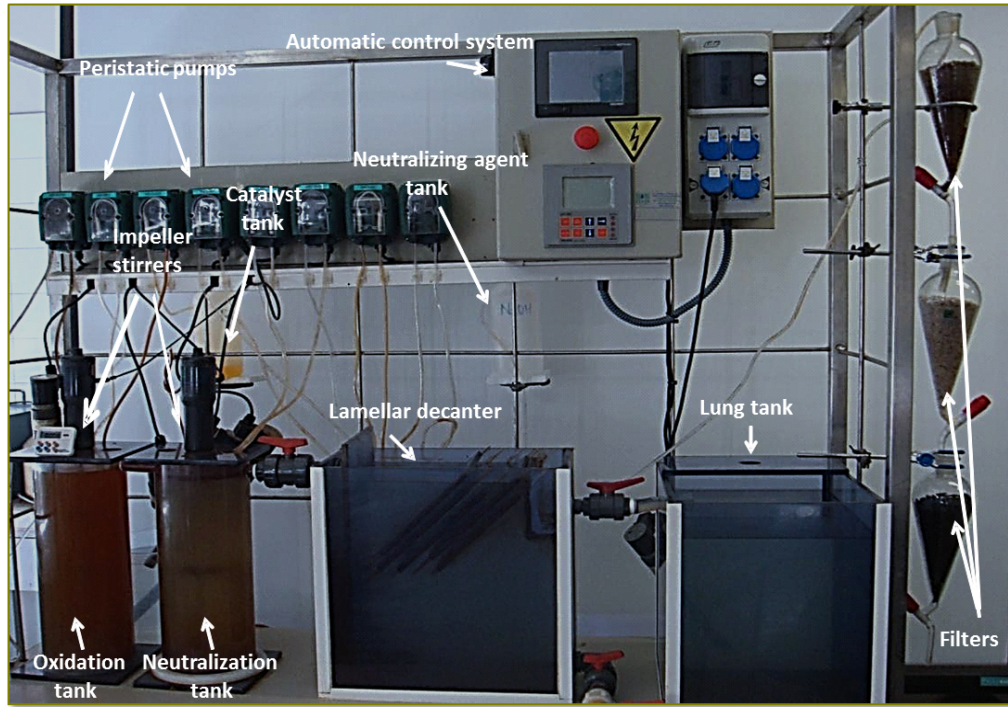


Figure 1.5. Pilot plant for secondary treatment of OMW-2 (Chemical Engineering Department, University of Granada).

The outlet stream of the oxidation tank was then directed to a stirred neutralization tank (Figure 1.5). It is important to underline that spontaneous acidification of OMW-2 occurred during the Fenton-like oxidation stage - pH fell rapidly to values around 3.0, at which the reaction optimally occurred - due to the addition of the catalyst and also to the cleavage of complex organic solutes into organic acids during this stage (Martínez Nieto et al., 2011a). Hence, a neutralizing agent (sodium hydroxide solution, 1N) was added to this second tank (see Figure 1.4), adjusting the pH of the effluent coming out of the Fenton-like oxidation tank to neutrality (pH = 6.0-9.0, as regulations demand).

As a beneficial side effect, precipitation of the iron colloidal particles present due to the previous addition of the ferric catalyst as well as to the natural dissolved iron initially found in the raw OMW-2 results promoted in the form of iron hydroxide.

A commercial anionic flocculant was added into the stirred neutralization tank, leading to the formation of an iron-rich sludge which finally sedimented in a lamellar decanter. The sludge was also recirculated to the oxidation tank to reduce the catalyst consumption.

Finally, a filtration-in-series stage was performed. The aim was removing the residual suspended solids as well as iron particles still present in the treated effluent prior to its discharge or in view of

an ulterior purification stage for its final purification (Figure 1.5). For this purpose, two different filtration sequences - (i) fine sand filter followed by olive stones filter vs. (ii) gravel filter followed by olive stones filter - were examined (Martínez-Nieto et al., 2010). The latter sequence showed better performance with respect to COD and total suspended solids (Tss) removal, whereas TPh and iron removal efficiencies were similar in both cases.

1.3.2 Characterization of OMW-2 exiting the secondary treatment

Results withdrawn from the pilot-scale secondary treatment are reported in Table 1.2. Fenton-like oxidation leads to high mineralization levels in relatively short residence times ($\tau = 3$ h). Up to 92.2 % COD and 99 % total phenols abatement values were measured at the exit of the homogeneous Fenton-like oxidation reactor, in good agreement with those observed on a lab scale in previous works by Martínez-Nieto et al. (2011a).

Furthermore, the iron-rich sludge (less than 12.3 % v/v) was recirculated to the oxidation reactor for its reuse in the Fenton-like process. This measure enables minimizing the catalyst consumption, hence rendering the secondary treatment much more cost-effective and environmentally friendly.

At the exit of the lamellar decanter, COD and total phenols removal efficiencies reached values of up to 92.7 % and 99.5 % respectively. However, significant residual iron concentration values (up to $5 \text{ mg}\cdot\text{L}^{-1}$) may be registered even after the sedimentation stage. Nevertheless, total iron concentration values at the outlet of the gravel filter followed by olive stones filter sequence were well below 1 ppm (Table 1.2).

The secondary treatment ensured major organic matter abatement, confirmed by the very high COD and phenolic compounds removal efficiencies. Finally, the treated effluent could be reused for irrigation purposes. The proposed secondary treatment has already been patented and transferred to an industrial scale by the ‘Chemical and Biochemical Processes Technology’ Research Group of the University of Granada (Martínez-Nieto et al., 2008).

Despite the significant removal of organic pollutants achieved by the Fenton-like secondary treatment, it was not able to reduce the high concentration of dissolved monovalent and divalent ions, which cannot be removed by conventional physicochemical treatments. Furthermore, higher EC values were noticed if compared to the raw OME-2. This was mainly owed to the increment in sodium and chloride content derived from the addition of the neutralizing agent and the catalyst into the flocculation and oxidation tanks, respectively.

Table 1.2. OMW-2 characterization at the outlet of each stage of the secondary treatment on a pilot scale.

Parameters	OMW-2 after Fenton-like oxidation	OMW-2 after flocculation-sedimentation	OMW-2 after gravel and olive stones filtration	OMW after fine sand and olive stones filtration
pH	3.2	7.9	7.7	7.8
EC, mS·cm⁻¹	3.81	3.62	3.43	3.43
Tss, mg·L⁻¹	141.2	80.5	13.1	32.3
COD, mg O₂·L⁻¹	315.9	295.2	150.8	226.6
Total phenols, mg·L⁻¹	0.9	0.8	0.4	0.3
Total iron, mg·L⁻¹	50.8	3.69	0.028	0.024
Cl⁻, mg·L⁻¹	1096.6	1,095.1	990.9	965.8
Na⁺, mg·L⁻¹	725.5	724.9	718.6	691.8

The proposed secondary treatment ensures compliance of the treated effluent with the parametric standards delimited in Spain by the Guadalquivir Hydrographical Confederation (G. H. C.) which at the present moment establishes limits with regard to pH, COD and BOD₅ parameters (Table 1.3). Nevertheless, recommendations pin-pointed by the Food and Agriculture Organization (F. A. O.) warn of the risk of employing regenerated waters presenting high salinity values for irrigation purposes (Table 1.4). Furthermore, in line with Directive 2000/60/CE, which aims to confer maximum protection to water and regenerated wastewater, quality standards to discharge the treated effluent in public waterways (Table 1.5) or in the municipal sewer treatment systems or even for reuse in the proper olive oil production process should be sought for. With this goal, an ulterior separation stage by membranes was conducted on a bench-scale.

Table 1.3 Parametric standard limits for discharge of OME in suitable terrains (Guadalquivir Hydrographical Confederation, 2006 - 2011)

Parameter	2002	2003	2004	2006	2011
pH	6 - 9	6 - 9	6 - 9	6 - 9	6 - 9
Tss, mg·L⁻¹	600	500	500	500	500
COD, mg O₂·L⁻¹	2,500	2,000	1,500	1,000	1,000
BOD₅, mg O₂·L⁻¹	2,000	-	-	-	-

Table 1.4. Water quality as a function of its salinity (Food and Agriculture Organization, FAO).

EC, dS·L ⁻¹	Water quality	Risk due to salinity
0 - 1	Excellent to good	Low to mid
1 - 3	Good to marginal	High
> 3	Marginal to unacceptable	Very high

In this regard, as regulations become more stringent every year, ion exchange (IE) technology offers many benefits in contrast with other separation processes. As the most relevant advantages we can point the fact that this technique is technologically simple and enables efficient removal of even traces of impurities from solutions. The operational and installation costs of IE processes are sensibly lower compared with other wastewater treatment processes like membrane filtration or granular activated carbon filtration process (Dabrowski et al., 2004). In this sense, this process is considered very attractive because of the relative simplicity of application and in many cases it has been proven to be an economic and effective technique to remove ions from wastewaters, particularly from diluted solutions (Pintar, 2001; Valverde et al., 2006).

In this sense, selective resins could reduce the residual concentration of sodium, total iron, chloride and phenols, which are the main pollutants present in OMW after the described advanced oxidation secondary treatment, below the maximum standard limits established by the Drinking Water Directive. Council Directive 98/83/EC set the maximum concentration in

drinking water at 200 mg L⁻¹ for iron, 200 mg L⁻¹ for sodium and 250 mg L⁻¹ for chloride (European Commission, 1998). On the other hand, a previous European legislation established a legal tolerance level of 5 µg L⁻¹ for total phenols in water intended for human consumption (European Commission, 1980). Thus, achieving the above mentioned standards, it would be possible to reuse the final treated effluent in the olives washing machines and finally closing the loop, thus rendering the production process cost-effective and environmentally respectful.

Table 1.5. Standard limits for discharge in public waterways (R.D. 606/2003).

Parameter	Limit value
pH	6 - 9
EC, mS·cm⁻¹	2
Tss, mg·L⁻¹	35
BOD₅, mg O₂·L⁻¹	25
COD, mg O₂·L⁻¹	125
Ammonia, mg NH₄·L⁻¹	15
Grease, mg·L⁻¹	20

1.4 Ion exchange technology for water purification

Among various water treatment technologies, IE has emerged as one of the most promising technologies for water treatment. The process in which exchange of an ion from a solution with a similarly charged ion present on a stationary solid particle, called IE resin, occurs in a reversible chemical reaction is named as IE. As it is previously mentioned, IE process is a more interesting technology from the economical point of view compared with other wastewater treatment processes such as membrane technology. On the other hand, this technology achieves high treatment capacity, high removal efficiency and presents fast kinetics.

The IE reaction is stoichiometric and reversible in nature. In the perspective of water purification, IE reaction occurs by the replacement of ionic impurities in the water with ions

released by an IE resin (Figure 1.6). The uptake of ions by IE resins is rather affected by certain variables such as pH, temperature, flow rate, ionic charge, initial pollutant concentration and contact time (Caetano and Valderrama, 2009). The resins must be periodically regenerated to restore its original ionic form. IE technology has been widely used for various applications on commercial scale with proven success.

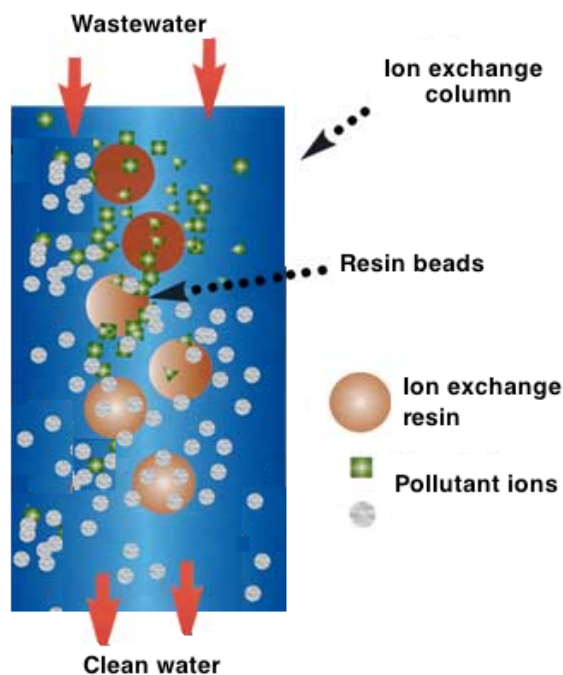


Figure 1.6. General scheme of IE process.

Various naturally occurring materials such as zeolites, montmorillonite, clay, and soil humus are representative ion exchangers (Zagorodni, 2007). Since long, cation- and anion-exchange resins have been widely employed for softening water and for removal of anions, respectively. On the other hand, the combination of cation- and anion-exchange resins is effective for deionization of water. The cation- and anion-exchange resins release positively and negatively charged ions, respectively, in exchange of the cationic and anionic impurities, respectively. The most efficient IE resins, which have been used for water treatment, are prepared from synthetic polymers such as styrene-divinylbenzene and are either sulfonated or aminated for targeted pollutants.

1.4.1. Heavy Metals Removal through Ion Exchange

IE processes have been widely used to remove heavy metals from wastewater due to their many advantages, such as high treatment capacity, high removal efficiency and fast kinetics (Kang et

al., 2004). IE resin, either synthetic or natural solid resin, has the specific ability to exchange its cations (innocuous) with the metals in the wastewater.

Among the materials employed in IE processes, synthetic resins are commonly preferred due to its effectiveness to nearly remove the heavy metals from the solution (Alyüz and Veli, 2009). The most common cation exchangers are strongly acidic resins with sulfonic acid groups (-SO₃H) and weakly acid resins with carboxylic acid groups (-COOH). Hydrogen ions in the sulfonic group or carboxylic group of the resin can be used as exchangeable ions with metal cations. As the solution containing heavy metal passes through the cations exchange column, metal ions are exchanged for the hydrogen ions on the resin with the following IE process:



The uptake of heavy metal ions by IE resins is rather affected by certain variables such as pH, temperature, initial metal concentration and contact time (Gode and Pehlivan, 2006). Ionic charge also plays an important role in IE process.

In addition to synthetic resins, natural zeolites, naturally occurring silicate minerals, have been widely used to remove heavy metal from aqueous solutions due to their low cost and high abundance.

Many researchers have demonstrated that zeolites exhibit good cation-exchange capacities for heavy metal ions under different experimental conditions (Motsi et al., 2009; Ostroski et al., 2009; Taffarel and Rubio, 2009).

Clinoptilolite is one of the most frequently studied natural zeolites that have received extensive attention due to its selectivity for heavy metals. Though there are many reports on the use of zeolites and montmorillonites as IE resin to remove heavy metal, they are limited at present compared with the synthetic resins.

1.4.2. Anionic Pollutants Removal through Ion Exchange

IE is one of the most effective and commonly used treatments for removal of anionic contaminants from aqueous solutions. The equilibrium between OH⁻-form resin and anionic pollutants may be simply represented by the following conventional IE equation:



Concerning nitrate decontamination, many researchers have considered IE the most appropriate technology given its simplicity, effectiveness, selectivity, relatively low capital and operating costs, and long effective lifetime of specific exchangers (Samatya et al., 2006; Pintar et al., 2001; Kim and Benjamin 2004).

On the other hand, only a few works have been reported dealing with sulfide removal. For instance, Chanda and Rempel (1995) compared the performance of a macroporous anion-exchange resin Reillex™HPQ with the common anion-exchange resin Dowex-I-X8, both in chloride form, for sulfide sorption from alkaline aqueous solutions. The obtained results pointed out the predominant sorption of sulfide as HS^- on HPQ(Cl^-) and as S^{2-} on Dowex-I(Cl^-).

In case of fluoride, its removal by anion-exchange resins has been reported as a difficult process because of selectivity issues (Meenakshi and Viswanathan 2007). As a result, cation/chelating resins have been employed for fluoride sorption. For instance, Meenakshi and Viswanathan (2007) evaluated and compared the performance of anionic and chelating-type resins under diverse equilibrating conditions and reported the last one as the most fluoride-selective material.

IE resins can be successfully applied for cyanide removal over wide ranges of concentrations (Osathaphan et al., 2008). As an example, Osathaphan et al., (2008) investigated the removal efficiencies of cyanide and a zinc-cyanide complex using a strong basic anion exchange resin, Amberlite IRA-402 Cl, based on crosslinked polystyrene with quaternary ammonium functional groups.

Several studies are based on the adsorption of phenol and its derivatives from contaminated water using synthetic resins and low-cost natural adsorbents (Su-Hsia and Ruey-Shin, 2009; Zhu et al., 2011). Instead of using commercial activated carbon and synthetic resins, researchers have worked on inexpensive materials such as coal fly ash, sludge, biomass, zeolites and other adsorbents, which have high adsorption capacity and are locally available.

Low-cost adsorbents have demonstrated outstanding removal capabilities for phenol and its derivatives compared to activated carbons. Adsorbents that stand out for high adsorption capacities are coal-reject, residual coal treated with H_3PO_4 , dried activated sludge, red mud, and cetyltrimethylammonium bromide-modified montmorillonite. Of these synthetic resins, HiSiv 1000 and IRA-420 display high adsorption capacity of phenol and XAD-4 has good adsorption capability for 2-nitrophenol. These polymeric adsorbents are suitable for industrial effluents containing phenol and its derivatives as mentioned previously (Su-Hsia and Ruey-Shin, 2009).

1.5 References

- AMA, Systems Olive oil production systems without OMW production: current status, Report No 1/94. Research Department, Ministry of Culture and Environment, Junta de Andalucía, 1994.
- Aktas, E.S., Imre, S., Esroy, L. (2001). Characterization and lime treatment of olive mill wastewater. *Water Research*, 35:2336–2340.
- Al-Malah, K., Azzam, M.O.J., Abu-Lail, N.I. (2000). Olive mills effluent (OME) wastewater post-treatment using activated clay. *Separation and Purification Technology*, 20:225-234.
- Ammary, B.Y. (2005). Treatment of olive mill wastewater using an anaerobic sequencing batch reactor. *Desalination*, 177:157-165.
- Annesini, M., Gironi, F. (1991). Olive oil mill effluent: ageing effects on evaporation behavior. *Water Research*, 25:1157–1960.
- Beltrán de Heredia, J., Garcia, J. (2005). Process integration: continuous anaerobic digestion - ozonation treatment of olive mill wastewater. *Ind. Eng. Chem. Res.*, 44:8750-8755.
- Bouranis, D.L., Vlyssides, A.G., Drossopoulos, J.B., Karvouni, G. (1995). Some characteristics of a new organic soil conditioner from the co-composting of olive oil processing wastewater and solid residue. *Communication in Soil Science and Plant Analysis*, 26:2461–2472.
- Caetano, C., Valderrama, A. (2009). Phenol removal from aqueous solution by adsorption and ion exchange mechanisms onto polymeric resins. *J. Colloid Interface Sci.*, 338:402–409.
- Cañizares, P., Martinez, L., Paz, R., Saéz, C., Lobato, J., Rodrigo, M.A. (2006). Treatment of Fenton-refractory olive oil mill wastes by electrochemical oxidation with boron-doped diamond anodes. *J. Chem. Technol. Biotechnol.*, 81(8):1331-1337.
- Cañizares, P., Paz, R., Sáez, C., Rodrigo, M.A. (2009). Costs of the electrochemical oxidation of wastewaters: a comparison with ozonation and Fenton oxidation processes. *Environ. Manage.*, 90:410-420.
- Cegarra, J., Paredes, C., Roig, A., Bernal, M.P., García, D. (1996). Use of olive mill wastewater compost for crop production. *International Biodeterioration and Biodegradation* 38(3–4):193–203.

Dabrowski, A., Hubicki, Z., Podkoscielny, P., Robens, E. (2004). Review: selective removal of the heavy metal ions from waters and industrial wastewaters by ion-exchange method. *Chemosphere*, 56:91–106.

De Caprariis, B., Di Rita, M., Stoller, M., Verdone, N., Chianese, A. (2012). Reaction-precipitation by a spinning disc reactor: Influence of hydrodynamics on nanoparticles production. *Chemical Engineering Science*, 76:73-80.

Di Giovacchino, L. (1985) Caratteristiche delle acque di vegetazione delle olive, Nota 1. *La Rivista Italiana delle Sostanze Grasse*, 62:411.

European Commission, 1980. Council Directive 80/778/EEC of 15 July 1980 on the quality of water intended for human consumption. 1980.

European Commission, 1998. Council Directive 98/83/EC of 3 November 1998 on the quality of water intended for human consumption. 1998.

Fezzani, B., Ben Cheikh, R. (2010). Two-phase anaerobic co-digestion of olive mill wastes in semi-continuous digesters at mesophilic temperature. *Bioresour. Technol.*, 10:1628-1634.

Fountoulakis, M.S., Dokianakis, S.N., Kornaros, M.E., Aggelis, G.G., Lyberatos, G. (2002). Removal of phenolics in olive mill wastewaters using the white-rot fungus *Pleurotus ostreatus*. *Water Res.*, 36:4735-4744.

Garrido Hoyos, S.E., Martínez Nieto, L., Camacho Rubio, F., Ramos Cormenzana, A. (2002). Kinetics of aerobic treatment of olive-mill wastewater (OMW) with *Aspergillus terreus*, *Process Biochemistry*, 37(10):1169-1176.

Grafias, P., Xekoukoulotakis, N. P., Mantzavinos, D., Diamadopoulos, E. (2010). Pilot treatment of olive pomace leachate by vertical-flow constructed wetland and electrochemical oxidation: an efficient hybrid process. *Water Research*, 44(9):2773-2780.

Hanafia, F., Belaoufi, A., Mountadar, M., Assobhei, O. (2011). Augmentation of biodegradability of olive mill wastewater by electrochemical pre-treatment: effect on phytotoxicity and operating cost. *J. Hazard. Mater.*, 190:94-99.

Hodaifa, G., Eugenia-Sánchez, M., Sánchez, S. (2008). Use of industrial wastewater from olive-oil extraction for biomass production of *Scenedesmus obliquus*. *Bioresource Technology*, 99:1111-1117.

- Hodaifa, G., Ochando-Pulido, J.M., Rodriguez-Vives, S., Martinez-Ferez, A. (2013). Optimization of continuous reactor at pilot scale for olive-oil mill wastewater treatment by Fenton-like process. *Chem. Eng. J.*, 220:117–124.
- Inan, H., Dimoglo, A., Şimşek, H., Karpuzcu, M. (2004). Olive oil mill wastewater treatment by means of electro-coagulation. *Separ. Purif. Technol.*, 36(1):23-31.
- Khoufi, S., Aloui, F., Sayadi, S. (2006). Treatment of olive oil mill wastewater by combined process electro-Fenton reaction and anaerobic digestion. *Water Res.*, 40:2007-2016.
- Lafi, W.K., Shannak, B., Al-Shannag, M., Al-Anber, Z., Al-Hasan, M. (2009). Treatment of olive mill wastewater by combined advanced oxidation and biodegradation. *Separ. Purif. Technol.*, 70(2):141-146.
- Marques, I.P. (2001). Anaerobic digestion treatment of olive mill wastewater for effluent re-use in irrigation. *Desalination*, 137:233-239.
- Martínez Nieto, L., Hodaifa, G., Rodríguez Vives, S., Giménez Casares, J.A. (2010). Industrial plant for olive mill wastewater from two-phase treatment by chemical oxidation. *J. Environ. Eng*, 136 (11):1309–1313.
- Martínez Nieto, L., Hodaifa, G., Rodríguez Vives, S., Giménez Casares, J.A., Ochando, J. (2011a). Degradation of organic matter in olive oil mill wastewater through homogeneous Fenton-like reaction. *Chemical Engineering Journal*, 173(2):503-510.
- Martínez Nieto, L., Hodaifa, G., Rodríguez Vives, S., Giménez Casares, J.A., Ochando, J. (2011b). Flocculation-sedimentation combined with chemical oxidation process. *Clean - Soil, air and water*, 39(10):949-955.
- Niaounakis, M., Halvadakis, C.P. (2006). Olive processing waste management literature review and patent survey, 2nd ed., Elsevier: Waste Management Series 5:23-64.
- Osathaphan, K., Boonpitak, T., Laopirojana, T. and Sharma, V. K. (2008). Removal of cyanide and zinc-cyanide complex by an ion-exchange process. *Water, Air, and Soil Pollution*, 194:179-183.
- Papadimitriou, E.K., Chatjipavlidis, I., Balis, C. (1997). Application of composting to olive mill wastewater treatment. *Environmental Technology*, 18(1):101–107.

Papastefanakis, N., Mantzavinos, D., Katsaounis, A. (2010). DSA electrochemical treatment of olive mill wastewater on Ti/RuO₂ anode. *J. Appl. Electrochem.*, 40(4):729-737.

Paraskeva, P., Diamadopoulos, E. (2006). Technologies for olive mill wastewater (OMW) treatment: a review. *Journal of Chemical Technology and Biotechnology*, 81:1475–1485.

Paraskeva, C.A., Papadakis, V.G., Tsarouchi, E., Kanellopoulou, D.G., Koutsoukos, P.G. (2007). Membrane processing for olive mill wastewater fractionation, *Desalination*, 213:218-229.

Pintar, J. (2001). Integrated ion exchange/catalytic process for efficient removal of nitrates from drinking water. *Chem. Eng. Sci.*, 56:1551–1559.

Rizzo, L., Lofrano, G., Grassi, M., Belgiorno, V. (2008). Pretreatment of olive mill wastewater by chitosan coagulation and advanced oxidation processes. *Separation and Purification Technology*, 63(3):648-653.

Sacco, O., Stoller, M., Vaiano, V., Ciambelli, P., Chianese, A., Sannino, D. (2012). Photocatalytic degradation of organic dyes under visible light on n-doped photocatalysts. *International Journal of Photoenergy*, doi:10.1155/2012/626759.

Sarika, R., Kalogerakis, N., Mantzavinos, D. (2005). Treatment of olive mill effluents. Part II. Complete removal of solids by direct flocculation with poly-electrolytes. *Environment International*, 31:297-304.

Stoller, M. (2009). On the effect of flocculation as pretreatment process and particle size distribution for membrane fouling reduction. *Desalination*, 240:209-217.

Stoller, M., Bravi, M. (2010). Critical flux analyses on differently pretreated olive vegetation wastewater streams: some case studies. *Desalination*, 250:578-582.

Su-Hsia, L., Ruey-Shin, J. (2009). Adsorption of phenol and its derivatives from water using synthetic resins and low-cost natural adsorbents: A review. *Journal of Environmental Management*, 90:1336-1349.

Tezcan Ün, Ü., Altay, U., Koparal, A.S., Ogutveren, U.B. (2008). Complete treatment of olive mill wastewaters by electrooxidation. *Chem. Eng. J.*, 139:445-452.

-

Tezcan Ün, Ü., Uğur, S., Koparal, A.S., Öğütveren, Ü.B. (2006). Electrocoagulation of olive mill wastewaters. *Separation and Purification Technology*, 52(1):136-141.

Valverde, A., DeLucas, M., Pérez, J.P., González, M., Rodríguez, J.F. (2006). Minimizing the environmental impact of the regeneration process of an ion exchange bed charged with transition metals. *Sep. Purif. Technol.*, 49:167–173.

Voreadou K. (1989). Olive mill wastewater: a trial for the water ecosystems, in: Proceedings of Symposium on Treatment of Wastes from Olive Mills, Greek Agrotechnical Society, Heraklion.

Zhu, L., Deng Y., Zhang, J., Chen, J. (2011). Adsorption of phenol from water by N butylimidazolium functionalized strongly basic anion exchange resin, *Journal of Colloidal and Interface Science*, 364:462-468.

CHAPTER 2

JUSTIFICATION AND OBJECTIVES

2.1 Justification

The present Doctoral Thesis is framed within the main research line of the Chemical and Biochemical Processes Technology Group (TEP025), from the Chemical Engineering Department of the University of Granada. In this research group, different treatments have been developed for industrial wastewaters purification through advanced oxidation processes, membrane technology as well as IE technique. Concretely, one of the research lines is focused on the depuration of olive mill effluents.

During the two-phase olive oil extraction system, two wastewater streams are mainly produced: the first one comes from the washing of the fruit, and is therefore called olives washing wastewater (OWW), and the second one is generated in the extraction of the olive oil, thus referred to as olive oil washing wastewater, OOW, a mixture of the olive-fruit humidity along with process-added water. These effluents are commonly known as olive mill wastewater (OMW).

Olives washing wastewater presents low organic load and constitutes the largest amount of the generated wastewater volume. On the other hand, olive oil washing wastewater has high organic load, highlighting the phenols content, which are phytotoxic and refractory, thus resistant to biological degradation. In moderate concentrations are often toxic to aquatic fauna and flora. Therefore, the wastewater from these industries great difficulty degrade by biological processes, both aerobic and anaerobic. Polyphenols gives a high antimicrobial activity inhibiting the development of flora responsible for self-purification processes, presenting phytotoxic activity.

Improper disposal of OMW to the environment or to domestic wastewater treatment plants is prohibited due to its toxicity to microorganisms, and also because of the consequent surface and groundwater potential contamination. Moreover, there is a legislation requiring the reduction of the global indicators concentration - COD and suspended solids - so these effluents can be reused or discharged. On the other hand, this wastewater also presents a high inorganic compounds concentration, especially high levels of potassium salts (60-70%) and sulfates, phosphates and chlorides of iron and calcium.

In previous research works, the “Chemical and Biochemical Processes Technology” Research Group (TEP025), from the Chemical Engineering Department of the University of Granada, has

developed an advanced physic-chemical process for OMW continuous treatment, which consists of the the following steps: (I) previous coagulation-flocculation step, (II) pseudo-Fenton advanced chemical oxidation process, (III) neutralizing / flocculation step, (IV) decanting process and finally (V) filtration in series through different kinds of filtrating materials (sand and olive stones).

In this context, the planned objectives for this thesis can be summarized as follows:

- Study of final purification of synthetic wastewater simulating olive mill effluent coming from the previously studied secondary treatment.
- Selection and characterization of four IE resins (strong-acid cationic resin, weak-acid cationic resin, strong-base anionic resin and weak-base anionic resin) for final purification step in the olive mill effluent:
- ✓ Recirculation-mode studies
 - Thermodynamic studies (Langmuir, Freundlich and Temkin models).
 - Kinetic studies (Pseudo-first order, Pseudo-second order and Intraparticle diffusion models).
- ✓ Continuous-mode studies
 - Breakthrough curves column studies (Thomas, Yoon-Nelson and Clark models). Determination of breakthrough times and maximum adsorption capacities.
- Optimization of operating variables affecting final purification of olive mill effluent through IE process: initial pH, temperature, flow rate, resins disposition, resins dosage, in order to fulfil the legislated standards for discharge of final water into public water courses and even for its reuse in the proper production process – for instance in the olives washing machines or during olive oil centrifugation process - thus closing the loop.
- Physicochemical characterization of the olive mill effluent exiting the optimized tertiary treatment through the following indicators:
 - ✓ Organic matter content, COD and total phenols.
 - ✓ Electroconductivity and pH values.
 - ✓ Analysis of the main inorganic ions content, including sodium, total iron and chloride concentrations.
- Study of the influence of main parameters on regeneration process of the studied resins: temperature, flow rate, regenerants nature and concentration.

2.2 Structure of the thesis

The thesis (experimental results) is divided in two sections, both of them devoted to all the main topics described above. The first section devoted to the study of the influence of main operating parameters on final purification of synthetic wastewater simulating olive mil effluent after secondary treatment through IE process. Furthermore, this first section also comprehends the theoretical studies (thermodynamic, kinetic and breakthrough curves studies) for the selected resins.

The second section refers to on the one hand the optimization of the operating factors involved in the final purification of real OMW by means of IE and on the other hand to the study of the effect of main parameters on the regeneration process for all the studied resins.

In this sense, first section includes chapters 4 to 10, while chapters 11 to 14 are covered in the second one.

A brief description of the chapters is detailed in the following points:

- In chapter 3 the IE resins used in the experimental section of this thesis are described as well as the equipment employed for IE experiments. Furthermore, operating conditions for recirculation and continuous mode experiments are detailed and common analytical methods employed in the experimental section are also completely described.
- Chapter 4 consists of a preliminary study in which IE was presented as an efficient pretreatment for reducing membrane fouling in the purification of OMW. Simultaneous removal of main pollutant ions from synthetic water simulating OMWST using Dowex Marathon C and Amberlite IRA-67 resins was examined by studying the disposition order of both resins in semi-batch system, as well as operating temperature in recirculation and continuous mode.
- In chapter 5, IE process is proposed as a suitable option for purification of synthetic OMW previously treated by means of the mentioned secondary treatment. The parametric requirements for drinking water production or at least for public waterways discharge were achieved using a combination of two IE columns working in series at bench scale. The IE resins used in this study were also Dowex Marathon C and Amberlite IRA-67. The effect of contact time, operating temperature and flow rate on simultaneous removal of sodium, total iron, chloride and phenols (the major pollutant species in OMWST) were investigated.
- Chapter 6 describes the performance of a fixed-bed IE system comprising strong-acid

cation exchange and weak-base anion exchange resins, which was fully examined for the removal of the ionic species responsible for the high salinity (sodium and chloride ions) of OMW from an olive mill working with the two-phase decanting technology exiting a primary-secondary treatment. In this chapter, the impacts of several key operating variables on the IE performance were examined, comprising the pH, the contact time and the initial concentration of these pollutant ionic species. Moreover, equilibrium isotherms were studied in order to gather information of the IE system equilibrium for Na^+ and Cl^- ions removal from this effluent. Finally, the continuous operation of the proposed IE process was addressed.

- In chapter 7, Dowex Marathon C resin was deeply investigated for removing iron from pretreated OMW after secondary treatment. The effect of the iron concentration in the pretreated effluent stream was investigated in the range $0.5\text{-}100\text{ mg L}^{-1}$. Moreover the equilibrium behaviour of this pollutant has been predicted by Langmuir, Freundlich and Temkin isotherms. Additionally, kinetics of iron adsorption on this resin was investigated using pseudo-first order, pseudo-second order and intraparticle diffusion models. Finally, the suitability of the proposed IE process and the final characteristics of the regenerated effluent were analysed.
- In chapter 8, the influence of iron inlet concentration and the system pH was studied with the aim of obtaining the equilibrium information related to the IE column breakthrough behaviour. More specifically, the IE process was modelled by fitting the experimental data to various adsorption models. Moreover, the impact of the regenerating conditions on the reusability of the resin and on the long-term IE efficiency was also determined by carrying out multiple adsorption–desorption–washing cycles, to address the potentiality for the industrial scale-up of the proposed process. Finally, the compliance of the real final treated effluent with irrigation standards was checked.
- Chapter 9 deals with the phenol removal from aqueous solution through Amberlyst A26, a strong-base anion exchange resin, and Amberlite IRA-67, a weak-base anion exchange resin. The influence of phenol concentration in the feedstream was investigated as well as the effect of recirculation time. Equilibrium data were fitted to the Langmuir, Freundlich and Temkin isotherms. In this chapter, Kinetic studies performed based on pseudo-first order, pseudo-second order and intraparticle diffusion models were also carried out. Results confirmed that Amberlyst A26 was more

efficient than Amberlite IRA-67 for the potential removal of phenol from industrial effluents.

- Chapter 10 describes the continuous-flow IE process for the recovery of phenols from OMW. Experiments were carried out in a packed column by means of both strong-base and weak-base anion exchange resins. The effect of initial pH on phenol removal was tested in the pH range 3-11. On the other side, Thomas, Yoon–Nelson and Clark models were applied to the experimental data to predict the breakthrough curves and model parameters such as rate constants and breakthrough times for three different inlet concentrations. Column regeneration studies showed that almost 100 % phenol recovery efficiencies were obtained. Finally, it was pointed out that IE process led to a solution of phenol susceptible to be concentrated and used in food, cosmetic or pharmaceutical sectors.
- Chapter 11 consists of an experimental study, whose aim was to test the best IE operating conditions (previously optimized with model olive mill effluent after secondary treatment) with real OMW after pretreatment and to compare the experimental results in terms of conductivity as well as ions concentrations. It was found that model OMW-2ST can be employed as a good simulating media to reproduce IE processes.
- In chapter 12, optimization of final purification of real OMW through strong-acid cation exchange resin and weak-base anion exchange resin is addressed. Central composite design was used for the optimization of the main variables affecting IE process (operating temperature, flow rate and initial pH). The obtained model was statistically tested using analysis of variance. Furthermore, resins dosage was also optimized. Under optimum conditions, the achieved concentrations for all contaminants in the final stream were maintained below the maximum established limits, complying with standards for reuse in the production process.
- Chapter 13 deals with the optimization of final purification of olive mill effluent through different combinations of the following IE resins: Dowex MAC 3 weak-acid cation exchange resin, Dowex Marathon C strong-acid cation exchange resin, Amberlite IRA-67 weak-base anion exchange resin and strong-base anion exchange resin Amberlyst A26. In this chapter, a comparison of all the possible resins combinations was carried out in order to elucidate the best option for purification of olive mill effluent in terms of ions concentration, COD and pH and electroconductivity values. Results showed the best option was to use the strong-acid cation exchange resin, i.e. Dowex Marathon C, followed by the Amberlite IRA-67 weak-base anion exchange

resin.

- The last chapter of this thesis, chapter 14, is devoted to the study of main parameters affecting the regeneration process all the resins, which were employed in the works throughout chapter 3 to chapter 12. In this chapter, the effect of temperature, flow rate as well as regenerants nature and concentration was investigated for each resin's regeneration.
- Finally, chapter 15 is devoted to the main conclusions of our work and chapter 16 is a summary in Spanish of the main results of the thesis.

CHAPTER 3

EXPERIMENTAL DETAILS

In this chapter the IE resins used in the experimental section of this thesis are described as well as the equipment employed for IE experiments. On the other side, operating conditions for recirculation and continuous mode experiments are detailed. Finally, common analytical methods and procedures employed in the experimental section are completely described.

3.1 Ion exchange resins

Four different IE resins were used for experiments with the aim of evaluating the suitability of different combinations among them (always combining one cationic resin and one anionic resin) for final purification of OMW after the secondary treatment.

The main physicochemical characteristics of each resin are detailed in Table 3.1 and Table 3.2.

In this point it is important to highlight the different matrix each resin presents as well as the total exchange capacity exhibited by the different resins. Furthermore, it is worthy to point out that strong-acid cationic resin and strong-base anionic resin present effective pH throughout the whole pH range (i.e. 0-14), whereas effective pH ranges are 5-14 and 0-7 for the weak-acid cationic resin and for the weak-base anionic resin, respectively.

Table 3.1. Physicochemical properties of Dowex Marathon C, Dowex MAC 3 cation exchange resins Amberlyst A 26 and Amberlite IRA-67 IE resins.





Properties	Dowex Marathon C	Dowex MAC 3
Type	Strong-acid cation	Weak acid-cation
Matrix	Styrene-DVB, gel	Polyacrylic, macroporous
Ionic form as shipped	H ⁺	H ⁺
Particle size	0.55-0.65 mm	0.3-1.2 mm
Effective pH range	0-14	5-14
Total exchange capacity	1.80 eq L ⁻¹	3.80 eq L ⁻¹
Shipping weight	800 g L ⁻¹	750 g L ⁻¹
Aspect		

Table 3.2. Physicochemical properties of Amberlyst A 26 and Amberlite IRA-67 IE resins anion exchange resins.

Properties	Amberlyst A 26	Amberlite IRA-67
Type	Strong-base anion	Weak-base anion
Matrix	Styrene-divinylbenzene	Tertiary amine
Ionic form as shipped	OH ⁻	OH ⁻
Particle size	0.56-0.70 mm	0.5-0.75 mm
Effective pH range	0-14	0-7
Total exchange capacity	0.80 eq L ⁻¹	1.60 eq L ⁻¹
Shipping weight	675 g L ⁻¹	700 g L ⁻¹
Aspect		

3.2 Ion exchange equipment

IE experiments were performed by using a bench-scale IE device (MionTec), which consisted mainly in a peristaltic pump (Ecoline VC-380) and two IE columns, as shown in Figure 3.1. IE columns employed in this study were made of an acrylic tube (540 mm height 46 mm internal diameter), provided with a mobile upper retaining grid, which could be fixed in the column to adjust it as a fixed bed or a semi-fluidized bed.

On other side, the IE device was equipped with a temperature-controlled thermostatic bath (Precisterm JP Selecta).

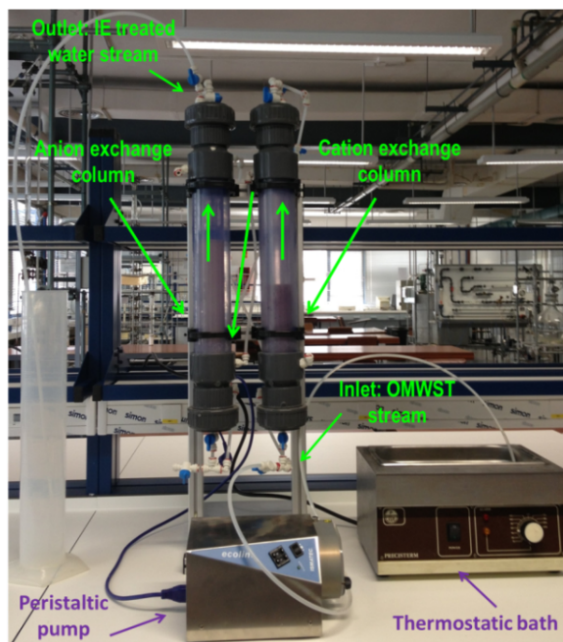


Figure 3.1. Ion exchange bench-scale equipment.

3.3 Analytical methods

Analytical grade reagents and chemicals with purity over 99 % were used for the analytical procedures. All analytical methods were applied at least in triplicate. Sodium, chloride, total iron, total phenols, EC and pH measurements were carried out on the raw OMW and at the end of each depuration step according to standard methods (Greenberg et al., 1992). A Helios Gamma UV-visible spectrophotometer (Thermo Fisher Scientific) served for COD and total iron measurements. OMW samples were diluted when necessary with MilliQ® water for their analysis, and IE treated samples were analysed directly without dilution.

For the measurement of the total iron concentration, all iron ions were reduced to iron ions (II) in a thioglycolate medium with a derivative of triazine, forming a reddish-purple complex that was determined photometrically at 565 nm (Standard German methods ISO 8466-1 and German DIN 38402 A51) (Greenberg et al., 1992).

For the measurement of the sodium concentration, a Crison GLP 31 Sodium Ion-Selective Electrode 96 50 was employed (see Figure 3.2), with autocorrection of temperature. 0.01, 0.1 and 1.0 g/L Na⁺ standard solutions required for the electrode calibration were prepared in the laboratory.

For the measurement of the chloride concentration, a Crison GLP 31 Chloride Ion-Selective Electrode 96 52 C was used (see Figure 3.2), with autocorrection of temperature. 0.01, 0.1 and 1.0 g/L Cl⁻ standard solutions required for the electrode calibration were prepared in the laboratory.



Figure 3.2. Crison GLP 31 device equipped with sodium and chloride ion-selective electrodes.

Total phenols and phenol derivatives reacted with a derivative thiazol, giving a purple azo dye, which was determined photometrically at 475 nm (Standard German methods ISO 8466-1 and DIN 38402 A51) (Greenberg et al., 1992).

EC and pH measurements were assessed with a Crison GLP31 conductivity-meter and a Crison GLP21 pH-meter, with autocorrection of temperature. Buffer standard solutions for conductivity (1,413 $\mu\text{S}\cdot\text{cm}^{-1}$ and 12.88 $\text{mS}\cdot\text{cm}^{-1}$) and pH (pH 4.01, 7.00 and 9.21) measurements respectively were supplied as well by Crison.

3.4 Recirculation and continuous mode experiments

3.4.1 Recirculation-mode experiments

The IE removal efficiencies of pollutant ions from OMW after secondary treatment were addressed by performing IE experiments in recirculation mode (see Figure 3.3). The flask containing the feed solution was magnetically stirred continuously during the whole course of the experiments.

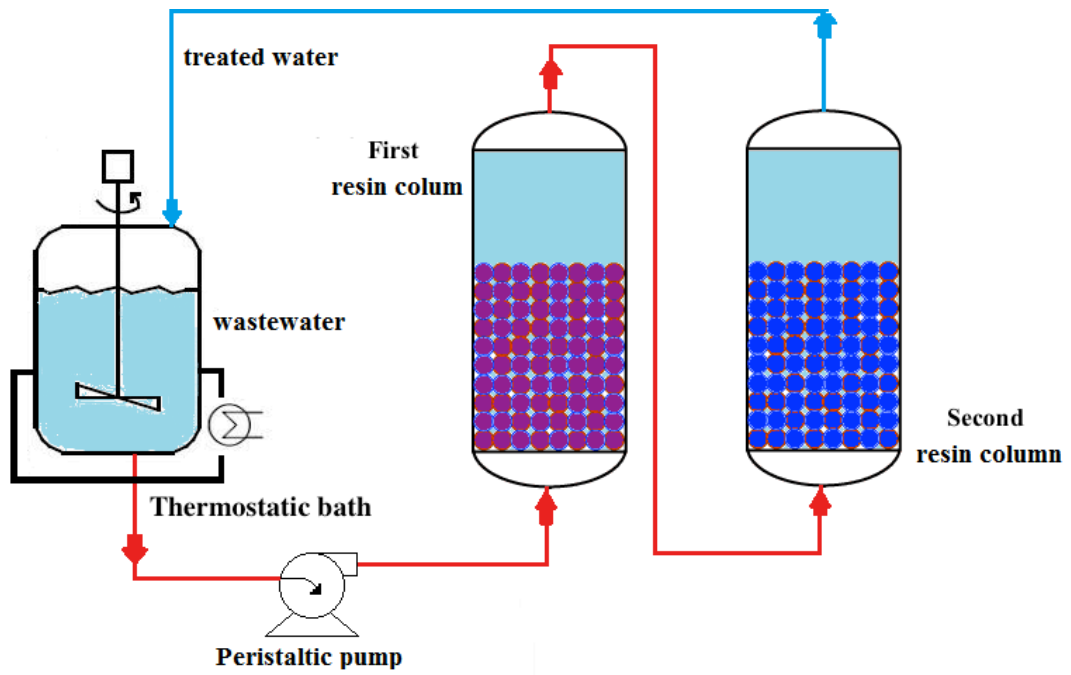


Figure 3.3. Flow-sheet scheme for IE recirculation-mode experiments.

3.4.2 Continuous-mode experiments

During continuous IE performance experiments, feedstream was introduced at the bottom of the first column in upflow mode, leaving this column by the top. Then, solution passed through the second column also in upflow mode from the bottom to the top (Figure 3.4).

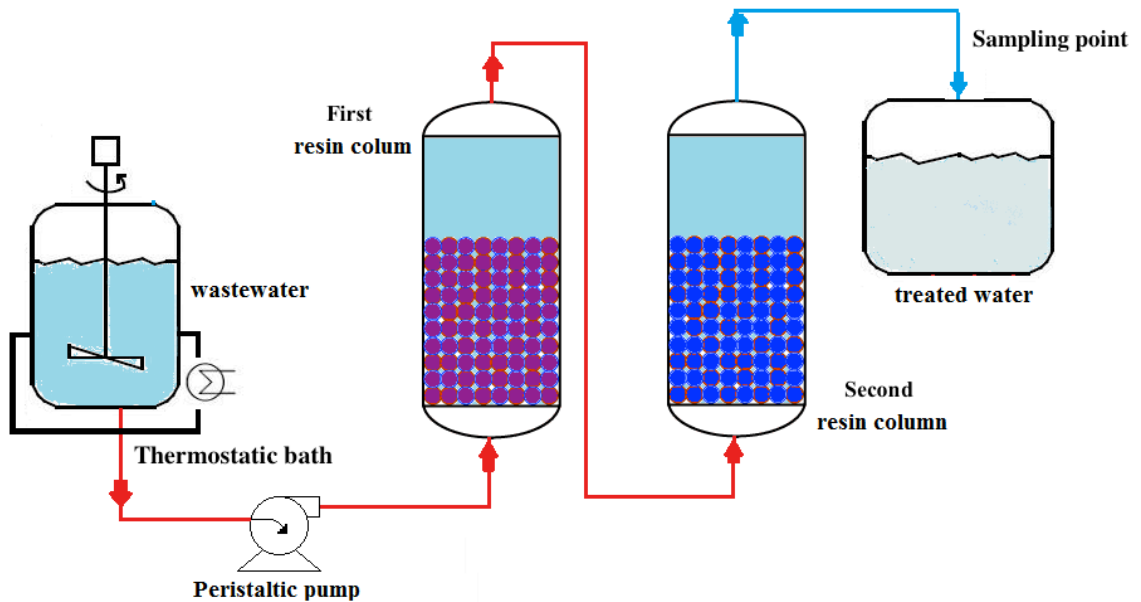


Figure 3.4. General flow diagram of IE continuous process.

In both cases, the percent of removal efficiency of the contaminant species was defined as follows:

$$\% \text{ Removal efficiency} = \frac{C_i - C_f}{C_i} \times 100 \quad (1)$$

where C_i and C_f are the initial and final species' concentration (mg L^{-1}), respectively.

3.5 References

Greenberg, A.E., Clesceri, L.S., Eaton, A.D. (1992). Standard Methods for the Examination of Water and Wastewater, APHA/AWWA/WEF, 16th ed., Washington DC. Cabs.

PART II

RESULTS

CHAPTER 4

ION EXCHANGE AS AN EFFICIENT PRETREATMENT SYSTEM FOR REDUCTION OF MEMBRANE FOULING IN THE PURIFICATION OF MODEL OMW.

M.D. Víctor-Ortega^{1*}, J.M. Ochando-Pulido¹, G. Hodaifa², A. Martínez-Ferez¹.

¹Chemical Engineering Department, University of Granada, 18071 Granada, Spain

²Molecular Biology and Biochemical Engineering Department, University of Pablo de Olavide, 14013 Seville

*email: mdvictor@ugr.es

Desalination

Publisher: ELSEVIER SCIENCE BV. PO BOX 211, 1000 AE AMSTERDAM, NETHERLANDS

Volume 343. Pages 198-207.

Year: 2014

ISSN: 0011-9164

DOI: <http://dx.doi.org/10.1016/j.desal.2013.11.011>

Impact factor: 3.756

Tertile: First



Abstract

Membrane technology is becoming increasingly accepted in the field of wastewater reclamation, but pretreatments are needed to prevent membrane fouling that limits system performance and recovery. In this research work, ion exchange (IE) is presented as an efficient pretreatment for reducing membrane fouling in the purification of olive mill wastewater (OMW). No previous studies are available in scientific literature regarding the treatment of OMW by means of IE technology. OMW was previously conducted to a secondary treatment comprising chemical oxidation with Fenton's reagent, coagulation–flocculation and filtration through olive stones. Chloride, sodium, iron and phenols are the major pollutants in OMW after secondary treatment (OMWST). A bench-scale study was undertaken to evaluate the performance of two IE columns working in serial connection. Simultaneous removal of those pollutants from synthetic water simulating OMWST using Dowex Marathon C and Amberlite IRA-67 resins was examined by studying the disposition order of both resins in semi-batch system, as well as operating temperature in batch and continuous mode. Results of continuous IE operation verify the patterns observed for the studied species in batch-run experiments. The IE system proposed, with average removal efficiencies (50–80%), will be contributed to reduce concentration polarization and membrane fouling.

Keywords: Ion exchange, Membrane fouling, Olive mill wastewater, Pretreatment, Simultaneous removal.

4.1 Introduction

As water becomes scarce and treatment regulations more stringent, purification systems like membranes and ion exchange (IE) processes have drawn more attention because of their attractive separation capabilities. Reverse osmosis (RO) membranes are able to effectively remove most organic and inorganic compounds and microorganisms from raw water and have been applied to drinking water treatment and wastewater reclamation (Bódalo et al., 2003; López et al., 2006). On the other hand, in order to produce water of superior quality like drinking water, the use of IE resins in desalination and wastewater reclamation has become more widespread. IE resins have been developed as a major option for pollutants removal in drinking water treatment (Bolto and Dixon, 2004) and wastewater reclamation over the past few decades (Demirbas et al., 2005; Fu and Wang, 2011; Su-Hsia and Ruey-Shin, 2009; van Deventer, 2011; Dabrowski et al., 2004).

Olive mill wastewater (OMW) is a hardly treated by-product generated during olive oil production which constitutes an important environmental problem, since its disposal into water

courses leads to deterioration of natural water bodies, pollution and environmental degradation (Danellakisa et al., 2011). This effluent is characterized by an acid pH value, black colour, very high and variable chemical oxygen demand (COD) and major concentration of microbial growth inhibiting compounds, such as phenolic compounds and tannins (Table 4.1). Also inorganic compounds such as chloride, sulfate and phosphoric salts of potassium, calcium, iron, magnesium, sodium, copper and traces of other elements are present in OMW (Garrido Hoyos et al., 2002). Management of this pollutant effluent is of major importance nowadays, especially in the Mediterranean countries. In this sense, there are some studies concerning OMW treatment by means of membrane filtration processes (Ochando-Pulido et al., 2012a; Canepa et al., 1988; Borsani and Ferrando, 1996; Turano et al., 2002; Stoller and Chianese, 2006; Ochando-Pulido et al., 2013a; Ochando-Pulido et al., 2012b; Stoller, 2011). As water treatment membrane systems increase in use throughout the world, pretreatment is needed to prevent fouling on membranes (Ochando-Pulido et al., 2012b; Stoller and Chianese, 2007; Stoller, 2009; Ochando-Pulido et al., 2012c; Ochando-Pulido et al., 2013b; Stoller, 2011). Phenols and some ions, like calcium and iron, are major foulants of membrane systems that cause severe fouling and limit system recovery (Stoller and Chianese, 2007; Ochando-Pulido et al., 2012c).

Table 4.1. Characterization of OMW used in the oxidation experiments (Martínez Nieto et al., 2011a).

Parameters	OMW from Jaén	OMW from Granada
pH	7.24	6.32
Total solids (% w/w)	0.24	0.83
Total suspended solids (% w/w)	0.005	0.001
Ash (% w/w)	0.08	0.50
Electric conductivity (mS cm⁻¹)	2.08	1.17
[Fe³⁺] (mg L⁻¹)	126.4	7.7
Total phenols (mg L⁻¹)	44.0	50.6
BOD5 (mg O₂ L⁻¹)	380.0	1100.0
COD (mg O₂ L⁻¹)	1672.9	4137.2

In our previous studies, an efficient and novel secondary treatment based on an advanced chemical oxidation process which comprises Fenton's reagent was used to break down organic and inorganic compounds of OMW in the laboratory and on a pilot scale (Martínez Nieto et al., 2011a; Hodaifa et al., 2013a), followed by a flocculation-sedimentation step and filtration-in-

series through olive stones as zero-cost filtration medium (Martínez Nieto et al., 2012; Hodaifa et al., 2013b). This depuration sequence succeeded to overcome the problem related to the presence of phenolic compounds and achieved very high reduction of COD and suspended solids concentration. Nevertheless, after this secondary treatment OMW presented a high concentration of dissolved monovalent and divalent ions, which cannot be removed by conventional physicochemical treatments.

IE is a separation process in which harmful or undesirable ions are removed from solution to the resin or other IE material and replaced by others which do not contribute to contamination of the environment, since in most cases the undesirable ion is changed by another one which is neutral within water bodies. The change continues until the ion exchanger achieves ionic equilibrium and then the capacity of the ion exchanger is exhausted and no exchange is possible any longer. After that, the IE column must be removed from service, regenerated and reused after the usage (Metcalf and Eddy, 2003). The method is technologically simple and enables efficient removal of even traces of impurities from solutions. The operational and installation costs of IE processes are sensibly lower compared with other wastewater treatment processes like membrane filtration or granular activated carbon (GAC) filtration process (Dabrowski et al., 2004). However, IE resins must be regenerated by chemical reagents when they are exhausted, a factor to be optimized to avoid causing secondary pollution. The uptake of ions by IE resins is rather affected by certain variables such as pH, temperature, flow rate, ionic charge, initial pollutant concentration and contact time.

Many studies on the adsorption of metal ions on IE resins such as Dowex A-1 (Mathur and Khopkar, 1985), Duolite GT-73 (Shaha et al., 2000) and NKA-9 (Xingcun and Yimin, 1997) have been reported. There are several examples of selective removal of heavy metal ions by IE which include removal of Pb(II), Hg(II), Cd(II), Ni(II), V(IV,V), Cr(III,VI), Cu(II) and Zn(II) from water and industrial wastewaters (Fu and Wang, 2011; Dabrowski et al., 2004; Gode and Pehlivan, 2006). Apart from that, there are many reports on the use of IE in hydrometallurgical applications for the recovery or purification of metal solutions or for effluent treatment, including the primary recovery of gold, uranium and rhenium, and the purification of cobalt electrolyte to ensure high-purity metal (van Deventer, 2011).

IE resins have also found an increasing application in the drinking water treatment sector over the last few decades, especially when there is a high concentration of natural organic matter (NOM) in contaminated water since high percentages on the removal efficiency of NOM by IE process are found (Bolto and Dixon, 2004). Phenolic compounds can also be successfully removed from wastewaters by IE technology (Su-Hsia and Ruey-Shin, 2009; Zhu et al., 2001; Roostaei and Tezel, 2004; Ku et al., 2004).

Selective resins can reduce the residual concentration of iron, sodium, chloride and phenols, which are the major pollutants in the olive mill wastewater effluent after the secondary treatment (OMWST), to limits which are not harmful for membrane systems performance. On the other hand, IE resins can reduce wastewater salinity, which is a main issue causing membrane concentration polarization and fouling problems. In this sense, IE is presented as an efficient pretreatment system for reduction of membrane fouling in the purification of OMW. The aim of this work was to examine the simultaneous removal of iron, sodium, chloride and phenols from synthetic water simulating OMWST using a Dowex Marathon C cation exchange resin and an Amberlite IRA-67 anion exchange resin, in serial connection. The present research work is focused on the disposition of the resins under study and the influence of the operating temperature, with the idea of implementing a combined system based on IE as pretreatment of a subsequent membrane process.

4.2 Experimental

4.2.1 OMW treatment

The secondary treatment of OMW consists of various stages: 1) Fenton-like oxidation, 2) flocculation–sedimentation, and 3) olive stones filtration.

4.2.1.1 Fenton-like oxidation

Olives and olive oil wastewaters were mixed in 1:1 (v/v) proportion in the laboratory to regulate the value of the organic load of OMW entering the depuration system and thus avoid fluctuations in the COD parameter. OMW was then conducted through a secondary advanced oxidation process consisting in chemical oxidation based on Fenton’s reagent. OMW was pumped into a stirred reaction tank in which an oxidizing agent (hydrogen peroxide) and a catalyst (ferric chloride) were added as it is shown in Figure 4.1. The best catalyst - regarding efficiency and low cost from among tested Mohr salt ($\text{Fe}(\text{SO}_4)_2(\text{NH}_4)_2\cdot 6\text{H}_2\text{O}$), ferric perchlorate and ferric chloride - and the best catalyst/ oxidant concentrations ratio were studied, as well as the optimal operating conditions with regard to pH, stirring velocity and temperature (Martínez Nieto et al., 2011a; Hodaifa et al., 2013a).

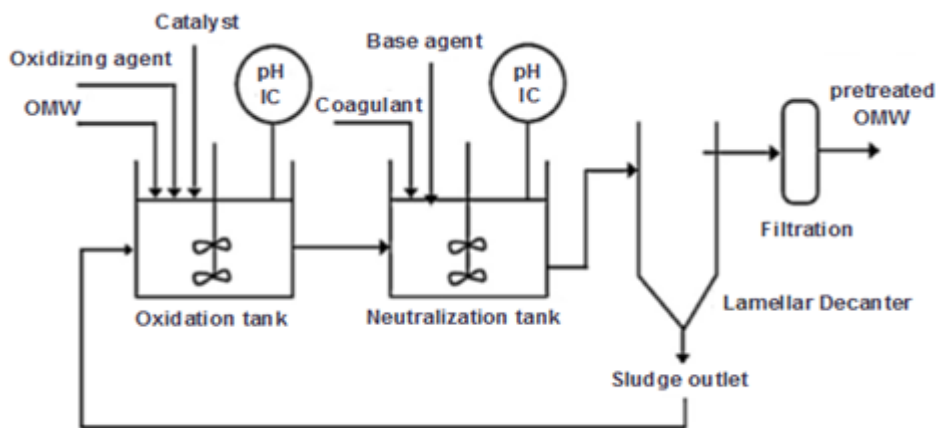


Figure 4.1. Flow diagram of the pretreatment process (Ochando-Pulido et al., 2012c).

4.2.1.2 Flocculation–sedimentation

Throughout the Fenton-like oxidation process, OMW pH fell spontaneously to values around 3.0 - at which the reaction optimally occurred - owed to the addition of the catalyst. For this reason, a neutralizing agent (sodium hydroxide solution, 5N) was added in a following stirred tank to the OMW coming out of the Fenton-like oxidation tank, adjusting its pH to neutrality (to pH values between 6.0 - 9.0, as regulations demand). This way, besides, the iron colloidal particles present in OMW due to the previous addition of the ferric catalyst became precipitated as iron hydroxide. Moreover, to attain rapid separation of the solid–liquid phases, several commercial coagulant–flocculants (QG-2001, QG-2002, DQGALFLOC-130H and Nalco-77171) were tested, leading to the formation of an iron-rich sludge which finally sedimented in a lamellar decanter. The sludge was recirculated to the oxidation tank to reduce the catalyst consumption. The optimum dosage of each flocculant was also studied (Martínez Nieto et al.; 2011b).

4.2.1.3 Olive stones filtration

In our previous research studies, the profit of olive stones as zero-cost adsorbent medium was investigated in detail (Martínez Nieto et al., 2012; Hodaifa et al., 2013b). Using olive stones directly as adsorbent for metal ions, instead of more expensive materials, such as activated carbon, was stated as an economically and environmentally interesting alternative for this thereby product of the olive oil industry.

Besides, it is well known that the presence of iron is harmful to nanofiltration (NF) and RO membranes, as in its form of insoluble complexes with hydroxyl ions (ferric hydroxide) at neutral and alkaline pH, these large metal hydroxides molecules cannot easily pass through the

membrane. As a result, they become deposited on the membrane surface, leading to cake enhanced concentration polarization, pore blockage and abrasive fouling phenomena. On the other hand, high iron levels reduce the effectiveness of IE resins. In this sense, olive stones could be profitable for removing the residual iron ions present in OMW at the outlet of the decanter of the above described process (see Figure 4.1) before the membrane separation steps. In this study, two different filtration sequences were examined: (i) fine sand filter followed by olive stones filter and (ii) gravel filter followed by olive stones filter (Martínez Nieto et al., 2012; Hodaifa et al., 2013b).

4.2.2 Ion exchange process

4.2.2.1 Synthetic water solutions

All experiments were conducted using model water simulating pretreated OMW prepared by dissolving reagent-grade sodium chloride, 30 % (w/w) iron (III) chloride aqueous solution and phenol (all of them provided by Panreac) in double distilled water. Model water solutions were prepared prior to the start of the experiments, stored at 4 °C and brought to room temperature before being used. Chloride and sodium were added as sodium chloride. On the other hand, iron was added as iron (III) chloride.

The target concentrations for chloride and sodium were fixed at the values registered on average at the outlet of the OMW secondary treatment: approximately 1130 mg/L and 730 mg/L, whereas about 1 mg/L and 0.4 mg/L for phenol and total iron, respectively (Martínez Nieto et al., 2011a; Hodaifa et al., 2013a).

4.2.2.2 Ion exchange resins

The IE resins used in this work were Dowex Marathon C strong-acid cation exchange and Amberlite IRA-67 weak-base anion exchange resins, both provided by Sigma Aldrich. The physical properties of both resins are shown in Table 4.2.

Table 4.2. Properties of Dowex Marathon C and Amberlite IRA-67 IE resins.

Properties	Dowex Marathon C	Amberlite IRA-67
Type	Strong-acid cation	Weak-base anion
Matrix	Styrene-DVB, gel	Tertiary amine
Ionic form as shipped	H ⁺	OH ⁻
Particle size	0.55-0.65 mm	0.5-0.75 mm
Effective pH range	0-14	0-7
Total exchange capacity	1.80 eq/L	1.60 eq/L
Shipping weight	800 g/L	700 g/L

4.2.2.3 Ion exchange equipment

A bench scale study was undertaken to evaluate the performance of a combination of two IE columns operating in serial connection for the purification of OMWST.

IE columns employed in this study were made of an acrylic tube of 540 mm height x 46 mm internal diameter. The columns had a mobile upper retaining grid, which was fixed in the column to adjust it as a fixed bed or a semi-fluidized bed. The IE device (MionTec) was equipped with a peristaltic pump (Ecoline VC-380) and a temperature-controlled thermostatic bath (Precisterm JP Selecta). The IE equipment used in this work is shown in Figure 4.2.

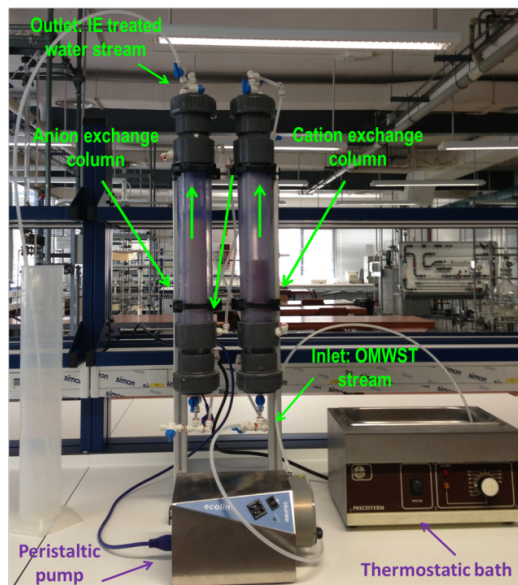


Figure 4.2. Ion exchange bench-scale equipment.

4.2.2.4 IE resins conditioning and performance

IE columns were prepared before the first use as follows: 400 mL MilliQ[®] water were pumped into each column in upflow mode, leaving the top of the columns uncovered to avoid creating vacuum. After that, each resin was introduced from the top of the corresponding column (346 g in case of Dowex Marathon C and 350 g Amberlite IRA-67). Then, each resin was washed with MilliQ[®] water at 10 L/h in the beginning and then at 20 L/h to create bed fluidization and resin expansion along the column. Taking account the shipping weight of each resin (800 g/L for Dowex Marathon C and 720 g/L for Amberlite IRA-67), the anionic resin bed expansion was higher than the cationic resin bed expansion. 4 L and 2 L MilliQ[®] water were spent to completely remove the Dowex Marathon C and Amberlite IRA-67 resins dye, respectively.

During the IE performance experiments, OMWST feed stream was introduced at the bottom of the first column (cationic resin) in upflow mode, leaving this column by the top. Then, OMWST passed through the second column (anionic resin) also in upflow mode from the bottom to the top.

4.2.2.5 Resins Regeneration

After each operational cycle, the Dowex Marathon C cation exchange resin was fully washed with a 2 % HCl aqueous solution for 30 minutes at 298 K. In a similar way, Amberlite IRA-67 anion exchange resin was washed with a 4 % NaOH aqueous solution for 40 minutes at 298 K. Then, the resins were washed with double distilled water to remove all excess of acid or base, respectively.

4.2.2.6 IE experiments

The batch IE experiments, for the removal of pollutant ions, Na⁺, Cl⁻, total iron and phenols, were carried out on the semi-fluidized bed operating on a closed loop system. In these experiments, the total sample volume of simulating OMWST solution, flow rate, and operation time used were 2 L, 10 L h⁻¹, and 180 min, respectively.

In continuous IE experiments, resins disposition was investigated by treating 100 L of simulating OMWST solution, at 10 L/h for 600 min.

In both batch and continuous experiments, metal ion concentrations were analyzed in the outlet stream at different contact times throughout the whole experiments. The treated amount was monitored as a function of contact time by removing 50 mL aliquot of solution for the ions concentration measurements. Also, the effect of temperature on the IE process performance was

studied by setting values equal to 298 K, 308 K and 318 K. For batch-mode experiments, 2 L of simulating OMWST solution were treated by the IE system for 180 min at a fixed flow rate of 10 L/h. For continuous-mode experiments, 25 L of simulating OMWST solution were treated, at 10 L/h for 150 min.

4.2.3 Analytical methods

Analytical grade reagents and chemicals with purity over 99 % were used for the analytical procedures. All analytical methods were applied at least in triplicate. Sodium, chloride, total iron, total phenols, conductivity (EC) and pH measurements were carried out on the raw OMW and at the end of each depuration step according to standard methods (Greenberg et al., 1992). A Helios Gamma UV-visible spectrophotometer (Thermo Fisher Scientific) served for COD and total iron measurements. OMW samples were diluted when necessary with MilliQ[®] water for their analysis and IE treated samples were analysed directly without dilution.

For the measurement of the total iron concentration, all iron ions were reduced to iron ions (II) in a thioglycolate medium with a derivative of triazine, forming a reddish-purple complex that was determined photometrically at 565 nm (Standard German methods ISO 8466-1 and German DIN 38402 A51) (Greenberg et al., 1992).

For the measurement of the sodium concentration, a Crison GLP 31 Sodium Ion-Selective Electrode 96 50 was employed, with autocorrection of temperature. 0.01, 0.1 and 1.0 g/L Na⁺ standard solutions to calibrate the electrode were prepared in the laboratory.

For the measurement of the chloride concentration, a Crison GLP 31 Chloride Ion-Selective Electrode 96 52 C was used, with autocorrection of temperature. 0.01, 0.1 and 1.0 g/L Cl⁻ standard solutions required for the electrode calibration were also prepared in the laboratory.

Total phenols and phenol derivatives were analyzed by reaction with a derivative thiazol, giving a purple azo dye which was determined photometrically at 475 nm (Standard German methods ISO 8466-1 and DIN 38402 A51) (Greenberg et al., 1992).

EC and pH measurements were assessed with a Crison GLP31 conductivity-meter and a Crison GLP21 pH-meter, provided with autocorrection of temperature. Buffer standard solutions for EC (1,413 $\mu\text{S}\cdot\text{cm}^{-1}$ and 12.88 $\text{mS}\cdot\text{cm}^{-1}$) and pH (pH 4.01, 7.00 and 9.21) measurements respectively were supplied as well by Crison.

4.3 Results and discussion

4.3.1 Characterization of OMWST

The physicochemical composition of the OMWST effluent is reported in Table 4.3. The secondary treatment achieved very high removal of COD and suspended solids and particularly succeeded to reduce the concentration of phenolic compounds. Nevertheless, it was not able to abate the high concentration of dissolved monovalent and divalent ions, which cannot be removed by conventional physicochemical treatments. High EC values were noticed in the OMWST, mainly due to the considerable EC of the raw OMW together with the further increment in sodium and chloride content derived from the addition of the catalyst and neutralizing agents within the secondary treatment (Martínez Nieto et al., 2011a; Hodaifa et al., 2013a; Martínez Nieto et al., 2012).

Table 4.3. Characteristics range of OMW after secondary treatment.

Parameters	Parametric value
pH	7.78 - 8.17
Conductivity, mS cm ⁻¹	3.15 - 3.55
COD, mg L ⁻¹	120.5 - 226.6
Total phenols, mg L ⁻¹	0.39 - 0.98
[Fe] Total, mg L ⁻¹	0.04 - 0.4
[Cl ⁻], mg L ⁻¹	875.83 - 1045.03
[Na ⁺], mg L ⁻¹	534.01 - 728.71

In this sense, the measured EC values in OMWST were well above the range 2 - 3 mS/cm, thus OMWST presents hazardous salinity levels with the goal of reusing the regenerated water for irrigation purposes according to the standard levels established by the Food and Agricultural Association (FAO) (Table 4.4). Moreover, iron load present in OMWST due to the ferric catalyst addition is particularly harmful for polymeric membranes, causing not only cake-enhanced concentration polarization and pore blockage and plugging but also abrasive deleterious colloidal fouling phenomena (Stoller, 2011; Zhu and Elimelech, 1997; Yiantsios and Karabelas, 2002).

Table 4.4. Water Quality according to Food and Agriculture Organization.

EC, mS/cm	Water Quality	Hazardous due to salinity
0-1	Excellent - Good	Low - Medium
1-3	Good - Poor	High
>3	Poor - Non-acceptable	Very high

4.3.2 Resins disposition

In first place, the disposition of both resins in the IE system was investigated at fixed conditions equal to 298 K and 10 L/h. These experiments were carried out on continuous operation mode for 600 min operation time, and 50 % removal efficiencies were set as main objective for all the studied ions. Ions concentration values in the outlet stream as a function of operating time are given in Figure 4.3.

In Figure 4.3a it can be observed that the chloride saturation was reached for the same operating time upon both resins dispositions (400 min of operating time, equivalent to 67 L of treated simulating OMWST). However, by using the A resins configuration higher volume could be treated and higher removal efficiencies were achieved for the same volume treated. When experiments were carried out according to the B configuration, from 80 min of operation on (approximately 13 L of treated simulating OMWST) chloride concentration at the outlet stream was higher than 600 g/L (50 % removal efficiency), whereas this happened from 170 min for the A configuration (around 28 L of treated simulating OMWST).

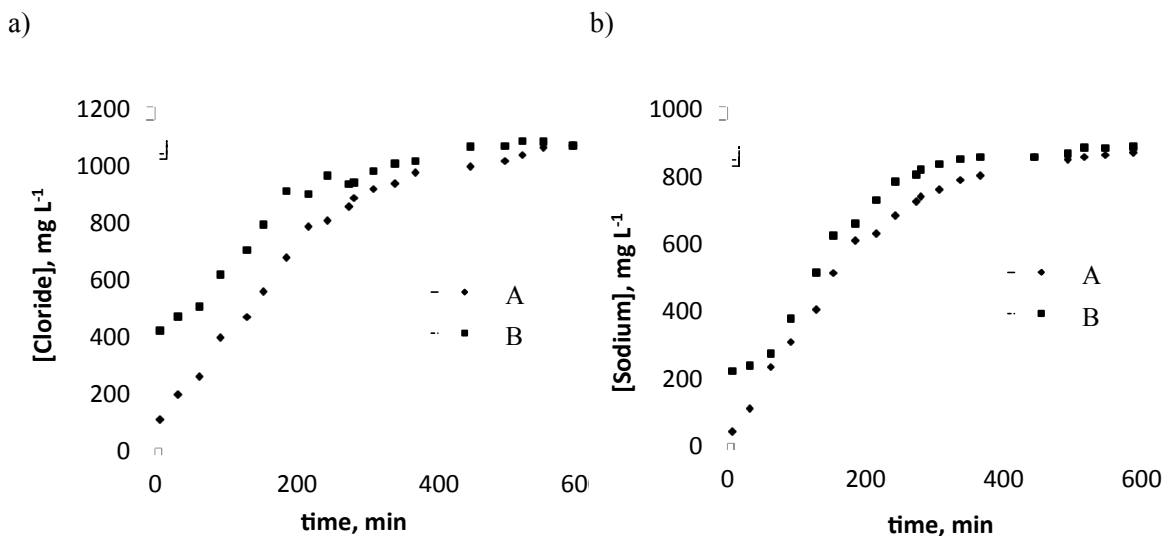
Analogously, Figure 4.3b shows the equilibrium sodium concentration in the outlet stream was reached in about 350 min for both resins dispositions (equivalent to 58 L of treated simulating OMWST). Nevertheless, by setting the A resins configuration higher volume could be treated and higher removal efficiencies were ensured for the same volume treated, following a similar pattern as the one observed for chloride ions. When experiments were carried out according to the B configuration, from 100 min of operation (approximately 17 L of treated simulating OMWST) concentration of sodium in the outlet stream was higher than 400 g/L (50 % removal efficiency), whilst this occurred from 130 min by employing the A configuration (about 22 L of treated simulating OMWST).

Total iron concentration in the outlet stream (Figure 4.3c) was lower than 0.2 mg/L throughout the entire experiments disregarding the chosen resins disposition. This meant removal

efficiencies higher than 50 % during the total operating time, with no significant differences between both configurations.

Considerably significant differences between the studied resins dispositions were found in case of phenols removal up to 180 min runtime (Figure 4.3d), but afterwards these differences became negligible. When experiments were carried out according to the B configuration, phenols concentration in the outlet stream above 0.5 g / L (50 % removal efficiency) was attained from 10 min of operation (roughly 1.7 L of treated simulating OMWST), whereas in the case of the A configuration this happened from 150 min (approx. 25 L of treated simulating OMWST). From 450 min operation, concentration of phenolic compounds in the outlet stream was higher than initial phenols concentration in simulating OMWST, which can be explained due to fact of phenols desorption.

On the other hand, the effect of resins disposition on the EC value (Figure 4.3e) in the outlet stream is represented. Within the first 30 min operation time, relevant EC differences between the A and B resins disposition were registered. For this operating time, the measured EC exiting in the A configuration was lower than for the B configuration. In this point, EC was about 0.4 mS/cm in the A configuration in contrast with the 0.9 mS/cm value in the B one. From 250 min operation (about 42 L simulating OMWST), conductivity was higher than 3 mS/cm in B configuration. Otherwise, in the A configuration this EC value was overcome from 300 min (5 L treated OMWST).



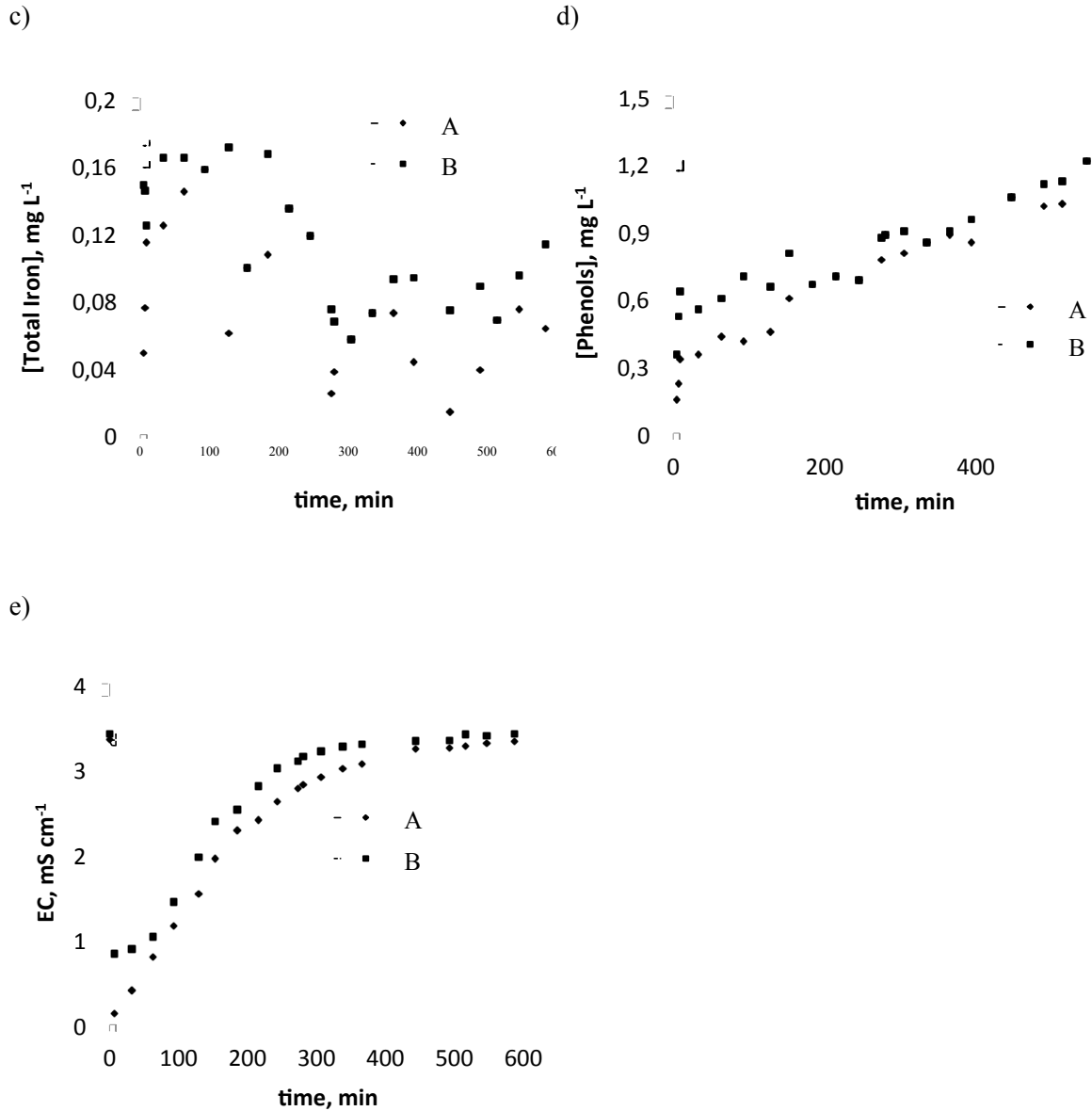


Figure 4.3. Effect of resins position (A: Cation + Anion, and B: Anion + Cation) on chloride, sodium, total iron, and total phenols concentrations, and electric conductivity (EC) values at the outlet of continuous IE system.

All these results confirmed that setting the cation exchange resin followed by the anion exchange one offers better results than in the opposite order. It is worth underlining the fact that this effect was particularly highly pronounced in the case of monovalent ions removal, such as sodium and chloride, especially during the first treatment hour. This may be owed to the high monovalent ions load ($[Cl^-] > [Na^+] > [Total\ phenols] > [Total\ Fe]$) in OMWST. On the other hand, chloride ions have similar ionic charge as hydroxide ions, and the same occurs to sodium ions with respect to hydrogen ions. This also can give advantage to monovalent ions exchange, since ionic charge plays an important role in the IE process. Resins have preference for certain ionic

species that have similar ionic charge characteristics. In general, the selectivity of the resins depends on the ionic charge and the ions size (Clifford and Walter, 1983). Also, similar results were obtained by Apell and Boyer (2010) when magnetic cation exchange resin (MIEX-Na) and magnetic anion exchange resin (MIEX-Cl) were combined (Apell and Boyer, 2010). They found that hardness removal appeared to be cumulative, while dissolved organic matter (DOM) removal was not cumulative. These results are explained by the fact that DOM-Ca⁺ complexes retain deprotonated carboxylic acid groups in the presence of calcium, so DOM-Ca⁺ can theoretically be removed by anion and cation exchange, depending on the ratio of calcium to carboxylic acid groups.

Monovalent ions and iron are removed by means of ionic exchange. The total exchange capacities of the employed resins are high enough (1.8 and 1.6 eq/L, Table 4.2) to justify the ion exchange. In case of phenols, the uptake in the resin is assumed to be accomplished by two ways: ion exchange and molecular adsorption.

Cations are exchanged in the first column (Dowex Marathon C), thus at the end of this column pH drops approximately to 1.5-2.5 (H⁺ species are released). In the second column (Amberlite IRA-67), anions are exchanged and pH progressively increases, being in the range 7-8 at the end of the process.

The phenol dissociation to phenol and phenolate can be considered as a function of the total concentration of phenol and the pH of the liquid solution (pH >8). At acidic pH (pH < 8) the phenol dissociation is low and therefore, the molecular adsorption process is the predominant one (Dowex Marathon C), whereas both adsorption and ion exchange are important at alkaline pH (Amberlite IRA-67) (Carmona et al., 2006). This fact justifies the optimal arrangement of resin columns: cationic + anionic, since the cationic one is active in the whole pH range and the anionic one is only active in the range 0-7 (Table 4.2).

4.3.3 Effect of temperature

4.3.3.1 Batch experiments

Figure 4.4 represents the ions concentration and electric conductivity in the outlet stream as a function of contact time. A guided focus on this figure permits to notice that the results showed considerable reduction of the concentrations of all species with increasing contact time. In addition, the equilibrium was obtained in about 30 min and from this point further removal efficiencies were over 90 %.

Chloride, sodium and total iron adsorption efficiencies were found to be not significantly affected by operating temperature (Figure 4.4a-c). Otherwise, phenol removal was deeply affected by this variable (Figure 4.4d). In this case, the best results were obtained at the lowest operating temperature (298 K). Similarly, Mustafa et al. (1997) noted no significant effect of temperature on the removal of chromate ions from different solutions upon temperature variation in the range 298-313 K by employing the strongly basic anion exchanger Amberlite IRA-400 in the chloride form (Mustafa et al., 1997). These results contrast with those found by Demirbas et al. (2005) in their study of the effect of temperature on the distribution coefficient (K_d) for the adsorption of divalent metal ions (Cu II, Zn II, Ni II, Pb II and Cd II) onto Amberlite IR-120 resin (Demirbas et al., 2005). K_d was defined as the ratio of metal ion concentration on the resin to that in aqueous solution. In the case of these divalent ionic species the K_d coefficient was very high for all metal ions and increased with temperature. This is due to the endothermic adsorption of divalent cations, which cause the equilibrium constants for this reaction to increase with temperature and thus the reaction products are favoured at high temperatures.

Otherwise, Roostaei and Tezel (2004) examined the liquid-phase adsorption of phenol from water by silica gel, HiSiv 3000, activated alumina, activated carbon, Filtrasorb-400 and HiSiv 1000 (Roostaei and Tezel, 2004). It was found that adsorption capacity decreased with increasing temperature (Ku et al., 2004). In other studies, adsorption of molecular phenol species on N-butylimidazolium functionalized strongly basic anion exchange resin with Cl⁻ anion (MCl) was found to be exothermic under acidic pH conditions. Similar results were observed in some other studies, where phenols were adsorbed on Purolite A-510, NDA103 and IRA96C resins at acidic pH (Ku et al., 2004; Erdem et al., 2005). At an initial solution pH of 12.6, where phenolate species dominated, the removal efficiency increased with the rise in the temperature, indicating that phenol uptake was favoured at higher temperatures at pH around 12.6. The adsorption of phenolate species on MCl was stated to be endothermic under alkaline pH conditions. This result are in conflict with the work by Ku et al. (2004), who reported that the temperature did not influence the adsorption of ionic phenol species on Purolite A-510 resin (Ku et al., 2004). From Zhu et al results (2011), it can be concluded that the molecular adsorption of phenol on MCl was exothermic and that the anion exchange of phenolate by MCl was endothermic (Zhu et al., 2011).

Figure 4.4e shows the EC values in the outlet stream of the IE process as a function of contact time for the three studied temperatures. As aforementioned, the equilibrium was obtained in about 30 min and from this point EC was well below 0.03 mS/cm for all cases.

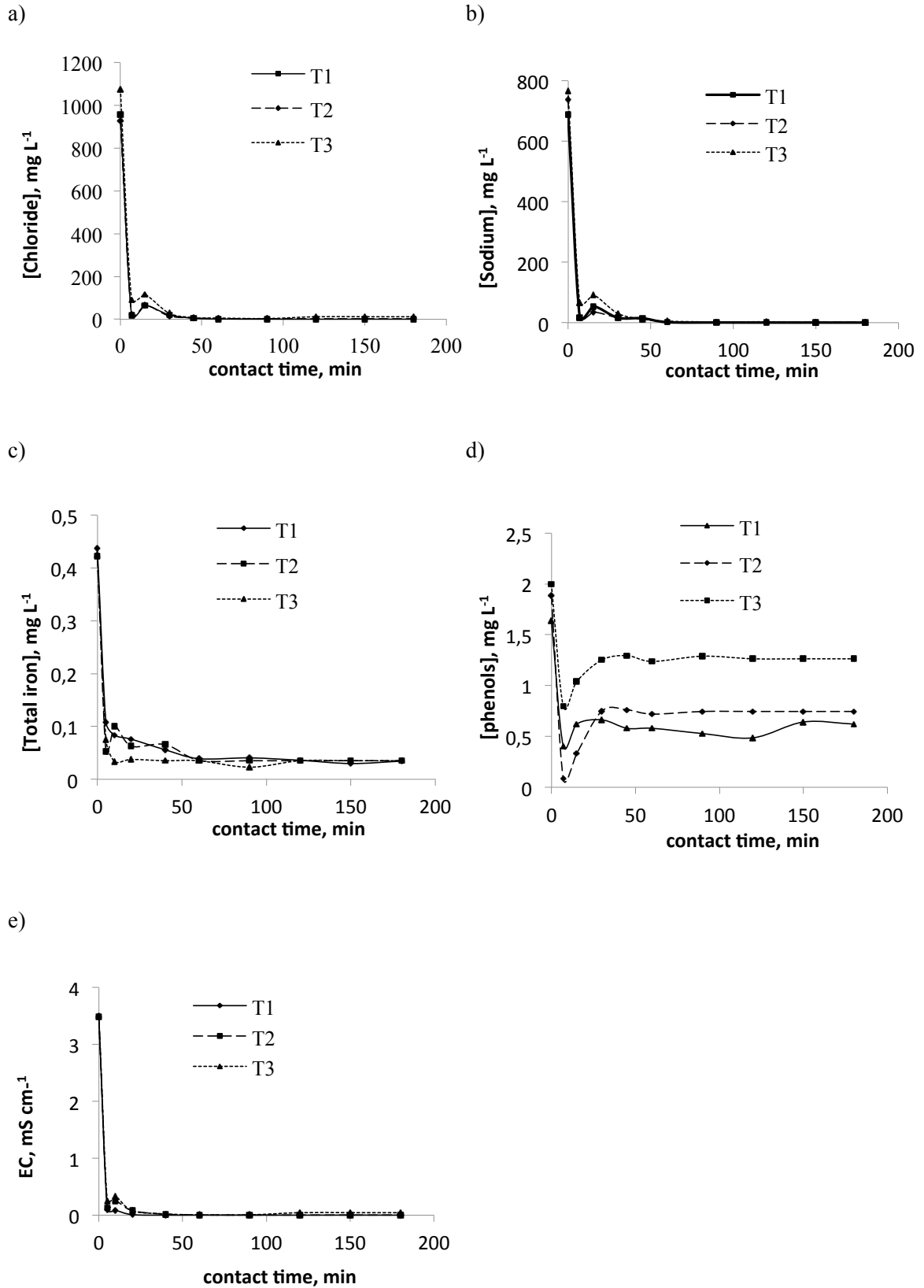
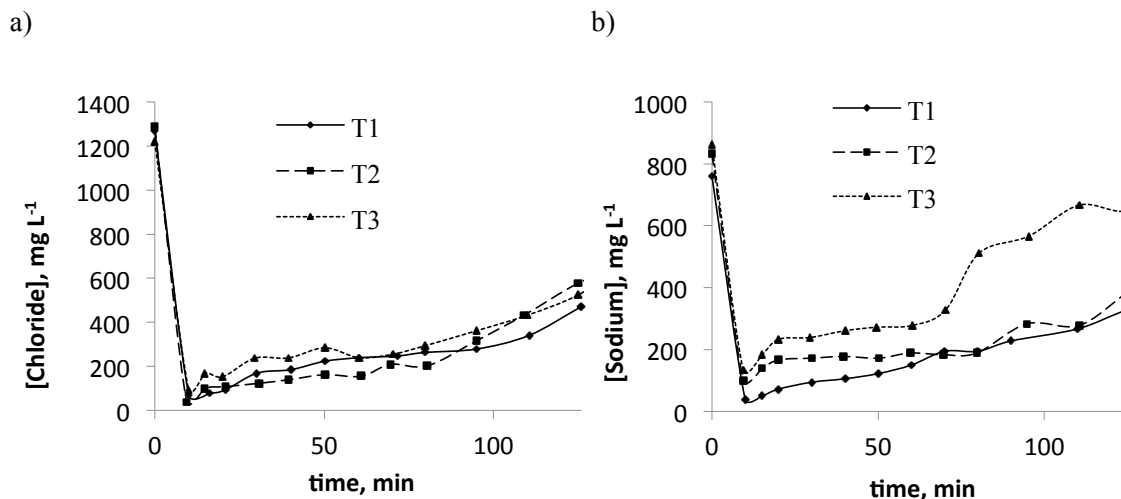


Figure 4.4. Effect of temperature (T1: 298 K; T2: 308 K; T3: 318 K) on chloride, sodium, total iron, and total phenols concentrations, and electric conductivity (EC) at the outlet of batch IE system.

The results confirmed that IE reduced efficiently the EC and the content of phenols (roughly 65 % phenols removal efficiency), which have molecular weights in the range 0.5-2 kDa and thus are in the same range as the membrane’s molecular weight cut off (MWCO). This fact is especially relevant for further scheduled membranes operations, as according to the pore blocking model, particles of certain size are prone to cause fouling on the membranes, which are those having a size (d_p) within the range of the mean pore diameter of the membrane (D_p). As a rule of thumb, blocking may statistically be significant when $0.1 < d_p/D_p < 10$ (Marco and Chianese, 2007; Stoller, 2009; Stoller, 2001). Therefore, pore blocking and plugging of NF and RO membranes by phenolic molecules would be certainly avoided and fouling probability reduced through the IE pretreatment.

4.3.3.2 Continuous experiments

The effect of temperature on the concentration of monovalent ions (chloride and sodium) as well as total iron and phenols was additionally investigated on a continuous operation mode (Figure 4.5a-d). Assays were carried out in the same conditions than the batch-run experiments and were conducted for 125 min operation time (about 21 L simulating OMWST). Figure 4.4b,d confirm that the best results for adsorption of sodium and phenols were obtained at the lowest studied temperature (298 K). Moreover, when experiments were carried out at the highest temperature (318 K) IE of these species was revealed as the most inefficient. However, chloride and total iron concentration in the outlet stream was not significantly affected by temperature (Figure 4.4a,c).



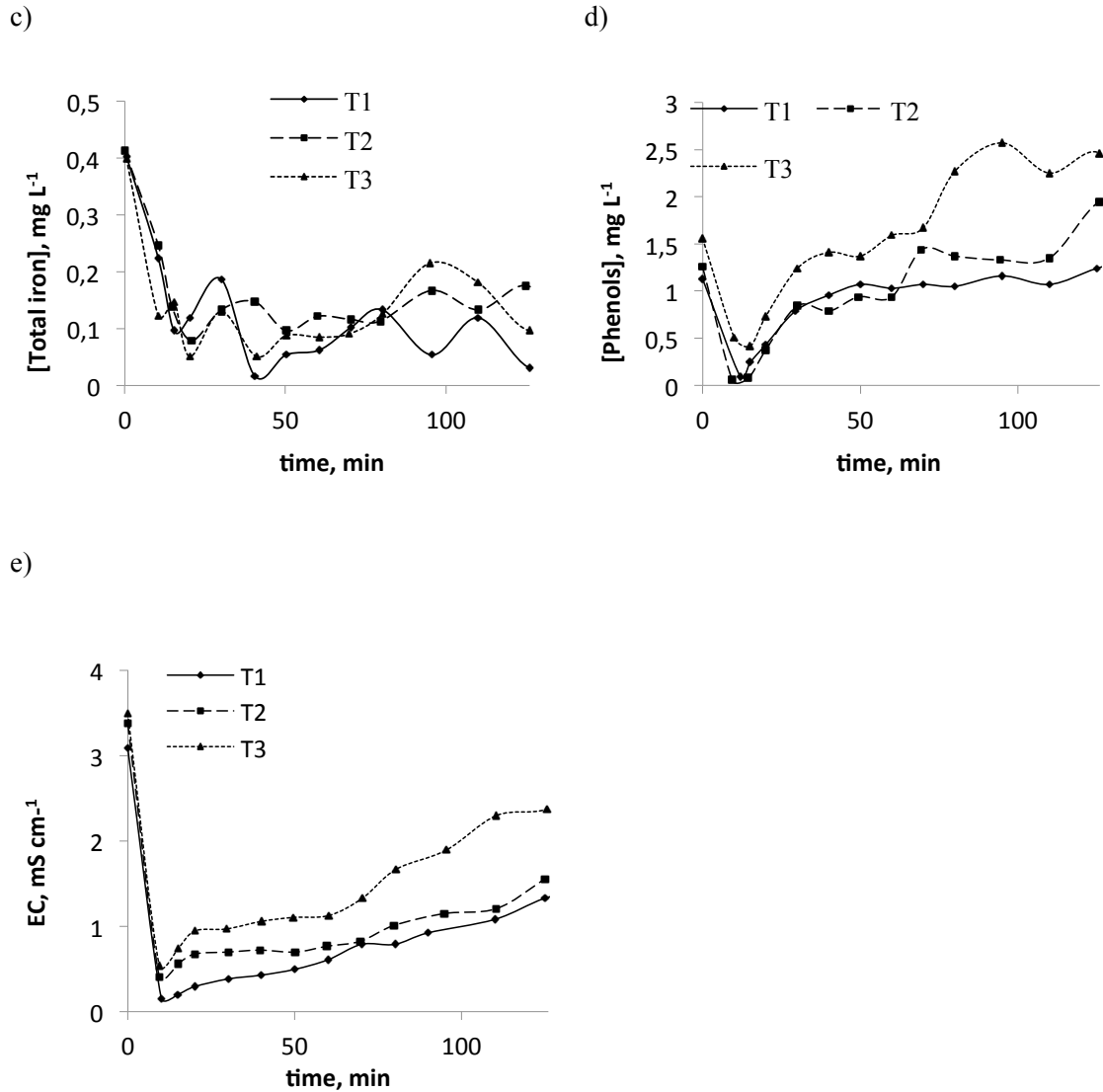


Figure 4.5. Effect of temperature (T1: 298 K; T2: 308 K; T3: 318 K) on chloride, sodium, total iron, and total phenols concentrations, and electric conductivity (EC) at the outlet of continuous IE system.

In the first IE treatment hour, the removal efficiencies of monovalent ions, such sodium and chloride, were around 80 % and 90 %, respectively, at the optimal temperature (298 K). Iron removal efficiency was higher than 60 % throughout all the experiments disregarding the operating temperature. However, phenols removal efficiency was over 50 % in the first 30 min of treatment and then decreased rapidly.

Figure 4.4e represents the effect of temperature on the EC value in the outlet stream. When experiments were carried out at 298 K, EC in the outlet stream was the lowest through the whole experiment. However, EC in the outlet stream was the maximum one upon assays conducted at the highest temperature (318 K). Regarding these results, EC reduction in the

outlet stream decreased with increasing temperature. At the end of experiments, EC was around 1.33 mS cm^{-1} , 1.55 mS cm^{-1} and 2.37 mS cm^{-1} in case of experiments at 298 K, 308 K and 318 K, respectively.

The effect of temperature on contaminant removal by anion exchange resin and cation exchange resin provides the opportunity to further discuss the removal mechanism. For example, the different behaviours of phenol, sodium, and EC in batch and continuous experiments may be due to different removal mechanisms and/or interactions between contaminants and resin.

Results on continuous IE operation mode verify the patterns observed for the studied species in the batch-run experiments. The average removal efficiencies provided by the proposed IE system (50 - 80 %) will help reduce concentration polarization and fouling issues on ulterior membrane processes. The lower concentration of ionic species reduces the shielding of the Donnan-effect and thus the polarization resistance would be minimized (Bartels et al., 2005). This is especially significant in the case of sodium and chloride ions, remaining in OMWST at high level, as well as iron ions, which present major shielding effect on the electronegativity of the membrane due to their highly positive charge. Minor approach of foulants to the active layer of the membrane as the repulsion force increases is expected to be relevant for minimization of further fouling development on the membrane surface. Furthermore, reduction of pore blockage and plugging as well as abrasive deleterious fouling phenomena by iron colloidal particles would be ensured (Stoller, 2011; Zhu and Elimelech, 1997; Yiantsios and Karabelas, 2002).

4.3.4 Regeneration and industrial application

Virgin anion and cation exchange resins were regenerated before their initial use to become fresh resin. The impact of the regeneration procedure on the efficiency of ions removal by Dowex Marathon C and Amberlite IRA-67 resins were investigated. Over the course of four regeneration cycles, the loss in efficiency in removing ions did not exceed 5%. This fact is useful from a practical point of view, since water treatment plants cannot use only fresh resins. Therefore, in all experiments of this work the same resins have been used, and a regeneration cycle between an experiment and other has been conducted.

In previous studies, Martínez Nieto et al. (2010) and Hodaifa et al. (2013) have designed and installed an industrial plant for treating olive oil mill wastewaters by chemical oxidation (Fenton reaction); the plant consists of the following operating units: (i) pretreatment of OMW, (ii) advanced oxidation treatment based on Fenton's reagent, (iii) followed by flocculation-sedimentation and (iv) olive stones filtration (Hodaifa et al., 2013 and Martínez Nieto et al., 2010).

In this scenario, additionally to the operations units already included in the industrial plant, our idea is to include two more operating units: (v) an intermediate operation unit consisting in ion exchange to reduce the salinity and a (vi) final operation unit consisting in NF or RO, depending on the final usage of the treated water: irrigation or reutilization in the process, respectively. It is Also worth indicating that the volumes produced by the regeneration of the resins and rejections of the last unit can be recycled to the reactor where organic matter oxidation is carried out.

4.4 Conclusions

To the author’s knowledge, no former studies focusing on IE treatment of olive oil industry effluents (OMW) are available in the scientific literature. In the present research work, IE is presented as an efficient membrane pretreatment for reducing membrane fouling in the purification of OMW. It has been shown that Dowex Marathon C and Amberlite IRA-67 resins reduce the residual concentration of chloride, sodium, total iron and phenols, which are the major pollutants in this previously treated OMW, to limits which are not harmful for the performance of an ulterior membrane system.

Results confirm that using the cation exchange resin followed by the anion exchange one gave better results than in the opposite order. This effect was highly pronounced in sodium and chloride removal. In batch experiments, the results showed that concentrations of all species were considerably reduced with increasing contact time. In addition, the equilibrium was obtained in about 30 min and from this point on removal efficiencies were above 90 % and conductivity was lower than 0.03 mS/cm. Sodium, chloride and total iron adsorption was not significantly affected by operating temperature. Otherwise, phenols removal was affected by this variable. In this case, the best results were obtained at the lowest operating temperature (298 K). In continuous IE process, the removal efficiencies of monovalent ions, such as sodium and chloride, were around 80% and 90%, respectively, at the optimal temperature (298 K) up to the first IE treatment hour. At that temperature, iron removal efficiency was higher than 60 % throughout the experiments. However, phenols removal efficiency was well above 50 % within the first 30 min of treatment and then rapidly decreased. In both operating modes, conductivity reduction in the outlet stream decreased as well with increasing temperature.

The obtained results are highly relevant since operating temperature is a key variable from a technical-economical point of view. In this regard, the examined resins work highly efficiently at ambient temperature conditions, hence giving a sensible economical boost to the IE process. All these with the final aim to recycle the regenerated OMW effluent to the olive oil production process and close the loop.

4.5 References

- Apell, J.N., Boyer, T.H. (2010). Combined ion exchange treatment for removal of dissolved organic matter and hardness. *Water Research*, 44:2419-2430.
- Bartels, C., Franks, R., Rybar, S., Schierach, M., Wilf, M. (2005). The effect of feed ionic strength on salt passage through reverse osmosis membranes. *Desalination*, 184:185-195.
- Bódalo, A., Gómez, J.L., Gómez, E., Máximo, F., Hidalgo A.M. (2003). Application of reverse osmosis to reduce pollutants present in industrial wastewater. *Desalination*, 155:101-108.
- Bolto, B., Dixon, D. (2004) Ion exchange for the removal of natural organic matter. *Reactive & Functional Polymer*, 60:171-182.
- Borsani, R., Ferrando, B. (1996). Ultrafiltration plant for olive vegetationwaters by polymeric membrane batteries. *Desalination*, 108:281–286.
- Canepa, P., Marignetti, N., Rognoni, U., Calgari, S. (1988). Olive mills wastewater treatment by combined membrane processes. *Water Res.*, 22(12):1491–1494.
- Carmona, M., De Lucas, A., Valverde, J.L., Velasco, B., Rodríguez, J.F. (2006). Combined adsorption and ion exchange equilibrium of phenol on Amberlite IRA-420. *Chemical Engineering Journal*, 117:155-160.
- Clifford, D., Weber, Jr., Walter, J. (1983). The determinants of divalent/monovalent selectivity in anion exchangers. *Reactive Polymers, Ion Exchangers, Sorbents*, 1:77-89.
- Dabrowski, A., Hubicki, Z., Podkoscielny, P., Robens, E. (2004). Review: Selective removal of the heavy metal ions from waters and industrial wastewaters by ion-exchange method. *Chemosphere*, 56:91-106.
- Danellakisa, D., Ntaikoub, I., Kornarosb, M., Dailianis, S. (2011). Olive oil mill wastewater toxicity in the marine environment: Alterations of stress indices in tissues of mussel *Mytilus galloprovincialis*. *Aquatic Toxicology*, 101:358-366.
- Demirbas, A., Pehlivan, E., Gode, F., Altun, T., Arslan, G. (2005). Adsorption of Cu(II), Zn(II), Ni(II), Pb (II) and Cd(II) from aqueous solution on Amberlite IR-120 synthetic resin. *J. of Colloid and Interface Science*, 282:20-25.
- van Deventer, J. (2011). Selected Ion Exchange Applications in the Hydrometallurgical Industry. *Solvent Extraction and Ion Exchange*, 29:695-718.

Erdem, E., Colgecen, G., Donat, R. (2005). The removal of textile dyes by diatomite earth. *J. Colloid Interface Sci.*, 282:314-319.

Fu, F., Wang, Q. (2011). Removal of heavy metal ions from wastewaters: A review. *Journal of Environmental Management*, 92:407-418.

Garrido Hoyos, S.E., Martínez Nieto, L., Camacho Rubio, F., Ramos Cormenzana, A. (2002). Kinetics of aerobic treatment of olive mill wastewater (OMW) with *Aspergillus terreus*. *Process Biochemistry*, 37(10):1169–1176.

Gode, F., Pehlivan, E. (2006). Removal of chromium (III) from aqueous solutions using Lewatit S 100: the effect of pH, time, metal concentration and temperature. *J. Hazard. Mater.*, 136:330-337.

Greenberg, A.E., Clesceri, L.S., Eaton, A.D. (1992). Standard Methods for the Examination of Water and Wastewater, APHA/AWWA/WEF, 16th ed., Washington DC. Cabs.

Hodaifa, G., Ochando-Pulido, J.M., Rodriguez-Vives, S., Martinez-Ferez, A. (2013a). Optimization of continuous reactor at pilot scale for olive-oil mill wastewater treatment by Fenton-like process. *Chem. Eng. J.*, 220:117-124.

Hodaifa, G., Ochando-Pulido, J.M., Ben-Driss-Alami, S., Rodriguez-Vives, S., Martinez-Ferez, A. (2013b). Kinetic and thermodynamic parameters of iron adsorption onto olive stones. *Ind. Crops Prod.*, 49:526-534.

Ku, Y., Lee, K., Wang, W. (2004). Removal of phenols form aqueous solutions by purolite A-510 resin. *Sep. Sci. Technol.*, 39:911–923.

López, J., Coello, M.D., Quiroga J.M. (2006) Comparative studies of reverse osmosis membranes for wastewater reclamation. *Desalination*, 191:137-147.

Ochando-Pulido, J.M., Rodriguez-Vives, S., Martinez-Ferez, A. (2012a). The effect of permeate recirculation on the depuration of pretreated olive mill wastewater through reverse osmosis membranes. *Desalination*, 286:145-154.

Ochando-Pulido, J.M., Stoller, M., Bravi, M., Martinez-Ferez, A., Chianese, A. (2012b). Batch membrane treatment of olive vegetation wastewater from two-phase olive oil production process by threshold flux based methods. *Sep. Purif. Technol.*, 101:34-41.

Ochando-Pulido, J.M., Hodaifa, G., Martinez-Ferez, A. (2012c). Fouling inhibition upon Fenton-like oxidation pretreatment for olive mill wastewater reclamation by membrane process. *Chemical Engineering and Processing*, 62:89– 98.

Ochando-Pulido, J.M., Hodaifa, G., Victor-Ortega, M.D., Martinez-Ferez, A. (2013a). Reuse of olive mill effluents from two-phase extraction process by integrated advanced oxidation and reverse osmosis treatment. *J. Hazard. Mater.*, 263:158-167.

Ochando-Pulido, J.M., Hodaifa, G., Victor-Ortega, M.D., Martinez-Ferez, A. (2013b). Effective treatment of olive mill effluents from two-phase and three-phase extraction processes by batch membranes in series operation upon threshold conditions. *J. Hazard. Mater.*, 263:168-176.

Martínez Nieto, L., Hodaifa, G., Rodríguez Vives, S., Giménez Casares, J.A., Ochando J. (2011a). Degradation of organic matter in olive oil mill wastewater through homogeneous Fenton-like reaction. *Chem. Eng. J.*, 173(2):503–510.

Martínez Nieto, L., Hodaifa, G., Rodríguez Vives, S., Giménez Casares, J.A., Ochando, J. (2011b). Flocculation–sedimentation combined with chemical oxidation process. *Clean - Soil, Air and Water*, 39(10):949–955.

Martínez Nieto, L., Ben Driss Alami, S., Hodaifa, G., Faur, C., Rodríguez Vives, S., Giménez Casares, J.A., Ochando, J. (2012). Adsorption of iron on crude olive stones. *Ind. Crops Prod.*, 32:467–471.

Mathur, J.N., Khopkar, P.K. (1985). Ion exchange behaviour of chelating resin dowex a-1 with actinides and lanthanides. *Solvent Extr. Ion Exch.*, 3:753-762.

Metcalf, Eddy, *Wastewater engineering: treatment and reuse* (4th internal edition ed.). New York: McGraw-Hill, 2003.

Mustafa, S., Bashir, H., Rehana, N., Naeem, A. (1997). Selectivity reversal and dimerization of chromate in the exchanger Amberlite IRA-400. *React. Funct. Polym.*, 34:135–144.

Roostaei, N., Tezel, F.H. (2004). Removal of phenol from aqueous solutions by adsorption, *J. Environ. Manag.*, 70:157–164.

Shaha, B., Iglesias, M., Cumming, I.W., Streat, M. (2000). Sorption of trace heavy metals by thiol containing chelating resins. *Solvent Extr. Ion Exch.*, 18:133-167.

Su-Hsia, L., Ruey-Shin, J. (2009). Adsorption of phenol and its derivatives from water using synthetic resins and low-cost natural adsorbents: A review. *Journal of Environmental Management*, 90:1336-1349.

Stoller, M., Chianese, A. (2006). Optimization of membrane batch processes by means of the critical flux theory. *Desalination*, 191:62–70.

Stoller, M., Chianese, A. (2007). Influence of the adopted pretreatment process on the critical flux value of batch membrane processes. *Ind. Eng. Chem. Res.*, 46:2249-2253.

Stoller, M. (2009). On the effect of flocculation as pretreatment process and particle size distribution for membrane fouling reduction. *Desalination*, 240:209-217.

Stoller, M. (2011). Effective fouling inhibition by critical flux based optimization methods on a NF membrane module for olive mill wastewater treatment. *Chemical Engineering Journal*, 168:1140–1148.

Turano, E., Curcio, S., De Paola, M.G., Calabrò, V., Iorio, G. (2002). An integrated centrifugation– ultrafiltration system in the treatment of olive mill wastewater. *J. Membr. Sci.*, 206:519–531.

Xingcun, H., Yimin, J. (1997). Adsorption of gold by NKA-9 resin and its mechanism. *Precious metals*, 18:35.

Yiantsios, S.G., Karabelas, A.J. (2002). An assessment of the Silt Density Index based on RO performance colloidal fouling experiments with iron oxide particles. *Desalination*, 151:229-238.

Zhu, X., Elimelech, M. (1997) Colloidal fouling of reverse osmosis membranes: measurements and fouling mechanisms. *Environmental Science & Technology*, 31:3654-3662.

Zhu, L., Deng, Y., Zhang, J., Chen, J. (2011). Adsorption of phenol from water by N butylimidazolium functionalized strongly basic anion exchange resin. *Journal of Colloidal and Interface Science*, 364:462-468.

CHAPTER 5

FINAL PURIFICATION OF SYNTHETIC OLIVE OIL MILL WASTEWATER TREATED BY CHEMICAL OXIDATION USING ION EXCHANGE: STUDY OF OPERATING PARAMETERS

M.D. Víctor-Ortega^{1*}, J.M. Ochando-Pulido¹, G. Hodaifa², A. Martínez-Ferez¹

¹ Chemical Engineering Department, University of Granada, 18071 Granada, Spain

*email: mdvictor@ugr.es

² Molecular Biology and Biochemical Engineering Department, University Pablo de Olavide, 41013 Seville, Spain

Chemical Engineering and Processing: Process Intensification

Publisher: ELSEVIER SCIENCE SA. PO BOX 564, 1001 LAUSANNE, SWITZERLAND

Volume 85. Pages 241-247.

Year: 2014

ISSN: 0255-2701

DOI: <http://dx.doi.org/10.1016/j.cep.2014.10.002>

Impact factor: 2.071

Tertile: Second



Abstract

In this research work, ion exchange (IE) is presented as a suitable option for purification of olive oil mill wastewater (OMW) previously treated by means of a secondary treatment (OMWST). This pretreatment consisted in Fenton-like oxidation process, followed by coagulation–flocculation and filtration through olive stones. The parametric requirements for drinking water production or at least for public waterways discharge were achieved using a combination of two IE columns working in series at bench scale. The IE resins used in this study were Dowex Marathon C and Amberlite IRA-67. The effect of contact time, operating temperature and flow rate on simultaneous removal of sodium, total iron, chloride and phenols (the major pollutant species in OMWST) were investigated. Removal percentages of sodium, chloride and total iron increased with incrementing the contact time. Equilibrium was obtained in about 30 minutes for all ions and ion concentrations values determined were lower than the maximum levels for drinking water standards. On the other hand, adsorption efficiencies of sodium, total iron and chloride ions were found to be not considerably affected by the operating temperature. The highest phenols removal percentage (around 100%) was obtained in the first minutes for 298 K and 10 L/h.

Keywords: Ion exchange; Olive oil mill wastewater; Drinking Water Directive; Simultaneous ions removal; Industrial waters cycles; Water recovery.

5.1 Introduction

Olive oil mill wastewater (OMW) generated by the olive oil production process is the main effluent of this industry. OMW derives from olives washing wastewater (OWW) and olive vegetation wastewater (OVW). Around $1.8 \cdot 10^6$ t of olive oil are produced annually worldwide and the Mediterranean countries are the major producers. For this reason, OMW represents a serious environmental problem in the Mediterranean basin and concretely in the southern European countries (Gomec et al., 2007). The amount of this effluent and its physicochemical properties are influenced by several factors such as the variety of the olives, the meteorological conditions and the extraction process (Martins and Quinta-Ferreira, 2011).

In the two-phase-based system the volume of OVW yielded (OVW-2) is reduced by one third as water injection is used only in the final vertical centrifugation step. Most of the organic matter stays in the solid waste (“alpeorujo”). This waste contains more humidity than its equivalent from the three-phase system (60% in two-phase systems vs. 45% in three-phase ones, OVW-3) and therefore OVW-2 presents lower pollutants load (Hermoso et al., 1998). In this work, the problem related to the reclamation of OVW-2 effluent was investigated.

In particular, what most characterizes this effluent is an acid pH value, black colour, very high chemical oxygen demand (COD) and high concentration of recalcitrant organic matter, such as phenolic compounds and tannins (Hodaifa et al., 2008). This is one of the highest organic loads of known concentrated effluents, which is 100–150 times higher than that of domestic wastewater. On the other hand, inorganic compounds such as chloride, sulfate and phosphoric salts of potassium, calcium, iron, magnesium, sodium, copper and traces of other elements are usually present in OMW (Garrido Hoyos et al., 2002).

The low pH of this wastewater, as well as the presence of phytotoxic and antimicrobial compounds and toxic fatty acids, makes it difficult to directly reuse this wastewater. Accordingly, the treatment of OMW is a very crucial need for environmental protection and has been studied by several methods such as composting, evaporation ponds, thermal, physicochemical and biological treatments, land spreading and membranes filtration (Achak et al., 2009; Ammary, 2005; Sarika et al., 2005; Martínez Nieto et al., 2011a; Beltrán de Heredia and García, 2005; Papastefanakis et al., 2010; Tezcan et al., 2008; Grafias et al., 2010; Lafi et al., 2009; Khoufi et al., 2006; Ochando-Pulido et al., 2012).

In previous research works, OMW from two-phase continuous centrifugation process was treated at a pilot scale by an advanced chemical oxidation process based on Fenton's reagent followed by a flocculation step and filtration in series through three different kinds of filtering materials (Martínez Nieto et al., 2010; Martínez Nieto et al., 2011b). This depuration sequence achieved a large reduction of phenolic compounds, COD and suspended solids. Nevertheless, after this treatment OMW presented a significant concentration of dissolved monovalent and divalent ions, which cannot be removed by conventional physicochemical treatments.

The IE process comprises the interchange of ions between a solution and an insoluble solid, i.e., polymeric or mineral ion exchangers such as IE resins (functionalized porous or gel polymer), natural or synthetic zeolites, montmorillonite, clay, etc. In a wastewater treatment system undesirable ions in water supply are replaced with innocuous ions. Water decontamination consists of removal of ionic pollutants such as phosphate, chloride, nitrate, ammonia, which appear in various types of agricultural, domestic and industrial wastewaters, or heavy metals discharged in effluent from electroplating plants, metal finishing operations, as well as a number of mining and electronics industries (Bochenek et al., 2011). Physicochemical methods of water purification such as chemical reactions, electro-flotation, reverse osmosis and adsorption may be under given conditions more effective than IE technology. However, the latter process is considered very attractive because of the relative simplicity of application and in many cases it has been proven to be an economic and effective technique to remove ions from wastewaters, particularly from diluted solutions (Pintar et al., 2001; Valverde et al., 2006). The use of IE

technique depends on various factors such as temperature, pH, flow rate, contact time, initial pollutant concentration and adsorbent characteristics (Caetano et al., 2009).

There are many studies on the adsorption of metal ions on IE resins, which have been reported in literature. Several studies of selective removal of heavy metal ions by IE which include removal of Pb(II), Hg(II), Cd(II), Ni(II), V(IV,V), Cr(III,VI), Cu(II) and Zn(II) from water and industrial wastewaters have been carried out in the last years (Shaha et al., 2000; Fu and Wang, 2011; Dabrowski et al., 2004; Gode and Pehlivan, 2006). Otherwise, there are many reports on the use of IE in hydrometallurgical applications for the recovery or purification of metal solutions or for effluent treatment, including the primary recovery of gold, uranium and rhenium, and the purification of cobalt electrolyte to ensure high-purity metal (van Deventer, 2011).

IE resins have also found an increasing application in the drinking water treatment sector over the last few decades, especially when there is a high concentration of natural organic matter (NOM) in the contaminated water, since high percentages on the removal efficiency of NOM by IE process are found (Eilers, 2008). Phenolic compounds can also be successfully removed from wastewaters by IE technology (Su-Hsia and Ruey-Shin, 2009; Zhu et al., 2011; Roostaei and Tezel, 2004; Ku et al., 2004). In case of phenols, Michelle Caetano et al. (Caetano et al., 2009) evaluated a strong anion exchange resin (Dowex XZ), a weak anion exchange (AuRIX 100) and non-functionalized resin (Macronet MN200) to remove phenol from aqueous solution.

In this sense, selective resins can reduce the residual concentration of sodium, total iron, chloride and phenols below the maximum standard limits established by the Drinking Water Directive. Council Directive 98/83/EC set the maximum concentration in drinking water at 200 $\mu\text{g L}^{-1}$ for iron, 200 mg L^{-1} for sodium and 250 mg L^{-1} for chloride (European Commission, 1998). On the other hand, it is important to avoid phenols presence as much as possible as it is phytotoxic and recalcitrant to biological degradation.

To the best of our knowledge, there are no previous studies in literature reported on the use of IE technology for drinking water production from OMW. In this research study, IE is presented as an efficient alternative for purification of OMW previously treated by means of the secondary treatment above described (OMWST), where iron, sodium, chloride and phenols are the major pollutants.

With the idea of achieving the parametric requirements for drinking water production or at least public waterways discharge, and close the loop or zero-discharge in olive-oil extraction plant, a bench scale study was undertaken to evaluate the performance of a combination of two IE

columns working in serial connection for the purification of OMWST. The aim of this work consists in investigating simultaneous removal of sodium, total iron, chloride and phenol species from synthetic water simulating OMWST using Dowex Marathon C and Amberlite IRA-67 resins. With this purpose, study the influence of several factors such as contact time, operating temperature and flow rate was carried out in a semi-batch IE system.

5.2 Materials and methods

5.2.1 Model water solutions

All experiments were carried out using model water simulating pretreated OMWST prepared by dissolving reagent-grade sodium chloride, iron (III) chloride 30 % (w/w) aqueous solution and phenol (all of them provided by Panreac) in double distilled water. Model water solutions were prepared prior to the start of the experiments, stored at 4 °C and brought to room temperature before being used.

The physicochemical composition of the OMWST effluent is reported in Table 5.1 (Martínez Nieto et al., 2011b; Hodaifa et al., 2013). The desired concentrations for chloride and sodium were fixed at the highest values registered on average at the outlet of the OMW secondary treatment: approximately 1045 mg/L and 730 mg/L, respectively, whereas about 1 mg/L and 0.4 mg/L for phenol and total iron.

Table 5.1. Physicochemical analysis of OMW determined after secondary treatment (OMWST) (Martínez Nieto et al., 2011b; Hodaifa et al., 2013).

Physicochemical properties	Parametric value
pH	7.78 - 8.17
Conductivity, mS cm⁻¹	3.15 - 3.55
COD, mg L⁻¹	121 - 227
Total phenols, mg L⁻¹	0.39 - 0.98
[Fe] Total, mg L⁻¹	0.04 - 0.4
[Cl], mg L⁻¹	876 - 1045
[Na⁺], mg L⁻¹	534 - 729

5.2.2 Ion Exchange system

Strong-acid cation exchange Dowex Marathon C and weak-base anion exchange Amberlite IRA-67 resins, both provided by Sigma Aldrich, were used in this study. Their properties and specifications as reported by the suppliers are shown in Table 5.2. Dowex Marathon C is generally used for softening and demineralization applications. Otherwise, Amberlite IRA-67 is widely used for industrial water treatment systems as well as pharmaceutical, chemical and food processing industries.

A bench-scale IE equipment was used to evaluate the performance of a combination of two IE columns operating in serial connection for the purification of OMWST. IE columns employed in this study were made of an acrylic tube of 540 mm height x 46 mm internal diameter. The columns are provided with a mobile upper retaining grid, which could be fixed in the column to adjust it as a fixed bed or a semi-fluidized bed. The IE device (MionTec) was equipped with a peristaltic pump (Ecoline VC-380) and a temperature-controlled thermostatic bath (Precisterm JP Selecta). The IE unit used in this work is shown in Figure 5.1.

Table 5.2. Properties of Dowex Marathon C and Amberlite IRA-67 IE resins.

Properties	Dowex Marathon C	Amberlite IRA-67
Type	Strong-acid cation	Weak-base anion
Matrix	Styrene-DVB, gel	Tertiary amine
Ionic form as shipped	H ⁺	OH ⁻
Particle size	0.55-0.65 mm	0.5-0.75 mm
Effective pH range	0-14	0-7
Total exchange capacity	1.80 eq L ⁻¹	1.60 eq L ⁻¹
Shipping weight	800 g L ⁻¹	700 g L ⁻¹

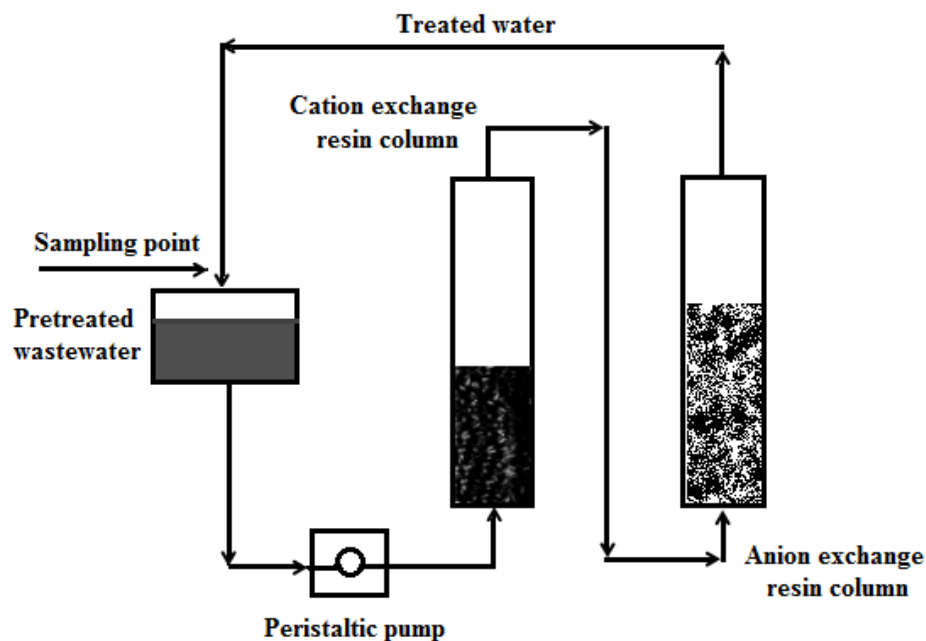


Figure 5.1. Flow-sheet scheme for complete IE recirculation operating cycle.

5.2.3 IE resins conditioning and regeneration

IE columns were pre-conditioned before the first use as follows: 400 mL MilliQ[®] water were pumped into each column in upflow mode, leaving the top of the columns uncovered to avoid creating vacuum. After that, each resin was introduced from the top of the corresponding column (346 g in case of Dowex Marathon C and 350 g Amberlite IRA-67). Then, each resin was washed with MilliQ[®] water at 10 L/h in the beginning and then at 20 L/h to create bed fluidization and resin expansion along the column. Taking into account the shipping weight of each resin (800 g L⁻¹ for Dowex Marathon C whereas 720 g L⁻¹ for Amberlite IRA-67), the anionic resin bed expansion was higher than the cationic resin bed expansion. Both IE resins were washed with MilliQ[®] water until the resins dyes were removed completely.

After each operational cycle, the Dowex Marathon C cation exchange resin was fully washed with 2 % HCl aqueous solution. In a similar way, Amberlite IRA-67 anion exchange resin was washed with 4 % NaOH aqueous solution. Finally, the resins were washed with double distilled water to remove all excess of acid or base, respectively.

5.2.4 Recirculation mode IE experiments

In our previous studies, a secondary treatment was used to break down organic and inorganic compounds of OMW in the laboratory and on a pilot scale (Martínez Nieto et al., 2011b). The secondary treatment of OMW consists of an advanced chemical oxidation process based on

Fenton's reagent, followed by a flocculation step and filtration in series through three different kinds of filtrating materials, highlighting the profit of olive stones as a zero-cost filtration medium (Martínez Nieto et al., 2010).

IE experiments were performed in recirculation mode in semi-fluidized bed, operating in a closed loop system. In these experiments, the total sample volume of simulating OMWST solution and operation time used were fixed at 2 L and 180 min, respectively.

During IE performance experiments, OMWST feed stream was introduced at the bottom of the first column (cation exchange resin) in upflow mode, leaving this column by the top. Then, OMWST passed through the second column (anion exchange resin) also in upflow mode from the bottom to the top.

Pollutant ions concentrations were analyzed in the outlet stream at different contact time intervals throughout the whole experiments. On the other hand, the treated amount was monitored as a function of contact time by removing 50 mL aliquot of solution for the ions concentration measurements. The effect of contact time on the adsorption of the pollutants of interest by both resins was examined at 298 K and 10 L/h.

The effect of temperature and flow rate on the IE process performance were also studied by setting values equal to 298 K, 308 K and 318 K and 5 L h⁻¹, 10 L h⁻¹, 15 L h⁻¹ and 20 L h⁻¹, respectively.

Efficiencies of metal ions removal were calculated with the following equation:

$$\% \text{ Efficiency of metal removal} = \frac{C_0 - C}{C_0} \times 100$$

5.2.5 Analytical methods

Analytical grade reagents and chemicals with purity over 99 % were used for the analytical procedures.

For the measurement of the total iron concentration, all iron ions were reduced to iron ions (II) in a thioglycolate medium with a derivative of triazine, forming a reddish-purple complex that was determined photometrically at 565 nm (Standard German methods ISO 8466-1 and German DIN 38402 A51) (Greenberg et al., 1992).

For the measurement of the sodium concentration, a Crison GLP 31 Sodium Ion-Selective Electrode 96 50 was employed, with autocorrection of temperature. To calibrate the electrode, 0.01, 0.1 and 1.0 g/L Na⁺ standard solutions were prepared in the laboratory.

For the measurement of the chloride concentration, a Crison GLP 31 Chloride Ion-Selective Electrode 96 52 C was used, with autocorrection of temperature. Standard solutions (0.01, 0.1 and 1.0 g/L Cl⁻) required for the calibration of the electrode were also prepared in the laboratory.

Total phenols and phenol derivatives were analyzed by reaction with a derivative thiazol, giving a purple azo dye which was determined photometrically using a Helios Gamma UV-visible spectrophotometer (Thermo Fisher Scientific) at 475 nm (Standard German methods ISO 8466-1 and DIN 38402 A51) (Greenberg et al., 1992).

EC and pH measurements were assessed with a Crison GLP31 conductivity-meter and a Crison GLP21 pH-meter, provided with autocorrection of temperature. Buffer standard solutions for EC (1,413 μ S cm⁻¹ and 12.88 mS cm⁻¹) and pH (pH 4.01, 7.00 and 9.21) measurements respectively were supplied as well by Crison.

Finally, all analytical methods were applied at least in triplicate.

5.3 Results and Discussion

In this research work, simultaneous removal of iron, sodium, chloride and phenols on Dowex Marathon C and Amberlite IRA-67 resins was studied by using IE recirculation technique.

In our previous studies, the disposition of both resins in this semi-batch system was investigated. The results confirmed that using the cation exchange resin followed by the anion exchange one gave better results than in the opposite order (V́ctor-Ortega et al., 2014).

5.3.1 Effect of recirculation time

The impact of the recirculation time on the IE performance is shown in Figure 5.2. The results from Figure 5.2 show that removal percentages of all species removal were considerably increased with incrementing contact time. In addition, the equilibrium was obtained in about 30 min for sodium, chloride and total iron. From this point, sodium and chloride removal efficiencies were close to 100 % and total iron removal efficiency was higher than 90 %. Consequently, concentrations were lower than the maximum established levels throughout the whole experiments.

On the other hand, the highest percentage of phenols removal (around 100 %) was obtained in the first minutes of IE treatment (Figure 5.2). From 7 to 45 min operation, efficiency of phenols removal decreased, which can be explained due to the fact of phenols desorption. Cations are exchanged in the first column (Dowex Marathon C), thus at the end of this column pH drops approximately to values ranging 1.5-2.5 (H^+ species are released). In the second column (Amberlite IRA-67), anions are exchanged and pH progressively increases (OH^- species release). Phenol adsorption by Amberlite IRA-67 was favoured at low pH, since this resin is only active in the range of 0-7. Moreover, there was a competitive adsorption of phenols and chloride ions onto the anionic resin. The result was likely due to a higher adsorption affinity of chloride ions relative to phenol species. For this reasons, phenols removal was higher at the beginning of IE treatment and then decreased. Equilibrium was found after 45 min contact time and percentage of phenols removal exceeded 70%.

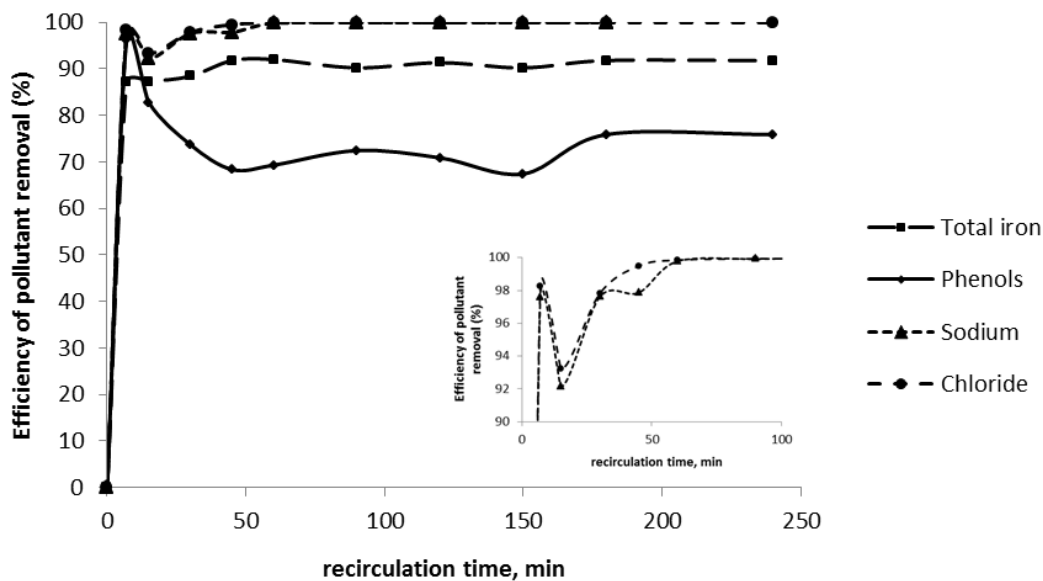


Figure 5.2. Effect of recirculation time on removal efficiency of ions (sodium, total iron, and chloride ions, and phenols removal). Operation conditions: 298 K, 10 L/h.

5.3.2 Effect of temperature

Sodium, total iron and chloride adsorption efficiencies were found to be not considerably affected by the operating temperature (Figure 5.3, Panels A, B and C). Furthermore, it was found that concentration of these pollutants was below the maximum standard levels established by the legislation for wastewater reuse throughout the whole IE experiments time (European

Commission, 1998). These results would have important implications in the cost-effectiveness of the final purification of OMWST by IE.

Analogously, Mustafa et al. (Mustafa et al., 1997) noted no significant effect of temperature on the removal efficiency of chromate ions from different solutions upon temperature variation in the range 293-313 K by employing the strongly basic anion exchanger Amberlite IRA-400 in the chloride form. These results contrast with those found by Demirbas et al. in their study of the effect of temperature on the adsorption of divalent metal ions (Cu II, Zn II, Ni II, Pb II and Cd II) onto Amberlite IR-120 resin (Demirbas et al., 2005). In the case of these divalent ionic species, the ratio of metal ion concentration on the resin to that in aqueous solution was very high for all metal ions and increased with temperature. This is due to the endothermic adsorption of divalent cations, which cause the equilibrium constants for this reaction to increase with temperature and thus the reaction products are favoured at high temperatures.

Otherwise, phenols removal was deeply affected by this variable (Figure 5.3, Panel D). In this case, the best results were obtained at the lowest operating temperature (298 K). At this temperature phenols removal efficiency was around 60 % when equilibrium was reached. However, when experiments were carried out at 318 K, adsorption of this pollutant was the most inefficient being the plateau value of the removal efficiency lower than 40 %. As it is mentioned before, the highest percentage of phenols removal (higher than 90 % at the optimal temperature) was obtained for the first minutes of IE treatment and then efficiency of phenols removal decreased, which can be owed to phenols desorption.

In case of phenolic species, Roostaei and Tezel (Roostaei and Tezel, 2004) proved that phenols adsorption capacity decreased with increasing temperature. The liquid-phase adsorption of phenols from water was studied by using silica gel, HiSiv 3000, activated alumina, activated carbon, Filtrasorb-400 and HiSiv 1000. In other studies, adsorption of molecular phenol species on N-butylimidazolium functionalized strongly basic anion exchange resin with Cl⁻ anion (MCl) was found to be exothermic under acidic pH conditions. Similar results were observed in some other studies, where phenols were adsorbed on Purolite A-510, NDA103 and IRA96C resins at acidic pH (Ku and Lee, 2004; Erdem et al., 2005). At an initial solution pH of 12.6, where phenolate species dominated, the removal efficiency increased with the rise in the temperature, indicating that phenols uptake was favored at higher temperatures at pH around 12.6. The adsorption of phenolate species on MCl was pointed to be endothermic under alkaline pH conditions. These results are in conflict with the work by Ku et al. (2004), who reported that the temperature did not affect the adsorption of phenolic species on Purolite A-510 resin (Ku et al., 2004). From Zhu et al. results (2011), it can be concluded that the molecular adsorption of

phenols on MCl was exothermic and that the anion exchange of phenolate by MCl was endothermic (Zhu et al., 2011).

It is worth highlighting that phenol molecule presents a pK_a value of 9.95, which implies that phenol is neutral in the pH range below 8.95. Thus in the current working conditions, phenol is in its neutral form and IE is probably not taking place. However, it has been observed that phenol is retained to a certain extension in the anionic resin, and the responsible mechanism of this retention could be adsorption/partition or size exclusion.

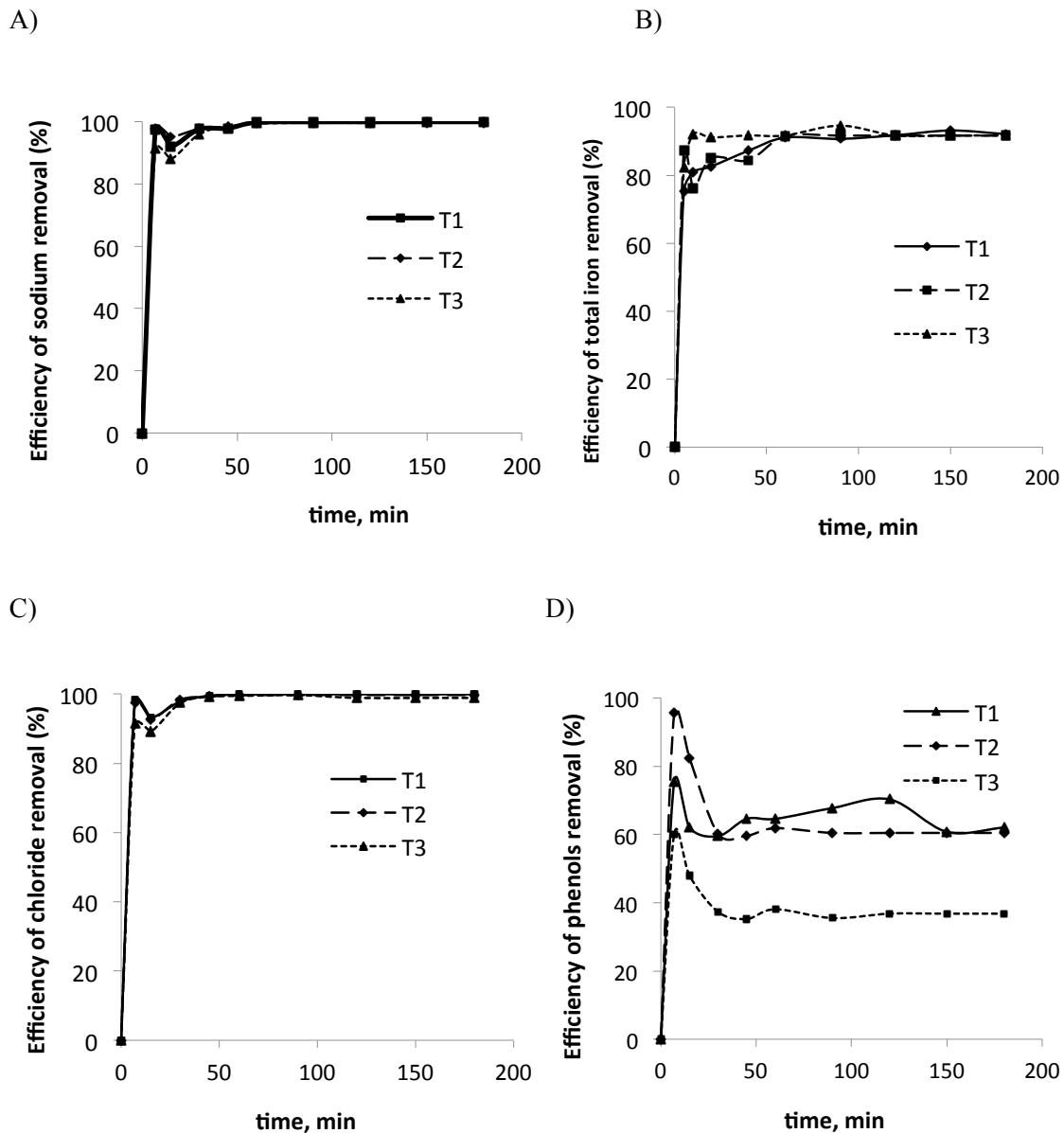


Figure 5.3. Effect of temperature on concentration of sodium (panel A), total iron (panel B), chloride (panel C) and phenols (panel D) in the outlet stream (T1: 298 K; T2: 308 K; T3: 318 K).

5.3.3 Effect of flow rate

No considerable differences were found for flow rates of 10 and 15 L/h for sodium and chloride adsorption and removal efficiency percentages around 100 % were observed for these ions (Figure 5.4 panels A and C). In case of total iron, during the first treatment minutes, certain differences were found between removal efficiencies at 10 L/h and the lowest at 5 L/h. However, these differences disappeared after 60 min of operation time. From this point, total iron removal efficiency was well above 90 % for the three studied flow rates. (Figure 5.4 panel B). Throughout the entire experiments, concentrations were lower than the maximum established levels.

The best results for adsorption of phenols were obtained at 10 L/h, which yielded phenols removal efficiency higher than 70 % at the end of the test. When experiments were carried out at 5 L/h and 15 L/h, phenols removal percentages were about 60 %. In addition, the required time to reach equilibrium decreased with increasing the flow rate.

Chen et al. (2002) found that at higher flow rate fixed, the waste does not have enough time to contact/react with the ion exchange resins (low residence times). On the other hand, too short flow rate is also not necessary. It is therefore worth pointing the existence of an optimum value of flow rate for the removal of each pollutant species. Despite of this fact, in the study by Chen et al. (2002) it can be observed that the effluent concentration curves are not much influenced by flow rate (Chen et al., 2002).

Hekmatzadeh et al. (2012) studied the effect of flow rate on nitrate adsorption by a nitrate selective anion exchange resin named IND NSSR (Hekmatzadeh et al., 2012). They concluded that the nitrate adsorption capacity was not very sensitive to variations in the flow velocity. This might signify that the rate of chemical reaction or selectivity and the sorption process were high and the assumption of local equilibrium was correct.

On the other hand, in the study carried out by Ostroski et al. (2009), flow rates in the range of 1–8 mL/min were investigated using NaY zeolite for exchange of Fe(III) and Zn(II) (Ostroski et al., 2009). In both systems it was observed a strong influence of the flow rate in the service time and in the saturation time of the column. Analyzing the results for the flow rates investigated, it could be concluded that 2 and 8 mL/min were the operational condition that minimize the mass transfer resistances for Fe(III) and Zn(II) uptake, respectively. This conclusion was based on the smallest values of mass-transfer zone (MTZ) for each cation obtained at these flow rates.

Fernández-Olmo et al. (2008) recommended low feed flow rate and high bath temperature (up to 55 °C) for high iron uptake (Fernández-Olmo et al., 2008).

Finally, Karadag et al. (2008) investigated the remediation of ammonium by using clinoptilolite (Karadag et al., 2008). They found that the highest saturation time was achieved in the case of the lowest flow rate. This was due to being driven of ammonium ions through the column before the complete exchange by clinoptilolite at higher flow rates.

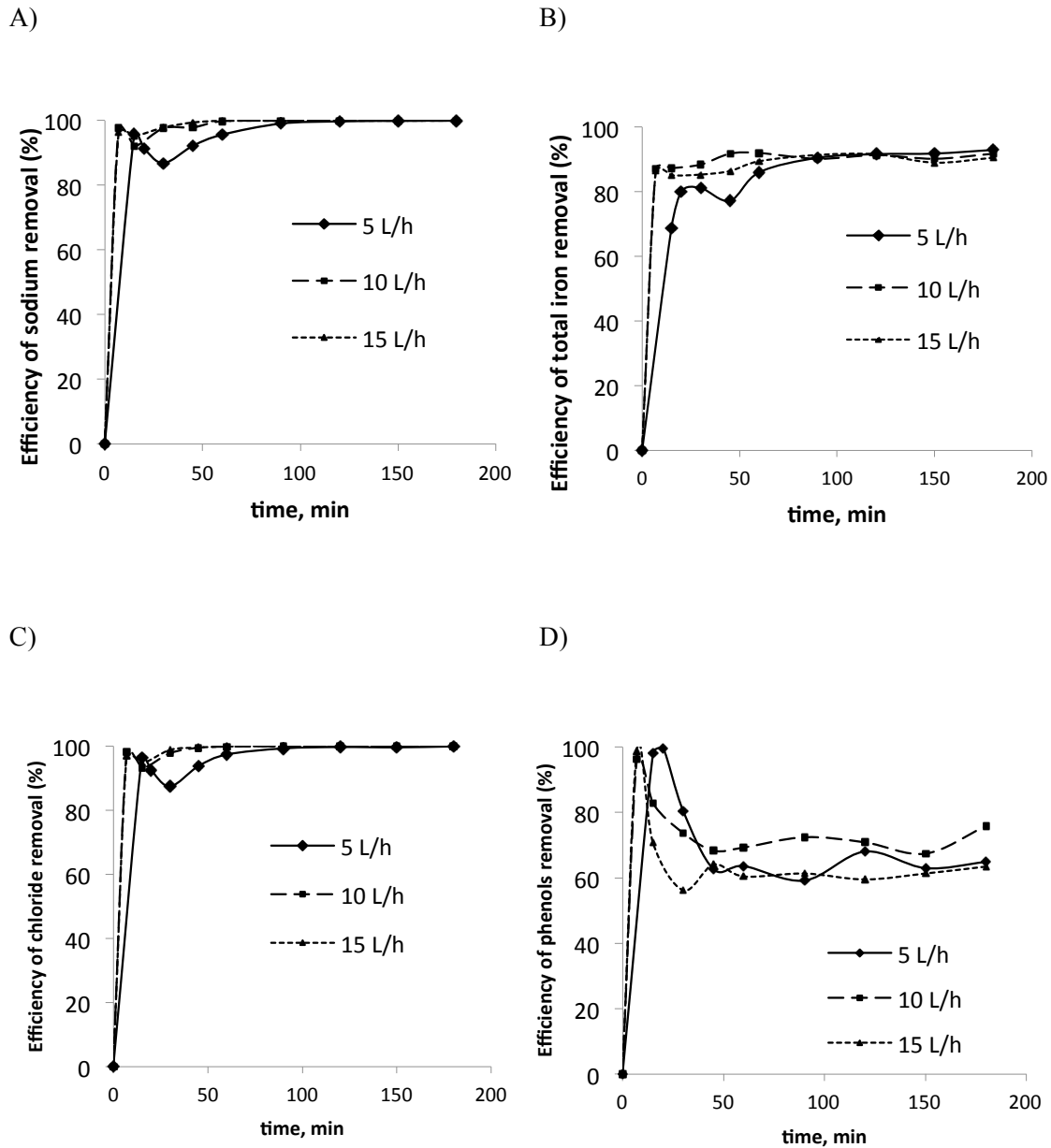


Figure 5.4. Effect of flow rate on removal efficiency of sodium (panel A), total iron (panel B), chloride (panel C) and phenols (panel D) in the outlet stream (Q1: 5 L/h; Q2: 10 L/h; Q3: 15 L/h). Recirculation mode IE experiments.

5.3.4 IE potential for the reuse of the final treated water in the olive-oil process

A comparison between the maximum legislated values requisite for drinking water production and the final treated effluent after the proposed integral process is reported in Table 5.3.

It was found that OMWST treated by the proposed IE methodology fulfils the legislated requirements for drinking water, been therefore suitable for its reuse in the process. This allows the reutilization of the final treated effluent in the olives washing machines and finally closing the loop, thus rendering the production process cost-effective and environmentally respectful.

Table 5.3. Comparison between the final values of water treated and the legislated values of drinking water.

Parameters	Drinking Water*	Purified OMWST**
Conductivity (mS cm ⁻¹)	2.50	0.0443
[Cl ⁻] (mg L ⁻¹)	250	12.1
[Na ⁺] (mg L ⁻¹)	200	0.988
[Fe ³⁺] (mg L ⁻¹)	0.200	0.0395
[Phenols] (mg L ⁻¹)	Non-legislated	0.615

*Required values for drinking water. ** Values for optimal conditions.

5.4 Conclusions

Remediation of sodium, total iron, chloride and phenols ions from synthetic wastewater solutions was successfully achieved using Dowex Marathon C and Amberlite IRA-67 IE resins. Removal percentages of all species were considerably increased with incrementing the contact time. In addition, the equilibrium was obtained in about 30 min for sodium, chloride and total iron, whereas the highest percentage of phenols removal was obtained for the first minutes of IE treatment. Sodium, total iron and chloride adsorption efficiencies seemed not to be affected by operating temperature, whereas the best results were obtained at the lowest temperature (298 K) for phenols removal.

On the other hand it is known that flow rate might affect this kind of IE processes. In this case it was found that flow rates of 10 and 15 L/h did not affect importantly to sodium, chloride and total iron adsorption after equilibrium was achieved. In this point, removal efficiency percentages around 90-100 % were ensured for these ions. The best results for adsorption of phenols were obtained at 10 L/h, achieving removal efficiency higher than 70 % at the end of the test. Concentrations were lower than the maximum established levels for drinking water

throughout the whole experiments. Therefore this treated OMWST can be reused in the process in order to close the loop.

5.5 References

Achak, M., Mandi, L., Ouazzani, N. (2009). Removal of organic pollutants and nutrients from olive mill wastewater by a sand filter. *Journal of Environmental Management*, 90:2771-2779.

Ammary, B.Y. (2005). Treatment of olive mill wastewater using an anaerobic sequencing batch reactor. *Desalination*, 177 (2005) 157-165.

Beltrán de Heredia, J., Garcia, J. (2005) Process integration: continuous anaerobic digestion - ozonation treatment of olive mill wastewater. *Ind. Eng. Chem. Res.*, 44:8750-8755.

Bochenek, R., Sitarz, R., Antos, D. (2011). Design of continuous ion exchange process for the wastewater treatment. *Chemical Engineering Science*, 66:6209-6219.

Caetano, M., Valderrama, C., Farran, A., Cortina, J.L. (2009). Phenol removal from aqueous solution by adsorption and ion exchange mechanisms onto polymeric resins. *Journal of Colloid and Interface Science*, 338:402-409.

Chen, J.P., Chua, M.L., Zhang, B. (2002). Effects of competitive ions, humic acid, and pH on removal of ammonium and phosphorous from the synthetic industrial effluent by ion exchange resins. *Waste Management*, 22:711-719.

Dabrowski, A., Hubicki, Z., Podkoscielny, P., Robens E. (2004). Review: Selective removal of the heavy metal ions from waters and industrial wastewaters by ion-exchange method. *Chemosphere*, 56:91-106.

Demirbas, A., Pehlivan, E., Gode, F., Altun, T., Arslan, G. (2005). Adsorption of Cu(II), Zn(II), Ni(II), Pb (II) and Cd(II) from aqueous solution on Amberlite IR-120 synthetic resin. *J. of Colloid and Interface Science*, 282:20-25.

van Deventer, J. (2011). Selected Ion Exchange Applications in the Hydrometallurgical Industry. *Solvent Ext. Ion Exch.*, 29:695-718.

Eilers, A.K. (2008). Ion exchange for NOM removal in drinking water treatment, Master of Science thesis in Civil engineering. Delft University of Technology.

Erdem, E., Colgecen, G., Donat, R. (2005). The removal of textile dyes by diatomite earth. *J. Colloid Interface Sci.*, 282:314-319.

European Commission. 1998. Council Directive 98/83/EC of 3 November 1998 on the quality of water intended for human consumption.

Fernández-Olmo, I., Ortiz, A., Urtiaga, A., Ortiz, I. (2008). Selective iron removal from spent passivation baths by ion exchange. *J. Chem. Technol. Biotechnol.*, 83:1616-1622.

Fu, F., Wang, Q. (2011). Removal of heavy metal ions from wastewaters: A review. *J. Environ. Manag.*, 92:407-418.

Garrido Hoyos, S.E., Martínez Nieto, L., Camacho Rubio, F., Ramos Cormenzana, A. Kinetics of aerobic treatment of olive-mill wastewater (OMW) with *Aspergillus terreus*. *Process Biochem.*, 37:1169-1176.

Gode, F., Pehlivan, E. (2006). Removal of chromium (III) from aqueous solutions using Lewatit S 100: the effect of pH, time, metal concentration and temperature. *J. Hazard. Mater.*, 136:330-337.

Gomec, C., Erdim, E., Turan, I., Aydin, A., Ozturk, I. (2007). Advanced oxidation treatment of physico-chemically pre-treated olive mill industry effluent. *J. Environ. Sci. Health Part B*, 46:741–747.

Grafias, P., Xekoukoulotakis, N.P., Mantzavinos, D., Diamadopoulos, E. (2010). Pilot treatment of olive pomace leachate by vertical-flow constructed wetland and electrochemical oxidation: an efficient hybrid process. *Water Res.*, 44(9):2773-2780.

Greenberg, A.E., Clesceri, L.S., Eaton, A.D. (1992). Standard Methods for the Examination of Water and Wastewater, APHA/AWWA/WEF, 16th ed., Washington DC. Cabs.

Hekmatzadeh, A.A., Karimi-Jashani, A., Talebbeydokhti, N., Kløve, B. (2012). Modeling of nitrate removal for ion exchange resin in batch and fixed bed experiments. *Desalination*, 284:22-31.

Hermoso Fernández, M., et al. Elaboracion de aceites de oliva de calidad. Obtencion por el sistema de dos fases. Junta de Andalucia, Consejeria de Agricultura, Pesca. Servicio de Publicaciones y Divulgacion, 1998, ISBN: 84-898-0237-8.

Hodaifa, G., Eugenia-Sánchez, M., Sánchez S. (2008). Use of industrial wastewater from olive-oil extraction for biomass production of *Scenedesmus obliquus*. *Bioresour. Technol.*, 99:1111-1117.

Hodaifa, G., Ochando-Pulido, J.M., Rodriguez-Vives, S., Martinez-Ferez, A. (2013). Optimization of continuous reactor at pilot scale for olive-oil mill wastewater treatment by Fenton-like oxidation process. *Chem. Eng. J.*, 220:117-124.

Karadag, D., Tok, S., Akgul, E., Turan, M., Ozturk, M., Demir, A. (2008). Ammonium removal from sanitary landfill leachate using natural Gördes clinoptilolite. *Journal of Hazardous Materials*, 153:60–66.

Khoufi, S., Aloui, F., Sayadi, S. (2006). Treatment of olive oil mill wastewater by combined process electro-Fenton reaction and anaerobic digestion. *Water Res.*, 40:2007-2016.

Ku, Y., Lee, K., Wang, W. (2004). Removal of phenols form aqueous solutions by purolite A-510 resin. *Sep. Sci. Technol.*, 39:911–923.

Lafi, W.K., Shannak, B., Al-Shannag, M., Al-Anber, Z., Al-Hasan, M. (2009). Treatment of olive mill wastewater by combined advanced oxidation and biodegradation. *Separ. Purif. Technol.*, 70(2):141-146.

Martínez Nieto, L., Hodaifa, G., Rodríguez Vives, S., Giménez Casares, J.A. (2010). Industrial plant for olive mill wastewater from two-phase treatment by chemical oxidation, *J. Environ. Eng.*, 136:1309-1313.

Martínez Nieto, L., Hodaifa, G., Rodríguez Vives, S., Giménez Casares, J.A. Ochando, J. (2011a). Flocculation–sedimentation combined with chemical oxidation process. *Clean - Soil, Air, Water*, 39(10):949-955.

Martínez Nieto, L., Hodaifa, G., Rodríguez Vives, S., Giménez Casares, J.A., Ochando, J. (2011b). Degradation of organic matter in olive oil mill wastewater through homogeneous Fenton-like reaction, *Chem. Eng. Journal*. 173 (2011) 503-510.

Martins, R.C., Quinta-Ferreira, R.M. (2011). Remediation of phenolic wastewaters by advanced oxidation processes (AOPs) at ambient conditions: comparative studies. *Chem. Eng. Sci.*, 66:3243–3250.

Mustafa, S., Bashir, H., Rehana, N., Naeem, A. (1997). Selectivity reversal and dimerization of chromate in the exchanger Amberlite IRA-400, *React. Funct. Polym.*, 34:135–144.

Ochando-Pulido, J.M., Stoller, M., Bravi, M., Martinez-Ferez, A., Chianese, A. (2012). Batch membrane treatment of olive vegetation wastewater from two-phase olive oil production process by threshold flux based methods. *Sep. Purif. Technol.*, 101:34-41.

- Ostroski, I.C., Barros, M., Silvab, E.A., Dantas, J.H., Arroyo, P.A., Lima, O. (2009). A comparative study for the ion exchange of Fe(III) and Zn(II) on zeolite NaY. *Journal of Hazardous Materials*, 161:1404-1412.
- Papastefanakis, N., Mantzavinos, D., Katsaounis, A. (2010). DSA electrochemical treatment of olive mill wastewater on Ti/RuO₂ anode. *J. Appl. Electrochem.*, 40(4):729-737.
- Pintar, A., Batista, J., Levec, J. (2001). Integrated ion exchange/catalytic process for efficient removal of nitrates from drinking water. *Chem. Eng. Sci.*, 56:1551-1559.
- Roostaei, N., Tezel, F.H. (2004). Removal of phenol from aqueous solutions by adsorption. *J. Environ. Manag.*, 70:157-164.
- Sarika, R., Kalogerakis, N., Mantzavinos, D. (2005). Treatment of olive mill effluents. Part II. Complete removal of solids by direct flocculation with poly-electrolytes. *Environ. Int.*, 31:297-304.
- Shaha, B., Iglesias, M., Cumming, I.W., Streat, M. (2000). Sorption of trace heavy metals by thiol containing chelating resins. *Solvent Extr. Ion Exch.*, 18:133-167.
- Su-Hsia, L., Ruey-Shin, J. (2009). Adsorption of phenol and its derivatives from water using synthetic resins and low-cost natural adsorbents: A review. *J. Environ. Manag.*, 90:1336-1349.
- Tezcan Ün, Ü., Altay, U., Koparal, A.S., Ogutveren, U.B. (2008). Complete treatment of olive mill wastewaters by electrooxidation. *Chem. Eng. J.*, 139:445-452.
- Valverde, J.L., DeLucas, A., Carmona, M., Pérez, J.P., González, M., Rodríguez, J.F. (2006). Minimizing the environmental impact of the regeneration process of an ion exchange bed charged with transition metals. *Sep.Purif.Technol.*, 49:167-173.
- Víctor-Ortega, M.D., Ochando-Pulido, J.M., Hodaifa, G., Martínez-Ferez, A. (2014). Ion exchange as an efficient pretreatment system for reduction of membrane fouling in the purification of model OMW. *Desalination*, 343:198-207.
- Zhu, L., Deng, Y., Zhang, J., Chen, J. (2011). Adsorption of phenol from water by N butylimidazolium functionalized strongly basic anion exchange resin. *J. Colloid. Interface Sci.*, 364:462-468.

CHAPTER 6

IMPACTS OF INTEGRATED STRONG-ACID CATION EXCHANGE AND WEAK-BASE ANION EXCHANGE PROCESS FOR SUCCESSFUL REMOVAL OF SALINE TOXICITY FROM MODEL OLIVE MILL WASTEWATER

M.D. Víctor-Ortega*, J.M. Ochando-Pulido, A. Martínez-Ferez

Chemical Engineering Department, University of Granada, 18071 Granada, Spain

*email: mdvictor@ugr.es

Ecological Engineering

Publisher: ELSEVIER SCIENCE BV. PO BOX 211, 1000 AE AMSTERDAM, NETHERLANDS

Volume 77. Pages 18-25.

Year: 2015

ISSN: 0925-8574

DOI: <http://dx.doi.org/10.1016/j.ecoleng.2015.01.005>

Impact factor: 2.580

Tertile: First



Abstract

In the present work, the performance of a fixed-bed ion exchange (IE) process comprising novel strong-acid cation exchange and weak-base anion exchange resins was examined for the removal of the ionic species, that is, sodium and chloride ions, responsible for the high salinity of olive mill wastewater from an olive mill working with the two-phase decanting technology exiting a primary-secondary treatment (OMW-2ST). Sodium IE efficiency was found to increase with an increment in the pH value up 5, whereas the optimum pH for chloride IE was equal to 1. Equilibrium behaviour of both species was accurately predicted by Langmuir isotherm, showing sodium uptake is 53.9 % higher than for chloride. Sodium and chloride removal efficiencies decreased (from 97.0 to 74.0 % and from 95.0 to 77.0 %, respectively) when their initial concentration increased from 250 - 1000 mg L⁻¹. Finally, the integrated IE system in continuous mode ensured 80 - 90 % average removal efficiencies for both ionic species and conductivity. IE efficiency loss below 5 % after several regeneration cycles is a technical-economical key fact. The final treated effluent complied with the standards established by the Food and Agricultural Association (FAO) with the goal of reusing the regenerated water for irrigation purposes.

Keywords: environmental impact, ion exchange, isotherm, pollutants, olive mill wastewater, wastewater reclamation.

6.1 Introduction

Olive oil industry, which is widely known to be currently one of the main agro-industrial activities of the Mediterranean Basin countries, by-produces mainly two wastewater streams: the first one comes from the washing of the fruit, and is therefore called olives washing wastewater (OWW), and the second one is generated in the extraction of the olive oil, thus referred to as olive oil washing wastewater, OOW, a mixture of the olive-fruit humidity along with process-added water. These effluents are commonly known as olive mill wastewater (OMW).

In traditional olive oil mills working with the ancient batch press method, increasingly less used, between 0.4 - 0.6 m³ of OMW were generated per ton of processed olives, while currently an average-sized modern olive oil factory leads to a sensibly higher amount of OMW: up to 10 - 15 m³ of OOW daily, in sum to 1 m³ d⁻¹ of OOW (Table 6.1). Taking the case of Spain, the main olive oil producer worldwide, this raises a total volume of more than 9 million m³ of OMW per year, which represents a huge amount of this highly pollutant effluents. What is more, olive oil production is steadily growing worldwide and it is now an emergent agro-food

industry in China and many other countries such as the USA, Australia and the Middle East. Hence, the treatment of the olive mill effluents is becoming a task of global concern.

Table 6.1. Flow rates of the different effluents of continuous extraction processes (Mendoza et al., 1996).

Effluent flow rate, L kg⁻¹	3-phase extraction	2-phase extraction
Washing of olives (OWW)	0.06	0.05
Horizontal centrifuge	0.90	0
Vertical centrifuge	0.20	0.15
Cleaning	0.05	0.05
Total	1.21	0.25

In the two-phase olive oil extraction system, water injection is only practiced in the final vertical centrifugation step, and thus the volume of liquid effluent by-produced (OMW-2) is reduced by one third on average if compared to the amount required for the three-phase system (OMW-3) (Table 6.1). The two-phase system appears to be more ecological, and for this reason this system has been strongly promoted in Spain. Nevertheless, the three-phase technology is still surviving in other countries where the scarcity of financial support has not permitted the technological switch yet.

Purification of the effluents from both decanting processes is specifically addressed to be a hard task given their highly variable physicochemical composition, which also depends on edaphoclimatic and cultivation parameters, the type, quality and maturity of the olives (Niaounakis and Halvadakis, 2006; Paraskeva and Diamadopoulos, 2006; Hodaifa et al., 2008). OMW-2 and OMW-3 are among the heaviest polluted agro-industrial effluents, typically characterized by strong odour nuisance, acid pH, intensive violet-dark colour and high saline toxicity, reflected by significant electroconductivity (EC) values (Table 6.2). In these effluents, major organic pollutants concentration is found, among which we should highlight phenolic compounds, organic acids, tannins and organohalogenated contaminants, mostly phytotoxic and recalcitrant to biological degradation. The presence of these substances would be hardly reflected by measurements of the biological oxygen demand (BOD₅), therefore the chemical oxygen demand (COD) seems to be more appropriate as a key parameter together with the total phenolic compounds (TPh) concentration (Table 6.2).

Table 6.2. Characteristics of effluents of batch or continuous olive oil extraction processes.

Process	ID	COD, g O ₂ L ⁻¹	BOD ₅ , g O ₂ L ⁻¹	TSS*, g L ⁻¹	TPh, g L ⁻¹	pH	EC, S cm ⁻¹
Olives cleaning	OWW	0.8 - 2.2	0.3 - 1.5	8 - 18	0 - 0.1	5.5 - 6.6	2.5 - 3.0
Batch press	OMW-P	130 - 130	90 - 100	10 - 12	1.0 - 2.4	4.5 - 5.0	2.0 - 5.0
Three phase	OMW-3	30 - 220	5 - 45	5 - 35	0.3 - 7.5	3.5 - 5.5	2.0 - 7.9
Two phase	OMW-2	4 - 18	0.8 - 6.0	2 - 7	0.1 - 1.0	3.5 - 6.0	1.5 - 2.5

*Tss: total suspended solids.

Uncontrolled disposal of these effluents causes serious environmental impacts, such as soil contamination, underground leakage and water body pollution (Hodaifa et al., 2008; Mendoza et al., 1996; Rozzi et al., 1988). However, at the moment there is no specific European legislation concerning the regulation of olive mill discharges, and standard procedures are delegated to individual countries. In spite of this fact, Directive 2000/60/CE highlights the necessity of conferring maximum protection to water and introducing the idea of the use of regenerated wastewater, thus encouraging the establishment of a legal framework capable of achieving this goal. Direct disposal of these effluents to surface waters or municipal sewage systems is thereof forbidden, and OMW cannot either be disposed directly for irrigation purposes as a general rule, though controlled partial discharge on suitable terrains is still allowed in some EU countries like Italy (Niaounakis and Halvadakis, 2006; Paraskeva and Diamadopoulos, 2006).

Until now, different treatments for the management and reclamation of OMW have been proposed (Niaounakis and Halvadakis, 2006). Biological treatment of OMW is a hard task and right now not applied on a large scale due to the resistance of OMW to biological degradation (Garrido Hoyos et al., 2002; Marques, 2001; Fountoulakis et al., 2002; Ammary, 2005; Taccari and Ciani, 2011). Other treatment processes have been developed in time, such as lagooning or natural evaporation and thermal concentration (Paraskeva, 2006; Annesini and Gironi, 1991), treatments with lime and clay (Aktas et al., 2001; Al-Malah et al., 2000), composting (Cegarra et al., 1996; Papadimitriou et al., 1997; Bouranis et al., 1995), physico-chemical procedures as coagulation-flocculation (Sarika et al., 2005; Martínez Nieto et al., 2011a; Stoller, 2009) and electrocoagulation (Inan et al., 2004; Tezcan et al., 2006), advanced oxidation processes including ozonation (De Heredia and Garcia, 2005), Fenton’s reagent (Martínez Nieto et al., 2011b; Hodaifa et al., 2013) and photocatalysis (Stoller and Bravi, 2010) and also electrochemical (Papastefanakis et al., 2010; Tezcan et al., 2008; Canizares et al., 2006) and hybrid processes (Grafias et al., 2010; Lafi et al., 2009; Khoufi et al., 2006; Rizzo et al., 2008).

Small size and geographical dispersion of traditional olive oil mills has made the management of OMW rather cost-ineffective. Nevertheless, these typical small olive oil mills are recently tending to group into bigger cooperatives. This fact can be an advantage for suitable treatment processes of these highly polluted effluents.

Within this framework, olive mill wastewater from an olive mill working with the two-phase decanting technology (OMW-2) was conducted to a primary-secondary treatment in previous work carried out in our research group by Martínez-Nieto et al., comprising Fenton's advanced oxidation, flocculation and filtration through cost-free olive stones in series (Martínez Nieto et al., 2011a; Martínez Nieto et al., 2011b; Martínez Nieto et al., 2010). This depuration sequence succeeded to solve the problem related to the presence of phenolic compounds and achieved very high reduction of the organic pollutants load (COD), suspended solids and total phenolic compounds, also exploiting a by-product residue of the proper olive oil production process, olive stones.

However, conventional and advanced physicochemical treatments are not able to abate the high salinity exhibited by OMW-2, principally in form of dissolved monovalent species such as sodium and chloride ions, which after the proposed treatment is increased owed to the addition of the catalyst (FeCl_3) and neutralizing agent (NaOH) (Martínez Nieto et al., 2011b; Hodaifa et al., 2013). EC values in the primary-secondary-treated OMW-2 (OMW-2ST) are well above the range 2-3 mS cm^{-1} , thus presenting hazardous salinity levels according to the standard limits established by the Food and Agricultural Association (FAO) with the goal of reusing the regenerated water for irrigation purposes (Table 6.3).

Table 6.3. Water Quality according to Food and Agriculture Organization (FAO).

EC, mS cm^{-1}	Water Quality	Hazardous due to salinity
0-1	Excellent - Good	Low - Medium
1-3	Good - Poor	High
>3	Poor - Non-acceptable	Very high

In this regard, the use of ion exchange (IE) technology can be a potential solution for the reclamation of these highly contaminated OMW-2 effluents. IE exhibits a series of characteristics which make it more attractive than classic separation processes, that is, simplicity, effectiveness, selectivity, recovery and relatively low cost (Inoue, 2008; Savari et al., 2008). Moreover, resins beds are modular and have a small footprint, they can be tailored to remove monovalent and

divalent ionic species apart from organic pollutants, they can also be successfully regenerated by using common acids and bases, and regeneration cycles can be minimized. What is more, IE processes can also be a suitable alternative to membrane technology for the final purification of OMW-2 (Ochando-Pulido et al., 2012a and 2012b), given that IE processes do not require high pressure pumps, variable speed drives and attendant control systems (Bassandeh et al., 2013), thus implying lower capital and operating costs.

In the present research work, the performance of a fixed-bed IE process comprising novel strong-acid cation exchange and weak-base anion exchange resins was fully examined for the removal of the ionic species responsible for the high salinity of OMW-2ST. With this purpose, sodium and chloride IE equilibrium was studied and modeled for model OMW2-ST. Modelling of the IE equilibrium is capital for the successful design and scale-up of IE processes. Subsequently, the impacts of several key operating variables on the IE performance were examined, comprising the pH, the contact time and the initial concentration of the pollutant ionic species. Finally, the continuous operation of the proposed IE process was addressed, and the water quality standards for reusing the purified effluent for irrigation purposes were checked with the goal of reducing the environmental damages caused by OMW in order to make the olive oil production a green process.

6.2 Experimental section

6.2.1 IE equipment and resins

IE experiments were performed by using a bench-scale IE device (MionTec) which consisted mainly in a peristaltic pump (Ecoline VC-380) and two IE columns, as shown in Figure 6.1. IE columns employed in this study were made of an acrylic tube (540 mm height x 46 mm internal diameter), provided with a mobile upper retaining grid which could be fixed in the column to adjust it as a fixed bed or a semi-fluidized bed.

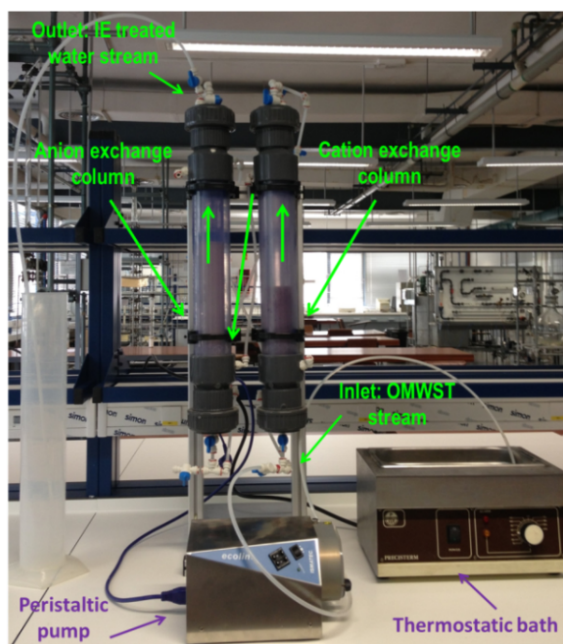


Figure 6.1. Ion exchange bench-scale equipment.

In this work, fixed-bed operation was chosen. The first column was filled with Dowex Marathon C strong-acid cation exchange resin, whereas the second one was filled with Amberlite IRA-67 weak-base anion exchange resin. The physical and chemical characteristics of the used resins are hereafter described in Table 6.4. Firstly, Dowex Marathon C was conditioned in hydrochloric acid solution and finally in water before being used in the IE and desorption experiments, whereas Amberlite IRA-67 was treated with sodium hydroxide solution and then washed with water following the advice given by the resin manufacturer.

Table 6.4. Physicochemical properties of Dowex Marathon C and Amberlite IRA-67 IE resins.

Properties	Dowex Marathon C	Amberlite IRA-67
Type	Strong-acid cation	Weak-base anion
Matrix	Styrene-DVB, gel	Tertiary amine
Ionic form as shipped	H ⁺	OH ⁻
Particle size, mm	0.55-0.65	0.5-0.75
Effective pH range	0-14	0-7
Total exchange capacity, eq L ⁻¹	1.80	1.60
Shipping weight, g L ⁻¹	800	700

6.6.2. Operating conditions in semi-batch IE experiments

The impacts of several key operating variables on the IE performance were examined in semi-batch operation, comprising the pH, the contact time and the initial concentration of the pollutant ionic species. For these series of experiments, model OMW-2ST solutions were prepared by dissolving reagent-grade sodium chloride (provided by Panreac) in double distilled water.

The IE performance of sodium and chloride ions was studied at different pH values in the range 1 - 9, adjusting the pH value of sodium and chloride in model OMW-2ST solutions by adding NaOH or HCl, depending on the desired value.

Otherwise, the impact of the initial concentration of both ionic species in the IE performance was examined by adjusting the desired concentrations of sodium at values equal to 250 mg L⁻¹, 500 mg L⁻¹, 750 mg L⁻¹ and 1000 mg L⁻¹, whereas chloride concentrations were set at 250 mg L⁻¹, 500 mg L⁻¹, 1000 mg L⁻¹ and 1500 mg L⁻¹.

6.2.3 IE equilibrium experiments

IE equilibrium was examined by performing semi-batch experiments at room temperature in order to obtain the basic equilibrium parameters of Na⁺/H⁺ and Cl⁻/OH⁻ systems, respectively (Figure 6.2). The extent of the IE equilibrium data of each species was determined by measuring the residual amount of these ions in the liquid phase. Previously, aqueous solutions of both contaminants were put in contact with the studied IE resins until equilibrium was achieved.

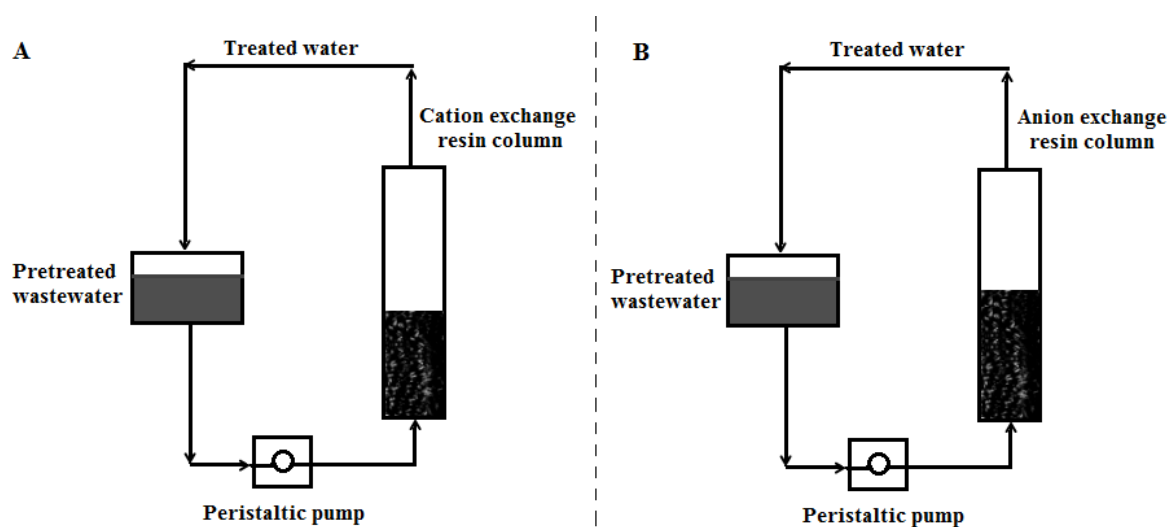


Figure 6.2. Flow-sheet scheme for IE recirculation operating cycle for sodium (panel A) and chloride removal (panel B).

The flask containing the feed solution was stirred continuously during the whole experiments. The flow rate and temperature were fixed at 10 L h⁻¹ and room temperature, respectively (V́ctor-Ortega et al., 2014), whereas the contact time was varied up to 60 minutes. The initial pH of the solution was adjusted to the optimum values found in the former semi-batch IE experiments.

The removal efficiency values for the contaminant ions were calculated according to the following equation:

$$\% \text{ Removal efficiency} = \frac{C_i - C_f}{C_i} \times 100 \quad (1)$$

where C_i and C_f are the initial and final ions concentration (mg L⁻¹), respectively.

6.2.4 Continuous IE experiments

Finally, continuous IE process was examined for the final purification of OMW-2ST. During continuous IE performance experiments, model OMW-2ST feedstream was introduced at the bottom of the first column (cationic resin) in upflow mode, leaving this column by the top. Then, OMW-2ST passed through the second column (anionic resin) also in upflow mode from the bottom to the top (Figure 6.1). Continuous IE experiments were performed at 10 L h⁻¹ and ambient temperature (25 ° C), and the evolution of the concentration of sodium and chloride ions as well as the conductivity values in the outlet stream were continuously measured during the operating time by removing 50 mL solution aliquots.

For continuous IE experiments, the target concentrations were fixed at the values registered on average in OMW-2 at the outlet of the proposed treatment (OMW-2ST), that is, around 1130 mg L⁻¹ and 730 mg L⁻¹ for chloride and sodium ions, whereas 1 mg L⁻¹ and 0.4 mg L⁻¹ for total phenolic compounds and total iron, prepared by dissolving phenol and 30 % (w/w) iron (III) chloride (provided by Panreac), respectively. (Table 6.5) (Ochando-Pulido et al., 2012a and 2012b; V́ctor-Ortega et al., 2014).

After each operational cycle, the Dowex Marathon C cation exchange resin was fully washed with a 2 % HCl aqueous solution for 30 minutes at 25 ° C. In a similar way, Amberlite IRA- 67 anion exchange resin was washed with a 4 % NaOH aqueous solution for 40 minutes at 25 ° C. Then, the resins were washed with double distilled water to remove all excess of acid or base, respectively.

Table 6.5. Physicochemical characteristics of OMW-2ST.

Parameters	Parametric value
pH	7.78 - 8.17
Conductivity, mS cm⁻¹	3.15 - 3.55
COD, mg L⁻¹	120.5 - 226.6
Total phenolic compounds, mg L⁻¹	0.39 - 0.98
Total [Fe], mg L⁻¹	0.04 - 0.4
[Cl⁻], mg L⁻¹	875.83 - 1045.03
[Na⁺], mg L⁻¹	534.01 - 728.71

6.2.5 Analytical methods

Analytical grade reagents and chemicals with purity over 99 % were used for the analytical procedures, applied at least in triplicate.

Sodium concentration values were determined by using a Crison GLP 31 Sodium Ion-Selective Electrode 96 50, with autocorrection of temperature. To calibrate the electrode in the laboratory, 0.01, 0.1 and 1.0 g L⁻¹ Na⁺ standard solutions were prepared.

Chloride concentration values were assessed by a Crison GLP 31 Chloride Ion-Selective Electrode 96 52 C, with autocorrection of temperature. To this end, 0.01, 0.1 and 1.0 g L⁻¹ Cl⁻ standard solutions required for the electrode calibration were also prepared in the laboratory.

EC and pH measurements were evaluated with a Crison GLP31 conductivity-meter and a Crison GLP21 pH-meter, provided with autocorrection of temperature. Buffer standard solutions for EC (1,413 μ S cm⁻¹ and 12.88 mS cm⁻¹) and pH (pH 4.01, 7.00 and 9.21) measurements respectively were supplied as well by Crison.

6.3 Results and discussion

6.3.1 Effect of pH

The influence of the pH value on sodium (Na⁺) and chloride (Cl⁻) IE performance is reported in Figure 6.3. The IE performance of sodium and chloride ions was studied at different pH values in the range 1 - 9.

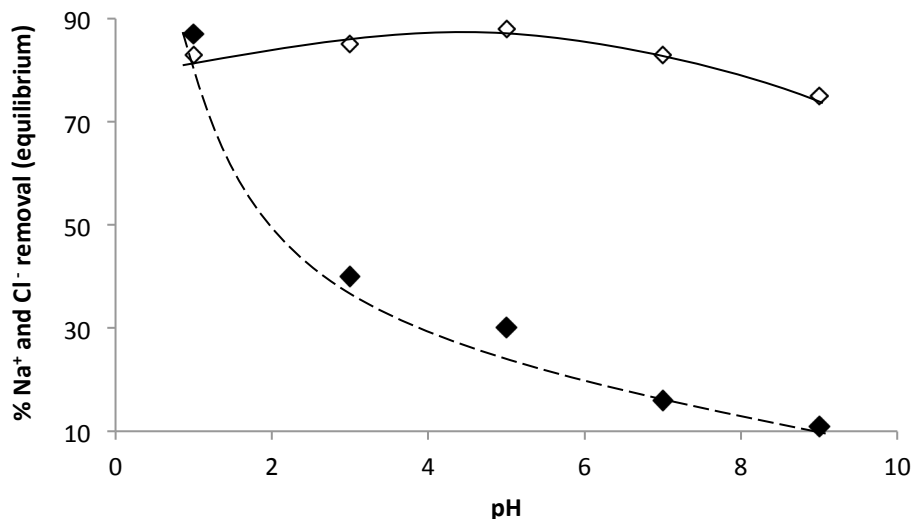


Figure 6.3. Effect of pH on Na⁺ removal (◇) onto Dowex Marathon C cation exchange resin (Na⁺ concentration = 750 mg L⁻¹, resin dose = 3.46 g 100 mL⁻¹ and equilibrium time = 1 h) and Cl⁻ removal (◆) onto Amberlite IRA-67 anion exchange resin (Cl⁻ Concentration = 1000 mg L⁻¹, resin dose = 3.5 g 100 mL⁻¹ and equilibrium time = 1 h).

As shown in Figure 6.3, sodium removal efficiency increased with an increase in the pH value up to 5, but it can be observed that higher pH values led to lower IE efficiency. It seems that the excessive protonation of the active sites of the Dowex Marathon C cation exchange resin at low pH values (below 5) hinders the formation of links between Na⁺ ions and the active sites of the cation exchange resin. Similar results were found by Senthil and Gayathri (2009) in their study on bael tree (BT) leaf powder as adsorbent to remove lead (Pb²⁺ ions) from aqueous solutions.

On the other hand, at moderate pH values (3 - 6) the linked H⁺ is released from the active sites of the cation exchange resin and as a result the extent of IE of sodium ions is found to increase.

Otherwise, the optimum pH value for IE of chloride ions resulted to be the lowest pH value studied, that is, about a value equal to 1 (Figure 6.3). Furthermore, the IE efficiency with regard to Cl⁻ ions was observed to steadily decrease by incrementing the pH value. This is due to the fact that Amberlite IRA-67 anion exchange resin exhibits weak-base properties, active in a pH range from 0 to 7.

Moreover, it is worth highlighting that the pH of the solution becomes increased as Cl⁻ ions are exchanged and OH⁻ ions are released from the anion exchange resin, thus making the removal efficiency of Amberlite IRA-67 to decrease. It is also important to highlight that some retention for Cl⁻ ions was observed even at pH values above the active range of the resin. This

phenomenon is most likely due to adsorption in the polymeric matrix (acrylic divinylbenzene copolymer) than to IE (Caetano et al., 2009).

6.3.2 Effect of initial concentration

The impact of the initial concentration of both ionic species (Na^+ and Cl^-) in model OMW-2ST solutions on the IE removal efficiency is reported in Figure 6.4, where it can be observed that the initial Na^+ concentration was varied from 250 to 1000 mg L^{-1} and the cation exchange resin dosage was maintained at 34.6 g L^{-1} , whereas the initial Cl^- concentration was varied from 250 to 1500 mg L^{-1} , keeping the anion exchange resin dosage at 35 g L^{-1} .

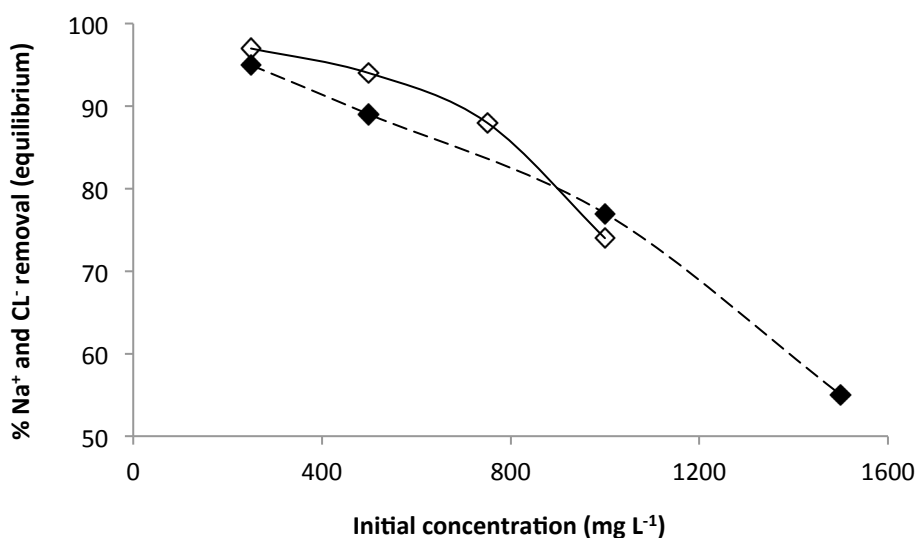


Figure 6.4. Effect of initial concentration on Na^+ removal (\diamond) onto Dowex Marathon C cation exchange resin (Na^+ concentration = 250 - 1000 mg L^{-1} , resin dose = 34.6 g L^{-1}) and Cl^- removal (\blacklozenge) onto Amberlite IRA-67 anion exchange resin (Cl^- concentration = 250 - 1500 mg L^{-1} , resin dose = 35 g L^{-1}).

The Na^+ removal efficiency was found to decrease from a value of 97.0 % for the lowest concentration studied, 250 mg L^{-1} , to a value equal to 74.0 % for the highest concentration examined, 1000 mg L^{-1} , upon the same IE operating conditions, that is, contact time and temperature (see Figure 6.4). Analogously, Cl^- removal efficiency was observed to decrease from 95.0 % to 55.0 % for the minimum and maximum initial concentrations studied, 250 mg L^{-1} to 1500 mg L^{-1} , by holding constant the same contact time and temperature (Figure 6.4). Also note that 77.0 % IE efficiency for Cl^- was registered upon a concentration of 1000 mg L^{-1} . The removal percentage of Na^+ and Cl^- ions becomes decremented with an increase in the initial concentration of each ion. This can be attributed to an increase in the number of each ionic species for the fixed amount of the respective resin (Senthil and Gayathri, 2009).

6.3.3 Equilibrium isotherms

Equilibrium isotherms, representing the amount of solute exchanged per unit of resin mass as a function of the equilibrium concentration in the bulk solution at constant temperature, were studied in order to gather information of the IE system equilibrium for Na⁺ and Cl⁻ ions removal from OMW-2ST. The initial pH values of the solutions were adjusted to the optimum values formerly found, that is, a pH value equal to 1 for chloride whereas a pH value of 5 for sodium.

The equilibrium data for both species were correlated by means of Langmuir, Freundlich and Temkin isotherms. The IE capacity of each resin was evaluated as a function of both pollutants concentration by determining their loading q_e (mg of pollutant / g of adsorbent) with the following expression:

$$q_e = (C_0 - C_e) \times \frac{V}{m_s} \quad (2)$$

where C_0 is the initial total concentration of each contaminant in the model OMW-2ST, C_e is the equilibrium total concentration (mg of Na⁺ or Cl⁻ L⁻¹ of solution), V (m³) is the volume of the model OMW-2ST, and m_s (kg) is the corresponding resin mass.

The Langmuir model (Langmuir, 1918) is based on the assumption that the maximum IE occurs when a saturated monolayer of solute molecules is present on the resin surface, the uptake (IE) energy is constant and there is no migration of the up-taken molecules in the surface plane. The Langmuir isotherm is given by the following expression:

$$q_e = \frac{q_m \times K_L \times C_e}{1 + K_L \times C_e} \quad (3)$$

where C_e is the equilibrium concentration in the solution (mg L⁻¹), q_m and K_L are the Langmuir constants, representing the maximum IE capacity for the solid phase (resin) loading and the energy constant related to the uptake heat respectively. The Langmuir isotherm can be linearized according to the following equation:

$$\frac{C_e}{q_e} = \frac{C_e}{q_m} + \frac{1}{K_L \times q_m} \quad (3')$$

The Freundlich isotherm model (Freundlich, 1906) is an empirical relationship describing the IE of solutes from a liquid phase to a solid surface which assumes that different sites with several uptake energies are involved. The Freundlich isotherm represents the relationship between the amounts of ionic species exchanged per unit mass of resin, q_e , and the concentration of the ionic species at equilibrium, C_e :

$$q_e = K_f C_e^{1/n} \quad (4)$$

where K_f and n are the Freundlich constants, characteristics of the system, whereas K_f and n are the indicators of the IE capacity and intensity, respectively. The logarithmic form of the Freundlich model is given by the following equation:

$$\log q_e = \log K_f + \frac{1}{n} \times \log C_e \quad (4')$$

Finally, the fitting of the experimental data to the Temkin isotherm is given by the equation proposed by Temkin and Pyzhev (1940):

$$q_e = B \times \ln (A \times C_e) \quad (5)$$

where A and B are Temkin isotherm constants. Temkin isotherm contains a factor that explicitly takes into the account resin-exchanged species interactions. This isotherm assumes that the uptake (IE) heat of all the molecules in the layer decreases linearly with the coverage due to resin-exchanged species interactions, and that IE is characterized by a uniform distribution of binding energies, up to some maximum binding energy.

Eq. (5) can be linearized by using the natural logarithmic as follows:

$$q_e = B \times \ln A + B \times \ln C_e \quad (5')$$

The results of the linear regression to the different isotherm models for each studied pollutant are hereafter reported in Table 6.6, and also given in Figure 6.5 for sake of comparison and comprehension. It is worth pointing that all three isotherm models represent the equilibrium data for sodium IE on Dowex Marathon C strong-acid cation exchange resin as well as for chloride IE on Amberlite IRA-67 weak-base anion exchange resin satisfactorily. Moreover, the calculated equilibrium IE capacities, q_e , are close to the experimental values, $q_{e,exp}$, for both ionic species.

Nevertheless, the Langmuir isotherm provides the most accurate prediction of the experimental results ($R^2 > 0.99$ for both ionic species). According to Table 6.6 the value of the K_L coefficient (Langmuir model) for sodium IE is more than twice higher (53.9 %) than that observed for chloride, explained by the fact that sodium uptake heat is higher than for chloride in OMW-2ST. This fact implies that the affinity of Dowex Marathon C strong-acid cation exchange resin for sodium is higher than that showed by Amberlite IRA-67 weak-base anion exchange resin for chloride ions. On the other hand, the maximum IE capacity, q_m , is similar for both ionic species.

Table 6.6. Langmuir, Freundlich and Temkin isotherm parameters for Na⁺ uptake on Dowex Marathon C and for Cl⁻ on Amberlite IRA-67 cation and anion exchange resins.

Pollutant	Strong-acid cation exchange resin								
	Langmuir model			Freundlich model			Temkin model		
	K _L (L mg ⁻¹)	q _m (mg g ⁻¹)	R ²	K _f (mg g ⁻¹)* (mg L ⁻¹) ^{-1/n}	n	R ²	A (L g ⁻¹)	B (J mol ⁻¹)	R ²
Sodium	0.05386	22.94	1	4.079	3.131	0.9346	0.8100	4.172	0.9788
	Weak-base anion exchange resin								
	Langmuir model			Freundlich model			Temkin model		
	K _L (L mg ⁻¹)	q _m (mg g ⁻¹)	R ²	K _f (mg g ⁻¹)* (mg L ⁻¹) ^{-1/n}	n	R ²	A (L g ⁻¹)	B (J mol ⁻¹)	R ²
Chloride	0.02483	25.06	0.9989	3.237	3.076	0.9500	0.3665	4.497	0.9664

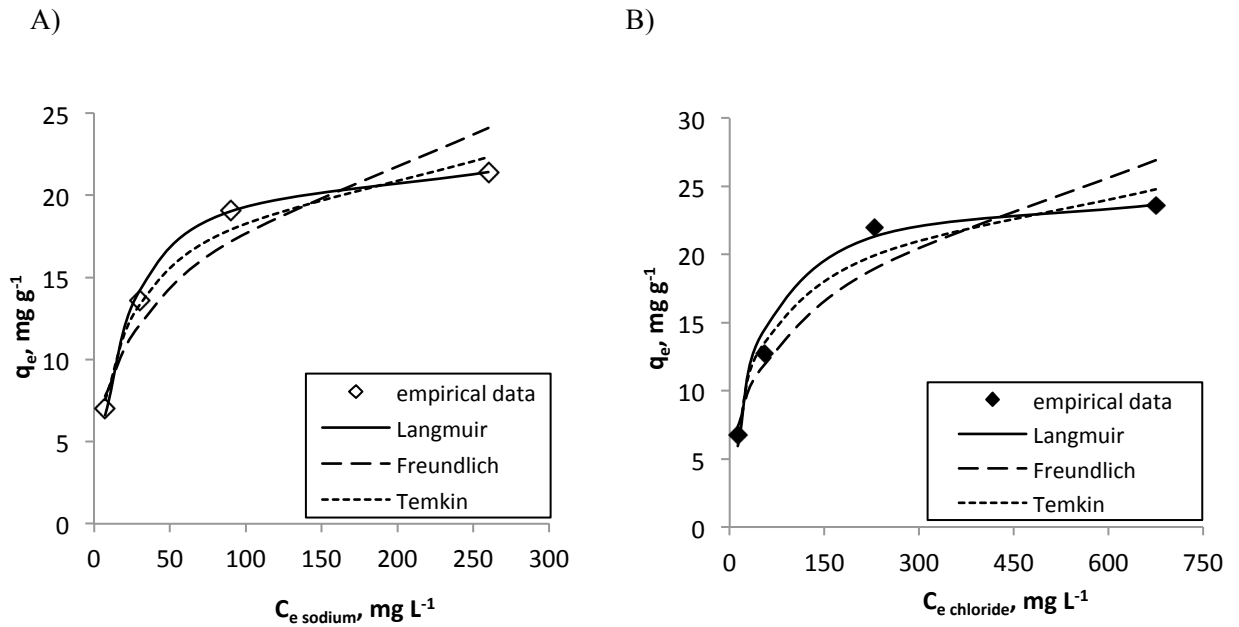


Figure 6.5. Equilibrium isotherms of Na⁺ on Dowex Marathon C cation exchange resin (panel A) and Cl⁻ on Amberlite IRA-67 anion exchange resin (panel B) in model OMW-2ST.

These patterns are supported by the results withdrawn from the Freundlich model, for which K_f constant values were also found to be higher (20.7 %) for sodium than for chloride IE. For both

ionic species the n coefficient is higher than 1, which indicates that the IE process is enhanced. Analogously, the A value in Temkin model, representing the equilibrium binding constant, is as well major for sodium IE than for chloride uptake (54.7 % higher), whereas similar values of the B parameter were observed for both pollutants.

Finally, the equilibrium was reached in about 30 min and from this point on the removal efficiencies were as high as 90 % for both pollutants at the optimal pH values. Thereby, the concentration values in the exiting stream were equal to 91.2 mg L⁻¹ and 133 mg L⁻¹ for chloride and sodium ionic species, respectively, thus complying with the standard limits for reuse of the purified effluent in the proper production process (200 mg L⁻¹ for sodium and 250 mg L⁻¹ for chloride), confirming the potential of the novel Dowex Marathon C strong-acid cation exchange and Amberlite IRA-67 weak-base anion exchange resins for sodium and chloride ions removal.

6.3.4 Continuous IE process

Results of continuous IE operation mode verify the patterns observed for the studied species in semi-batch experiments. The evolution of the concentration of sodium and chloride ions in the outlet stream as a function of IE operating time is reported in Figure 6.6, whereas the evolution of the conductivity in the outlet stream as a function of operating time is given in Figure 6.7.

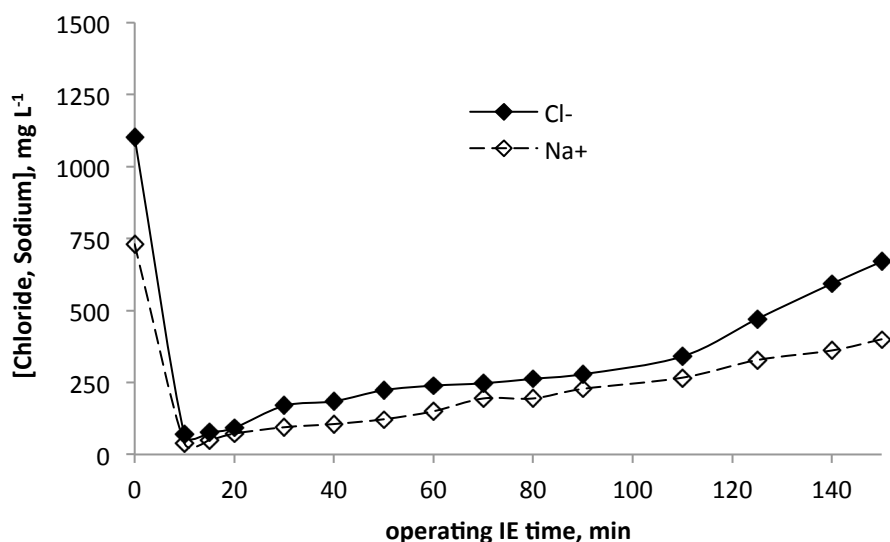


Figure 6.6. Evolution of sodium (◊) and chloride (◆) concentration in the outlet stream as a function of operating time during continuous IE experiments.

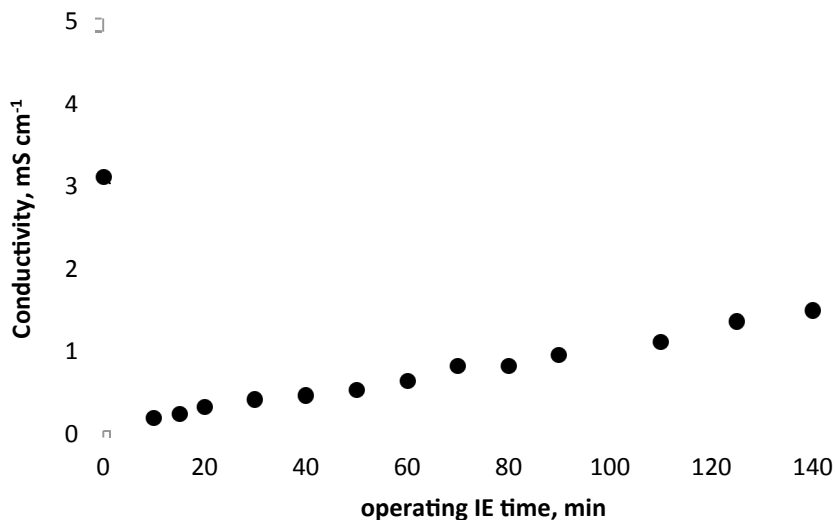


Figure 6.7. Evolution of conductivity in the outlet stream as a function of operating time during continuous IE experiments.

The integrated IE system consisting in two IE columns in serial connection, that is, the cation exchange resin column followed by the anion exchange resin column, ensured average removal efficiencies ranging from 80 - 90 % for the purification of both sodium and chloride ionic pollutants in OMW-2ST after the first IE treatment hour.

This means that by taking into account the standard limits for sodium and chloride (200 mg L^{-1} and 250 mg L^{-1} , respectively) to reuse the purified effluent in the proper production process, the maximum OMW-2ST treated volume would be equal to 11.67 L, which corresponds to 70 min operating time.

This is supported by the pattern of the evolution of the conductivity in the outlet stream as a function of the IE operating time (Figure 6.7): for an operating time up to 70 min, the conductivity in the outlet stream was about $0.7882 \text{ mS cm}^{-1}$, thus in the range of high quality irrigation water (see Table 6.3 and Table 6.7). On the other hand, when operating time was about 100 min, conductivity was close to a value of 1, hence the water quality was excellent-good ($1\text{-}2 \text{ mS cm}^{-1}$) for irrigation purposes (Table 6.3 and Table 6.7), implying a volume of treated OMW-2ST around 16.67 L.

Moreover, in all experiments in the present work the same resins have been used, and a regeneration cycle between one experiment and another has been conducted. It is very important to highlight that the loss in the IE efficiency was well below 5 % during the course of the whole regeneration cycles. This fact is key from a technical and economical point of view, since water treatment plants cannot use only fresh resins.

Table 6.7. Characteristics range of the final treated effluent.

Parameters	Value
pH	5.7-7.3
Conductivity, mS cm⁻¹	0.78 - 1
Total phenolic compounds, mg L⁻¹	0.3 - 0.4
Total [Fe], mg L⁻¹	0.04 - 0.07
[Cl⁻], mg L⁻¹	227.7 - 340.3
[Na⁺], mg L⁻¹	194.4 - 327.7

Within this scenario, a final operation unit consisting in an integrated strong-acid cation exchange and weak-base anion exchange IE process can be successfully implemented after the proposed secondary treatment (Ochando-Pulido et al., 2012a and 2012b) for the removal of the high saline toxicity from OMW-2ST. It is also worth indicating that the volumes produced by the regeneration of the resins and rejections of the last unit can be recycled to the reactor where organic matter oxidation is carried out. The proposed IE process can thus be a suitable alternative to membrane technology for the final purification of OMW-2 (Ochando-Pulido et al., 2012b), saving capital and operating costs.

Finally, an effluent with good quality standards according to the recommendations of the Food and Agricultural Association (FAO) with the goal of reusing the regenerated water for irrigation purposes was obtained, also complying with the water quality standard values established by the Guadalquivir Hydrographical Confederation (Spain) for discharge into public waterways, and thus permits reducing the environmental impact of the industrial olive oil production process.

6.4 Conclusions

In the present research work, the performance of a fixed-bed IE system comprising novel strong-acid cation exchange and weak-base anion exchange resins was fully examined for the removal of the ionic species, that is, sodium and chloride ions, responsible for the high salinity of olive mill wastewater from an olive mill working with the two-phase decanting technology exiting a primary-secondary treatment (OMW-2ST).

Sodium removal efficiency was found to increase with an increase in the pH value up 5, whereas the optimum pH value for IE of chloride ions resulted to be the lowest pH value studied, that is, about a value equal to 1. Otherwise, sodium removal efficiency was found to

decrease from a value of 97.0 % for the lowest concentration studied, 250 mg L⁻¹, to a value equal to 74.0 % for the highest concentration examined, 1000 mg L⁻¹, whereas chloride removal efficiency was observed to decrease from 95.0 % to 55.0 % for the minimum and maximum initial concentration values studied, 250 mg L⁻¹ to 1500 mg L⁻¹.

Moreover, the Langmuir isotherm provided the most accurate prediction of the equilibrium results for both ionic species, showing that sodium IE capacity is more than twice higher (53.9 %) than that observed for chloride, due to the fact that the uptake heat for sodium IE is higher than for chloride in OMW-2ST. This fact implies that the affinity of the strong-acid cation exchange resin for sodium is higher than that showed by the weak-base anion exchange resin for chloride ions.

Finally, the integrated IE process consisting in two IE columns in serial connection, that is, the cation exchange resin column followed by the anion exchange resin column working in continuous mode, ensured average removal efficiencies ranging from 50 - 80 % for the purification of both ionic pollutants in OMW-2ST, supported by the conductivity in the outlet stream as a function of the operating time.

This final IE process can be successfully implemented after the proposed primary-secondary treatment for the removal of the high saline toxicity in OMW-2ST. This permits obtaining an effluent with good quality standards according to the recommendations of the Food and Agricultural Association (FAO) with the goal of reusing the regenerated water for irrigation purposes, and also complies with the water quality standard values established by the Guadalquivir Hydrographical Confederation (Spain) for discharge into public waterways, thus permitting reducing the environmental impact of the industrial olive oil production process.

6.5 References

- Aktas, E.S., Imre, S., Esroy, L. (2001). Characterization and lime treatment of olive mill wastewater. *Water Res.*, 35:2336-2340.
- Al-Malah, K., Azzam, M.O.J., Abu-Lail, N.I. (2000). Olive mills effluent (OME) wastewater post-treatment using activated clay. *Separ. Purif. Technol.*, 20:225-234.
- Ammary, B.Y. (2005). Treatment of olive mill wastewater using an anaerobic sequencing batch reactor. *Desalination*, 177:157-165.
- Annesini, M., Gironi, F. (1991). Olive oil mill effluent: ageing effects on evaporation behavior. *Water Res.*, 25:1157-1960.

Bassandeh, M., Antony, A., Le-Clech, P., Richardson, D., Leslie, G. (2013). Evaluation of ion exchange resins for the removal of dissolved organic matter from biologically treated paper mill effluent. *Chemosphere*, 90:1461–1469.

Bouranis, D.L., Vlyssides, A.G., Drossopoulos, J.B., Karvouni, G. (1995). Some characteristics of a new organic soil conditioner from the co-composting of olive oil processing wastewater and solid residue. *Commun. Soil Sci. Plant Anal.*, 26:2461-2472.

Canizares, P., Martinez, L., Paz, R., Saéz, C., Lobato, J., Rodrigo, M.A. (2006). Treatment of Fenton-refractory olive oil mill wastes by electrochemical oxidation with boron-doped diamond anodes. *J. Chem. Technol. Biotechnol.*, 81(8):1331-1337.

Cegarra, J., Paredes, C., Roig, A., Bernal, M.P., García, D. (1996). Use of olive mill wastewater compost for crop production. *Int. Biodet. Biodegrad.*, 38(3-4):193-203.

De Heredia, J.B., Garcia, J. (2005). Process integration: continuous anaerobic digestion-ozonation treatment of olive mill wastewater. *Ind. Eng. Chem. Res.*, 44:8750-8755.

Fountoulakis, M.S., Dokianakis, S.N., Kornaros, M.E., Aggelis, G.G., Lyberatos, G. (2002). Removal of phenolics in olive mill wastewaters using the white-rot fungus *Pleurotus ostreatus*. *Water Res.*, 36:4735-4744.

Freundlich, H.M.F. (1906). Over the adsorption in solution. *J. Phys. Chem.*, 57:385-471.

Garrido Hoyos, S.E., Martínez Nieto, L., Camacho Rubio, F., Ramos Cormenzana, A. (2002). Kinetics of aerobic treatment of olive mill wastewater (OMW) with *Aspergillus terreus*. *Process Biochem.*, 37(10):1169-1176.

Grafías, P., Xekoukoulotakis, N,P., Mantzavinos, D., Diamadopoulou, E. (2010). Pilot treatment of olive pomace leachate by vertical-flow constructed wetland and electrochemical oxidation: an efficient hybrid process. *Water Res.*, 44(9), 2773-2780.

Hodaifa, G., Eugenia-Sánchez, M., Sánchez, S. (2008). Use of industrial wastewater from olive-oil extraction for biomass production of *Scenedesmus obliquus*. *Bioresour. Technol.*, 99:1111-1117.

Hodaifa, G., Ochando-Pulido, J.M., Rodriguez-Vives, S., Martinez-Ferez, A. (2013). Optimization of continuous reactor at pilot scale for olive-oil mill wastewater treatment by Fenton-like process. *Chem. Eng. J.*, 220:117-124.

Inan, H., Dimoglo, A., Şimşek, H., Karpuzcu, M. (2004). Olive oil mill wastewater treatment by means of electro-coagulation. *Separ. Purif. Technol.*, 36(1):23-31.

Inoue, H. (2003). Removal of sodium ion from bile acid solution using diffusional dialysis with cation exchange membrane. *Separ. Purif. Technol.*, 33:189-197.

Khoufi, S., Aloui, F., Sayadi, S. (2006). Treatment of olive oil mill wastewater by combined process electro-Fenton reaction and anaerobic digestion. *Water Res.*, 40:2007-2016.

Lafi, W.K., Shannak, B., Al-Shannag, M., Al-Anber, Z., Al-Hasan, M. (2009). Treatment of olive mill wastewater by combined advanced oxidation and biodegradation. *Separ. Purif. Technol.*, 70(2):141-146.

Langmuir, I. (1918). The adsorption of gases on plane surfaces of glass, mica and platinum. *J. Am Chem Soc.*, 40(8):1361-1403.

Marques, I.P. (2001). Anaerobic digestion treatment of olive mill wastewater for effluent re-use in irrigation. *Desalination*, 137:233-239.

Martínez Nieto, L., Hodaifa, G., Rodríguez Vives, S., Giménez Casares, J.A. (2010). Industrial plant for olive mill wastewater from two-phase treatment by chemical oxidation. *J. Environ. Eng.*, 136(11):1309-1313.

Martínez Nieto, L., Hodaifa, G., Rodríguez Vives, S., Giménez Casares, J.A., Ochando, J. (2011a). Flocculation–sedimentation combined with chemical oxidation process. *Clean - Soil, Air, Water*, 39(10):949-955.

Martínez Nieto, L., Hodaifa, G., Rodríguez Vives, S., Giménez Casares, J.A., Ochando, J. (2011b). Degradation of organic matter in olive oil mill wastewater through homogeneous Fenton-like reaction. *Chem. Eng. J.*, 173 (2), 503-510.

Mendoza, A., Hidalgo-Casado, F., Ruiz-Gómez, M.A., Martínez-Román, F., Moyano-Pérez, M.J., Cert-Ventulá, A., Pérez-Camino, M.C., Ruiz-Méndez, M.V. (1996). Characteristics of olive oils from First and second centrifugation. *Oil and Grease*, 47, 163-181.

Niaounakis, M., Halvadakis, C.P. (2006). Olive processing waste management literature review and patent survey. 2nd ed., Elsevier: Waste Management Series 5, 23-64.

Ochando-Pulido, J.M., Hodaifa, G., Martínez-Férez, A. (2012a). Fouling inhibition upon Fenton-like oxidation pretreatment for olive mil wastewater reclamation by membrane process. *Chemical Engineering and Processing: Process Intensification*, 62:89-98.

Ochando-Pulido, J.M., Hodaifa, G., Rodriguez-Vives, S., Martinez-Ferez, A. (2012b). Impacts of operating conditions on reverse osmosis performance of pretreated olive mill wastewater. *Water Res.*, 46(15):4621-4632.

Papadimitriou, E.K., Chatjipavlidis, I., Balis, C. (1997). Application of composting to olive mill wastewater treatment, *Environ. Technol.*, 18(1):100-107.

Papastefanakis, N., Mantzavinos, D., Katsaounis, A. (2010). DSA electrochemical treatment of olive mill wastewater on Ti/RuO₂ anode. *J. Appl. Electrochem.*, 40(4):729-737.

Paraskeva, P., Diamadopoulos, E. (2006). Technologies for olive mill wastewater (OMW) treatment: A review. *J. Chem. Technol. Biotechnol.*, 81:475-1485.

Rizzo, L., Lofrano, G., Grassi, M., Belgiorno, V. (2008). Pretreatment of olive mill wastewater by chitosan coagulation and advanced oxidation processes. *Separ. Purif. Technol.*, 63(3):648-653.

Rozzi, A., Limoni, N., Menegatti, S., Boari, G., Liberti, L., Passino, R. (1988). Influence of Na and Ca alkalinity on UASB treatment of olive mill effluents. *Part I. Preliminary results. Process Chem.*, 23:86-90.

Sarika, R., Kalogerakis, N., Mantzavinos, D. (2005). Treatment of olive mill effluents. Part II. Complete removal of solids by direct flocculation with poly-electrolytes. *Environ. Int.*, 31:297-304.

Savari, S., Sachdeva, S., Kumar, A. (2008). Electrolysis of sodium chloride using composite poly (styrene-co-divinylbenzene) cation exchange membrane. *J. Membr. Sci.*, 310:246–261.

Senthil Kumar, P., Gayathri, R. (2009). Adsorption of Pb²⁺ ions from aqueous solutions onto bael tree leaf powder: isotherms, kinetics and thermodynamics study. *J. Eng. Sci. Technol.*, 4(4):381-399.

Stoller, M. (2009). On the effect of flocculation as pretreatment process and particle size distribution for membrane fouling reduction. *Desalination*, 240:209-217.

Stoller, M., Bravi, M. (2010). Critical flux analyses on differently pretreated olive vegetation wastewater streams: some case studies. *Desalination*, 250:578-582.

Taccari, M., Ciani, M. (2011). Use of *Pichia fermentans* and *Candida* sp. Strains for the biological treatment of stored olive mill wastewater. *Biotechnol. Lett.*, 33:2385-2390.

Temkin, M.J., Pyzhev, V. (1940). Recent modifications to Langmuir isotherms. *Acta Physicochim URSS.*, 12:217-222.

Tezcan Ün, Ü., Uğur, S., Koparal, A.S., Öğütveren, Ü.B. (2006). Electrocoagulation of olive mill wastewaters. *Separ. Purif. Technol.*, 52(1):136-141.

Tezcan Ün, Ü., Altay, U., Koparal, A.S., Ogutveren, U.B. (2008). Complete treatment of olive mill wastewaters by electrooxidation. *Chem. Eng. J.*, 139:445-452.

Víctor-Ortega, M.D., Ochando-Pulido, J.M., Hodaifa, G., Martínez-Férez A. (2014). Ion exchange as an efficient pretreatment system for reduction of membrane fouling in the purification of model OMW. *Desalination*, 343:198-207.

CHAPTER 7

**THERMODYNAMIC AND KINETIC STUDIES ON IRON REMOVAL BY MEANS OF
A NOVEL STRONG-ACID CATION EXCHANGE RESIN FOR OLIVE MILL
EFFLUENT RECLAMATION**

M.D. Víctor-Ortega¹, J.M. Ochando-Pulido¹, A. Martínez-Ferez¹.

¹Chemical Engineering Department, University of Granada, 18071 Granada, Spain

email: mdvictor@ugr.es

Accepted for publication:

Ecological Engineering

Publisher: ELSEVIER SCIENCE BV. PO BOX 211, 1000 AE AMSTERDAM,
NETHERLANDS

Volume

Year: 2015

ISSN: 0925-8574

Impact factor: 2.580

Tertile: First



Abstract

Removal of metal ions from industrial wastewaters is a vital issue for the sustainable development of industries. In the present work, the performance of a fixed-bed ion exchange (IE) process with a novel strong-acid cation exchange resin has been tested for the removal of iron from secondary-treated olive mill wastewater (OMW-2ST). This secondary treatment is based on Fenton reaction and it uses iron (III) chloride as catalyst, therefore concentrations of iron up to 5 mg L^{-1} could be present in OMW-2ST. The influence of the concentration of iron in the feedstream has been investigated, and equilibrium behaviour has been modeled by means of Langmuir, Freundlich and Temkin isotherms. It was found that Langmuir isotherm provides the most accurate prediction of the experimental data ($R^2 > 0.99$). Results reveal that the adsorption process is spontaneous (negative value of ΔG°). Iron IE process was found to undergo pseudo-second order kinetics, as supported by the high square fit ($R^2 > 0.999$) and low sum of squared error values. It can be deduced that the assayed resin provides fast kinetics in the uptake of iron (up to $4.96 \text{ g mg}^{-1}\text{min}^{-1}$) as well as higher sensibly sorption capacity (28.0 mg g^{-1}) than biosorbents like olive stones (2.12 mg g^{-1}). This resin supposes also minor operating costs in comparison with other synthetic ones. The equilibrium was reached after 30 min, providing removal efficiency close to 100 %. Thereby, iron concentration in the eluting stream was maintained below the standard limit for reuse of the purified effluent in the proper production process ($200 \text{ } \mu\text{g L}^{-1}$).

Keywords: Adsorption isotherms, Kinetic study, Industrial wastewater, Ion exchange, Iron removal.

7.1 Introduction

Iron is one commonly employed metal, due mainly to its hardness and low price. Indeed it corresponds with 95% (w/w) in metal world production. From the ecological point of view, metals suppose a key issue due to their high toxicity above certain concentrations for living organisms, including human being (Volesky, 2001). Namely, high concentrations of iron in public water supplies cause turbidity and unpleasant taste and odour. It also causes troubles in distribution systems since it supports the growth of iron bacteria, resulting in clogging of pipes and increasing the rugosity coefficient (Ostroski et al., 2009). Steel and iron industries, metal plating, mining and metals corrosion industries, among others, are potential sources of environmental pollution in terms of metal ions in general and iron in particular.

Chemical precipitation has traditionally been the most commonly employed treatment method for metal ions removal. Although this treatment is relatively simple and inexpensive, it

presents a serious drawback, which is the generation of a large volume of sludge, which needs further disposal (Ostroski et al., 2009). Moreover, after precipitation processes residual iron can be normally detected in the fluid phase. Therefore, feasible processes to minimize the pollution caused by iron discharges in order to reduce the risks associated to its presence in the environment are very welcome. Ion exchange (IE) and water softening (Vaarama and Lehto, 2003), activated carbon and other filtration materials (Munter et al., 2005), supercritical fluid extraction (Andersen and Bruno, 2003), bioremediation (Berbenni et al., 2000) and limestone treatment (Aziz et al., 2004), oxidation by aeration, chlorination, ozonation followed by filtration (Ellis et al., 2000), by ash (Das et al., 2007), by aerated granular filter (Cho, 2005) and by means of adsorption (Tahir et al., 2004; Hodaifa et al., 2014, 2013) can be cited among other methods employed for removal of iron in water purification processes. It is a fact that adsorption and IE processes are nowadays universally accepted as two of the most effective pollutant removal methods, due mainly to their low cost, easiness in handling, low consumption of reagents, as well as scope for recovery of added-value components through desorption and regeneration of adsorbent/IE resin. (Abdel-Ghani et al., 2007).

Olive mill wastewater from olive mills working with the two-phase decanting technology (OMW-2) must be treated before its disposal according to current European environmental rules. This fact constitutes a high cost for olive oil manufacturers. Moreover, it is difficult to implement online/inline treatment systems for OMW due to the small size of most olive oil production factories. Thus, new, feasible and flexible solutions would be very welcome, especially for little plants (Hodaifa et al., 2013).

Within this context, advanced oxidation processes (AOPs) including ozonation (De Heredia and Garcia, 2005), Fenton's homogeneous catalysis (Martínez Nieto et al., 2010), heterogeneous photocatalysis (Stoller and Bravi, 2010), electrochemical (Papastefanakis et al., 2010 and Tezcan Ün et al., 2008) or hybrid processes (Grafias et al., 2010; Lafi et al., 2009) are required for the depuration of these bio-refractory wastewaters (Paraskeva and Diamadopoulos, 2006). Among them, Fenton's process has been well considered due to its cost-efficiency, which is mainly based on its simplicity from the instrumental and operational points of view. Also, Fenton's processes can be carried out at ambient operating conditions, which supposes an important advantage over other treatment methodologies. (Martínez Nieto et al., 2010).

In previous studies, OMW-2 was previously treated by means of an AOP based on Fenton-like reaction in prior research transferred to an industrial scale (Martínez Nieto et al., 2010). A ferric catalyst is used during this secondary treatment with the aim of promoting oxidation of the present organic matter and for this reason, the final olive mill effluent presents traces of iron (up to 5.0 mg L^{-1}). Thus, a complementary treatment, such as IE, is needed. IE involves the

use of synthetic resins where a presaturant ion on the solid phase is exchanged for the unwanted ions in the effluent (Shalini and Pragnesh, 2012). Thus, selective cation exchange resins might be targeted to reduce the residual concentration of iron below the maximum standard limit for iron in drinking water, established by the Drinking Water Directive (European Commission, 1998). This is a must in order to reuse purified effluents coming from production processes.

In the present work, the performance of a fixed-bed IE process comprising Dowex Marathon C, a novel strong-acid cation exchange resin, was assayed for removing iron from pretreated olive mill wastewater after secondary treatment (OMW-2ST). The effect of the concentration of iron in the OMW-2ST stream was investigated in the range 0.5-100 mg L⁻¹. Moreover, the equilibrium behaviour of this pollutant has been predicted by Langmuir, Freundlich and Temkin isotherms. Additionally, kinetics of iron adsorption on this resin has been investigated using pseudo-first order, pseudo-second order and intraparticle diffusion models. Finally, the suitability of the proposed IE process and the final characteristics of the regenerated effluent have been analysed.

7.2 Experimental

7.2.1 Materials

Analytical grade reagents and chemicals with purity over 99 % were used for the analytical procedures, applied at least in triplicate.

For the experiments, model solutions were prepared by dissolving reagent-grade iron (III) chloride (provided by Panreac) in double distilled water. In addition, the initial pH of the solution was adjusted with 37 % hydrochloric acid solution (supplied by Panreac).

The resin used in this research work was Dowex Marathon C (provided by Sigma Aldrich), whose physical and chemical characteristics are hereafter described in Table 7.1.

Table 7.1. Physicochemical properties of Dowex Marathon C resin.

Type	Strong-acid cation
Matrix	Styrene-DVB, gel
Ionic form as shipped	H ⁺
Particle size, mm	0.55-0.65
Effective pH range	0-14
Total exchange capacity, eq L⁻¹	1.80
Shipping weight, g L⁻¹	800

7.2.2 Ion exchange equipment

IE experiments were performed with continuous packed bed column system, which is shown in Figure 7.1. The IE equipment (MionTec) consisted of a peristaltic pump (Ecoline VC-380) and an IE column containing Dowex Marathon C strong-acid cation exchange resin. The IE column employed in this study was made of an acrylic tube (540 mm height x 46 mm internal diameter), provided with a mobile upper retaining grid which could be fixed in the column to adjust it as a fixed bed or a semi-fluidized bed. The dead volume of this column was 0.55 L.

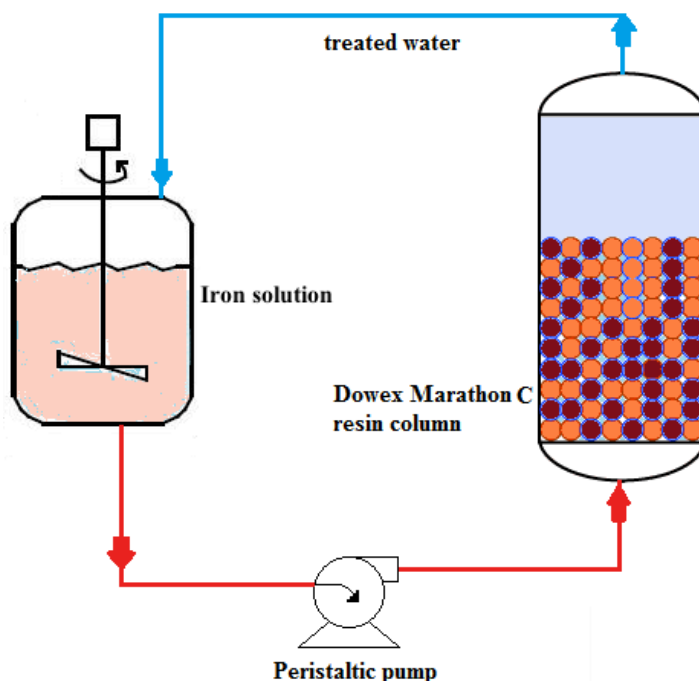


Figure 7.1. Flow-sheet scheme for IE recirculation operating device for iron removal.

7.2.3 Iron ion exchange experiments

To evaluate the effect of both the contact time and feedstream concentration, IE experiments were carried out during different operating-cycle periods. The effect of the initial concentration of iron was examined at the levels: 0.5 mg L⁻¹, 10 mg L⁻¹, 20 mg L⁻¹, 40 mg L⁻¹, 50 mg L⁻¹ and 100 mg L⁻¹.

On the other hand, adsorption isotherm studies were carried out with different initial iron concentrations ranging from 0.5 mg L⁻¹ to 100 mg L⁻¹ at constant resin dosage (3.5 g L⁻¹). Resulting data was fitted according to the following isotherm models: Langmuir, Freundlich and Temkin. Also, for the determination of the kinetics at different iron initial levels, data were fitted to the following kinetic models: first-order kinetic model, second-order kinetic model and intraparticle diffusion model.

With the aim of obtaining the corresponding parameters for iron/H⁺ equilibrium, IE experiments in recirculation mode were carried (Figure 7.1). Aqueous solutions of the contaminant were put in contact with the IE resin until equilibrium was achieved. The extent of the IE equilibrium data of this pollutant was determined by measuring the residual amount of iron in the liquid phase. The flask containing the feed solution was stirred continuously during the whole experiment. The flow rate and temperature were fixed at 10 L h⁻¹ and room temperature, respectively, since these were the optimum values obtained in previous studies (V́ctor-Ortega, 2014). Furthermore, the contact time was varied up to 60 min in order to ensure equilibrium conditions. The initial pH of the solution was adjusted to the optimum value (pH = 4.0) found in former semi-batch IE experiments. In these experiments, it was observed that iron IE efficiency increased with an increase in the pH value up 4. However, lower IE efficiency was noted upon higher pH because of formation of iron hydroxide causing hindrance of the cation exchange capacity.

The removal efficiency was estimated through the sorption percentage (Eq.1):

$$\% \text{ Sorption} = \frac{C_o - C_e}{C_o} \times 100 \quad (1)$$

where C_o and C_e refers to the initial and equilibrium iron concentration (mg L⁻¹), respectively.

7.2.4 Procedures

Briefly, for determination of the iron concentration, all iron in solutions was reduced to iron (II) in a thioglycolate medium with a derivative of triazine, which gave rise to the formation of a

reddish-purple complex which was photometrically monitored at 565 nm (Standard German methods ISO 8466-1 and German DIN 38402 A51) (Greenberg et al., 1992).

The analysis of the adsorption isotherms and kinetic models was performed using the Excel program.

Dowex Marathon C was previously conditioned in hydrochloric acid solution and then in water before being used in the IE and desorption experiments, following the advice given by the resin manufacturer. In this work, fixed-bed operation was chosen. After each operational cycle, the resin was regenerated by using hydrochloric acid (4 %) aqueous solutions and washed with double distilled water to remove the excess of acid.

7.3. Results and discussion

7.3.1 Effect of feedstream concentration

The effect of the feedstream iron concentration on the IE removal efficiency as well as on the amount of adsorbed iron per unit mass of resin is plotted in Figure 7.2. To carry out this study iron concentration was varied between 0.5 to 100 mg L⁻¹ and the cation exchange resin dosage was kept at 3.5 g L⁻¹.

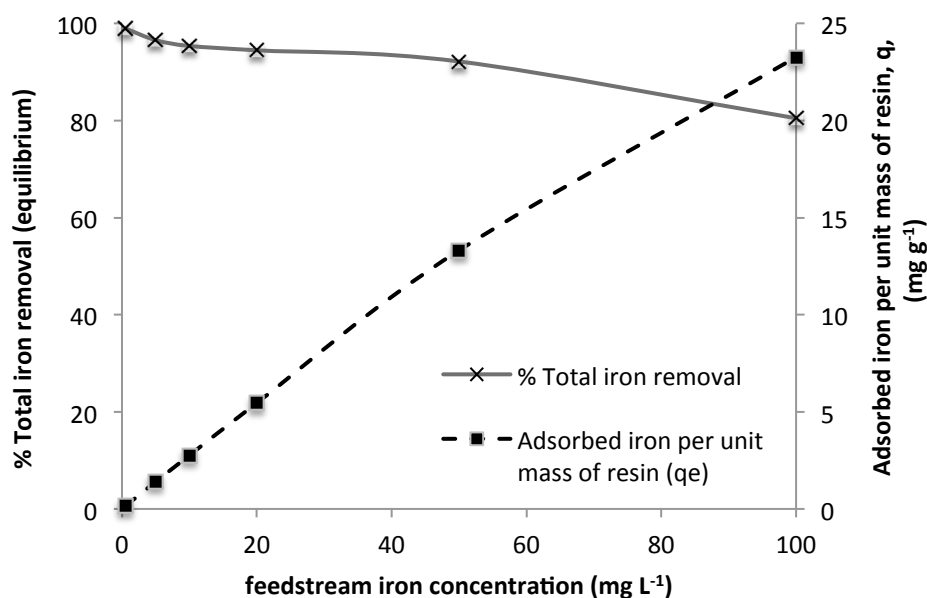


Figure 7.2. Effect of feedstream concentration on iron removal and on adsorption capacity of Dowex Marathon C, q_e (iron concentration = 0.5 - 100 mg L⁻¹, resin dosage = 3.5 g L⁻¹, temperature = 298 K, pH = 4.0 and volume = 2 L).

Results showed that iron ions sorption onto the resin is strongly influenced by its concentration in the feedstream. It was obtained that the adsorption of iron onto Dowex Marathon C increases as feedstream iron concentration increased, from 0.143 mg g^{-1} for 0.5 mg L^{-1} initial iron concentration, to 23.27 mg g^{-1} for 100 mg L^{-1} iron in the feedstream. This tendency was also observed by Bulai and Cioanca, 2011, for iron adsorption on Purolite S930-H.

On the contrary, it was found that the iron removal efficiency decreases from 97.0 % for 0.5 mg L^{-1} iron in the feedstream, to 81.0 % for the highest assayed concentration (100 mg L^{-1} iron in the feedstream) under identical IE operating conditions in terms of contact time and temperature. The decrease in the removal % with the iron concentration in the feedstream could be related to saturation of the IE resin (Senthil and Gayathri, 2009).

However, the decrease in the IE efficiency with iron concentration in the feedstream was confirmed to be significantly lower than that reported by other authors. For instance, Bulai and Cioanca, 2011, reported that the removal efficiency on Purolite S930-H decreased from 95 % (for 10 mg L^{-1} iron) to 20 % (for 300 mg L^{-1} iron), at a fixed resin dosage equal to 1.0 g L^{-1} .

Finally, the equilibrium was reached in about 30 min and from this point forward the removal efficiency was above 96 % (Fig. 2) for iron concentrations in the feedstream between 0.5 and 5 mg L^{-1} , which is the range of interest for iron removal from OMW-2ST (iron concentrations usually are below 5 mg L^{-1} after the mentioned secondary treatment). Thereby, the concentration value in the eluting stream was ensured to be lower than the legislated limits for reuse of the purified effluent.

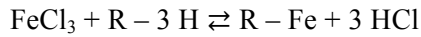
7.3.2 Equilibrium isotherms

The experimental data at equilibrium amount of adsorbed iron on Dowex Marathon C (q_e) and the concentration of iron in the liquid phase (C_e) at a constant temperature were used to describe the optimum isotherm model. The linear forms of Langmuir, Freundlich and Temkin equations were used to describe the equilibrium data. The performance of each form was judged through the correlation coefficients (R^2).

Ion exchange resins, after coming in contact with the solution, exchanges counter ions and attain equilibrium. The exchange is reversible in nature and the concentration ratio of both ions might not be the same in the two phases i.e. resin and solution phase (Helferrich, 1962).

The description of the equilibrium in the IE system is usually made by equilibrium isotherms, which represent the distribution of the adsorbed solute in the resin (Fe_{adsorbed}) and the free solute in the fluid phase (Fe_{solution}), in equilibrium.

The IE reaction of the iron system using the cationic resin Dowex Marathon C can be represented by:



When iron solution takes contact with Dowex Marathon C, the resin fixes iron ions and releases protons.

In this work, the IE capacity of the resin has been evaluated as a function of the pollutant concentration by determining its loading capacity q_e (mg of pollutant / g of adsorbent) (Eq. 2).

$$q_e = (C_0 - C_e) \cdot \frac{V}{m_s} \quad (2)$$

C_0 represents the initial iron concentration in the inlet stream, C_e refers to the equilibrium iron concentration (mg of iron L⁻¹ of solution), V (m³) is the volume of the iron solution and m_s (kg) is the corresponding resin amount.

Adsorption isotherms play a crucial role in the predictive modelling procedures for the analysis and design of adsorption systems, which are essential for real-scale operation (Ould Brahim et al., 2014).

Langmuir isotherm model is employed to predict the IE of aqueous compounds onto a solid phase (Langmuir, 1918). This mechanistic model accepts that a monolayer of adsorbed material is adsorbed over a uniform adsorbent surface (a flat surface of solid phase) at a constant temperature, and that the distribution of the compound between the two phases is controlled by the equilibrium constant. Hence, under equilibrium conditions rates corresponding to adsorption and desorption processes should be equal. The Langmuir isotherm is given by the following expression:

$$q_e = \frac{q_m \times K_L \times C_e}{1 + K_L \times C_e} \quad (3)$$

where C_e is the equilibrium concentration in the solution (mg L⁻¹), q_m and K_L are the Langmuir constants, representing the maximum IE capacity for the solid phase (resin) loading and the energy constant related to the uptake heat, respectively.

Freundlich isotherm model is an empirical relationship describing the IE of solutes from a liquid phase to a solid surface, which assumes that different sites with several uptake energies are involved (Freundlich, 1906). It is commonly used to describe the adsorption characteristics for heterogeneous surfaces. Freundlich isotherm represents the relationship between the amounts of

ionic species exchanged per unit mass of resin, q_e , and the concentration of the ionic species at equilibrium, C_e . The Freundlich exponential equation is given as:

$$q_e = K_f C_e^{1/n} \quad (4)$$

where K_f and n are the Freundlich constants, characteristic of the system, indicators of the IE capacity and intensity, respectively.

Also, Temkin isotherm model was finally tested to model the adsorption potential of Dowex Marathon C resin towards iron. This model takes into account the effects of indirect adsorbent (resin) /adsorbate (iron) interactions on the adsorption process. The model is given by Eq.(5), like follows:

$$q_e = B \cdot \ln(A \cdot C) \quad (5)$$

where A ($L \text{ mg}^{-1}$) is the equilibrium binding constant, corresponding to the maximum binding energy, and constant B is related to the heat of adsorption. Temkin isotherm contains a factor that explicitly takes into account the resin-exchanged species interactions. This isotherm assumes that the uptake (IE) heat of all molecules in the layer decreases linearly with the coverage due to resin-exchanged species interactions, and that IE is characterized by a uniform distribution of binding energies, up to some maximum binding energy.

The isotherm experimental data as well as the fit to the three tested isotherm models are shown in Figure 7.3. The relevant coefficients of each model and the calculated linear fit means squares are also reported in Table 7.2.

For Langmuir isotherm, the adsorption of iron onto Dowex Marathon C resin is described by means of q_m , K_L and R^2 values. The results indicate that the linear form of Langmuir model fits well with experimental data, as indicated by the high value of the regression coefficient ($R^2 > 0.99$) (Figure 7.3). On the other hand, the maximum IE capacity, q_m , was calculated as 28.01 mg g^{-1} (Table 7.2). Furthermore, the separation factor R_L is a good characteristic of the Langmuir isotherm, which can be expressed in Eq.(6):

$$R_L = \frac{1}{1 + K_L \cdot C_0} \quad (6)$$

R_L values between 0 and 1 indicate favourable adsorption. In this case, the R_L values were in the range of 0.04-0.89, which is less than unity, for feedstream iron concentrations ranging $100\text{--}0.5 \text{ mg L}^{-1}$. These R_L values indicate that the adsorption of iron ions onto Dowex Marathon C cation exchange resin is a favourable process, and the data fit accurately the Langmuir isotherm model.

As it can be observed in Table 7.2, the maximum IE capacity (q_m) found for iron removal by Dowex Marathon C resin (28.0 mg g^{-1}) is much higher than that obtained for iron adsorption onto olive stones (2.12 mg g^{-1}) (Hodaifa et al., 2013). This fact suggests that Dowex Marathon C resin is around ten times more efficient than this natural adsorbent.

Furthermore, Ostroski et al. (2009) studied iron adsorption onto Zeolite NaY by Langmuir model. In this case, results showed that maximum adsorption capacity was 2.93 meq g^{-1} .

On the other hand, Bulai and Cioanca, 2011, observed that maximum experimental iron adsorption capacity was close to 30 mg g^{-1} for Purolite S930, when initial iron concentration was 100 mg L^{-1} . This value was similar to that found by the authors for 100 mg L^{-1} initial iron concentration (23.27 mg g^{-1}).

Table 7.2. Langmuir, Freundlich and Temkin isotherm parameters for iron ions uptake on Dowex Marathon C resin.

Pollutant	Langmuir model				Freundlich model			Temkin model		
	$q_{m, \text{exp}}$	K_L	q_m	R^2	K_f	n	R^2	A	B	R^2
Iron	23.27	0.247	28.0	0.996	4.06	1.64	0.977	4.72	4.80	0.952

* Coefficient Units: $q_{m, \text{exp}}$ (mg g^{-1}); K_L (L mg^{-1}); q_m (mg g^{-1}); K_f (L mg^{-1}); A (L g^{-1})

Otherwise, concerning the equilibrium adsorption data of iron ions onto the studied resin adjusted to Freundlich isotherm model, the linear form of the isotherm at room temperature is employed to determine the value of K_f and n (Table 7.2). The value of R^2 (0.977) of Freundlich model was found to be lower than the value of R^2 (0.996) of Langmuir isotherm. The value of the n coefficient is higher than 1, which highlights the favourability of the adsorption process. Considering Figure 7.3, it can be noticed that Freundlich model is able to describe the adsorption empirical data with less reliability. Analogously, Pehlivan et al. demonstrated that Langmuir model described in a better way than Freundlich model the experimental data for adsorption of Cu^{2+} , Zn^{2+} , Ni^{2+} , Cd^{2+} and Pb^{2+} ions on Dowex 50W strong-acid cation exchange resin (Pehlivan and Altun, 2006).

On the other hand, the A and B parameters of the Temkin equation were calculated for iron ions adsorption (Table 7.2). It was obtained that the value of R^2 for Temkin model (0.952) is lower than that calculated for Freundlich model (0.977). The data of equilibrium isotherms for the system iron / Dowex Marathon C is better described by the Temkin model as it can be observed

in Figure 7.3. In addition, the heat of sorption process, estimated by Temkin isotherm model is 4.80 J mol^{-1} .

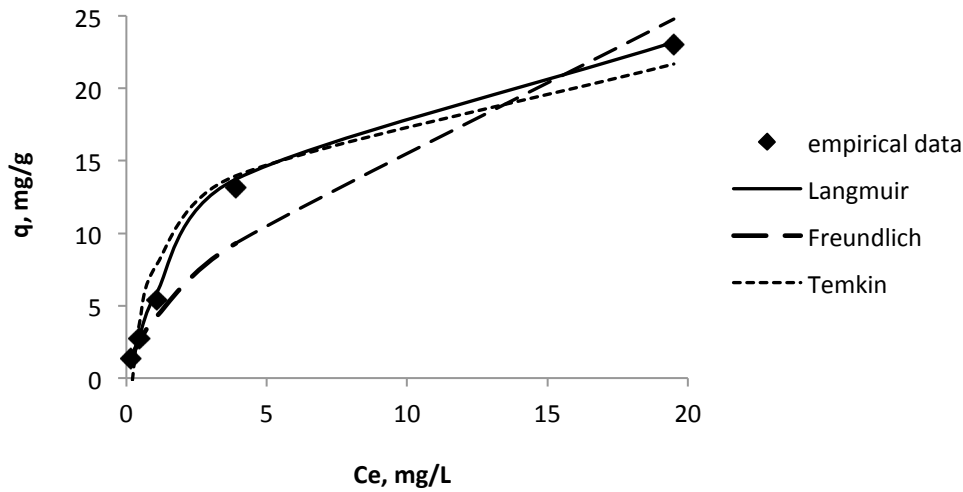


Figure 7.3. Langmuir, Freundlich and Temkin isotherms (iron concentration = $0.5 - 100 \text{ mg L}^{-1}$, resin dosage = 3.5 g L^{-1} , temperature = 298 K , pH = 4.0 and volume = 2 L).

7.3.3 IE kinetics

In order to study the adsorption rate of iron on the selected strong-acid cation exchange resin, experimental data obtained at several initial concentrations were fitted to different kinetic models. Namely the pseudo-first-order, the pseudo-second order and intraparticle diffusion models were tested. The reliability of these kinetic models was determined by measuring the coefficients of determination (R^2) and the sum of squares error (SSE). The SSE was calculated by the following equation (Eq. 6):

$$\text{SSE} = (q_{e,\text{exp}} - q_{e,\text{cal}})^2 \quad (7)$$

The adsorption rate constant could be determined from the pseudo first-order equation given by Lagergren et al. (1898), which is expressed as follows:

$$\log(q_e - q_t) = \log q_e - \left(\frac{k_1}{2.303}\right) \cdot t \quad (8)$$

where q_e and q_t refers to the amounts of iron adsorbed (mg g^{-1}) at equilibrium and time t (min), respectively, and k_1 is the first-order adsorption rate constant (min^{-1}).

Otherwise, the pseudo second-order equation based on equilibrium adsorption (Ho and McKay, 1999) can be expressed as:

$$\frac{dq}{dt} = \frac{1}{(k_2 q_e^2)} + \frac{1}{q_e} \cdot t \quad (9)$$

where, k_2 ($\text{g mg}^{-1} \text{min}^{-1}$) is the adsorption rate constant of pseudo second-order adsorption rate.

Finally, in order to investigate any possible mechanisms of iron adsorption onto Dowex Marathon C, intra-particle diffusion-based mechanism was also studied. According to this model, the uptake of the adsorbate by the adsorbent varies almost proportionately with the square root of the contact time ($t^{1/2}$). Weber and Morris (1962) proposed the most widely applied intra-particle diffusion equation for sorption systems as:

$$q_t = k_{id} t^{1/2} \quad (10)$$

where, q_t is the amount of iron adsorbed per unit mass of adsorbent (mg g^{-1}) at a time t , and k_{id} the intraparticle diffusion rate constant ($\text{mg g}^{-1} \text{min}^{-1/2}$). The rate parameter k_{id} of stage i is obtained from the slope of the straight line resulting of plotting q_t versus $t^{1/2}$.

The results of the fit of the experimental IE data to the different tested kinetic models are hereafter summarized in Tables 7.3 and 7.4. The values for parameters obtained after application of the kinetic models were used to predict the variation of adsorbed iron ions with time. The resulting curves and kinetic parameters are shown in Figures 7.4, 7.5 and 7.6.

For the first-order kinetics model, the values of k_1 and q_e were calculated from the slope and the intercept of the plots of $\log(q_e - q_t)$ versus t respectively at different concentrations (Figure 7.4). The results summarized in Table 7.3 show that the values of R^2 are relatively low and the experimental q_e values do not agree well with the calculated values. This reveals that the adsorption of iron onto Dowex Marathon C resin does not follow first-order kinetics.

Otherwise, the value of q_e and k_2 could be calculated from the slope and intercept of the plot of t/q_t versus t respectively. The results plotted in Figure 7.5 show linear plots for all the assayed initial concentrations, with very high values of R^2 in addition to the good agreement between the experimental and calculated values of q_e (Table 7.3). Therefore, the adsorption rate of iron onto Dowex Marathon C fits with utmost accuracy the pseudo second-order kinetics.

On the other hand, if the intraparticle diffusion is the controlling mechanism of the adsorption process, then the plot of q_t versus $t^{1/2}$ should be linear, and if it passes through the origin, the rate limiting process is only due to the intraparticle diffusion (Elmorsi, 2011).

Table 7.3. Adsorption kinetic parameters for the adsorption process (iron concentration = 0.5 - 100 mg L⁻¹, resin dosage = 3.5 g L⁻¹, temperature = 298 K, pH = 4.0 and volume = 2 L).

First-order kinetic model						Second-order kinetic model			
[Iron]	q _{e, exp}	q _{e, cal}	k ₁	R ²	SSE	q _{e, cal}	k ₂	R ²	SSE
0.5	0.143	0.227	0.050	0.956	0.007	0.145	4.96	1.0000	0.0038
5	1.40	0.302	0.054	0.915	0.118	1.422	0.420	0.9998	0.0532
10	2.76	1.00	0.062	0.969	0.226	2.87	0.120	0.9998	0.0904
20	5.46	2.533	0.067	0.971	0.556	5.80	0.043	0.9995	0.2191
50	13.32	6.05	0.066	0.946	1.824	14.205	0.017	0.9991	0.7545
100	23.27	11.074	0.064	0.978	3.044	24.752	0.0095	0.9995	1.2677

Units used of the above terms are as follow: [Iron], mg L⁻¹, q_e = mg g⁻¹, k₁ = min⁻¹, k₂ = g mg⁻¹min⁻¹.

Fig. 6 reports the results of the fit of the experimental data to the intraparticle diffusion model for the studied feedstream concentrations range. The results indicate that the plots of t_q vs. $t^{1/2}$ are not linear over the whole operating time. Furthermore, it can be seen that the intraparticle diffusion of iron occurred in two sequential stages: the first straight portion is attributed to the macropore diffusion (phase I) whereas the second linear portion might be mainly related to micropore diffusion (phase II) (Weber and Morris, 1962). The intraparticle diffusion constants for these two stages (k_{1d} and k_{2d}) are given in Table 7.4. Results indicated that the adsorption of iron onto the investigated resin involved more than one process. Such finding is supported by former results obtained in previous works on metal ions adsorption by Elmorsi (Ho and McKay, 1999). In addition, the sorption rate was generally fast and the intraparticle diffusion was found to be the rate-limiting step, which occurred in the same way in case of sorption of other metal ions (Prasad and Saxena, 2004).

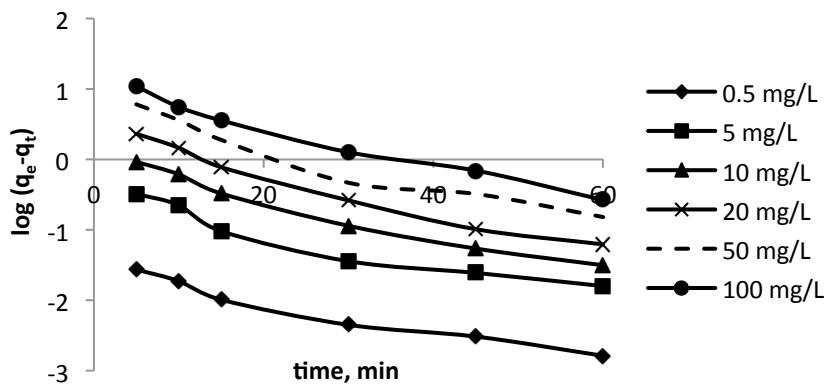


Figure 7.4. Pseudo-first-order kinetics for the adsorption process (iron concentration = 0.5 - 100 mg L⁻¹, resin dosage = 3.5 g L⁻¹, temperature = 298 K, pH = 4.0 and volume = 2 L).

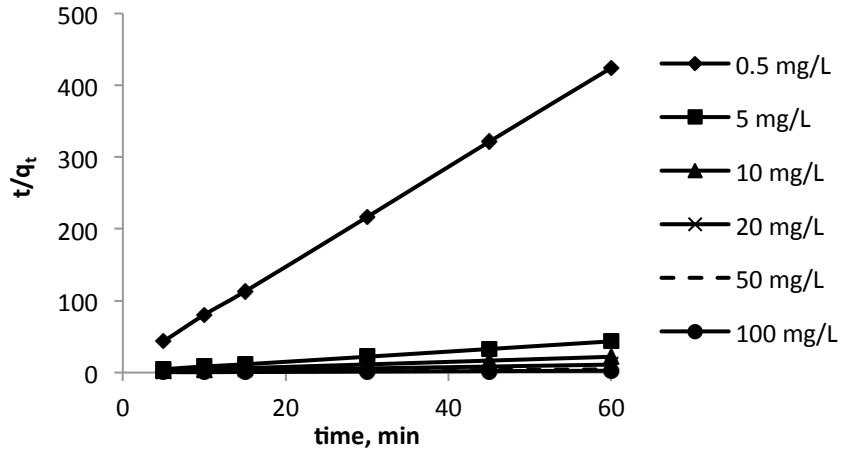


Figure 7.5. Pseudo-second-order kinetics for the adsorption process (iron concentration = 0.5 - 100 mg L⁻¹, resin dosage = 3.5 g L⁻¹, temperature = 298 K, pH = 4.0 and volume = 2 L).

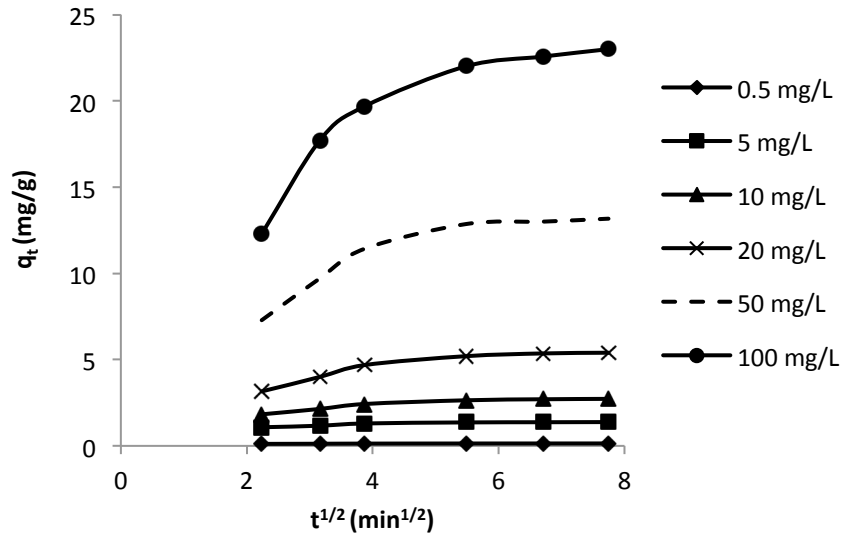


Figure 7.6. Intraparticle diffusion plot for the IE process (iron concentration = 0.5 - 100 mg L⁻¹, resin dosage = 3.5 g L⁻¹, temperature = 298 K, pH = 4.0 and volume = 2 L).

As it can be seen, the relative errors of the second-order model are lower than in both other models, and the correlation coefficients of the second-order model were found to be higher, indicating that this model describes better the adsorption of iron on Dowex Marathon C. On the other hand, results indicate that the adsorption kinetic coefficients were dependent on the initial iron concentration. Table 7.3 shows that the lowest differences between the theoretical $q_{e,cal}$ and the experimental $q_{e,exp}$ equilibrium adsorption capacity values are ensured by the second order rate equation. Nevertheless, the intraparticle diffusion equations also provide a good fitting of the experimental data points for the whole set of the tested initial concentrations. Considering all these results, the kinetics of iron adsorption on the selected strong-acid cation exchange resin

could be satisfactorily described by both pseudo-second order and intraparticle diffusion model equations.

Table 7.4. Weber-Morris parameters (iron concentration = 0.5 - 100 mg L⁻¹, resin dosage = 3.5 g L⁻¹, temperature = 298 K, pH = 4.0 and volume = 2 L).

[Iron]	k_{1d} (mg g ⁻¹ min ^{-1/2})	R^2	k_{2d} (mg g ⁻¹ min ^{-1/2})	R^2
0.5	0.0104	0.9943	0.0031	0.9976
5	0.1381	0.9783	0.0088	0.9989
10	0.3652	0.9977	0.0369	0.9589
20	0.9417	0.9999	0.0894	0.9213
50	2.5354	0.9995	0.1378	0.9897
100	4.5869	0.9652	0.4415	0.9989

Finally, the standard free energy (ΔG°) was calculated with the following equations (Alzaydien, 2009):

$$\Delta G = -RT \ln K_c \quad (11)$$

$$K_c = \frac{q_e}{C_e} \quad (12)$$

where T is the temperature (K), R is the ideal gas constant (kJ mol⁻¹K⁻¹), K_c is the standard thermodynamic equilibrium constant (L g⁻¹), q_e is the amount of adsorbed iron per unit mass of resin at equilibrium (mg g⁻¹) and C_e is the equilibrium aqueous concentration of iron. The Gibbs free energy change (ΔG°) was found to be -22.03 kJ mol⁻¹, indicating that the adsorption process of iron onto Dowex Marathon C is spontaneous.

To sum up, the performance of the tested kinetic models compared by judging the value of SSE (listed in Table 7.3) confirms that the pseudo-second-order kinetic model yielded the lowest SSE values (from 0.0038 to 1.2677). However, intraparticle diffusion should either be considered. Otherwise, the first-order model led to much higher values of SSE (from 0.007 to 3.044). A similar trend was reported by Gupta et al., who pointed out that the majority of the studies of metal ions adsorption might be divided into either pseudo first-order or second-order kinetics. This division was established on the basis of the best fit obtained by various research groups, although the second-order kinetics was found to be the predominant one (Gupta and

Bhattacharyya, 2011). This is in agreement with the previous values of both R^2 and $q_{e, cal}$ formerly obtained (Table 7.3), and supports the suitability of the pseudo-second-order kinetic model to describe the adsorption process of iron onto strong-acid cation exchange Dowex Marathon C resin.

7.4 Conclusions

The adsorption of iron onto Dowex Marathon C strong-acid cation exchange resin has been investigated on the basis of the feedstream iron concentration and contact time effects. The aim of the studies was to examine the potential of this ion exchange (IE) resin towards the removal of iron from Fenton-like secondary-treated olive mill wastewater (OMW-2ST).

The achieved results reveal that the removal efficiency of iron decreases as the concentration of iron in the feedstream increases. The equilibrium was reached after 30 min and from this point forward the removal efficiency was above 96 % for initial iron concentrations ranging between 0.5 and 5 mg L⁻¹ (typical concentration range in OMW-2ST). Thereby, the concentration of this compound in the eluting stream after IE was lower than the legislated limits for reuse of the purified effluent. Moreover, the IE efficiency towards iron was up to 92.2 % for concentration values as high as 50 mg L⁻¹. This means that Dowex Marathon C strong-acid cation exchange resin exhibits very significant potential for the removal of metal ions not only from the effluents by-produced in olive oil industries, but also from other contaminated wastewaters over a wide range of concentrations.

On the other hand, a thorough thermodynamic study of the IE process has been performed. The equilibrium behaviour of this pollutant has been accurately predicted by Langmuir isotherm ($R^2 > 0.99$). Furthermore, pseudo-first order, pseudo-second order and intraparticle diffusion models have been employed to predict the kinetics of iron adsorption on Dowex Marathon C. The results show that the correlation coefficients of the second-order model were the highest and also that the sum of squared errors (SSE) values were the lowest, both indicating that this model describes with utmost accuracy the adsorption of iron onto this IE resin.

This strong-acid cation exchange resin was confirmed to be considerably more efficient than natural adsorbents (such as olive stones or olive tree pruning) for the removal of iron from industrial effluents. This resin was found to provide fast kinetics in the uptake of iron (up to 4.96 g mg⁻¹ min⁻¹) as well as sensibly higher sorption capacity (28.0 mg g⁻¹) than biosorbents like olive stones (2.12 mg g⁻¹), and its price is lower than for similar synthetic resins used for metals removal.

7.5 References

Abdel-Ghani, N.T., Hefny, M., El-Chagbaby, G.A.F. (2007). Removal of Lead (II) from aqueous solution using low cost abundantly available adsorbents. *Int. J. Environ. Sci. Tech.*, 4(1):67-73.

Alzaydien, A.S. (2009). Adsorption of Methylene Blue from Aqueous Solution onto a Low-Cost Natural Jordanian Tripoli. *American Journal of Applied Sciences*, 5(3):197-208.

Andersen, W.C., Bruno, T.J. (2003). Application of gas-liquid entraining rotor to supercritical fluid extraction: removal of iron (III) from water. *Anal. Chim. Acta*, 485:1-8.

Aziz, H.A., Yusoff, M.S., Adlan, M.N., Adnan, N.H., Alias, S. (2004). Physicochemical removal of iron from semiaerobic landfill leachate by limestone filter. *Water Manage.*, 24:353-358.

Berbenni, P., Pollice, A., Canziani, R., Stabile, L., Nobili, F. (2000). Removal of iron and manganese from hydrocarbon-contaminated groundwaters. *Bioresour. Technol.*, 74:109-114.

Bulai, P., Cioanca, E. (2011). Iron removal from wastewater using chelating resin Purolite S930. *Tehnomus Journal*, 18:63-68.

Cho, B.Y. (2005). Iron removal using an aerated granular filter. *Process Biochem.*, 40:3314-3320.

Das, B., Hazarika, P., Saikia, G., Kalita, H., Goswami, D.C., Das, H.B., Dube, S.N., Dutta, R.K. (2007). Removal of iron by groundwater by ash: a systematic study of a traditional method. *J. Hazard. Mater.*, 141:834-841.

Beltrán De Heredia, J., Garcia, J. (2005). Process integration: continuous anaerobic digestion - ozonation treatment of olive mill wastewater. *Ind. Eng. Chem. Res.*, 44:8750-8755.

Ellis, D., Bouchard, C., Lantagne, G. (2000). Removal of iron and manganese from groundwater by oxidation and microfiltration. *Desalination*, 130:255-264.

Elmorsi, T.M. (2011). Equilibrium isotherms and kinetic studies of removal of methylene blue dye by adsorption onto miswak leaves as a natural adsorbent. *Journal of Environmental Protection*, 2:817-827.

European Commission, Council Directive 98/83/EC of 3 November 1998 on the quality of water intended for human consumption. Brussels, Belgium. 1998.

Freundlich, H.M.F. (1906). Over the adsorption in solution. *J. Phys. Chem.*, 57:385-471.

Grafias, P., Xekoukoulotakis, N.P., Mantzavinos, D., Diamadopoulos, E. (2010). Pilot treatment of olive pomace leachate by vertical-flow constructed wetland and electrochemical oxidation: an efficient hybrid process. *Water Res.*, 44(9):2773-2780.

Greenberg, A.E., Clesceri, L.S., Eaton, A.D. (1992). Standard Methods for the Examination of Water and Wastewater, APHA/AWWA/WEF, 16th ed., Washington DC. Cabs.

Gupta, S.S., Bhattacharyya, K.G. (2011). Kinetics of adsorption of metal ions on inorganic materials: A review. *Advances in Colloid and Interface Science*, 162:39-58.

Helfferich, F.G. 1962. Ion Exchange. McGraw Hill Book Company, New York.

Ho, Y.S., McKay, G. (1999). Pseudo-Second Order Model for Sorption Processes. *Process Biochemistry*, 34:735-742.

Hodaifa, G., Ochando-Pulido, J.M., Alami, S.B.D., Rodríguez-Vives, S., Martínez-Férez, A. (2013). Kinetic and thermodynamic parameters of iron adsorption onto olive stones. *Industrial Crops and Products*, 49:526-534.

Hodaifa, G., Alami, S.B.D., Ochando-Pulido, J.M., Víctor-Ortega, M.D. (2014). Iron removal from liquid effluents by olive stones on adsorption column: breakthrough curves. *Ecological Engineering*, 73:270-275.

Lafi, W.K., Shannak, B., Al-Shannag, M., Al-Anber, Z., Al-Hasan, M. (2009). Treatment of olive mill wastewater by combined advanced oxidation and biodegradation. *Separ. Purif. Technol.*, 70(2):141-146.

Lagergren, S. (1898). Zur theorie der sogenannten adsorption gelöster stoffe, Kungliga Svenska Vetenskapaskademiens. *Handlingar*, 24(4):1-39.

Langmuir, I. (1918). The adsorption of gases on plane surfaces of glass, mica and platinum. *J. Am Chem Soc.*, 40(8):1361-1403.

Martínez Nieto, L., Hodaifa, G., Rodríguez Vives, S., Giménez Casares, J.A. (2010). Industrial plant for olive mill wastewater from two-phase treatment by chemical oxidation. *J. Environ. Eng.*, 136(11):1309-1313.

Munter, R. Ojaste, H., Sutt, J. (2005). Complexed iron removal from ground water. *J. Environ. Eng.*, 131:1014-1020.

- Ostroski, I.C., Barros, M.A.S.D., Silva, E.A., Dantas, J.H., Arroyo, P.A., Lima, O.C.M. (2009). A comparative study for the ion exchange of Fe(III) and Zn(II) on zeolite NaY. *J. Hazard. Mater.*, 161:1404-1412.
- Ould Brahim, I., Belmedani, I.M., Belgacem, A., Hadoun, H., Z. Sadaoui, Z. (2014). Discoloration of azo dye solutions by adsorption on activated carbon prepared from the cryogenic grinding of used tires. *Chemical Engineering Transactions*, 38:121-126.
- Papastefanakis, N., Mantzavinos, D., Katsaounis, A. (2010). DSA electrochemical treatment of olive mill wastewater on Ti/RuO₂ anode. *J. Appl. Electrochem.*, 40(4):729-737.
- Paraskeva, P., Diamadopoulos, E. (2006). Technologies for olive mill wastewater (OMW) treatment: A review. *J. Chem. Technol. Biotechnol.*, 81, 475-1485.
- Pehlivan, E., Altun, T. (2006). The study of various parameters affecting the ion exchange of Cu²⁺, Zn²⁺, Ni²⁺, Cd²⁺, and Pb²⁺ from aqueous solution on Dowex 50W synthetic resin. *J. Hazard. Mater.*, 134:149-156.
- Prasad, M., Saxena, S. (2004). Sorption mechanism of some divalent metal ions onto low-cost mineral adsorbent. *Industrial & Engineering Chemistry Research*, 43(6):1512-1522.
- Senthil Kumar, P., Gayathri, R. (2009). Adsorption of Pb²⁺ ions from aqueous solutions onto bael tree leaf powder: isotherms, kinetics and thermodynamics study. *J. Eng. Sci. Technol.*, 4(4):381-399.
- Shalini, C., Pragnesh, N.D. (2012). Removal of iron for safe drinking water. *Desalination*, 303:1-11.
- Stoller, M., Bravi, M. (2010). Critical flux analyses on differently pretreated olive vegetation wastewater streams: some case studies. *Desalination*, 250:578-582.
- Tahir, S.S., Rauf, N. (2004). Removal of Fe²⁺ from the waste water of a galvanized pipe manufacturing industry by adsorption onto bentonite clay. *J. Environ. Manage.*, 73:285-292.
- Temkin, M.J., Pyzhev, V. (1940). Recent modifications to Langmuir isotherms. *Acta Physicochim URSS.*, 12:217-222.
- Tezcan Ün, Ü., Altay, U., Koparal, A.S., Ogutveren, U.B. (2008). Complete treatment of olive mill wastewaters by electrooxidation. *Chem. Eng. J.*, 139:445-452.

-
Vaaramaa, K., Lehto, J. (2003). Removal of metals and anions from drinking water by ion exchange. *Desalination*, 155:157-170.

Victor-Ortega, M.D., Ochando-Pulido, J.M., Hodaifa, G., Martínez-Férez, A. (2014). Final purification of synthetic olive oil mill wastewater treated by chemical oxidation using ion exchange: Study of operating parameters. *Chem. Eng. Process.*, 85:241-247.

Volesky, B. (2001). Detoxification of metal-bearing effluents: biosorption for the next century. *Hydrometallurgy*, 59:203-216.

Weber Jr., W.J., Morris, J.C. (1962). Kinetic of Adsorption on Carbon from Solution. *Journal of the Sanitary Engineering Division*, 89:31-59.

CHAPTER 8

IRON REMOVAL AND REUSE FROM FENTON-LIKE PRETREATED OLIVE MILL WASTEWATER WITH NOVEL STRONG-ACID CATION EXCHANGE RESIN FIXED-BED COLUMN

M.D. Víctor-Ortega*, J.M. Ochando-Pulido, A. Martínez-Ferez

Chemical Engineering Department, University of Granada, 18071 Granada, Spain

*email: mdvictor@ugr.es

Submitted for publication. Current status: under review.

Journal of Industrial and Engineering Chemistry

Publisher: ELSEVIER SCIENCE INC. 360 PARK AVE SOUTH, NEW YORK, NY 10010-1710

Year: 2015

ISSN: 1226-086X

Impact factor: 3.50

Tertile: First



Abstract

The performance of a fixed-bed cation exchange process was examined for final purification of the iron load derived from catalyst usage in the secondary treatment of olive mill wastewater, which led to unacceptable iron levels. Results showed an increase in the pH value up to 4 enhanced the iron IE efficiency, which decreased upon higher pH. Furthermore, Thomas model provided utmost accurate dynamic behaviour modelling for all inlet concentrations studied (20, 50 and 100 mg L⁻¹). Additionally, up to 100 % recovery efficiencies were maintained even after 10 complete cycles. Finally, an effluent with quality for irrigation reuse was obtained.

Keywords: Breakthrough curves, Industrial wastewaters, Olive mil wastewater, Ion exchange, Iron, Strong-acid cation exchange resin.

8.1 Introduction

In the past few decades, water resources are becoming insufficient in order to satisfy the increasing demand of fresh water worldwide. Water scarcity specially concerns agricultural irrigation, which demands more than 70 % of the total water consumption worldwide (FAO, 2003). What is more, the intensive development of industry is causing deterioration of the environmental quality. Within this context, removal of metal ions from industrial wastewaters is vital for the development of industries. Contamination due to the presence of iron species can be found currently in natural waters (Ahmetli and Tarlan, 2007), mining effluents (Gaikwad, 2010), hydrometallurgical solutions (McKevitt and Dreisinger, 2009) and a range of other industrial wastes (Agrawal et al., 2009).

On the other hand, there is a certain potential to use regenerated wastewater for irrigation purposes, representing a solution with very positive environmental and economic benefits. Several methods have been employed to remediate contaminated solutions including precipitation (Once et al., 2013), coagulation–flocculation (Abu Baker and Halim, 2013), adsorption (Kyzas and Kostoglou, 2014; Kyzas and Kostoglou, 2014; Nguyen et al., 2013), ion exchange (IE) (Amin et al., 2014; Badawy et al., 2013), membrane filtration (Mungray et al., 2012), flotation (Dai et al., 2012; Zak, 2012) and electrochemical procedures (Shafaei et al., 2011).

In particular, IE and adsorption processes may be a potential solution for wastewater reclamation when metal ions are present in moderate concentrations in the effluent. Concretely, IE is of particular interest since the metals can be potentially recovered, and the technology is simple and effective (Dabrowski et al., 2004). Compared with conventional separation and purification methods, IE provides several advantages involving lower operational costs, ease in

handling, low consumption of reagents if properly optimized, as well as the possibility of recovering added-value components through desorption and regeneration of IE resins (Bulai and Cioanca, 2011; Abdel-Ghani et al., 2007).

In the present work, the performance of a fixed-bed IE process was addressed for the final purification of the iron load in a secondary-treated olive mill wastewater stream (OMW-2ST). Industrial effluents from olive oil industry are among the most recalcitrant and organic-polluted, up to a hundred times more than urban wastewaters, also presenting high saline toxicity. In previous work, the authors optimized and scaled-up a secondary treatment process for olive mill wastewater based on Fenton-like advanced oxidation, which successfully achieved high organic matter abatement efficiencies. However, the use of a ferric catalyst during the process leads to an increase of the iron concentration in the treated effluent exiting the Fenton-like reactor (Martínez Nieto et al., 2010; Hodaifa et al., 2013a) up to unacceptable levels (more than 14 mg L⁻¹) (European Commission, 1998).

Within this framework, continuous packed-bed column IE system may be a suitable and cost-efficient solution for the remediation of heavy metals in aqueous systems. Some studies can be found in the literature dealing with iron removal by means of strong acid-cation exchange resins (Kaya et al., 2002; Benítez et al., 2002; Marañón et al., 2005; Millar et al., 2015), chelating IE resins (Benítez et al., 2002; Lasanta et al., 2005; Woodberry et al., 2007; Rao et al., 2005) as well as weak acid cation exchange resins (Riveros, 2004).

Nevertheless, some researchers have underlined the lack of scientific literature focusing on the fundamental of IE process involved in the treatment of dilute iron solutions (Agrawal et al., 2009; Millar et al., 2015). Deeper insight into the column behaviour of the IE process is needed to provide a better understanding of the practical application for the effective transference to industrial scale.

In the present research work, the performance of a fixed-bed IE process based on a strong-acid cation exchange resin was fully investigated. The influence of some key parameters on the IE performance and removal efficiency was elucidated, comprising the inlet concentration, the system pH and the equilibrium information related to the IE column breakthrough behaviour, which provides information about the dynamic behaviour of the metal concentration in time indispensable for appropriate column design (Sag et al., 2001; Guangyu and Viraraghavan, 2001). Column experiments were carried out to examine the breakthrough curves for different inlet iron concentrations. Moreover, the IE process was also modelled by fitting the experimental data to various adsorption models.

Ultimately, the impact of the regenerating conditions on the reusability of the resin and on the long-term IE efficiency was also determined by carrying out multiple adsorption–desorption–washing cycles, to address the potentiality for the industrial scale-up of the proposed process. Finally, the compliance of the real final treated effluent with irrigation standards was checked.

8.2 Methods and materials

8.2.1 Ion exchange resin

The resin used in this research work was a strong-acid cation exchange resin (Dowex Marathon C), which was supplied by Sigma Aldrich. Firstly, the selected cation exchange resin was conditioned in hydrochloric acid solution and finally in water before being used in the IE and desorption experiments, following the advice given by the resin manufacturer. The chosen resin presents sulfonic acid functional group and the ionic form H^+ , in styrene-DVB gel matrix. The physical and chemical characteristics of the used resin are hereafter summarized in Table 8.1.

Table 8.1. Physicochemical properties of Dowex Marathon C resin.

Type	Strong-acid cation
Matrix	Styrene-DVB, gel
Ionic form as shipped	H^+
Functional group	Sulfonic acid
Particle size, mm	0.55-0.65
Effective pH range	0-14
Total exchange capacity, eq L⁻¹	1.80
Shipping weight, g L⁻¹	800

8.2.2 Ion exchange bench-scale plant

The IE column, set-up as fixed-bed, was made of an acrylic tube with dimensions 540 mm height x 46 mm internal diameter. The IE equipment was provided with a mobile upper retaining grid, which could be fixed in the column to adjust it as a fixed bed or a semi-fluidized bed. A fixed amount of 69.2 g of the selected cation exchange resin was packed in the column, which resulted in 25.5 cm bed height of adsorbent. The desired effluent flow rate through the IE column could be adjusted and controlled by means of a peristaltic pump (Ecoline VC-380). A flow-scheme of the used IE plant is shown in Figure 8.1.

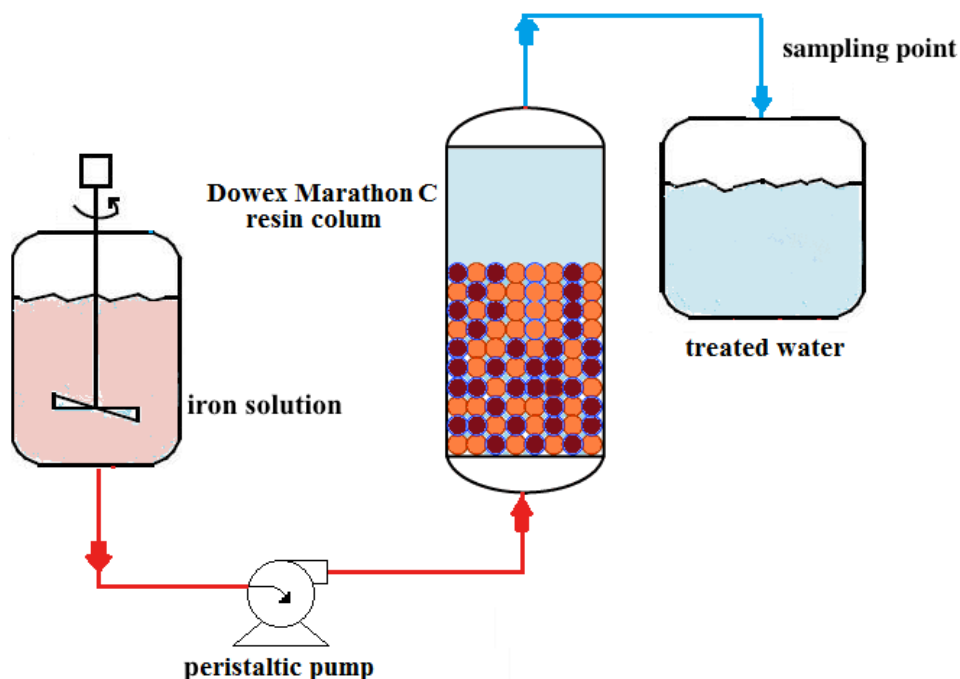


Figure 8.1. Flow-sheet scheme of packed-bed IE continuous system operation.

For the experiments, iron solutions were prepared by dissolving reagent-grade iron (III) chloride 30% (w/w) aqueous solution (provided by Panreac) in double distilled water. On the other hand, HCl 37% solution, which was used in the regeneration process, was also provided by Panreac.

8.2.3 Analytical methods

Analytical grade reagents and chemicals with purity over 99% were used for the analytical procedures, applied at least in triplicate. For the measurement of the total iron concentration, all iron ions were reduced to iron ions (II) in a thioglycolate medium with a derivative of triazine, forming a reddish-purple complex that was determined photometrically at 565 nm (Standard German methods ISO 8466-1 and German DIN 38402 A51) (Greenberg et al., 1992).

8.2.4 Inlet pH impact

The impact of the inlet pH (pH_0) on the IE performance for the final purification of the iron load in OMW-2ST was examined by varying the pH_0 values in the range 1 - 7, conducting recirculation mode experiments. With this purpose, the pH_0 value was adjusted by adding 0.1N NaOH or HCl solution, depending on the desired value, while maintaining the resin dosage constant (3.5 g L^{-1}). The flow rate and the temperature were fixed at 10 L h^{-1} and room temperature, respectively (V́ctor-Ortega et al., 2014), whereas the contact time was varied up to 60 min in order to reach equilibrium.

IE equilibrium was examined by performing recirculation mode experiments with the goal of obtaining the key equilibrium parameters of total iron/H⁺ IE process. The extent of the IE equilibrium data of iron species was determined by measuring the residual total iron concentration in the liquid phase. Previously, aqueous solutions of this contaminant were put in contact with the IE resin until equilibrium was achieved. The flask containing the feed solution was stirred continuously during the whole course of the experiments.

The removal efficiency was determined by computing the sorption percentage with Eq.(1):

$$\% \text{ Sorption} = \frac{C_0 - C_e}{C_0} \times 100 \quad (1)$$

where C_0 and C_e are the initial and equilibrium iron concentration (mg L^{-1}), respectively.

8.2.5 Fixed-bed column studies

Fixed-bed studies were performed by pumping iron solutions with different concentration values equal to 20 mg L^{-1} , 50 mg L^{-1} and 100 mg L^{-1} , at a flow rate of 10 L h^{-1} through the IE column, maintaining the pH at the value (2.6 ± 0.1) in the range of the one typically measured in the effluent exiting the secondary treatment (OMW-2ST).

Iron solutions at the outlet of the column were collected at regular time intervals. Aliquots were removed periodically, and the concentration of iron present in the effluent was spectrophotometrically determined as thoroughly described in *section 2.3*. The amount of adsorbed iron was calculated on the basis of the difference between the inlet concentration (C_0) and outlet concentration (C_t).

The IE efficiency of the cationic exchange fixed-bed column was evaluated by determining the breakthrough curves. The time for breakthrough appearance and the shape of the breakthrough curves are very important characteristics for determining the operation performance and the dynamic response of adsorption columns.

In order to avoid discrepancies and for utmost accuracy of the results, the breakthrough curves were represented as a function of treated volume in terms of normalized concentration, C_t/C_0 , defined as the ratio of outlet iron concentration, C_t (mg L^{-1}) to inlet iron concentration, C_0 (mg L^{-1}). The experimental curves were mathematically modelled by means of non-linear regression, and the parameters were estimated using the *MS Excel 2011* program.

The breakthrough time t_B is defined as the time required for the concentration of metal ions in the effluent to reach 5 % of the inlet concentration. Otherwise, the exhaustion time t_E makes reference to the time at which the concentration of metal ions in the effluent becomes 90 % of

the feedstream concentration.

The breakthrough volumes VB and exhaustion volumes VE are the effluent volumes at breakthrough time and exhaustion time, respectively. The effluent volume (V_{eff}) can be calculated with the following equation (Eq. (2)):

$$V_{\text{eff}} = Q \cdot t_{\text{total}} \quad (2)$$

where t_{total} and Q are the total flow time (min) and the volumetric flow rate (ml min^{-1}), respectively. The area under the breakthrough curve (A), obtained by integrating the adsorbed concentration C_{ad} (mg L^{-1}) vs. t (min) plot, was used to calculate the total adsorbed metal quantity, that is, the maximum column capacity.

The total adsorbed metal quantity q_{total} (mg g^{-1}) in the column for a given feed concentration and flow rate (Q) can be calculated as follows:

$$Q_{\text{total}} = Q \cdot \frac{(C_0 - C_t)}{1,000} \cdot t_{\text{total}} \quad (3)$$

The total amount of metal ions sent to the IE column (m_{total}) was calculated from the following equation:

$$m_{\text{total}} = \frac{C_0 \cdot Q}{1,000} \cdot t_{\text{total}} \quad (4)$$

The total removal efficiency of iron is the ratio of the maximum capacity of the column (q_{total}) to the total amount of iron driven into the column (m_{total}):

$$\text{Total removal efficiency (\%)} = \frac{q_{\text{total}}}{m_{\text{total}}} \cdot 100 \quad (5)$$

The equilibrium metal uptake (q_{eq}) or maximum column capacity is defined by Eq. (5) as the total amount of metal sorbed (q_{total}) per gram of sorbent (X) at the end of the total flow time:

$$q_{\text{eq}} = \frac{q_{\text{total}}}{X} \quad (6)$$

8.2.6 IE process modelling: breakthrough curves

The time or bed volume for breakthrough appearance as well as the shape of the breakthrough curve are key parameters for the estimation of the operation and dynamic response of an adsorption column (XiaoFeng et al., 2014). In addition, the successful design for an adsorption column requires the prediction of the concentration-time profile from the breakthrough curve for the effluent discharged from the column. In order to describe and model the adsorption

process of iron on the selected IE resin, several models were therefore used to correlate the adsorption breakthrough curves’ experimental data.

The models, hereafter described in the following sections, were fitted to the experimental breakthrough curves by non-linear regression methods. The regression coefficient (R^2) was used to evaluate the fitting of the experimental data to the non-linearized forms of Thomas, Yoon-Nelson, and Clark equations, whereas the sum of the squares of the errors (SSE) calculated according to Eq. (7) served as an indicator of the goodness of the adjustment between the experimental data and predicted values of C/C_0 used for plotting the breakthrough curves:

$$SSE = (q_{e,exp} - q_{e,cal})^2 \quad (7)$$

where the subscripts ‘calc’ and ‘exp’ make reference to the calculated and experimental values, respectively, and n is the number of measurements.

8.2.6.1 Thomas model

Thomas model is applicable in systems with a constant flow rate and no axial dispersion, and its behavior matches the Langmuir isotherm and the second-order reversible reaction kinetics. The linearized form of the model is given by the following equation (Thomas, 1944):

$$\text{Ln} \left(\frac{C_0}{C_t} - 1 \right) = \frac{K_{Th} q_0 M}{Q} - \frac{K_{Th} C_0 M}{Q} V \quad (8)$$

where K_{Th} ($\text{ml mg}^{-1} \text{min}^{-1}$) is the Thomas rate constant, q_0 (mg g^{-1}) is the equilibrium adsorbate uptake, Q (ml min^{-1}) is the flow rate, and V (ml) is the effluent volume; C_t is the concentration of metal ion at time t and C_0 is the initial metal ion concentration.

8.2.6.2 Yoon–Nelson model

Yoon–Nelson model is based on the assumption that the increase in rate or decrease in the probability of adsorption for each adsorbate molecule is proportional to the probability of adsorbate adsorption and the probability of adsorbate breakthrough on the adsorbent. The Yoon–Nelson model not only is less complicated than other models but also requires no detailed data concerning the characteristics of the adsorbate, the type of adsorbent, and the physical properties of the adsorption bed.

The linearized model equation for a single-component system is represented by the following expression (Yoon and Nelson, 1984):

$$\text{Ln} \left(\frac{C_0}{C_t} - 1 \right) = K_{YN} \cdot t - \tau \cdot K_{YN} \quad (9)$$

where K_{YN} (min^{-1}) is the Yoon–Nelson rate constant, τ is the time required for 50 % adsorbate breakthrough (min), and t is the sampling time (min), whereas C_t is the concentration of metal ion at time t and C_0 is the initial metal ion concentration.

For a given bed:

$$q_{0YN} = \frac{C_0 \cdot Q \cdot \tau}{1.000 X} \quad (10)$$

where q_{0YN} is the adsorption capacity, C_0 is the initial metal ion concentration, Q is the flow rate, X is the weight of adsorbent, and τ is the 50 % breakthrough time.

8.2.6.3 Clark model

Clark model relies on the use of a mass-transfer concept, but in the form of the Freundlich adsorption equation (Clark, 1987). The linearized form of the model is given by the following expression:

$$\ln\left[\left(\frac{C}{C_0}\right)^{n-1} - 1\right] = -rt + \ln A \quad (11)$$

with

$$A = \left(\frac{C_0^{n-1}}{C_b^{n-1}} - 1\right) e^{rt_b} \quad (12)$$

and

$$r = \frac{\beta}{U} v_m (n - 1) \quad (13)$$

where n is the Freundlich constant, C_b is the concentration of sorbate at breakthrough time t_b (mg L^{-1}), and v_m is the migration velocity of the concentration front in the bed (cm h^{-1}).

8.2.7 Regeneration and reuse of the ion exchange resin

For the regeneration of the selected strong-acid cation exchange resin, a protocol consisting in washing with 200 mL 4 % HCl aqueous solution was carried out at room temperature. Iron ions were thereby removed and the concentration was determined as described in *section 2.2*. The resin was then washed with distilled water for the removal of the excess of acid and recondition. This procedure was carried out after each adsorption/regeneration cycle.

8.3 Results and discussion

8.3.1 Effect of inlet pH

The influence of the inlet value (pH_0) on iron IE efficiency is reported in Figure 8.2. The adsorption of iron ions was studied at different pH values in the range 1 - 7.

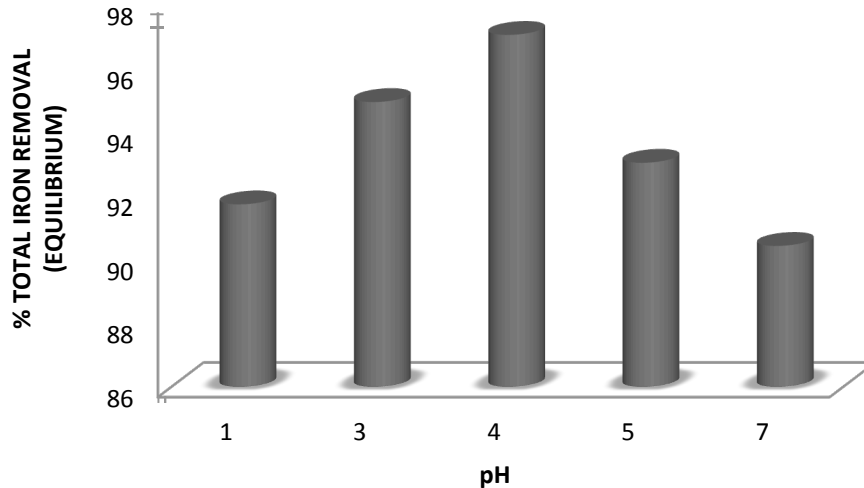


Figure 8.2. Effect of pH on iron removal onto Dowex Marathon C cation exchange resin (iron concentration = 50 mg L^{-1} , resin dose = 3.5 g L^{-1} and equilibrium time = 1 h).

As shown in Figure 8.2, iron ions IE removal efficiency increased with an increase in the pH value up to 4 - in line with the optimum pH for Fenton-like secondary treatment performance (Martínez Nieto et al., 2010) - but it can be observed that higher pH values led to lower IE efficiency. This is explained by the excessive protonation of the active sites of the selected strong-acid cation exchange resin at low pH values (below 4), which seems to hinder the formation of links between iron ions and the active sites of the cation exchange resin. Similar results were found by Senthil and Gayathri (2009) in their study on bael tree leaf powder as adsorbent to remove lead ions from aqueous solutions (Senthil and Gayathri, 2009).

On the other hand, at moderate pH_0 (3 - 5) the linked H^+ is released from the active sites of the cation exchange resin, and the extent of IE of iron ions is found to increase as a result of the acidification of the medium. However, further increasing the pH_0 , that is, above a value of 5, leads to decreased IE removal efficiencies, due to the fact that undesirable precipitation of metal hydroxides as dominant mechanism may yield reduced IE efficiency and hindrance of the cation exchange capacity.

These results are in the same line as those reported by other researchers with regard to pH as an

important parameter affecting IE process mechanisms. Millar et al. (2015) pointed out that adjusting the solution pH to a constant value of 2.2 by addition of sodium bicarbonate produced a favorable equilibrium isotherm (Millar et al., 2015). In contrast, the unmodified experiment wherein the pH was lowered due to release of protons from the resin resulted in an unfavorable exchange isotherm. In the column studies conducted by Rao et al. (2005) the solution pH was also noted to be an influential factor controlling the removal of iron from solution with a chelating IE resin (Rao et al., 2005). These authors observed that iron sorption efficiency decreased with increasing pH value on Duolite ES 467 resin. Approximately 30 % less iron was loaded on the resin at pH of 3 compared to pH equal to 2. Meanwhile, Hodaifa et al. (2013) found an initial pH equal to 2.9 as the optimum value in order to promote the adsorption performance of iron ions onto olive stones (Hodaifa et. al, 2013b).

8.3.2 Breakthrough curves experiments

The IE efficiency of the fixed-bed strong-acid cation exchange column was evaluated by determining the breakthrough curves. Column experiments were carried out to examine the breakthrough curves for different inlet iron concentrations. Breakthrough curves can be an effective tool for the appropriate design and operation of adsorption columns, as they provide information about the dynamic behavior of the metal concentration in time (Sag et al., 2001; Guangyu and Viraraghavan, 2001). The success of the column design for the adsorption process requires predicting the effect profile concentration-time curves of the effluents.

In particular, the time or bed volume for breakthrough appearance as well as the shape of the breakthrough curve are key parameters for the estimation of the operation and dynamic response of an adsorption column (XiaoFeng et al., 2014). Over the years, various mathematical models have been developed to analyze the column performances in the laboratory, key for the ulterior transference to industrial scale. In this research study, the mathematical models of Thomas, Clark and Yoon-Nelson in nonlinear forms were applied.

8.3.2.1 Effect of initial iron concentration on breakthrough curves

In our previous research works, a secondary treatment process for olive mill wastewater based on Fenton-like advanced oxidation was optimized and scaled-up, successfully achieving high organic matter abatement efficiencies. However, the use of a ferric catalyst during the process leads to an increase of the iron concentration in the treated effluent exiting the Fenton-like reactor (OMW-2ST) (Martínez Nieto et al., 2010; Hodaifa et al., 2013a) up to unacceptable levels (more than 14 mg L^{-1}) (European Commission, 1998). Moreover, these concentration values may become increased as a result of the fluctuations in the inlet concentrations of the

olive mill effluent.

To cope with this fact, the impact of the iron concentration in the OMW-2ST stream on the performance of the fixed-bed IE process was addressed for the final purification of the iron load in this effluent. With this purpose, the effect of the initial iron concentration on the profiles of the breakthrough curves was examined. Several initial concentrations (20, 50 and 100 mg L⁻¹) were studied, under constant flow rate and fixed bed height.

Figure 8.3 reports the effect of inlet iron concentration on the breakthrough curves for iron adsorption onto the selected strong-acid cation exchange resin in a fixed-bed column operating in continuous mode. In this figure, S-shaped curves can be observed for all three iron concentrations investigated. A focus on this figure also shows that increasing initial concentration values resulted in an earlier breakthrough curve. Moreover, the highest volume could be treated upon the lowest initial concentration, as a result of the increased diffusion or mass transfer coefficient.

Integration of the area above the breakthrough curve was performed for the determination of the iron loading on the IE resin. The obtained results of the iron loading capacity values were equal to 31.80, 45.16 and 59.24 mg Fe g⁻¹ when the initial concentrations were set at 20, 50 and 100 mg L⁻¹, respectively (see Table 8.2). This increase in the IE capacity could be explained by the fact that a higher influent iron concentration results in a higher driving force for the transfer process to overcome the mass transfer resistance (XiaoFeng et al., 2014). Similarly, Hodaifa et al. (2014) found the maximum adsorption capacity of iron onto olive stones on a packed column as 1.5 mg g⁻¹ for both inlet iron concentrations of 5 and 20 mg L⁻¹ (Hodaifa et al., 2014).

Table 8.2. Results of breakthrough curves’ estimated parameters at different inlet iron concentrations. Resin amount = 69.2 g; Temperature = 298 K; Flow rate = 10 L h⁻¹; pH = 4.

Inlet iron concentration (mg L ⁻¹)	t _{total} (min)	m _{total} (mg)	q _{total} (mg)	q _{eq} (mg g ⁻¹)	Removal %
20	390	2200	903	31.80	41.0
50	375	3050	1984	45.16	65.0
100	245	4100	3320	59.24	81.0

As it can be observed, the breakthrough curves are steeper with increasing pollutant concentrations. Similar results were also noticed in one hand by Hodaifa et al. (2014) for iron adsorption onto olive stones (at 5 and 20 mg L⁻¹ iron concentration) and on the other hand by

Rao et al. (2005) for 50 and 100 mg L⁻¹ in the treatment of wastewater containing Pb and Fe by IE (Hodaifa et al., 2014; Rao et al., 2005). These authors found as well that the breakthrough point was around 8 bed volumes (BV) for 100 mg L⁻¹ iron load while about 15 BV for 50 mg L⁻¹. In addition, Ortiz et al. (2009) obtained breakthrough curves for iron IE with a chelating resin (Ortiz et al., 2009). The breakthrough profile was as similarly complex as the ones identified in this study, with evidence of a region of rapid elution of iron ions into the treated water followed by a period of relative increased iron uptake. On the other hand, McKevitt and Dreisinger (2009) demonstrated that a wide variety of resins gave rise to breakthrough curves comparable to the one shown in Figure 8.3 (McKevitt and Dreisinger, 2009).

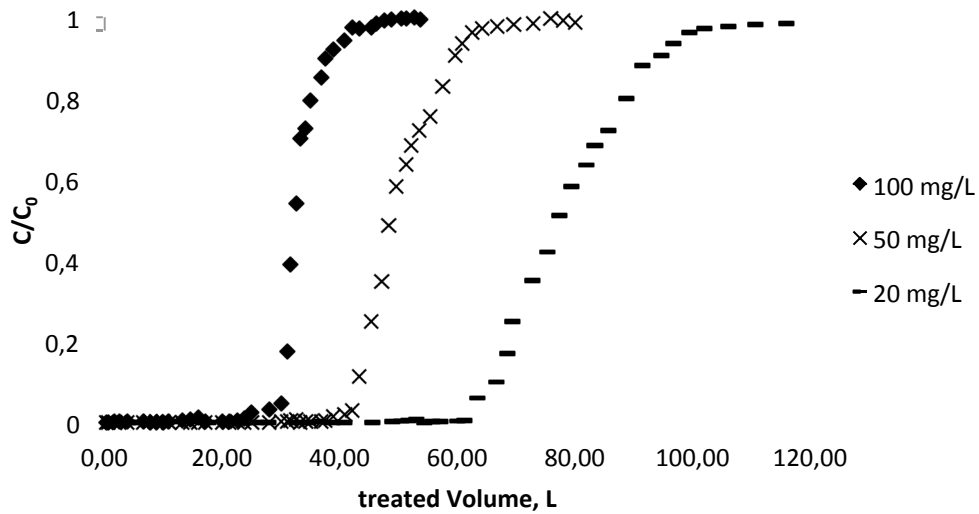


Figure 8.3. Breakthrough curves for two different iron concentrations in the influent: (-) 20 mg L⁻¹ (×) 50 mg L⁻¹ and (♦) 100 mg L⁻¹ inlet iron concentrations. Common conditions: flow rate = 10 L h⁻¹, resin amount = 69.2 g and operating temperature = 298 K.

8.3.2.2 Ion Exchange process breakthrough curves modelling

Several models - comprising Thomas, Yoon-Nelson, and Clark equations - were used to correlate the IE breakthrough curves' experimental data so as to describe and model the adsorption process of iron on the selected resin, for proper dimension, operation and reliable scale-up.

The results obtained from the modelling of the fixed-bed IE process for the final purification of the iron load in OMW-2ST with the different model equations used are graphically reported Figure 8.4, Figure 8.5 and Figure 8.6 for inlet iron concentrations equal to 20 mg L⁻¹, 50 mg L⁻¹ and 100 mg L⁻¹, respectively.

The values of the parameters obtained from the fitting of the experimental iron IE data to Thomas model are hereafter reported in Table 8.3, comprising mainly the Thomas rate constant K_{Th} together with the equilibrium adsorbate uptake q_0 . Thomas model was applied to the experimental IE data for C/C_0 ratios ranging from 0.01 to 0.99 while varying the initial iron concentration.

Table 8.3. Thomas model parameters of iron ions adsorption onto the selected cation exchange resin at different inlet concentration using linear regression analysis.

Inlet iron concentration (mg L ⁻¹)	Thomas model parameters			
	k_{Th} (ml min ⁻¹ mg ⁻¹)	q_0 (mg g ⁻¹)	R ²	SSE
20	0.075	22.16	0.9868	0.030
50	0.064	36.52	0.9476	0.107
100	0.058	48.23	0.9655	0.117

A focus on Table 8.3 permits noticing that upon an increment of C_0 , the value of q_0 noticeably increased, but the value of k_{Th} decreased. This is attributed to the difference in the adsorption driving force related to the concentration gradient (XiaoFeng et al., 2014). Therefore, the higher driving force resulting from the higher iron ion concentration led to a major q_0 value. Additionally, it was found that the values of q_0 estimated using the Thomas model are very close to the q_e values obtained from the experimental results with varying C_0 conditions. The high values of the non-linear regression coefficients demonstrated the accuracy of the linearized Thomas model equation for the fitting of the experimental iron IE data (Table 8.3). Furthermore, comparing the R² and SSE values for various models revealed that the Thomas model described with utmost suitability the iron ions IE process in a fixed-bed column.

Otherwise, the results obtained from the modelling with Yoon-Nelson model are briefly summarized in Table 8.4, where the estimated values of the Yoon-Nelson constant K_{YN} , the adsorption capacity q_0 , the 50 % adsorbate breakthrough τ , and additional statistical parameters are reported. As it can be observed, the value of K_{YN} was noted to decrease with increasing the initial iron concentration in the effluent. Furthermore, the values of τ were found to be significantly minor than the t value at 50 % breakthrough experimentally observed under all conditions assayed. These results point for the fact that Yoon- Nelson model is not very accurate in the prediction of the τ value, probably because of Yoon-Nelson model is simple and theoretical.

Finally, Clark model was applied for the performance modelling of the fixed-bed IE process for the final purification of the iron load in OMW-2ST. The results obtained are reported in Table 8.5.

The value of the Freundlich constant ($n = 1.64$), which was obtained from the batch tests in our previous work (Victor-Ortega et al, 2015), was used in the Clark model to calculate the other model parameters, A and r , which were, respectively, determined from Eq. (11). The observed increase in the rate of mass transfer (r) with increasing flow rate can be explained because of the fact that higher flow rates shorten the distance for the molecular diffusion of adsorbates through the stationary layer of water that surrounds adsorbent particles. The rate of mass transfer also increased with increasing initial iron concentration, and along with it the driving force and mass transfer of the adsorbate to the adsorbent surface. As seen in Table 8.5, R^2 values were lower in comparison to the previous models examined, and the corresponding SSE values were calculated to be higher, indicating that the Clark model predicts worst the breakthrough curve of iron adsorption process among all tested model equations.

Table 8.4. Yoon-Nelson model parameters of adsorption of iron ions onto the selected cation exchange resin at different inlet concentration using linear regression analysis.

Inlet iron concentration (mg L ⁻¹)	Yoon and Nelson model parameters				
	K _{YN} (min ⁻¹)	τ (min)	q ₀ (mg g ⁻¹)	R ²	SSE
20	0.0313	504.8	24.31	0.8704	0.379
50	0.0313	288.7	34.77	0.9650	2.406
100	0.0465	198.2	47.74	0.9465	0.358

Table 8.5. Clark model parameters of adsorption of iron ions the selected cation exchange resin at different inlet concentration using linear regression analysis.

Inlet iron concentration (mg L ⁻¹)	Clark model parameters				
	r (min ⁻¹)	A	t _b (min)	R ²	SSE
20	0.0159	1079.9	330.60	0.8669	0.436
50	0.0159	347.48	257.17	0.8380	2.617
100	0.0213	106.18	181.73	0.8719	1.817

The obtained results are supported by the S-shaped pattern modellings reported in Figure 8.4, Figure 8.5 and Figure 8.6, for the range of inlet iron concentrations examined, in which it can be clearly observed Thomas model fitted with the utmost accuracy the experimental data for the studied IE process. On the other hand, the behaviour of this system was accurately simulated as a Langmuir adsorption, which matched our conclusion from previous batch study (Hodaifa et al., 2014), since Thomas model is based on Langmuir isotherm.

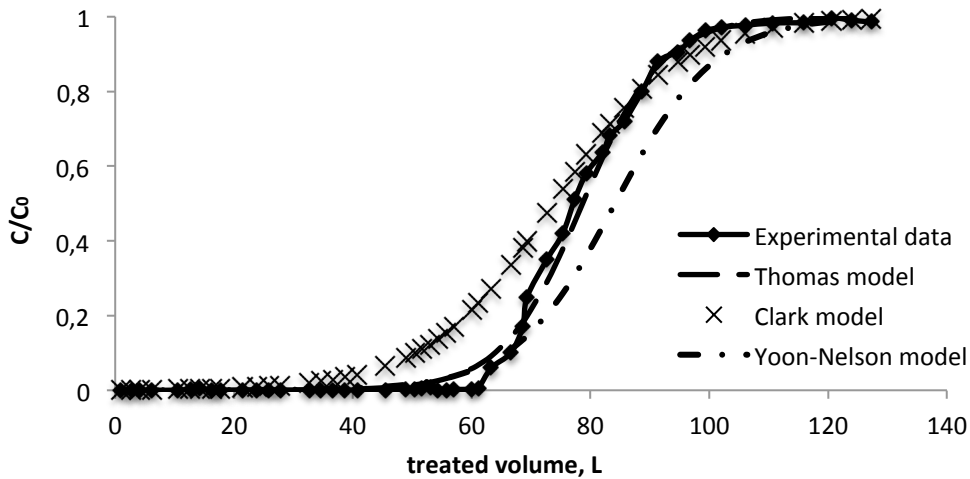


Figure 8.4. Breakthrough curves comparison for experimental and predicted data for the three studied models. Common conditions: inlet iron concentration = 20 mg L^{-1} , flow rate = 10 L h^{-1} , resin amount = 69.2 g and operating temperature = 298 K .

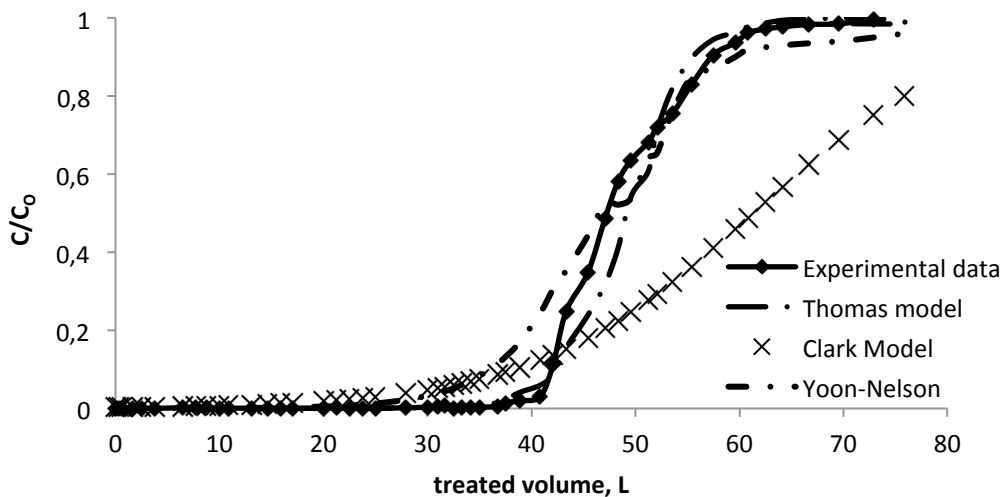


Figure 8.5. Breakthrough curves comparison for experimental and predicted data for the three studied models. Common conditions: inlet iron concentration = 50 mg L^{-1} , flow rate = 10 L h^{-1} , resin amount = 69.2 g and operating temperature = 298 K .

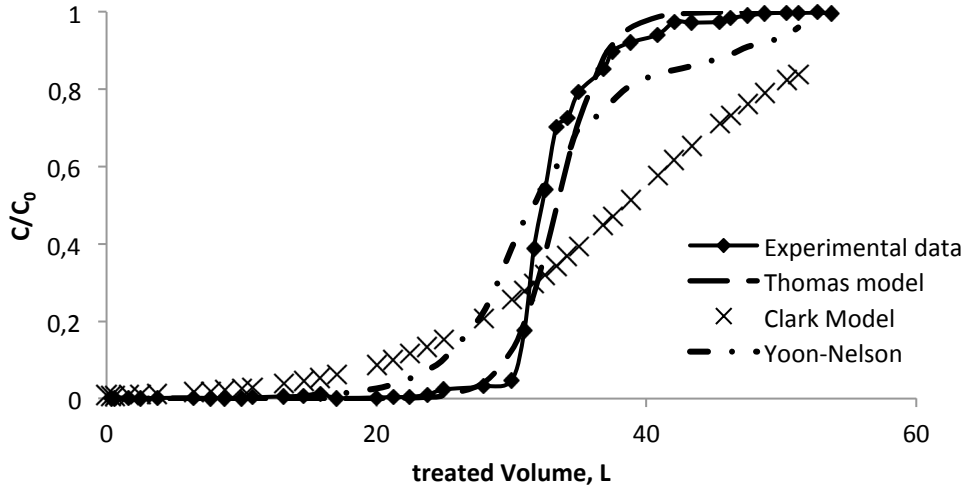


Figure 8.6. Breakthrough curves comparison for experimental and predicted data for the three studied models. Common conditions: inlet iron concentration = 100 mg L^{-1} , flow rate = 10 L h^{-1} , resin amount = 69.2 g and operating temperature = 298 K .

8.3.3 Regeneration and industrial application

In each experimental cycle the selected IE resin was loaded with iron until exhaustion, followed by elution by pumping 4 % HCl aqueous solution at 2.5 L h^{-1} and room temperature. Finally, the eluted resin was washed with distilled water at 2.5 L h^{-1} during the 5 first minutes and then increasing the flow rate until 20 L h^{-1} , following the manufacturer’s recommendations.

The adsorption–desorption–washing process was carried out for up to 10 cycles. It is very important to highlight that it was observed that even after 10 cycles the loading capacity of iron by the resin fluctuated in a narrow range of $60.5\text{--}57.5 \text{ g L}^{-1}$. Results are shown in Figure 8.7.

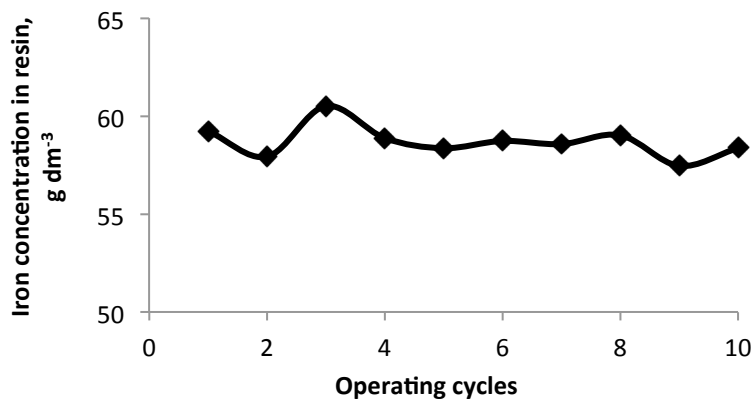


Figure 8.7. Recyclability of Dowex Marathon C resin (Adsorption: 100 mg Fe L^{-1} , 40 L solution, 69.2 g resin; Desorption: 200 mL 4% HCl aqueous solution; Washing: 500 mL of distilled water).

Desorption results by the proposed protocol therefore ensure close to 100 % iron recovery efficiencies. It may be stated that, in acidic medium, protons compete with iron ions and displace almost completely the adsorbed iron. Millar et al. (2015) have also used hydrochloric acid solutions to remove iron from strong-acid cation exchange resins (Millar et al., 2015). They obtained iron regeneration efficiencies higher than 90 % using 10 % HCl, and 89.6 % by regenerating with 5 % HCl. Also, Marañón et al. (1999) regenerated a series of cation and chelating resins loaded with iron using hydrochloric acid solutions (Marañón et al., 1999). In general, the regeneration efficiency was considerably higher with strong-acid cation resins (70–90%) compared to chelating resins (20–40%).

It is very important to highlight that the loss in the IE efficiency was well below 1 % during the course of the whole regeneration cycles. This fact is key from a technical and economical point of view for the cost-efficiency of the industrial scale-up of the proposed integral process for olive mill wastewater reclamation.

In the previous work by our research group, iron (III) chloride was used as catalyst during the secondary treatment of olive mill wastewater. This treatment consisted of an advanced chemical oxidation process based on Fenton’s reagent followed by a flocculation step and filtration in series through three different kinds of filtrating materials (Martínez Nieto et al., 2010; Hodaifa et al., 2013a; Hodaifa et al., 2013b; Hodaifa et al., 2014). Before the last filtration-in-series step, iron concentrations were in the range of 20 mg L⁻¹, and even higher concentrations are attained at the outlet of the oxidation reactor. Moreover, fluctuations in the inlet concentrations of the olive mill effluent may lead to increasing concentration values.

According to the results obtained in the present research work, the proposed final IE process with cation exchange resin can be successfully used in order to provide complete iron removal, in replacement of the filtration-in-series stage, and even the decanting step, which would imply important time, space and economic savings.

Moreover, the possibility of the effective iron recovery through the proposed IE process (up to 100 % iron recovery efficiencies were ensured upon applying the proposed regeneration protocol) enable its reuse in the Fenton reactor as catalyst, since the regeneration stream is acid, promoting Fenton reaction and thus boosting the cost-efficiency of the integral process for olive mill wastewater reclamation. Figure 8.8 shows the scheme of the whole integral process for olive mill wastewater purification. Moreover, these results may also apply to iron removal from several others industrial wastewaters, such as mining and hydrometallurgical effluents, among others, which could present iron levels in the same range. Finally, an effluent with quality to permit its reuse for irrigation purposes was obtained (Table 8.6).

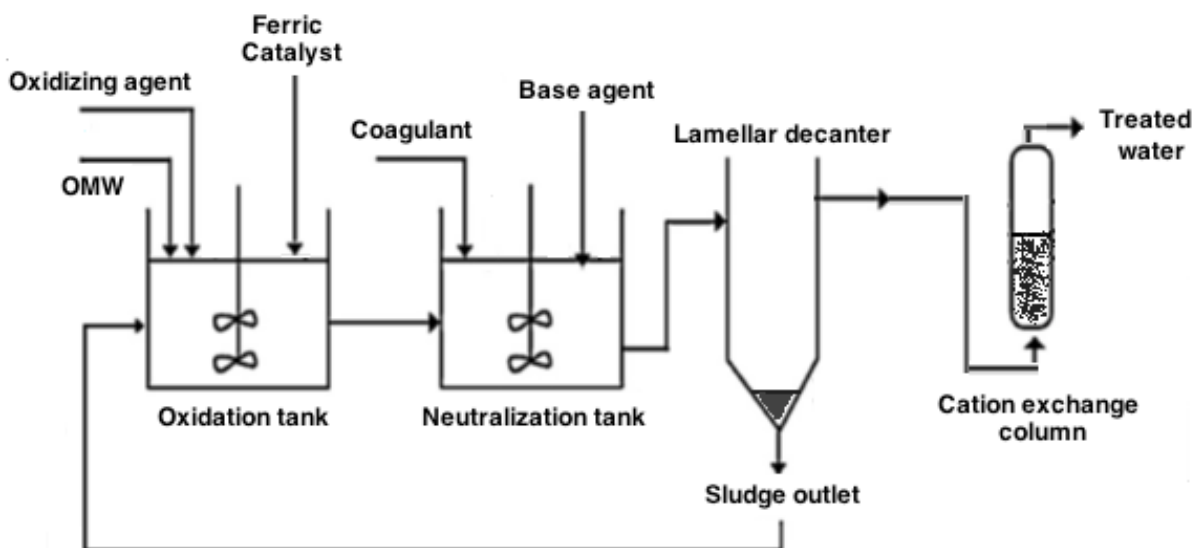


Figure 8.8. Flow diagram of the whole process for OMW-2 purification

Table 8.6. Characteristics range of the final treated effluent.

Parameters	Value
pH	5.7-7.3
Conductivity, dS m ⁻¹	0.78 - 1
Total phenolic compounds, µg L ⁻¹	300 - 400
Total [Fe], µg L ⁻¹	40 - 70

8.4 Conclusions

In the present work, the performance of a fixed-bed IE process with a strong-acid cation exchange resin was fully investigated for the final purification of the iron load in a secondary-treated olive mill wastewater stream (OMW-2ST). In previous work, the authors optimized and scaled-up a secondary treatment process for olive mill wastewater based on Fenton-like advanced oxidation, successfully achieving high organic matter abatement efficiencies. However, the use of a ferric catalyst during the process leads to an increase of the iron concentration in the treated effluent up to unacceptable levels.

Results showed that iron IE efficiency increased with an increase in the pH value up 4, but lower IE efficiency was observed upon higher pH due to formation of iron hydroxide causing hindrance of the cation exchange capacity. On the other hand, experimental data withdrawn from breakthrough curves demonstrated up to 59.24 mg g⁻¹ maximum iron adsorption capacity

onto the selected strong-acid cation exchange resin. Moreover, the iron equilibrium uptake efficiency was observed to strikingly increase with the increment of the inlet iron ion concentration. Both the breakthrough point and the exhaustion time decreased with an increase of the inlet iron ion concentration.

Furthermore, modeling of the proposed IE process was performed with utmost accuracy by means of Thomas model for all three inlet iron concentrations studied, providing the necessary information about the dynamic behavior of the iron IE process for appropriate column design and operation.

Finally, up to 100 % iron recovery efficiencies were maintained even after 10 complete-exhaustion IE cycles, upon the proposed protocol, thus fully regenerating the IE resin capacity. This feature, together with the possibility of effectively recovering the iron load through the proposed IE process to permit its reuse in the Fenton reactor as catalyst, would sensibly boost the cost-efficiency of the integral process for olive mill wastewater reclamation. At the end, an effluent with irrigation reuse quality compliance was obtained.

8.5 References

Abdel-Ghani, N.T., Hefny, M., El-Chagbaby, G.A.F. (2007). Removal of Lead (II) from aqueous solution using low cost abundantly available adsorbents. *Int. J. Environ. Sci. Tech.*, 4(1):67-73.

Abu Bakar, A.F., Halim, A.A. (2013). Treatment of automotive wastewater by coagulation–flocculation using poly-aluminum chloride (PAC), ferric chloride (FeCl₃) and aluminum sulfate (alum). *AIP Conference Proceedings*, 1571:524–529.

Agrawal, A., Kumari, S., Sahu, K.K. (2009). Iron and copper recovery/removal from industrial wastes: a review. *Ind. Eng. Chem. Res.*, 48(13):6145–6161.

Ahmetli, G., Tarlan, E. (2007). Fe(II/III) adsorption onto styrene/divinyl benzene based polymers. *J. Appl. Polym. Sci.*, 104(4):2696–2703.

Amin, N.K., Abdelwahab, O., El-Ashtoukhy, E.S.-Z. (2014). Removal of Cu(II) and Ni(II) by ion exchange resin in packed rotating cylinder. *Desalination and Water Treatment*, 3:1–11.

Badawy, N., Rabah, M.A., Hasan, R. (2013). Separation of some heavy metal species from electroplating rinsing solutions by ion exchange resin. *Int. J. Environ. Waste. Manag.*, 12(1):33-51.

Benítez, P., Castro, R., Barroso, C.G. (2002). Removal of iron, copper and manganese from white wines through ion exchange techniques: effects on their organoleptic characteristics and susceptibility to browning. *Anal. Chim. Acta*, 458(1):197-202.

Bulai, P., Cioanca, E. (2011). Iron removal from wastewater using chelating resin Purolite S930, *Tehnomus Journal*, 18:64-7.

Clark, R.M. (1987). Evaluating the cost and performance of field-scale granular activated carbon systems. *Environ. Sci. Technol.*, 21:573-580.

Dabrowski, A., Hubicki, Z., Podkoscielny, P., Robens, E. (2004). Selective removal of the heavy metal ions from waters and industrial wastewaters by ion-exchange method. *Chemosphere*, 56(2):91–106.

Dai, S.J., Yang, S.Y., Zhou, D.Q. (2012). The influence of coexisting ions on adsorption-flotation of Pb^{2+} in water by *Gordonia amarae*. *AMR*, 433:183-187.

European Commission, Council Directive 98/83/EC of 3 November 1998 on the quality of water intended for human consumption, 1998. Brussels, Belgium.

Food and Agricultural Organization (FAO), Review of world water resources by country, Water reports 23, Rome, Italy, 2003.

Gaikwad, R.W. (2010). Review and research needs of active treatment of acid mine drainage by ion exchange. *Electron. J. Environ. Agric. Food Chem.*, 9:1343–1350.

Greenberg, A.E., Clesceri, L.S., Eaton, A.D. (1992). Standard Methods for the Examination of Water and Wastewater, APHA/AWWA/WEF, 16th ed., Washington DC. Cabs.

Guangyu, Y., Viraraghavan, T. (2001). Heavy metal removal in a biosorption column by immobilized *M. rouxii* biomass. *Bioresour. Technol.*, 78:243-249.

Hodaifa, G., Ochando-Pulido, J.M., Rodríguez-Vives, S., Martínez-Ferez, A. (2013a). Optimization of continuous reactor at pilot scale for olive-oil mill wastewater treatment by Fenton-like process. *Chem. Eng. J.*, 220:117-124.

Hodaifa, G., Ochando-Pulido, J.M., Alami, S.B.D., Rodríguez-Vives, S., Martínez-Férez, A. (2013b). Kinetic and thermodynamic parameters of iron adsorption onto olive stones. *Industrial Crops and Products*, 49:526-534.

Hodaifa, G., Alami, S.B.D., Ochando-Pulido, J.M., Víctor-Ortega, M.D. (2014). Iron removal from liquid effluents by olive stones on adsorption column: breakthrough curves. *Ecol. Eng.*, 73:270-275.

Kaya, Y., Vergili, I., Acarbabacan, S., Barlas, H. (2002). Effects of fouling with iron ions on the capacity of demineralization by ion exchange process. *Fresenius Environ. Bull.*, 11:885-888.

Kyzas, G., Kostoglou, M. (2014). Green adsorbents for wastewaters: a critical review. *Materials*, 7(1):333–364.

Lasanta, C., Caro, I., Pérez, L. (2005). Theoretical model for ion exchange of iron(III) in chelating resins: application to metal ion removal from wine. *Chem. Eng. Sci.*, 60(13):3477-3486.

Lim, A.P., Aris, A.Z. (2014). A review on economically adsorbents on heavy metals removal in water and wastewater. *Rev. Environ. Sci. Biotechnol.*, 13(2):163–181.

Marañón, E., Suárez, F., Alonso, F., Fernández, Y., Sastre, H. (1999). Preliminary study of iron removal from hydrochloric pickling liquor by ion exchange. *Ind. Eng. Chem. Res.*, 38(7):2782–2786.

Marañón, E., Fernández, Y., Castrillón L. (2005). Ion exchange treatment of rinse water generated in the galvanizing process. *Water Environ. Res.*, 77(7):3054-3058.

Martínez Nieto, L., Hodaifa, G., Rodríguez Vives, S., Giménez Casares, J.A. (2010). Industrial plant for olive mill wastewater from two-phase treatment by chemical oxidation. *J. Environ. Eng.*, 136(11):1309-1313.

McKevitt, B., Dreisinger, D. (2009). A comparison of various ion exchange resins for the removal of ferric ions from copper electrowinning electrolyte solutions part I: electrolytes containing no other impurities. *Hydrometallurgy*, 98(1–2):116–121.

Millar, G.J., Schot, A., Couperthwaite, S.J., Shilling, A., Nuttall, K., de Bruyn, M. (2015). Equilibrium and column studies of iron exchange with strong acid cation resin. *J. Environ. Chem. Eng.*, 3:373-385.

Mungray, A.A., Kulkarni, S.V., Mungray, A.K. (2012). Removal of heavy metals from wastewater using micellar enhanced ultrafiltration technique: a review. *Cent. Eur. J. Chem.*, 10(1):27–46.

Nguyen, T.A., Ngo, H.H., Guo, W.S., Zhang, J., Liang, S., Yue, Q.Y., Li, Q., Nguyen, T.V.

(2013). Applicability of agricultural waste and by-products for adsorptive removal of heavy metals from wastewater. *Bioresour. Technol.*, 148:574–585.

Oncel, M.S., Muhcu, A., Demirbas, E., Kobya, M. (2013). A comparative study of chemical precipitation and electrocoagulation for treatment of coal acid drainage wastewater. *J. Environ. Chem. Eng.*, 1(4):989–995.

Ortiz, A., Fernández-Olmo, I., Urtiaga, A., Ortiz, I. (2009). Modeling of iron removal from spent passivation baths by ion exchange in fixed-bed operation. *Ind. Eng. Chem. Res.*, 48(15):7448–7452.

Rao, K.S., Dash, P.K., Sarangi, D., Chaudhury, G.R., Misra, V.N. (2005). Treatment of wastewater containing Pb and Fe using ion-exchange techniques. *J. Chem. Technol. Biotechnol.*, 80(8):892-898.

Riveros, P.A. (2004). The extraction of Fe(III) using cation-exchange carboxylic resins. *Hydrometallurgy*, 72(3-4):279-290.

Sag, Y., Yalcuk, A., Kutsal, T. (2001). Use of a mathematical model for prediction of the performance of the simultaneous biosorption of Cr(VI) and Fe(III) on *Rhizopus arrhizus* in a semi-batch reactor. *Hydrometallurgy*, 59:77-87.

Senthil Kumar, P., Gayathri, R. (2009). Adsorption of Pb²⁺ ions from aqueous solutions onto bael tree leaf powder: isotherms, kinetics and thermodynamics study. *J. Eng. Sci. Technol.*, 4(4):381-399.

Shafaei, A., Pajootan, E., Nikazar, M., Arami, M. (2011). Removal of Co(II) from aqueous solution by electrocoagulation process using aluminum electrodes. *Desalination*, 279(1–3):121-126.

Thomas, H.C. (1944). Heterogeneous ion exchange in a flowing system. *J. Am. Chem. Soc.*, 66:1664-1666.

Víctor-Ortega, M.D., Ochando-Pulido, J.M., Godaifa, H., Martínez-Férez, A. (2014). Final purification of synthetic olive oil mill wastewater treated by chemical oxidation using ion exchange: Study of operating parameters. *Chem. Eng. Process.*, 85:241-247.

Víctor-Ortega, M.D., Ochando-Pulido, J.M., Martínez-Ferez, A. (2015). Thermodynamic and kinetic studies on iron removal by means of a novel strong-acid cation exchange resin for olive mill effluent reclamation. *Ecol. Eng.*, “under review”.

Woodberry, P., Stevens, G., Northcott, K., Snape, I., Stark, S. (2007). Field trial of ion exchange resin columns for removal of metal contaminants, Thala valley tip, Casey Station, Antarctica. *Cold Reg. Sci. Technol.*, 48(2):105–117.

XiaoFeng, S., Tsuyoshi, I., Masahiko, S., Takaya, H., Koichi, Y., Ariyo, K., Shiori, N. (2014). Adsorption of phosphate using calcined Mg₃-Fe layered double hydroxides in a fixed-bed column study. *Journal of Industrial and Engineering Chemistry*, 20:3623-3630.

Yoon, Y.H., Nelson, J.H. (1984). Application of gas adsorption kinetics. I. A theoretical model for respirator cartridge service time. *Am. Ind. Hyg. Assoc. J.*, 45:509-516.

Zak, S. (2012). Treatment of the processing wastewaters containing heavy metals with the method based on flotation. *Ecol. Chem. Eng.*, 19:433-438.

CHAPTER 9

PHENOLS REMOVAL FROM INDUSTRIAL EFFLUENTS THROUGH NOVEL POLYMERIC RESINS: KINETICS AND EQUILIBRIUM STUDIES

M.D. Víctor-Ortega^{1*}, J.M. Ochando-Pulido¹, A. Martínez-Ferez¹.

¹Chemical Engineering Department, University of Granada, 18071 Granada, Spain

*email: mdvictor@ugr.es

Submitted for publication. Current status: under review.

Journal of the Taiwan Institute of Chemical Engineers

Publisher: ELSEVIER SCIENCE BV. PO BOX 211, 1000 AE AMSTERDAM, NETHERLANDS

Year: 2015

ISSN: 1876-1070

Impact factor: 3.0

Tertile: First



Abstract

The efficient removal of phenols from wastewaters has increasingly become a significant environmental concern due to its high toxicity even at low concentrations. In this research work, phenols removal from aqueous solution was evaluated by using Amberlyst A26, a strong-base anion exchange resin, and Amberlite IRA-67, a weak-base anion exchange resin. The influence of phenols concentration in the feedstream was investigated as well as the effect of recirculation time. Equilibrium data fitted to the Langmuir, Freundlich and Temkin isotherms revealed Langmuir isotherm provided the best correlation for both resins ($R^2 = 0.99$). Kinetic studies performed based on pseudo-first order, pseudo-second order and intraparticle diffusion models showed that although the correlation coefficients of the second-order model were the highest ($R^2 = 1$) and also the SSE values were the lowest ($< 2\%$), the kinetics of phenols uptake could be also satisfactorily described by intraparticle diffusion. On the other hand, results revealed that phenols uptake is a spontaneous process for Amberlyst A26 ($\Delta G^\circ = -1.55 \text{ kJ mol}^{-1}$), whereas it is not spontaneous for Amberlite IRA-67 ($\Delta G^\circ = 3.06 \text{ kJ mol}^{-1}$). Finally, Amberlyst A26 was confirmed to be considerably more efficient than Amberlite IRA-67 for the potential removal of phenols from industrial effluents.

Keywords: Adsorption isotherms, Anionic resins, Industrial effluents, Kinetics, Phenols removal.

9.1 Introduction

Phenols are pollutants presenting high toxicity, refractoriness as well as persistence and accumulation in the environment, and thus its removal is a main environmental issue. Phenolic compounds exist in wastewaters from olive mill, oil refineries, plastics, leather, paint, pharmaceutical and steel industries (Carmona et al., 2006). Phenols are also present in domestic effluents and vegetation decay (Gupta et al., 2004). Considering the great prevalence of phenolic compounds in different wastewaters along with their toxicity to living beings even at low concentrations, and within the framework of the actual environment regulations, these compounds must be removed before discharge of wastewater into water bodies (Jain et al., 2004).

Different methods have been proposed to eliminate phenolic compounds from polluted waters, including chemical oxidation (Kavitha and Palanivelu, 2004; Barros et al., 2003; Fan et al., 2003; Wu et al., 2000), chemical coagulation (Tomaszewska et al., 2004; Özbelge et al., 2002), extraction with solvents (Lazarova and Boyadzhieva, 2004), membrane technology (Kujawski et al., 2004; Zagklisa et al., 2015) adsorption (Al-Asheh et al., 2003; Chern and Chien, 2002;

Vinod and Anirudhan, 2002; Juang et al., 1996) and ion exchange (IE) (Zagklisa et al., 2015; Costa and Rodrigues, 1985; Abburi, 2003; Ku and Lee, 2000; Juang and Shiau, 1999; Lee et al., 2004; Ku et al., 2004; Caetano et al., 2009; Zhu et al., 2011; Víctor-Ortega et al., 2014; Juang et al., 1999; Bertin et al., 2011). In this scenario, adsorption technology is currently being applied widely for the removal of organic micropollutants from aqueous solutions. Concretely, in the past two decades, polymeric adsorbents have become a promising choice for efficient removal of aromatic pollutants. These polymeric resins present several advantages, especially those about regeneration, which can be accomplished by simple, non-destructive means, such as solvent washing, thus providing the potential for solute recovery (Caetano et al., 2009).

Adsorption on selective resins has also been investigated for the removal of phenols from aqueous solutions, either through molecular adsorption or IE mechanisms. Caetano et al. (2009) tested the removal of phenol through IE mechanism on polymeric resins followed by desorption with methanol/water mixtures (Caetano et al., 2009). Zhu et al. (2011) tested the adsorption of phenol on N-butylimidazolium functionalized strongly basic anion exchange resin and the results showed that at acidic pH the dominant mechanism was molecular adsorption whereas at alkaline pH phenol was removed through IE mechanism (Zhu et al., 2011). Juang et al. studied the adsorption of phenol and 4-chlorophenol on XAD4, XAD7, and XAD16 (Juang et al., 1999). Furthermore, Bertin et al. examined the direct adsorption of olive mill wastewater (OMW) phenols on XAD7 and XAD16 resins followed by desorption with different solvents (Bertin et al., 2011). The results were very encouraging, exhibiting high adsorption percentages, with 95% of the adsorbed phenols being desorbed with acidified ethanol. Ku et al. investigated phenol removal from aqueous solutions by using Purolite A-510 resin in the chloride form and found that phenol removal increased steadily with increasing pH (Ku et al., 2004). Nevertheless, they consider that the uptake of phenol compounds occurs only on the active sites of the resin by either molecular adsorption or IE. Thus, the same resin sites are considered to be accessible for both modes of uptake and so the ratio of the solute uptake through molecular adsorption and IE depends on the solution pH. The presence of OH^- ions in solution would involve multicomponent exchange namely between hydroxyl, phenolate and the anion initially in the resin. Significant dissociation of phenol occurs at a pH higher than its pKa (9.83), allowing its uptake by IE, which is an economic, effective and useful technique to remove pollutant ions from wastewaters and replace them by non-contaminant ions released from the ion exchanger (Carmona et al., 2006). Anasthas and Gaikar have also used the IE technique for the separation of alkylphenols from non-aqueous systems. They found that the separation is mainly governed by acid–base interactions between phenolic OH^- groups and the basic groups of the resin structure (Anasthas and Gaikar, 1999).

In the present work, a strong-base anion exchange resin (Amberlyst A26) and a weak-base anion exchange (Amberlite IRA-67) were evaluated to remove phenols from aqueous solution. The effect of the phenols concentration in the feedstream was investigated in the range 1-200 mg L⁻¹ as well as the influence of recirculation time. On the other hand, the equilibrium behaviour of this pollutant has been described by Langmuir, Freundlich and Temkin isotherms. Additionally, kinetics of experimental data have been analysed using pseudo-first order, pseudo-second order and intraparticle diffusion models. Finally, the suitability of the proposed IE resins has been investigated through thermodynamic parameters.

9.2 Experimental

9.2.1 Materials

Analytical grade reagents and chemicals with purity over 99 % were used for the analytical procedures, applied at least in triplicate.

For the IE experiments, model solutions were prepared by dissolving reagent-grade phenol (provided by Panreac) in double distilled water. On the other hand, regeneration solutions were prepared by dissolving reagent-grade NaOH (supplied by Panreac) in double distilled water.

In this research work, two anion exchange resins were used: Amberlyst A26 strong base anion exchange resin and Amberlite IRA-67 weak base anion exchange resin. Typical physical and chemical characteristics of these resins are described in Table 9.1.

Table 9.1. Physicochemical properties of the resins.

Properties	Amberlyst A26	Amberlite IRA-67
Type	Strong-base anion	Weak-base anion
Matrix	Styrene-divinylbenzene	Tertiary amine
Ionic form as shipped	OH ⁻	OH ⁻
Particle size, mm	0.56-0.70	0.50-0.75
Effective pH range	0-14	0-7
Total exchange capacity, eq L⁻¹	0.80	1.60
Shipping weight, g L⁻¹	675	700

9.2.2 Ion exchange equipment

Figure 9.1 shows the flow-sheet scheme of the experimental apparatus (MionTec), which consisted of a peristaltic pump (Ecoline VC-380) and a column containing IE resin. The IE column employed in this study was made of an acrylic tube (540 mm height x 46 mm internal diameter), provided with a mobile upper retaining grid which could be fixed in the column to adjust it as a fixed bed or a semi-fluidized bed.

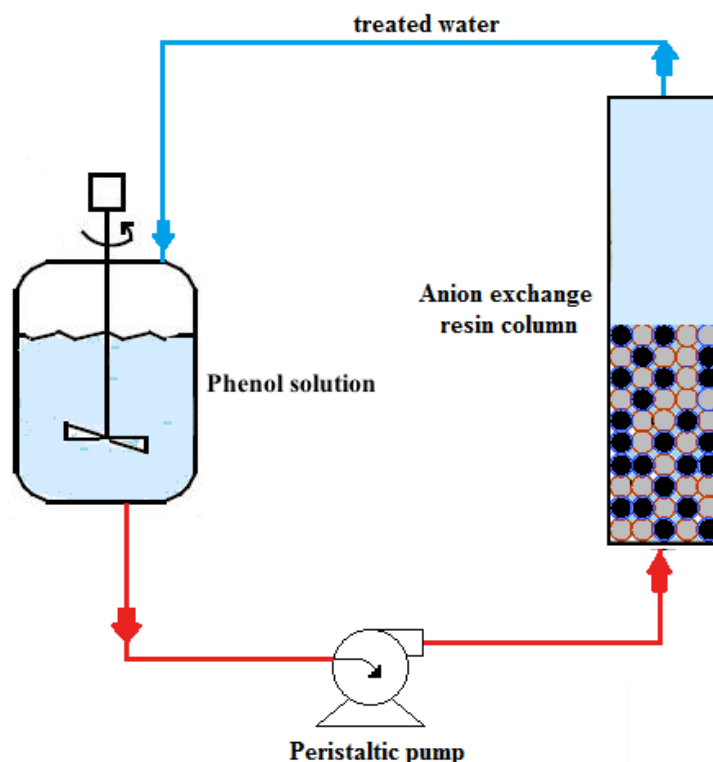


Figure 9.1. Flow-sheet scheme of IE recirculation operating device for phenols removal.

9.2.3 Equilibrium experiments

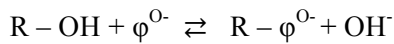
The uptake of phenols was carried out by performing recirculation mode experiments in order to evaluate the effect of both the recirculation time and feedstream concentration. The effect of the initial concentration of phenols was examined in the range 1-200 mg L⁻¹, until equilibrium was achieved.

On the other hand, adsorption isotherm studies were carried out with different initial phenols concentrations ranging from 1mg L⁻¹ to 200 mg L⁻¹ at constant resin dosage (7 g L⁻¹ for both anionic resins). Resulting data were fitted according to the following isotherm models: Langmuir, Freundlich and Temkin.

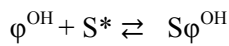
Furthermore, for the determination of the kinetics at different phenols initial levels, data were fitted to the following kinetic models: first-order kinetic model, second-order kinetic model and intraparticle diffusion model.

In the solid phase it was assumed that two mechanisms for the uptake of phenols into the resin beads take place, one by IE and another by molecular adsorption (Carmona et al., 2006). The following equations describe these mechanisms.

(a) Exchange of phenolate anion with the counter-ion (OH) of the resin:



(b) Adsorption of the molecular phenol on the free polymeric surface:



where S^* and $S\varphi^{OH}$ represent active and occupied adsorption sites of the resin, respectively.

The corresponding parameters for phenol/ OH^- equilibrium uptake were obtained by means of experiments in recirculation mode (Figure 9.1). Model solutions of phenols were put in contact with each IE resin until equilibrium was achieved. The flask containing the feed solution was stirred continuously during the whole experiment. The flow rate and temperature were fixed at 10 L h^{-1} and room temperature, respectively, whereas the recirculation time was varied up to 60 min in order to ensure equilibrium conditions.

The extent of the uptake was determined by measuring the residual amount of phenols in the liquid phase.

The removal efficiency was determined by computing the percentage sorption using the formulae in Eq. (1):

$$\% \text{ Phenols sorption} = \frac{C_o - C_e}{C_o} \times 100 \quad (1)$$

where C_o and C_e refers to the initial and equilibrium phenol concentration (mg L^{-1}), respectively.

9.2.4 Procedures

Total phenols and phenol derivatives were analysed by reaction with a derivative thiazol, giving a purple azo dye which was determined photometrically using a Helios Gamma UV–visible spectrophotometer (Thermo Fisher Scientific) at 475 nm (Standard German methods ISO 8466-1 and DIN 38402 A51) (Greenberg et al., 1992).

Both IE resins were initially washed several times with double distilled water, following the advice of resins manufacturers, in order to get proper swelling prior to adsorption experiments. In this work, fixed-bed operation was chosen. After each operational cycle, the strong-base and weak-base anion exchange resins were regenerated by using NaOH (4 %) and NaOH (2%) aqueous solutions, respectively. Subsequently, both resins were washed with double distilled water to remove the excess of base.

The analysis of the adsorption isotherms and kinetic models was performed using the Excel program.

9.3 Results and discussion

9.3.1 Effect of recirculation time and initial concentration

The impact of the recirculation time on the phenols uptake for different initial phenols concentration is shown in Figure 9.2a and b. Results show that phenols removal efficiency was considerably increased with incrementing recirculation time for both resins. For Amberlyst A26 resin (Figure 9.2a), it can be observed that the equilibrium was obtained in about 7 min for initial concentrations lower than 20 mg L⁻¹, whereas it was reached after 15 minutes for initial phenols levels in the range 20 – 200 mg L⁻¹.

On the other hand, Figure 9.2b shows that equilibrium was achieved around the first 15 minutes for all the studied initial phenols concentrations, for Amberlite IRA-67 resin.

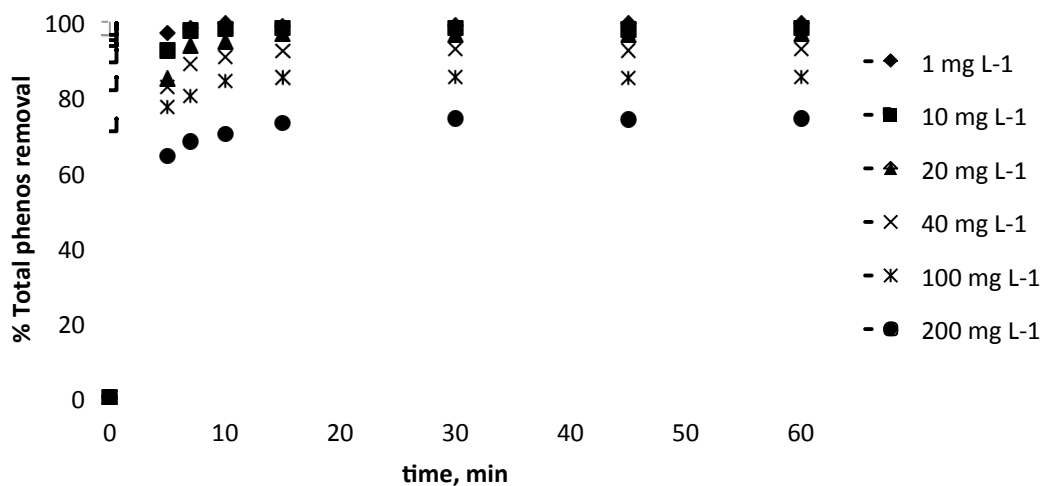


Figure 9.2a. Effect of recirculation time on phenols uptake through Amberlyst A26 (phenols concentration = 1 - 200 mg L⁻¹, resin dosage = 7 g L⁻¹, recirculation time = 60 minutes, temperature = 298 K and volume = 2 L).

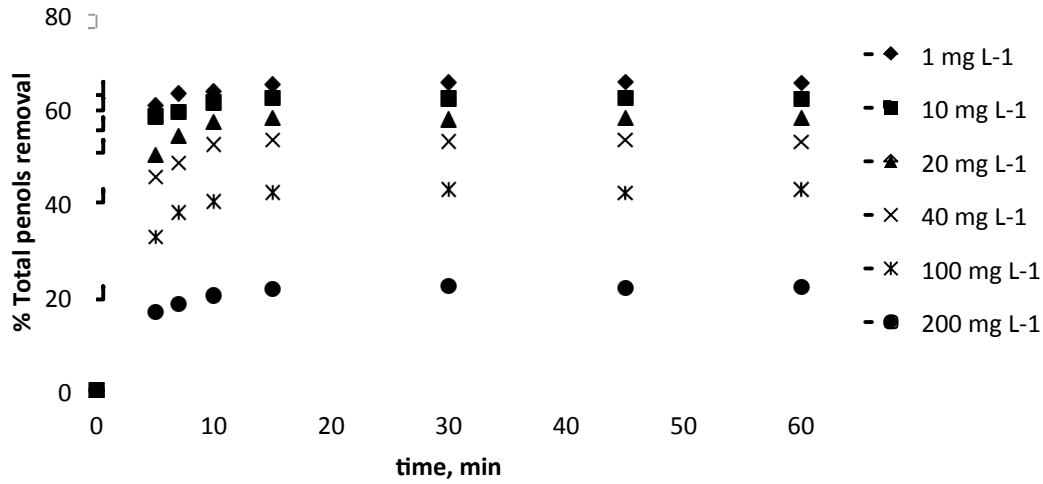


Figure 9.2b. Effect of recirculation time on phenols uptake through Amberlite IRA-67 (phenols concentration = 1 - 200 mg L⁻¹, resin dosage = 7 g L⁻¹, recirculation time = 60 minutes, temperature = 298 K and volume = 2 L).

The effect of the initial phenols concentration on the removal efficiency is plotted in Figure 9.3. To carry out this study phenols concentration was varied between 1 to 200 mg L⁻¹ and the anion exchange resins dosages were kept at 7.0 g L⁻¹.

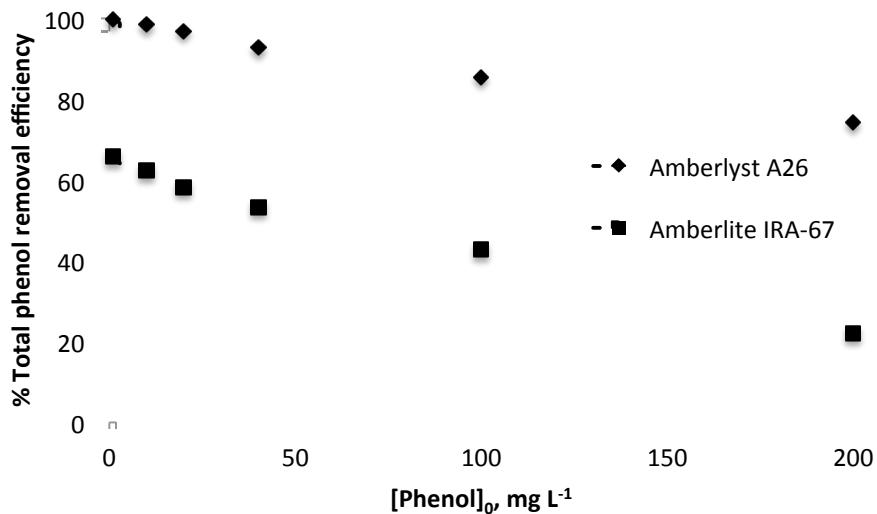


Figure 9.3. Effect of initial concentration ($[\text{Phenols}]_0$) on phenols uptake through Amberlyst A26 and through Amberlite IRA-67 (phenols concentration = 1 - 200 mg L⁻¹, resin dosages = 7 g L⁻¹, recirculation time = 60 minutes, temperature = 298 K and volume = 2 L).

Results show that phenols removal through both resins is considerably influenced by its concentration in the feedstream. It was found that the phenols removal efficiency decreases from

99.6 % for 1 mg L⁻¹ phenols in the feedstream, to 74.2 % for the highest assayed concentration (200 mg L⁻¹ phenols in the feedstream) under identical IE operating conditions in terms of recirculation time and temperature for the strong-base anion exchange resin. In this case, it can be ensured that IE was the predominant process responsible of the phenols ion removal since the increase in pH in the outlet stream was directly proportional to the removal efficiency for each assayed initial concentration. This fact is due to phenol OH⁻ ions are replaced by hydroxide. Hence, the decrease in the removal percentage with the phenol concentration in the feedstream could be related to saturation of the IE resin (Senthil Kumar and Gayathri, 2004).

On the other hand, phenols removal efficiency was found to decrease from 65.7 % for 1 mg L⁻¹ phenols in the feedstream, to 22.1 % for the highest assayed concentration (200 mg L⁻¹ phenols in the feedstream) under the same conditions for the weak-base anion exchange resin. In this case, the removal percentage decrease was more pronounced. The phenols removal efficiency dropped around 25% for the strong-base anion exchange resin. Otherwise, this drop was about 44 % (almost the double) for the weak-base anion exchange resin. In this case, phenols IE by Amberlite IRA-67 would be favored at low pH, since this resin is only active in the range of 0–7 (see Table 9.1). In addition, the phenol dissociation to phenol and phenolate can be considered as a function of the total concentration of phenols and the pH of the liquid solution (pH > 8). At acidic pH (pH < 8) the phenol dissociation is low and therefore, the molecular adsorption process is the predominant one, whereas both adsorption and IE are important at alkaline pH (Carmona et al., 2006). Consequently, it can be assumed that the adsorption is the main responsible process for phenols removal through Amberlite IRA-67. Caetano et al., who studied the phenol removal by means of weak and a strong-base anion exchange resins, found similar results in the initial concentration range 5-20 mg L⁻¹ (Caetano et al., 2009).

9.3.2 Equilibrium isotherms

The description of the equilibrium in the IE system is usually made by equilibrium isotherms, which represent the distribution of the adsorbed solute in the resin (Phenol_{adsorbed}) and the free solute in the fluid phase (Phenol_{solution}), in equilibrium.

The experimental data at equilibrium amount of adsorbed phenols on Amberyst A26 and Amberlite IRA-67 (q_e) and the concentration of phenols in the liquid phase (C_e) at a constant temperature were used to describe the optimum isotherm model. The linear forms of Langmuir, Freundlich and Temkin equations were employed to describe the equilibrium data. The performance of each form was judged through the correlation coefficients (R^2).

In this work, the IE capacity of both selected resins was evaluated as a function of the pollutant concentration, by determining its loading capacity q_e (mg of pollutant / g of adsorbent) (Eq. 2):

$$q_e = (C_0 - C_e) \cdot \frac{V}{m_s} \quad (2)$$

C_0 represents the initial phenols concentration in the inlet stream (mg of phenol L⁻¹ of solution), V (m³) is the volume of the phenols solution and m_s (kg) is the corresponding resin amount.

Adsorption isotherms play a crucial role in the predictive modelling procedures for the analysis and design of adsorption systems, which are essential for real-scale operation (Ould Brahim et al., 2014).

Langmuir isotherm model describes quantitatively the formation of a monolayer adsorbate on the outer surface of the adsorbent, and after that no further adsorption takes place (Langmuir, 1918). Thereby, the Langmuir model represents the equilibrium distribution of ions between the solid and liquid phases. The Langmuir isotherm is valid for monolayer adsorption onto a surface containing a finite number of identical sites.

This model assumes uniform energies of adsorption onto the surface and no transmigration of adsorbate in the plane of the surface. Based upon these assumptions, the Langmuir isotherm is represented by the following equation (Eq. 3):

$$q_e = \frac{q_m \times K_L \times C_e}{1 + K_L \times C_e} \quad (3)$$

where C_e is the equilibrium concentration in the solution (mg L⁻¹), q_m and K_L are the Langmuir constants, representing the maximum IE capacity for the solid phase (resin) loading and the energy constant related to the uptake heat, respectively.

Freundlich isotherm model is an empirical relationship between the concentrations of a solute on the surface of an adsorbent to the concentration of the solute in the liquid with which it is in contact. This model assumes that different sites with several uptake energies are involved (Freundlich, 1906). It is commonly used to describe the adsorption characteristics for heterogeneous surfaces. Freundlich isotherm represents the relationship between the amounts of ionic species exchanged per unit mass of resin, q_e , and the concentration of the ionic species at equilibrium, C_e .

The Freundlich exponential equation is described as follows:

$$q_e = K_f C_e^{1/n} \quad (4)$$

where K_f and n are the Freundlich constants, characteristic of the system, indicators of the IE capacity and intensity, respectively.

On the other hand, Temkin isotherm model was finally tested to modelize the adsorption potential of both anionic resins towards phenolic compounds. This model takes into account the effects of indirect adsorbent (resin) /adsorbate (phenols) interactions on the adsorption process (Temkin and Pyzhev, 1940). The model is given by Eq.(5), as follows:

$$q_e = B \cdot \ln(A \cdot C) \quad (5)$$

where A is the Temkin isotherm equilibrium binding constant (L/g) and B is the constant related to heat of sorption (J/mol). Temkin isotherm contains a factor that explicitly takes into account the resin-exchanged species interactions. This isotherm assumes that the uptake (IE) heat of all molecules in the layer decreases linearly with the coverage due to resin-exchanged species interactions, and that IE is characterized by a uniform distribution of binding energies, up to some maximum binding energy.

The isotherm experimental data as well as the fit to the three tested isotherm models are shown in Figure 9.4a and 9.4b. The relevant coefficients of each model for both resins and the calculated linear fit means squares are also reported in Table 9.2.

The results indicate that the linear form of Langmuir model fits with utmost accuracy the experimental data for both resins, as indicated by the high value of the regression coefficient ($R^2 = 0.99$). Furthermore, as it can be observed in Table 9.2, the maximum IE capacity, q_m , was calculated as 22 mg g⁻¹ for Amberlyst A26, whereas it was 7.5 mg g⁻¹ for Amberlite IRA-67. This means the strong-base anion exchange resin (Amberlyst A26) has triple phenols removal capacity compared to the weak-base anion exchange resin (Amberlite IRA-67). On the other hand, the separation factor R_L is a good characteristic of the Langmuir isotherm, which can be expressed in Eq.(6):

$$R_L = \frac{1}{1 + K_L \cdot C_0} \quad (6)$$

R_L values between 0 and 1 indicate favourable adsorption. The R_L values were in the ranges of 0.02-0.77 and 0.12-0.96, for Amberlyst A26 and Amberlite IRA-67, respectively. In both cases, R_L is less than unity, indicating that the adsorption of phenols onto the studied resins is a favourable process, and the data fit accurately the Langmuir isotherm model. However, it is

important to highlight that phenols adsorption is more favoured in case of Amberlyst A26 since R_L values are lower than for Amberlite IRA-67.

Caetano et al. studied phenols adsorption onto AuRix 100 (weak base anion exchange resin) and Dowex XZ (strong anion exchange resin) for initial phenols concentrations in the range 5-2000 mg L⁻¹. In this case, the maximum IE capacity (q_m) was found to be 46.2 mg g⁻¹ (pH 3) and 75.8 mg g⁻¹ (pH 11) for Aurix 100, whereas it was 43.5 mg g⁻¹ (pH 3) and 76.8 mg g⁻¹ (pH 11) for Dowex XZ (Caetano et al., 2009). It is worthy to highlight that for the same data, the slope of the Langmuir equation decreases considerably with increasing C_e (and therefore with increasing C_i). On the other hand, q_m is indirectly proportional to the slope. This fact could explain why q_m is higher for studies from Caetano et al., since their isotherms experiments were based on higher initial phenols concentrations (5-2000 mg L⁻¹ vs. 1-200 mg L⁻¹).

In addition, the linear form of the Freundlich isotherm at room temperature was employed to determine the value of K_f and n (Table 9.2). The R^2 values of Freundlich model were found to be lower than the R^2 value of Langmuir isotherm for the studied resins. In both cases, the value of the n coefficient is higher than 1, which highlights the favourability of the adsorption process. In this sense, the value of n was higher for Amberlyst A26 (1.8 vs 1.4), indicating that adsorption process was more favoured for this resin. Considering Figure 9.4a and b, it can be noticed that Freundlich model is able to describe the adsorption empirical data with less reliability in both cases.

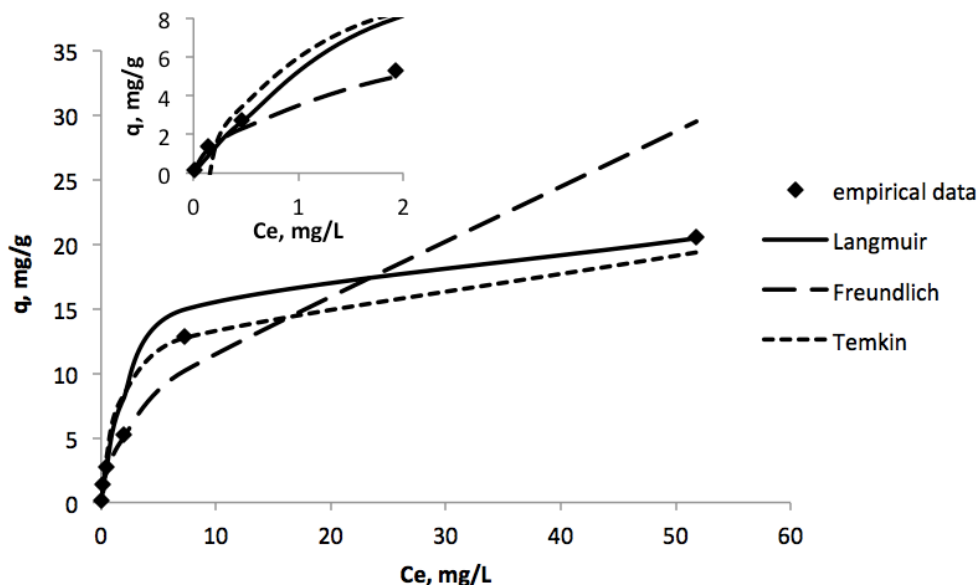


Figure 9.4a. Langmuir, Freundlich and Temkin isotherms for phenols uptake by Amberlyst A26 (phenols concentration = 1 - 200 mg L⁻¹, resin dosage = 7 g L⁻¹, recirculation time = 60 minutes temperature = 298 K and volume = 2 L).

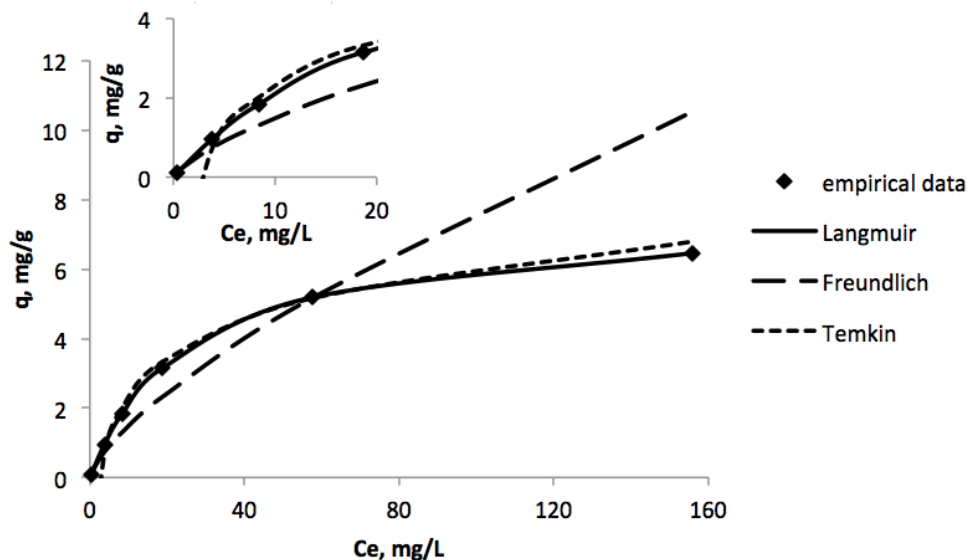


Figure 9.4b. Langmuir, Freundlich and Temkin isotherms for phenols uptake by Amberlite IRA-67 (phenols concentration = 1 - 200 mg L⁻¹, resin dosage = 7 g L⁻¹, recirculation time = 60 minutes temperature = 298 K and volume = 2 L).

Similar results were found by Caetano et al. in their study on phenols adsorption on both strong and weak-base anion exchange resins, which indicated R^2 values in the range 0.90 - 0.98 for Freundlich isotherms, while R^2 values of Langmuir model were equal to 0.99 for both resins (Caetano et al., 2009).

Finally, the A and B parameters of the Temkin model equation were calculated for phenols adsorption (Table 9.2). It was obtained that the value of R^2 for Temkin model (0.95) was lower than that calculated for Freundlich model (0.98) for Amberlyst A26. However, Temkin model seems to be closer to empirical data than Freundlich model (Figure 9.4a). This fact is right but only for C_e higher than 2 mg L⁻¹, namely C_i above 40 mg L. On the contrary, Freundlich model fits better the empirical data than Temkin model for C_i below 40 mg L⁻¹. Taking into account that the majority of data were in the C_i range 1-40 mg L⁻¹ (4 points vs. 2 points), it is logical the fact that R^2 value is higher for Freundlich model. On the other hand, Figure 9.4b reveals that Temkin model also fits the empirical data better than Freundlich model for Amberlite IRA-67, although R^2 value is in the same range (0.95) for both models (Table 9.2). In addition, the heat of sorption process, estimated by Temkin isotherm model, was found to be 5.8 J mol⁻¹ and 0.41 J mol⁻¹ for Amberlyst A 26 and Amberlite IRA-67, respectively.

Table 9.2. Langmuir, Freundlich and Temkin isotherm parameters for phenols uptake by Amberlyst A26 and Amberlite IRA-67 resins.

	Langmuir model			Freundlich model			Temkin model		
	K_L	q_m	R^2	K_f	n	R^2	A	B	R^2
Amberlyst A26	0.30	22	0.99	3.5	1.8	0.98	5.8	3.4	0.94
Amberlite IRA-67	0.038	7.5	0.99	0.29	1.4	0.95	0.41	1.6	0.95

* Coefficient Units: K_L (L mg⁻¹); q_m (mg g⁻¹); K_f (L mg⁻¹); A (L g⁻¹); B (J mol⁻¹)

9.3.3 Kinetic characterization

Information on the kinetics of pollutants uptake is required for selecting the optimum operational conditions for full-scale pollutants removal processes. Determination of the kinetic parameters and explanation of the mechanism in heterogeneous systems is often a complex procedure, as surface effects can be superimposed on chemical effects (Deliyanni et al. 2006).

The removal of phenols by means of both resins increased with time, attaining a maximum value during the first 5 min for initial phenols concentrations up to 20 mg L⁻¹ and at about 30–60 min for higher initial phenols concentrations. Thereafter phenols removal remained constant, as presented in Figure 9.5a and b. Results from these figures clearly indicate that the recirculation time required for maximum uptake (or to reach equilibrium) of phenols by Amberlyst A26 as well as Amberlite IRA-67 was dependant on the initial phenols concentration. In addition, the removal rate of phenols by both resins initially was fast up to 10–15 min, and then gradually decreased with increase in recirculation time.

In order to evaluate the kinetics parameters, experimental data obtained at several initial phenols concentrations were fitted to different kinetic models. Namely the pseudo-first order, the pseudo-second order and intraparticle diffusion models were tested. The reliability of these kinetic models was determined by measuring the coefficients of determination (R^2) and the sum of squares error (SSE). The SSE was calculated by the following equation (Eq. 6):

$$SSE = (q_{e,exp} - q_{e,cal})^2 \quad (7)$$

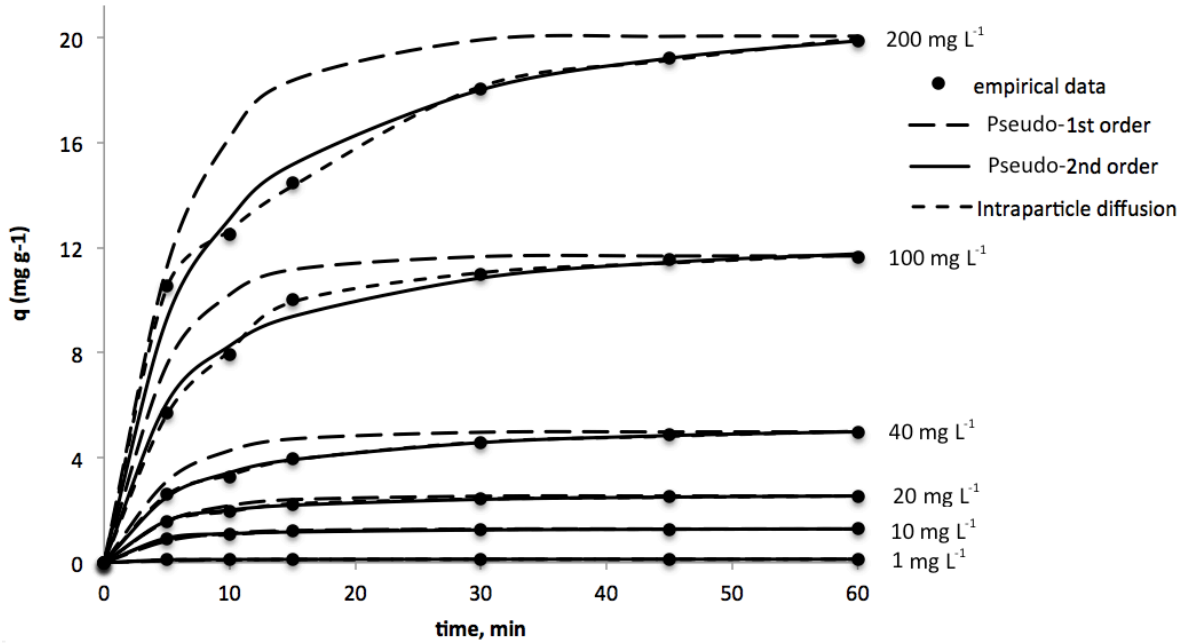


Figure 9.5a. Pseudo-first order kinetics, Pseudo-second order kinetics and Intraparticle diffusion equations for phenols uptake by Amberlyst A26 (phenols concentration = 1 - 200 mg L⁻¹, resin dosage = 7 g L⁻¹, recirculation time = 60 minutes temperature = 298 K and volume = 2 L).

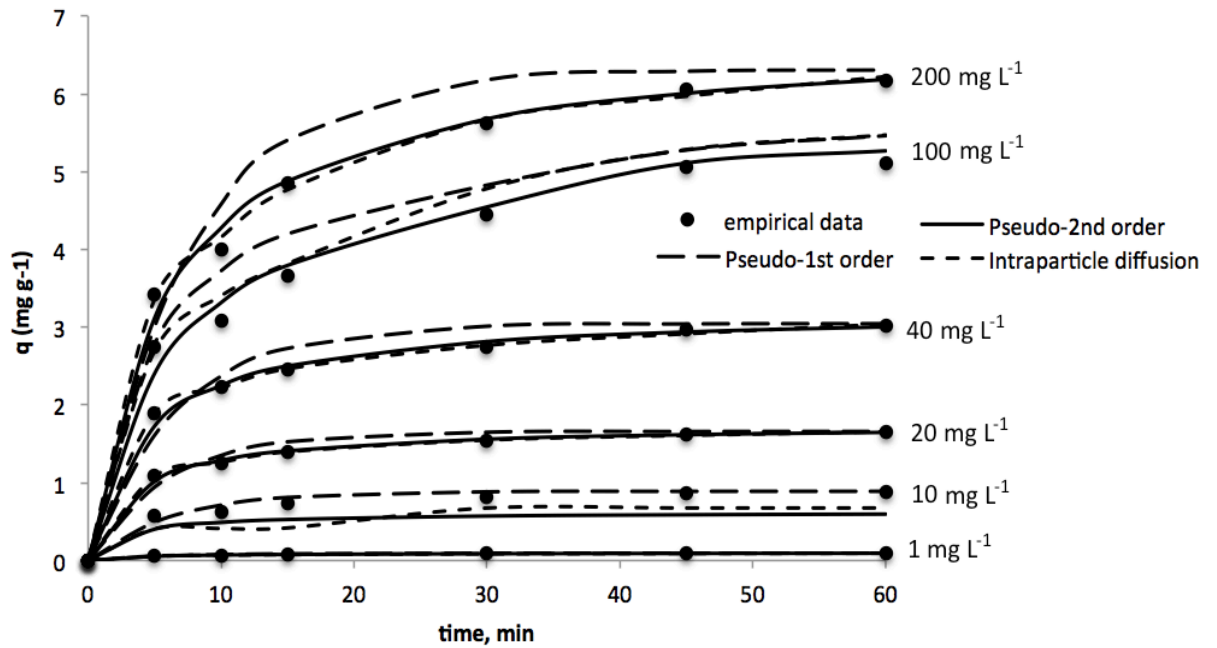


Figure 9.5b. Pseudo-first order kinetics, Pseudo-second order kinetics and Intraparticle diffusion equations for phenols uptake by Amberlite IRA-67 (phenols concentration = 1 - 200 mg L⁻¹, resin dosage = 7 g L⁻¹, recirculation time = 60 minutes temperature = 298 K and volume = 2 L).

Pseudo-first order model is one of the most widely used procedures for the adsorption of a solute from aqueous solution. The adsorption rate constant could be determined from the pseudo-first order equation given by Lagergren et al. (1898), which is expressed as follows (Lagergren, 1898):

$$q_t = q_e(1 - e^{-k_1 t}) \quad (8)$$

where q_e and q_t refers to the amounts of phenols adsorbed (mg g^{-1}) at equilibrium and time t (min), respectively, and k_1 is the first-order adsorption rate constant (min^{-1}).

The pseudo-second order equation is based on the equilibrium capacity of the solid phase. This model predicts the behaviour over the whole range of adsorption. The pseudo-second order equation can be expressed in the form (Ho and McKay, 1999):

$$q_t = \frac{q_e^2 k_2 t}{1 + q_e k_2 t} \quad (9)$$

where, k_2 ($\text{g mg}^{-1} \text{min}^{-1}$) is the adsorption rate constant of pseudo-second order adsorption rate.

Finally, in order to investigate any possible mechanisms of phenols adsorption onto both strong-base and weak-base anion exchange resins, intra-particle diffusion-based mechanism was also studied. According to this model, the uptake of the adsorbate by the adsorbent varies almost proportionately with the square root of the recirculation time ($t^{1/2}$). Weber and Morris (1962) proposed the most widely applied intra-particle diffusion equation for sorption systems as (Weber and Morris, 1962):

$$q_t = k_{id} t^{1/2} \quad (10)$$

where, q_t is the amount of phenols adsorbed per unit mass of adsorbent (mg g^{-1}) at a time t , and k_{id} the intraparticle diffusion rate constant ($\text{mg g}^{-1} \text{min}^{-1/2}$). The rate parameter k_{id} of stage i is obtained from the slope of the straight line resulting of plotting q_t versus $t^{1/2}$.

The results of the fit of the experimental uptake data to the different tested kinetic models for the studied resins are hereafter summarized in Tables 9.3 and 9.4. The values for the parameters obtained after application of the kinetic models were used to predict the variation of adsorbed phenols with time. The resulting curves are shown in Figure 9.5a and b.

For the first-order kinetics model, the rate constants k_1 were found to be in the range of 0.072–0.090 min^{-1} for Amberlyst A26 and in the range of 0.056–0.074 min^{-1} for the initial phenols concentration values of 1–200 mg L^{-1} (see Table 9.3).

The pseudo-second order adsorption rate constants k_2 values were found to be in the ranges of 0.0065-6.1 and 0.025-2.3 $\text{g mg}^{-1}\text{min}^{-1}$ for Amberlyst A26 and Amberlite IRA-67, respectively. The values of k_2 decreased with increase in initial phenols concentrations from 1 to 200 mg L^{-1} . This decrease is more pronounced for Amberlyst A26 as k_2 is reduced 10 times more than for Amberlyte IRA-67. Several authors have observed this trend (the k_2 decrease) in adsorption of different pollutants onto diverse adsorbent materials, such as metals adsorption onto synthetic IE resins (Zewail and Yousef, 2015), lead removal through clinoptilolite (Günay et al., 2007) and adsorption of methylene blue onto bamboo-based activated carbon (Hameed et al., 2007).

On the other hand, Figure 9.5a and b demonstrate that the initial uptake rate increased with increase in initial concentrations.

The results summarized in Table 9.3 show that the values of R^2 for first-order kinetics model are lower than for second-order-kinetics in both resins. Furthermore, the experimental q_e values do not agree well with the calculated values for the first-order kinetics model. This reveals that the uptake of phenols onto Amberlyst A26 and Amberlite IRA-67 resins does not follow first-order kinetics.

Nevertheless, the results reported in Figure 9.5a and b show pseudo-second model plots for all the assayed initial phenols concentrations, with very high values of R^2 in addition to the good agreement between the experimental and calculated values of q_e (Table 9.3) for second-order-kinetics in both resins. Therefore, the adsorption rate of phenols onto Amberlyst A26 and Amberlite IRA-67 (about 1.0) fits with utmost accuracy the pseudo-second order kinetics.

On the other hand, if the intraparticle diffusion is the controlling mechanism of the uptake, then the plot of q_t versus $t^{1/2}$ should be linear, and if it passes through the origin, the rate limiting process is only due to the intraparticle diffusion (Elmorsi, 2011).

Figure 9.5a and b also reports the results of the fit of the experimental data to the intraparticle diffusion model for the studied feedstream concentrations range. The intraparticle diffusion of phenols occurred in two sequential stages: the first straight portion is attributed to the macropore diffusion (phase I) whereas the second linear portion might be mainly related to micropore diffusion (phase II) (Weber and Morris, 1962). The intraparticle diffusion constants for these two stages (k_{1d} and k_{2d}) are given in Table 9.4. Results indicated that the phenols uptake through the investigated resins involved more than one process. In addition, the uptake rate was generally fast and the intraparticle diffusion was found to be the rate-limiting step, which occurred in the same way in case of sorption of many other different ions (Prasad and Saxena, 2004).

Table 9.3. Adsorption kinetic parameters for the phenols uptake process (phenols concentration = 1 - 200 mg L⁻¹, resin dosages: 7 g L⁻¹Amberlyst A26 and 7 g L⁻¹Amberlite IRA-67, temperature = 298 K and volume = 2 L).

	First-order kinetic model						Second-order kinetic model			
	[Ph]	$q_{e, exp}$	$q_{e, cal}$	k_1	R^2	SSE	$q_{e, cal}$	k_2	R^2	SSE
A	1	0.13	0.025	0.073	0.97	0.0071	0.13	6.1	1.0	0.0042
	10	1.3	0.43	0.090	0.97	0.11	1.3	0.36	1.0	0.059
	20	2.5	1.3	0,084	0.99	0.27	2.7	0.11	1.0	0.063
	40	5.0	4.0	0.085	0.99	0.28	5.5	0.031	1.0	0.21
	100	12	8.6	0.090	0.99	0.81	13	0.014	1.0	0.84
	200	20	16	0.072	0.98	1.5	22	0.0065	1.0	1.6
B	1	0.094	0.054	0.072	0.99	0.00031	0.10	2.3	1.0	0.0057
	10	0.89	0.50	0.070	0.98	0.048	0.62	0.58	1.0	0.069
	20	1.7	0.87	0.073	0.99	0.048	1.75	0.16	1.0	0.077
	40	3.0	1.6	0.065	0.99	0.087	3.2	0.072	1.0	0.18
	100	6.1	4.3	0.074	0.99	0.37	6.7	0.025	1.0	0.55
	200	6.3	3.7	0.056	0.99	0.26	6.8	0.025	1.0	0.42

A: Amberlyst A26 resin; B: Amberlite IRA-67 resin

Units used of the above terms are as follow: [Ph] ([Phenols]), mg L⁻¹, $q_e = \text{mg g}^{-1}$, $k_1 = \text{min}^{-1}$, $k_2 = \text{g mg}^{-1}\text{min}^{-1}$.

As it can be seen, the relative errors of the second-order model are lower than in both other models, and the correlation coefficients of the second-order model were found to be higher, indicating that this model describes better the phenols uptake by means of the studied resins. On the other hand, results indicate that the adsorption kinetic coefficients were dependent on the initial phenols concentration. Table 9.3 shows that the lowest differences between the theoretical $q_{e, cal}$ and the experimental $q_{e, exp}$ equilibrium adsorption capacity values are ensured by the second order rate equation.

Table 9.4. Weber-Morris parameters (phenols concentration = 1 - 200 mg L⁻¹, resin dosages: 7 g L⁻¹ Amberlyst A26 and 7 g L⁻¹ Amberlite IRA-67, temperature = 298 K and volume = 2 L).

	[Phenols]	k _{1d} (mg g ⁻¹ min ^{-1/2})	R ²	k _{2d} (mg g ⁻¹ min ^{-1/2})	R ²
A	1	0.011	0.97	0.00073	0.95
	10	0.18	1.0	0.0068	0.96
	20	0.41	1.0	0.051	0.93
	40	0.81	0.99	0.18	0.90
	100	2.6	1.0	0.30	0.88
	200	2.4	0.99	0.81	0.99
B	1	0.011	1.0	0.0033	0.89
	10	0.10	0.93	0.0031	0.98
	20	0.19	1.0	0.048	0.96
	40	0.35	1.0	0.12	0.88
	100	0.69	0.95	0.20	0.88
	200	0.86	0.96	0.24	0.93

Nevertheless, the intraparticle diffusion equations also provides a satisfactory fitting of the experimental data points for the whole set of the tested initial concentrations as it can be seen in Figure 9.5 and b. In this case, R² for the first straight portion was higher than for the second one. This trend was observed for both resins as well as for all the studied initial concentrations. Considering all the above results, the kinetics of phenols uptake on the selected strong-base and weak-base anion exchange resin could be satisfactorily described by both pseudo-second order and intraparticle diffusion model equations.

9.3.4 Gibbs free energy

Gibbs free energy was also calculated from the standard thermodynamic equilibrium constant, K_C (L g⁻¹), which was defined as follows:

$$K_C = \frac{qe}{ce} \quad (11)$$

where q_e is the amount of adsorbed phenols per unit mass of resin at equilibrium (mg g^{-1}) and C_e is the equilibrium aqueous concentration of phenols.

K_C can be obtained by plotting a straight line of $\ln (q_e/C_e)$ vs. q_e (Figure 9.6) and extrapolating q_e to zero (Khan and Singh, 1987). Its intercept gives the values of K_C .

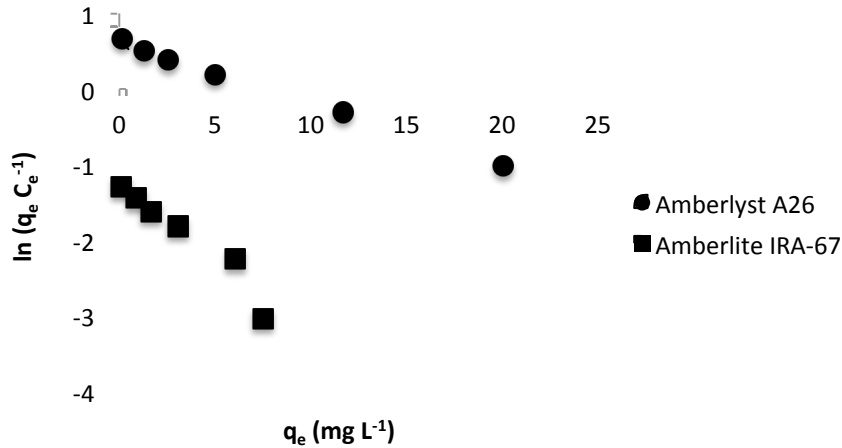


Figure 9.6. Plots of $\ln (q_e/C_e)$ vs. q_e for uptake of phenols by Amberlyst A26 and Amberlite IRA-67.

The standard Gibbs free energy changes (ΔG°) can be calculated according to the following equation (Alzaydien, 2009):

$$\Delta G^\circ = -RT \ln K_C \quad (12)$$

where T is the temperature (K) and R is the ideal gas constant ($\text{kJ mol}^{-1}\text{K}^{-1}$).

The values obtained are shown in Table 9.5. The ΔG° was found to be $-1.55 \text{ kJ mol}^{-1}$ for Amberlyst A26, indicating that the uptake process of phenols by this strong-base anion exchange resin is spontaneous at room temperature. Notwithstanding, the free energy changes in phenol-Amberlite IRA-67 system were 3.06 kJ mol^{-1} . In this case, the positive value points out that the uptake process is not spontaneous at room temperature.

Table 9.5. Equilibrium constant and Gibbs free energy of uptake of phenols by Amberlyst A26 and Amberlite IRA-67.

	Amberlyst A26	Amberlite IRA-67
Intercept, $\ln K_C$	0.63	-1.24
ΔG° (kJ mol^{-1})	-1.55	3.06
R^2 (linear)	0.99	0.94

9.4 Conclusions

The phenols uptake by weak-base anion exchange resin (Amberlite IRA-67) and strong-base anion exchange resin (Amberlyst A26) has been investigated on the basis of the feedstream phenols concentration and recirculation time effects. The aim of this study was to examine the potential of these IE resins towards the removal of phenols for its application to several industrial wastewaters.

For Amberlyst A26 resin, the equilibrium was obtained in about 7 min for initial concentrations lower than 20 mg L^{-1} , whereas it was reached after 15 minutes for initial phenols levels in the range $20 - 200 \text{ mg L}^{-1}$. Nonetheless, the equilibrium was achieved around the first 15 minutes for all the studied initial phenols concentrations, for Amberlite IRA-67 resin.

The phenols removal efficiency decreases considerably as the initial phenols concentration increases. In this sense, the phenols removal efficiency decreased from 99.6 % for 1 mg L^{-1} phenols in the feedstream, to 74.2 % for the highest assayed concentration (200 mg L^{-1}) for the strong-base anion exchange resin. In this case, it can be ensured that IE was the predominant process responsible of phenols removal. On the other hand, phenols removal efficiency decreased from 65.7 % for 1 mg L^{-1} phenols in the feedstream, to 22.1 % for the highest assayed concentration (200 mg L^{-1}) for the weak-base anion exchange resin. In this case, the decrease was more pronounced and it can be assumed that the adsorption is the main responsible process for phenols removal through this resin.

Considering all isotherm models, Langmuir isotherm provided the best correlation for both IE resins ($R^2 = 0.99$). The R_L values were in the ranges of 0.02-0.77 and 0.12-0.96, for Amberlyst A26 and Amberlite IRA-67. These results indicate that phenols adsorption is more favoured in case of Amberlyst A26 since the separation factor R_L values are lower than for Amberlite IRA-67.

Results demonstrated that phenols uptake onto Amberlyst A26 resin is a spontaneous process ($\Delta G^\circ = -1.55 \text{ kJ mol}^{-1}$), whereas it is not spontaneous for the phenols-Amberlite IRA-67 system ($\Delta G^\circ = 3.06 \text{ kJ mol}^{-1}$).

Furthermore, the results show that the second-order model describes with utmost accuracy the phenols uptake through the studied IE resin, although the kinetics of phenols uptake on the selected strong-base and weak-base anion exchange resin could be also satisfactorily described by intraparticle diffusion model. Moreover, the strong-base anion exchange resin was found to provide faster kinetics in the uptake of phenols (up to $6.1 \text{ g mg}^{-1}\text{min}^{-1}$ vs. $2.3 \text{ g mg}^{-1}\text{min}^{-1}$) as well as sensibly higher sorption capacity (22.0 mg g^{-1} vs. 7.5 mg g^{-1}) than the weak-base anion one. All

the above results reveal that Amberlyst A26 was confirmed to be considerably more efficient than Amberlite IRA-67 for the potential removal of phenols from industrial effluents.

9.5 References

Abhuri, K. (2003). Adsorption of phenol and p-chlorophenol from their single and bisolute aqueous solutions on Amberlite XAD-16 resin. *J. Hazard. Mater.*, 105:143-156.

Al-Asheh, S., Banat, F., Abu-Aitah, L. (2003). Adsorption of phenol using different types of activated bentonites. *Sep. Purif. Technol.*, 33:1-10.

Alzaydien, A.S. (2009). Adsorption of Methylene Blue from Aqueous Solution onto a Low-Cost Natural Jordanian Tripoli. *American Journal of Applied Sciences*, 5:197-208.

Anasthas, H., Gaikar, V. (1999). Adsorptive separations of alkylphenols using ion exchange resins. *Reactive Funct. Polym.*, 39:227-237.

Bertin, L., Ferri, F., Scoma, A., Marchetti, L., Fava, F. (2011). Recovery of high added value natural polyphenols from actual olive mill wastewater through solid phase extraction. *Chem. Eng. J.*, 171:1287-1293.

Barros, L., Macedo, G., Netto, W., Becerra, M. (2003). Phenol removal by biological and photochemical–biological processes. *Afinidad*, 60:568-572.

Caetano, M., Valderrama, C., Farran, A., Cortina, J.L. (2009). Phenol removal from aqueous solution by adsorption and ion Exchange mechanisms onto polymeric resins. *J. Colloid. Interface Sci.*, 338:402-409.

Carmona, M., De Lucas, A., Valverde, J.L., Velasco, B., Rodríguez, J.F. (2006). Combined adsorption and ion exchange equilibrium of phenol on Amberlite IRA-420. *Chem. Eng. J.*, 117:155-160.

Chern, J., Chien, Y. (2002). Adsorption of nitrophenol onto activated carbon: isotherms and breakthrough curves. *Water Res.*, 36:647-655.

Costa, C., Rodrigues, A. (1985). Part I. Phenol adsorption on polymeric adsorbents. *AIChE J.*, 31:1645-1654.

Deliyanni, E.A., Nalbandian, L., Matis, K.A. (2006). Adsorptive removal of arsenites by a nanocrystalline hybrid surfactant–akaganeite sorbent. *J. Colloid Interface Sci.*, 302:458-466.

- Elmorsi, T.M. (2011). Equilibrium isotherms and kinetic studies of removal of methylene blue dye by adsorption onto miswak leaves as a natural adsorbent. *Journal of Environmental Protection*, 2(6):817-827.
- Fan, C., Sun, Y., Min, Y., Hao, X., Li, X., Li, F. (2003). Photocatalytic degradation of phenol in aqueous solution using TiO₂/Ti thin film photocatalyst. *Trans. Nonferrous Met. Soc. China*, 13:1008-1012.
- Freundlich, H.M.F. (1906). Over the adsorption in solution. *J. Phys. Chem.*, 57:385-471.
- Greenberg, A.E., Clesceri, L.S., Eaton, A.D. (1992). Standard Methods for the Examination of Water and Wastewater, APHA/AWWA/WEF, 16th ed., Washington DC. Cabs.
- Günay, A., Arslankaya, E., Tosun, I. (2007). Lead removal from aqueous solution by natural and pretreated clinoptilolite: Adsorption equilibrium and kinetics. *J. Hazard. Mater.*, 146:362-371.
- Gupta, V.K., Ali, I., Saini, V.K. (2004). Removal of Chlorophenols from Wastewater Using Red Mud: An Aluminum Industry Waste. *Environ. Sci. Technol.*, 38:4012-4018.
- Jain, A.K., Gupta, V.K., Jain, S. (2004). Removal of Chlorophenols Using Industrial Wastes. *Environ. Sci. Technol.*, 38:1195-1200.
- Juang, R., Wu, F., Tseng, R. (1996). Adsorption isotherms of phenolic compounds from aqueous solutions onto activated carbon fibers. *J. Chem. Eng. Data*, 41:487-492.
- Juang, R.S., Shiau, J. (1999) Adsorption isotherms of phenols from water onto macroporous resins. *J. Hazard. Mater.*, 70:171-183.
- Juang, R.S., Shiau, J.Y., Shao, H.J. (1999). Effect of temperature on equilibrium adsorption of phenols onto nonionic polymeric resins. *Sep. Sci. Technol.*, 34:1819-1831.
- Hameed, B.H., Din, A.T.M., Ahmad, A.L. (2007). Adsorption of methylene blue onto bamboo-based activated carbon: Kinetics and equilibrium studies. *J. Hazard. Mater.*, 141:819-825.
- Ho, Y.S., McKay, G. (1999). Pseudo-Second Order Model for Sorption Processes. *Process Biochemistry*, 34:735-742.
- Kavitha, V., Palanivelu, K. (2004). The role of ferrous ion in fenton and photofenton process for degradation of phenol. *Chemosphere*, 55:1235-1243.

- Khan, A.A., Singh, R.P. (1987). Adsorption thermodynamics of carbofuran on Sn(IV) arsenosilicate in H^+ , Na^+ and Ca^{2+} forms. *Colloids Surf.*, 24:33-42.
- Ku, Y., Lee, K.C. (2000). Removal of phenol from aqueous solutions by XAD-4 resin. *J. Hazard. Mater.*, 80:59-68.
- Ku, Y., Lee, K., Wang, W. (2004). Removal of phenols from aqueous solutions by purolite A-510 resin. *Sep. Sci. Technol.*, 39:911-923.
- Kujawski, W., Warszawski, A., Ratajczak, W., Porebski, T., Capala, W., Ostrowska, I. (2004). Removal of phenol from wastewater by different separation techniques. *Desalination*, 163:287-296.
- Lagergren, S. (1898). Zur theorie der sogenannten adsorption gelöster stoffe, Kungliga Svenska Vetenskapaskademiens. *Handlingar* 24(4):1-39.
- Langmuir, I. (1918). The adsorption of gases on plane surfaces of glass, mica and platinum. *J. Am. Chem. Soc.*, 40:1361-1403.
- Lazarova, Z., Boyadzhieva, S. (2004). Treatment of phenol-containing aqueous solutions by membrane-based solvent extraction in coupled ultrafiltration modules. *Chem. Eng. J.*, 100:129-138.
- Lee, J., Shim, W., Ko, J., Moon, H. (2004). Adsorption equilibria, kinetics, and column dynamics of chlorophenols on a nonionic polymeric sorbent, XAD-1600. *Sep. Sci. Technol.*, 39:2041-2065.
- Ould Brahim, I., Belmedani, I.M., Belgacem, A., Hadoun, H., Sadaoui, Z. (2014). Discoloration of azo dye solutions by adsorption on activated carbon prepared from the cryogenic grinding of used tires. *Chemical Engineering Transactions*, 38:121-126.
- Özbelge, T., Özbelge, Ö., Baskaya, S. (2002). Removal of phenolic compounds from rubber-textile wastewaters by physicochemical methods. *Chem. Eng. Process.*, 41:719-730.
- Prasad, M., Saxena, S. (2004). Sorption mechanism of some Divalent Metal Ions onto Low-Cost Mineral Adsorbent. *Industrial & Engineering Chemistry Research*, 43:1512-1522.
- Senthil Kumar, P., Gayathri, R. (2004). Adsorption of Pb^{2+} ions from aqueous solutions onto bael tree leaf powder: isotherms, kinetics and thermodynamics study. *J. Eng. Sci. Technol.*, 4(4):381-399.

Temkin, M.J., Pyzhev, V. (1940). Recent modifications to Langmuir isotherms. *Acta Physicochim URSS.*, 12:217-222.

Tomaszewska, M., Mozia, S., Morawski, W. (2004). Removal of organic matter by coagulation enhanced with adsorption on PAC. *Desalination*, 162:79-87.

Víctor-Ortega, M.D., Ochando-Pulido, J.M., Godaifa, H., Martínez-Férez, A. (2014). Final purification of synthetic olive oil mill wastewater treated by chemical oxidation using ion exchange: Study of operating parameters. *Chem. Eng. Process.*, 85:241-247.

Vinod, V., Anirudhan, T. (2002). Effect of experimental variables on phenol adsorption on activated carbon prepared from coconut husk by single-step steam pyrolysis: mass transfer process and equilibrium studies. *J. Sci. Ind. Res.*, 61:128-138.

Weber, W.J., Morris, J.C. (1962). Kinetic of Adsorption on Carbon from Solution. *Journal of the Sanitary Engineering Division*, 89:31-59.

Wu, J., Rudy, K., Sapark, J. (2000). Oxidation of aqueous phenol by ozone and peroxidase. *Adv. Environ. Res.*, 4:339-346.

Zagklisa, D.P., Vavourakia, A.I., Kornarosa, M.E., Paraskevat, C.A. (2015). Purification of olive mill wastewater phenols through membrane filtration and resin adsorption/desorption. *J. Hazard. Mater.*, 285:69-76.

Zewail, T.M., Yousef, N.S. (2015). Kinetic study of heavy metal ions removal by ion exchange in batch conical air spouted bed. *Alexandria Engineering Journal*, 54:83-90.

Zhu, L., Deng, Y., Zhang, J., Chen, J. (2011). Adsorption of phenol from water by N-butylimidazolium functionalized strongly basic anion exchange resin. *J. Colloid Interface Sci.*, 364:462-468.

CHAPTER 10

PERFORMANCE AND MODELLING OF CONTINUOUS ION EXCHANGE PROCESSES FOR PHENOLS RECOVERY FROM OLIVE MILL WASTEWATER

M.D. Víctor-Ortega^{1*}, J.M. Ochando-Pulido¹, A. Martínez-Ferez¹

¹ Chemical Engineering Department, University of Granada, 18071 Granada, Spain

Tel: +34958241581; Fax: +34958248992;

*email: mdvictor@ugr.es

Submitted for publication. Current status: under review.

Separation and Purification Technology

Publisher: ELSEVIER SCIENCE BV. PO BOX 211, 1000 AE AMSTERDAM, NETHERLANDS

Year: 2015

ISSN: 1383-5866

Impact factor: 3.091

Tertile: First



Abstract

A continuous-flow ion exchange process for the recovery of phenols from olive mill wastewaters (OMWs) was examined in a packed column by means of both strong-base and weak-base anion exchange resins. The effect of initial pH showed that phenols removal efficiency increased with an increase in the pH value up to 7. Moreover, it can be observed that IE efficiency remains virtually constant at higher pH values for Amberlyst A26. On the other hand, phenols IE removal efficiency for Amberlite IRA-67 also increased with an increase in the pH value up to 7, reaching phenols removal efficiencies close to 57 %, but higher pH values led to lower IE efficiency. On the other side, Thomas, Yoon–Nelson and Clark models were applied to the experimental data to predict the breakthrough curves and model parameters such as rate constants and breakthrough times. In the perspective of a process scale-up, the simulation of the best-performing operational condition was used to evaluate the process performances for different inlet phenols concentrations (5, 25 and 100 mg L⁻¹). The results showed an increase in initial phenols concentration improved the adsorption capacity. In both cases, the Thomas model was found to give best fit to experiment data for the three initial phenols concentrations, followed by the Yoon-Nelson and Clark models. Finally, column regeneration studies showed that almost 100 % phenols recovery efficiencies were obtained. IE process led to a solution of phenols susceptible to be concentrated and used in food, cosmetic or pharmaceutical sectors.

Keywords: Breakthrough curves, Industrial effluents, Phenols recovery, Strong-base anion exchange resin, Weak-base anion exchange resin.

10.1 Introduction

The food industry generates high wastewater volumes, which contain inherent reusable substances of high value. The target products can be separated from the wastewater stream and further processed into secondary products of high commercial value, usually through highly time-consuming and expensive processes (Hajji et al., 2014). One example could be the case of olive mill wastewater (OMW), which presents considerable concentration of phenolic compounds of high-added value because of their antibacterial, antifungal, antiviral, antioxidant and anti-inflammatory activities as well as health-beneficial properties, with high potential for commercial use (Tsagaraki et al., 2007).

On the other hand, the discharge of this heavily polluted wastewater has become a serious economical and environmental issue worldwide. This fact is of particular concern in the Mediterranean area since more than 75% of the world olive oil is produced in this region (Roig

et al., 2006).

Summarized physicochemical characterization of OMW is reported in Table 10.1, highlighting the high phenols content (around 80 mg L⁻¹).

Table 10.1. Physicochemical characterization of OMW (Ochando-Pulido et al., 2015).

Parameters	OMW*
pH	5.7
Moisture, %	99.5
Total solids, %	0.44
Organic substances, %	0.29
Ashes, %	0.14
BOD₅, mg O₂ L⁻¹	645.1
COD, mg O₂ L⁻¹	4100.3
Total phenols, mg L⁻¹	80.5
EC, mS cm⁻¹	1.1

* OMW: 1:1 (v/v) olive oil washing wastewater and olives washing wastewater

It is well known that phenol and phenolic compounds are one the most common organic pollutants of wastewaters requiring a proper treatment before being discharged into the water courses. It is worthy to mention that drinking water pollution due to phenols at even a concentration of 1 mg L⁻¹ could result in significant taste and odor problems making it unsuitable for use (Aksu and Gönen, 2004).

In last years, several alternatives of valorisation and treatment have been developed for OMW, including physical, chemical and biological treatments. The use of lagoons for OMW evaporation is one of the most popular option for treating this effluent. This technique is favoured in the Mediterranean region due to the weather (Jarboui et al., 2010). Various coagulation-flocculation works on OMW, based on the use of several commercial coagulants, have also been reported (Azbar et al., 2004). Furthermore, there are some studies focused on the use of membrane technology with the final objective of reducing the organic load of OMW (Akdemir and Ozer, 2009; Paraskeva et al., 2007; Stoller and Bravi, 2010; Turano et al., 2002; Ochando-Pulido et al., 2013). In these research works, microfiltration (MF), ultrafiltration (UF), nanofiltration (NF) and reverse osmosis (RO) were employed.

On the other hand, several authors investigated microbiological treatments for purification of

OMW. However, the presence of phenolic compounds hinders the microbiological treatment of the OMW. In this regard, aerobic treatments have been developed for the remediation of OMW, especially for the degradation of phenolic compounds, which are the main responsible for the OMW phytotoxicity (Garcia-Castello et al., 2010). The composting is the most used method to recycle and transform OMW into fertilizers. In this case, Tomati et al. produced fertilizers without phytotoxicity from OMW through co-composting (Tomati et al., 1995).

As it is aforementioned, the main inconvenient concerning the treatment and use of phenolic compounds is its phytotoxicity. In contrast with this, phenols are widely employed by pharmaceutical, cosmetic and nourishment industries (De Marco et al., 2007).

Regarding phenolic compounds separation from OMW, solvent extraction by acidic ethyl acetate can be named as the most commonly employed technique. However, supercritical fluids and acidified ethanol were also successfully used for this purpose (Kalogerakis et al., 2013; Lafka et al., 2011; De Leonardis et al., 2007; Galanakis et al., 2010). These chemical methods for phenolic compounds synthesis make increase final prices of these compounds. Therefore, it could be economically and environmentally interesting to extract phenols from OMW by means of an easier and cheaper way. There are some researches about the extraction and removal of phenols from OMW by employing several fungi such as *Phanerochaete chrysosporium*, *Aspergillus niger*, *Aspergillus terreus* and *Geotrichum candidum* (García García et al., 2000; Bouzid et al., 2005). In addition, membrane technology has been efficiently used in several studies by combinations of membrane separation processes, which were proposed either as a pretreatment step before further unit operations, or as a complete phenols removal process (El-Abbassi et al., 2014; Zagklisa et al., 2015; Garcia-Castello et al., 2010; Conidi et al., 2014). Finally, IE resins have been employed for phenol recovery from OMW, such as XAD4, XAD7, XAD16 and XAD7HP (Bertin et al., 2011; Zagklisa et al., 2015).

In this scenario, the continuous adsorption in fixed-bed column is often desired from an industrial point of view since it is simple to operate and can be scaled-up from a laboratory process (Chern and Chien, 2002). In order to design and operate fixed-bed IE processes successfully, the breakthrough curves under specified operating conditions must be predictable. The shape of this curve is influenced by the individual transport process in the column and in the adsorbent (Vázquez et al. 2006). In this regard, several models have been used for the prediction of breakthrough time. Among them, Thomas model, Yoon-Nelson model and Clark model have become three of the most used.

The purpose of this research work was to evaluate the performance of two fixed-bed IE processes, based on both strong-base and weak-base anion exchange resins, for phenols

separation from OMW. This phenols separation would represent the first step of a wider OMW valorization process in order to get a high-added value product from this wastewater. The influence of some key parameters on the IE performance and removal efficiency was elucidated, comprising the inlet phenols concentration, the system pH and the equilibrium information related to the IE column breakthrough behaviour, which provides information about the dynamic behaviour of phenols concentration in time indispensable for appropriate column design. Column experiments were carried out to examine the breakthrough curves for three different inlet phenols concentrations for each resin. Subsequently, the IE processes were also modelled by fitting the experimental data to Thomas, Yoon-Nelson and Clark models.

10.2 Methods and materials

10.2.1 Materials

In this research work, two anion exchange resins were used: Amberlyst A26 strong base anion exchange resin and Amberlite IRA-67 weak base anion exchange resin. Firstly, both resins were conditioned in NaOH solution and finally in water before being used in the IE/adsorption experiments, following the advice given by the resin manufacturer. Typical physical and chemical characteristics of these resins are described in Table 10.2.

For these experiments, model solutions were prepared by dissolving reagent-grade phenol (provided by Panreac) in double distilled water. In addition, regeneration solutions were prepared by dissolving reagent-grade NaOH (supplied by Panreac) in double distilled water.

Table 10.2. Physicochemical properties of the resins.

Properties	Amberlyst A26	Amberlite IRA-67
Type	Strong-base anion	Weak-base anion
Matrix	Styrene-divinylbenzene	Tertiary amine
Ionic form as shipped	OH ⁻	OH ⁻
Particle size, mm	0.56-0.70	0.50-0.75
Effective pH range	0-14	0-7
Total exchange capacity, eq L⁻¹	0.80	1.60
Shipping weight, g L⁻¹	675	700

10.2.2 Analytical methods

Analytical grade reagents and chemicals with purity over 99 % were used for the analytical procedures, applied at least in triplicate.

Total phenols and phenol derivatives were analysed by reaction with a derivative thiazol, giving a purple azo dye which was determined photometrically using a Helios Gamma UV–visible spectrophotometer (Thermo Fisher Scientific) at 475 nm (Standard German methods ISO 8466-1 and DIN 38402 A51) (Greenberg et al., 1992).

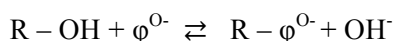
10.2.3 Initial pH study experiments

The IE performance for phenols removal was studied at different pH values in the range 3 - 11 by conducting recirculation mode experiments. With this purpose, the pH value was adjusted by adding 1N NaOH or HCl, depending on the desired value, while maintaining the resin dosage constant (7 g L⁻¹).

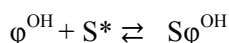
The flow rate and temperature were fixed at 10 L h⁻¹ and room temperature, respectively (Victor-Ortega et al., 2014), whereas the contact time was varied up to 60 min in order to reach equilibrium.

In the solid phase it was assumed that two mechanisms for the uptake of phenols into the resins beads take place, one by IE and another by molecular adsorption (Carmona et al., 2006). The following equations describe these mechanisms.

(a) Exchange of phenolate anion with the counter-ion (OH) of the resin:



(b) Adsorption of the molecular phenol on the free polymeric surface:



where S* and S φ^{OH} represent active and occupied adsorption sites of the resin, respectively.

IE/adsorption equilibrium was examined in order to obtain the basic thermodynamic parameters. The extent of the IE equilibrium data of this pollutant was determined by measuring the residual total phenols concentration in the liquid phase. Previously, aqueous solutions of the contaminant were put in contact with the IE resin until equilibrium was achieved. The flask containing the feed solution was stirred continuously during the whole course of the experiments.

The removal efficiency was determined by computing the sorption percentage using the formulae in Eq.(1):

$$\% \text{ Sorption} = \frac{C_o - C_e}{C_o} \times 100 \quad (1)$$

where C_o and C_e are the initial and equilibrium phenols concentration (mg L^{-1}), respectively.

10.2.4 Continuous-mode IE studies

The fixed-bed column was made of an acrylic tube (540 mm height x 46 mm internal diameter), provided with a mobile upper retaining grid, which could be fixed in the column to adjust it as a fixed bed or a semi-fluidized bed. A fixed amount of 35 g of Amberlyst A26 and Amberlite IRA-67 resins was packed in the column. Phenols solutions with concentrations of 5, 25 and 500 mg L^{-1} at pH optimum value, were pumped through the column at a flow rate of 10 L h^{-1} controlled by a peristaltic pump (Ecoline VC-380) (see Figure 10.1).

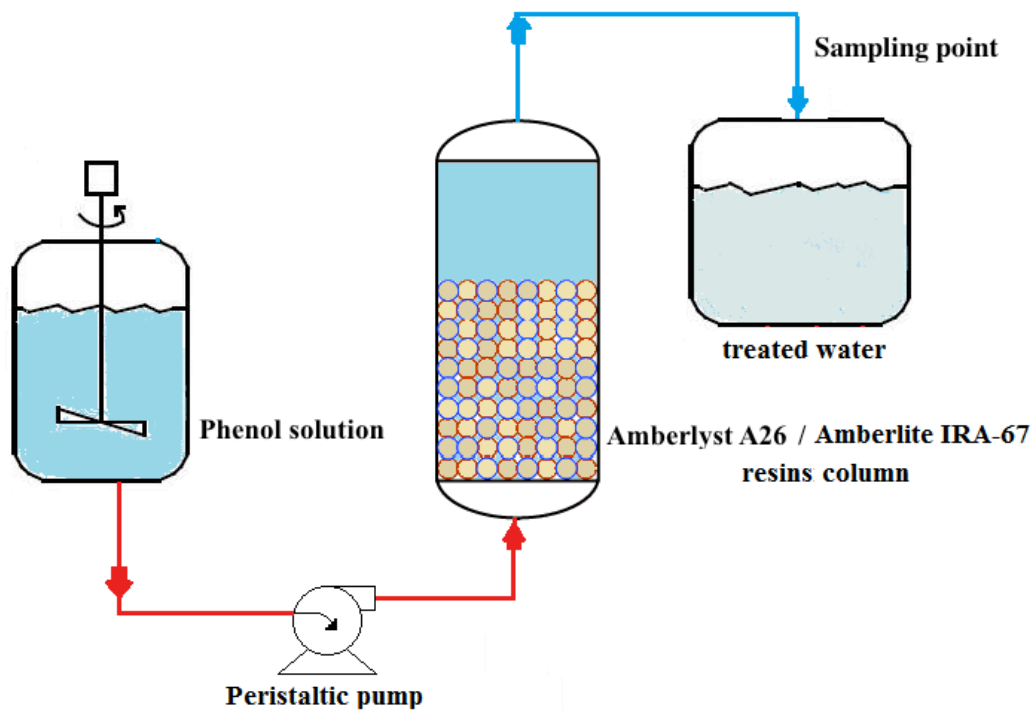


Figure 10.1. Flow-sheet scheme of column IE studies continuous operation for phenols removal.

The phenols solutions at the outlet of the column were collected at regular time intervals. Aliquots were removed periodically, and the concentration of phenols present in the effluent was spectrophotometrically determined as thoroughly described in *section 2.2*. The amount of the pollutant adsorbed was calculated on the basis of the difference between the inlet

concentration (C_0) and outlet concentration (C_t).

The efficiency of the column was evaluated by determining the breakthrough curves for each resin. The breakthrough curves, which showed the performance of the fixed-bed column, were plotted in terms of normalized concentration, C_t/C_0 , defined as the ratio of outlet phenols concentration, C_t (mg L^{-1}), to inlet phenols concentration, C_0 (mg L^{-1}), as a function of time. The experimental curves were mathematically modelled using non-linear regression, and the parameters were estimated using the *MS Excel 2011* program.

The breakthrough time t_B is defined as the time required for the concentration of pollutant in the effluent exiting the IE column to reach 5 % of the inlet concentration. Otherwise, the exhaustion time t_E is defined as the time when the concentration of phenols in the effluent becomes 90 % of the feedstream concentration.

The breakthrough volumes VB and exhaustion volumes VE are the effluent volumes at breakthrough time and exhaustion time, respectively. The effluent volume (V_{eff}) can be calculated from the following equation (Eq 2):

$$V_{\text{eff}} = Q \cdot t_{\text{total}} \quad (2)$$

where t_{total} and Q are the total flow time (min) and volumetric flow rate (ml min^{-1}), respectively. The area under the breakthrough curve (A), obtained by integrating the adsorbed concentration C_{ad} (mg L^{-1}) vs. t (min) plot, can be used to find the total adsorbed pollutant quantity (maximum column capacity). The total adsorbed phenols quantity q_{total} (mg g^{-1}) in the column for a given feed concentration and flow rate (Q) can be calculated from the following equation:

$$Q_{\text{total}} = Q \cdot \frac{(C_0 - C_t)}{1,000} \cdot t_{\text{total}} \quad (3)$$

The total amount of phenols sent to column (m_{total}) was calculated from the following equation:

$$m_{\text{total}} = \frac{C_0 \cdot Q}{1,000} \cdot t_{\text{total}} \quad (4)$$

The total removal efficiency of phenols is the ratio of the maximum capacity of the column (q_{total}) to the total amount of phenols driven into the column (m_{total}) from the following equation:

$$\text{Total removal efficiency (\%)} = \frac{q_{\text{total}}}{m_{\text{total}}} \cdot 100 \quad (5)$$

The phenols equilibrium uptake (q_{eq}) (or maximum capacity of the column) in the column is defined by Eq. (5) as the total amount of phenols sorbed (q_{total}) per gram of sorbent (X) at the

end of the total flow time:

$$q_{eq} = \frac{qt_{total}}{X} \quad (6)$$

10.2.5 Breakthrough curves modelling

The time or bed volume for breakthrough appearance and the shape of the breakthrough curve are important characteristics for determining the operation and dynamic response of an adsorption column (XiaoFeng et al., 2014). Moreover, the successful design for an adsorption column requires the prediction of the concentration-time profile from the breakthrough curve for the effluent discharged from the column. In order to describe the adsorption process of phenols on both Amberlyst A26 and Amberlite IRA-67 resins, several models were used to fit the adsorption breakthrough curves.

The used models, hereafter described in the following sections, were fitted to experimental breakthrough curves using non-linear regression methods. Coefficient of linearity (R^2) was calculated to describe the fit between experimental data and non-linearized forms of Thomas, Yoon-Nelson, and Clark equations, whereas the sum of the squares of the errors (SSE), calculated according to Eq. (7), served as an indicator of the fit goodness between the experimental data and predicted values of C/C_0 used for plotting the breakthrough curves:

$$SSE = (q_{e,exp} - q_{e,cal})^2 \quad (7)$$

where the subscripts ‘calc’ and ‘exp’ make reference to the calculated and experimental values, respectively, and n is the number of measurements.

10.2.5.1 Thomas model

Thomas model is applicable in systems with a constant flow rate and no axial dispersion, and its behaviour matches the Langmuir isotherm and the second-order reversible reaction kinetics. The linearized form of the model is given by the following equation (Thomas, 1944).

$$\ln\left(\frac{C_0}{C_t} - 1\right) = \frac{K_{Th} q_0 M}{Q} - \frac{K_{Th} C_0 M}{Q} V \quad (8)$$

In this expression, K_{Th} ($\text{ml mg}^{-1} \text{min}^{-1}$) is the Thomas rate constant, q_0 (mg g^{-1}) is the equilibrium adsorbate uptake, Q (ml min^{-1}) is the flow rate, and V (ml) is the effluent volume; C_t is the concentration of phenols at time t and C_0 is the initial pollutant concentration.

10.2.5.2 Yoon–Nelson model

Yoon–Nelson theoretical model was applied to investigate the breakthrough behaviour of phenols on the selected IE resins. This model is based on the assumption that the increase in rate or decrease in the probability of adsorption for each adsorbate molecule is proportional to the probability of adsorbate adsorption and the probability of adsorbate breakthrough on the adsorbent. The Yoon–Nelson model is not only less complex than other sorption models but also requires no detailed data concerning the characteristics of the adsorbate, the type of adsorbent, and the physical properties of the adsorption bed. The linearized model for a single-component system can be expressed by the following equation (Yoon and Nelson, 1984).

$$\text{Ln} \left(\frac{C_0}{C_t} - 1 \right) = K_{YN} \cdot t - \tau \cdot K_{YN} \quad (9)$$

where K_{YN} (min^{-1}) is the Yoon–Nelson rate constant, τ is the time required for 50 % adsorbate breakthrough (min), and t is the sampling time (min), whereas C_t is the concentration of phenols at time t and C_0 is the initial pollutant concentration.

For a given bed:

$$q_{0YN} = \frac{C_0 \cdot Q \cdot \tau}{1.000 X} \quad (10)$$

where q_{0YN} is the adsorption capacity, C_0 is the initial phenols concentration, Q is the flow rate, X is the weight of adsorbent, and τ is the 50 % breakthrough time.

10.2.5.3 Clark model

Another model developed by Clark was based on the use of a mass-transfer concept, but in the form of the Freundlich adsorption equation (Clark, 1987). The linearized form of the model is given by the following expression:

$$\text{Ln} \left[\left(\frac{C}{C_0} \right)^{n-1} - 1 \right] = -rt + \text{Ln } A \quad (11)$$

with

$$A = \left(\frac{C_0^{n-1}}{C_b^{n-1}} - 1 \right) e^{rt_b} \quad (12)$$

and:

$$r = \frac{\beta}{U} v_m (n - 1) \quad (13)$$

where n is the Freundlich constant, C_b is the concentration of sorbate at breakthrough time t_b (mg L^{-1}), and v_m is the migration velocity of the concentration front in the bed (cm h^{-1}).

10.2.6 Resins regeneration and phenols recovery

For the resins regeneration, the Amberlyst A26 strong-base anion exchange resin was fully washed with 100 mL 4 % NaOH aqueous solution whereas the Amberlite IRA-67 weak-base anion exchange resin was rinsed with 100 mL 2% NaOH aqueous solution, both at room temperature. Phenols were completely removed from the resins and recovered in aqueous solution, and its concentration was determined as described previously. The resins were then washed with distilled water to remove the excess of base and recondition. This procedure was carried out after each adsorption/regeneration cycle.

10.3 Results and discussion

10.3.1 Effect of initial pH

The influence of the initial pH value (pH_0) on phenols removal through the studied resins is reported in Figure 9.2. The adsorption/IE of phenols was studied at different pH_0 values in the range 3–11, for both Amberlyst A26 and Amberlite IRA-67 resins.

As shown in Figure 9.2, phenols removal efficiency increased, from 57 % to values above 94%, with an increase in the pH_0 value up to 7 for Amberlyst A26 strong-base anion IE resin. Moreover, it can be observed that IE efficiency remains virtually constant at higher pH values for Amberlyst A26. Therefore, pH 7 could be chosen as the optimum value, since it would be not necessary to add base to increase the pH value as the removal efficiency increase for pH values higher than 7 is not significant. It is worthy to highlight that phenol uptake occurs by adsorption at acidic pH since phenol is neutral at this pH. On the contrary, phenol removal takes place by both adsorption and ion exchange at alkaline pH, where phenol is present as phenolate ions exchangeable by OH^- ions. This fact was also corroborated by Carmona et al., by investigating phenol uptake through a different strong-base anion exchange resin, which is Amberlite IRA-420. They observed that phenol removal increased at pH values from 9 to 14 and remained constant below 8 (Carmona et al., 2006).

On the other hand, Figure 9.2 shows that phenols IE removal efficiency for Amberlite IRA-67 weak-base anion IE resin also increased with an increase in the pH value up to 7, reaching phenols removal efficiencies close to 57 %. However, it can be observed that higher pH values led to lower IE efficiency. This fact could be explained since phenols IE by this weak-base resin would be favored at low pH, as this resin is only active in the range of 0–7 (see Table 9.2). In

addition, the phenol dissociation to phenol and phenolate can be considered as a function of the total concentration of phenol and the pH of the liquid solution ($\text{pH} > 8$). At acidic pH ($\text{pH} < 8$) the phenol dissociation is low and therefore, the molecular adsorption process is the predominant one, whereas both adsorption and IE are important at alkaline pH (Carmona et al., 2006). Consequently, it can be assumed that the adsorption is the main responsible process for phenol removal through the selected weak-base resin. M. Caetano et al., who studied phenol removal by means of weak and a strong-base anion exchange resins, found similar results in the initial concentration range $5\text{-}20 \text{ mg L}^{-1}$ (Caetano et al., 2009).

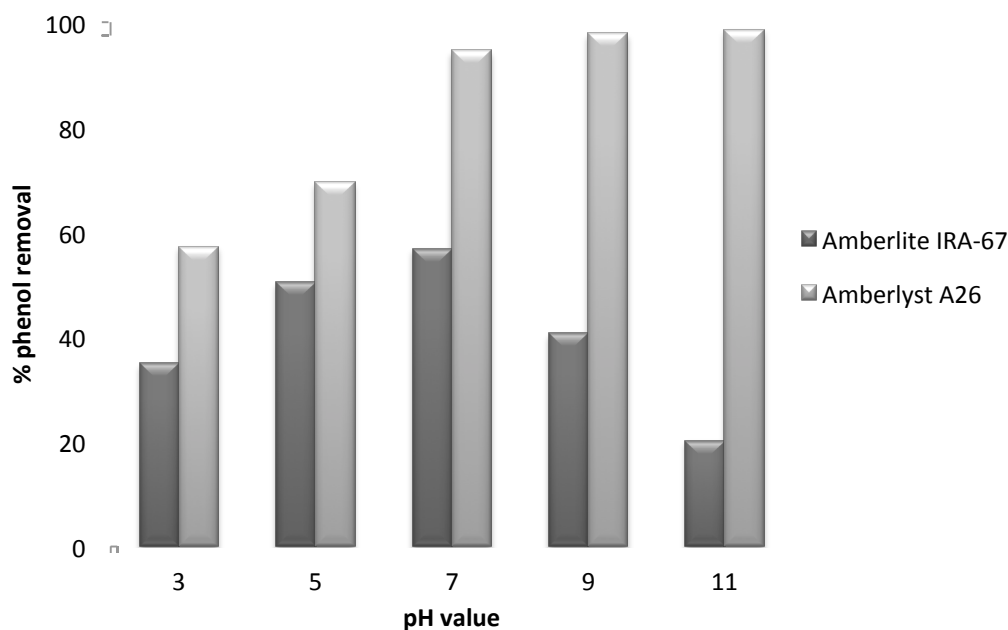


Figure 10.2. Effect of pH_0 on phenol removal through Amberlyst A26 strong-base anion exchange resin and Amberlite IRA-67 weak-base anion exchange resin (phenol concentration = 50 mg L^{-1} , resin dose = 3.5 g L^{-1} and equilibrium time = 1 h).

10.3.2 Breakthrough curves studies

The success of the column design for the adsorption process requires predicting the effect of concentration profile-time curves of the effluents. With this regard, various mathematical models have been developed to analyse the column studies in the laboratory, in order to plan columns on an industrial scale. In this research study the mathematical models of Thomas, Clark and Yoon-Nelson were applied in nonlinear forms.

10.3.2.1 Effect of inlet phenols concentration on breakthrough curves

In order to investigate the effect of the initial phenols concentration on the profiles of the breakthrough curves, three inlet concentrations ($5, 25$ and 100 mg L^{-1}) were used under a

constant flow rate and with a fixed bed height. Figure 9.3 shows the effect of inlet phenols concentration on breakthrough curves for phenols adsorption onto both Amberlyst A26 strong-base and Amberlite IRA-67 weak-base anion exchange resins in a column operating in continuous mode. In this figure, S-shaped curves can be observed for all the studied concentrations in both resins. Furthermore, increasing the initial concentration resulted in an earlier breakthrough curve, and upon the lowest initial concentration the highest volume could be treated, which can be attributed to the increased diffusion or mass transfer coefficient.

Integration of the area above the breakthrough curve was performed for the determination of the phenols loading on both resins, whose maximum values were found to be 148.6 and 76.30 mg phenols g⁻¹ when the initial concentration was 100 mg L⁻¹, for Amberlyst A26 and Amberlite IRA-67, respectively (see Table 10.3). This increase in capacity could be explained by the fact that a higher influent phenols concentration provided a higher driving force for the transfer process to overcome the mass transfer resistance (XiaoFeng et al., 2014). In previous studies, Srivastava et al. found the maximum sorptive capacity of bagasse fly ash for phenol to be 9.93 mg g⁻¹ for initial concentrations of 100 mg L⁻¹ (Srivastava et al., 2008).

From Table 10.3, it can be concluded that Amberlyst A26 resin has considerably higher potential for phenols removal than Amberlite IRA-67.

Table 10.3. Results of breakthrough curve at different inlet phenols concentrations. Resins amount = 35 g; Temperature = 298 K; Flow rate = 10 L h⁻¹; pH = 7.

Inlet phenols concentration (mg L ⁻¹)	t _{total} (min)	m _{total} (mg)	q _{total} (mg)	q _{eq} (mg g ⁻¹)	Removal %
Amberlyst A26					
5	882	735	475.15	20.43	64.6
25	500	2082.5	1476.53	59.5	70.9
100	325	5420	4228.2	148.6	78.0
Amberlite IRA-67					
5	390	325	166.73	9.29	51.3
25	255	1062.5	555.48	30.36	52.3
100	160	2670	1250.3	76.3	46.8

As it can be observed in Figure 10.3a,b, breakthrough curves are steeper with increasing pollutant concentration from 5 to 100 mg L⁻¹. Similar results were obtained by Srivastava et al. for phenol adsorption onto bagasse fly ash, by varying phenol concentration between 50 and 500 mg L⁻¹. In the same way, Aksu and Gönen investigated phenol uptake by immobilized activated sludge in a continuous packed bed, in the same phenol concentrations range, obtaining the same conclusions (Aksu and Gönen, 2004).

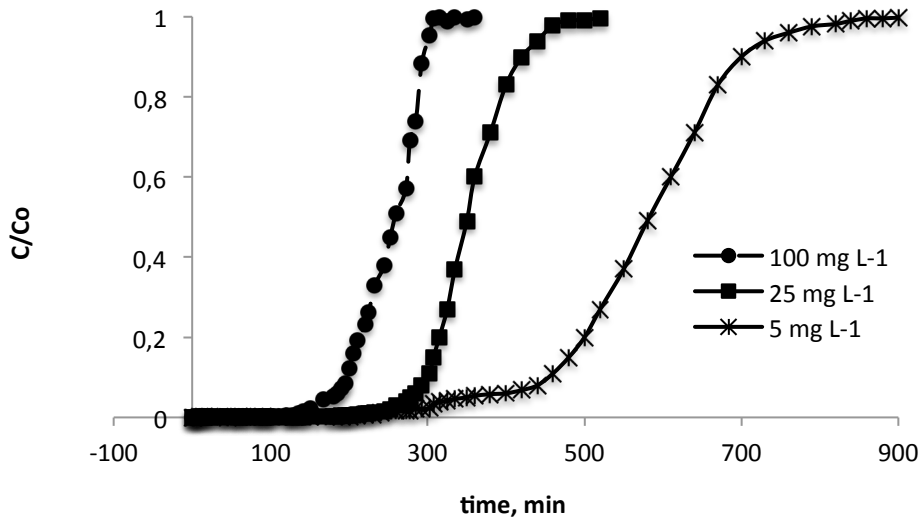


Figure 10.3a. Breakthrough curves for three different phenols concentrations in the influent: 5, 25 and 100 mg L⁻¹ inlet phenols concentrations. Common conditions: flow rate = 10 L h⁻¹, resin

amount = 35 g and operating temperature = 298 K. Resin: Amberlyst A26

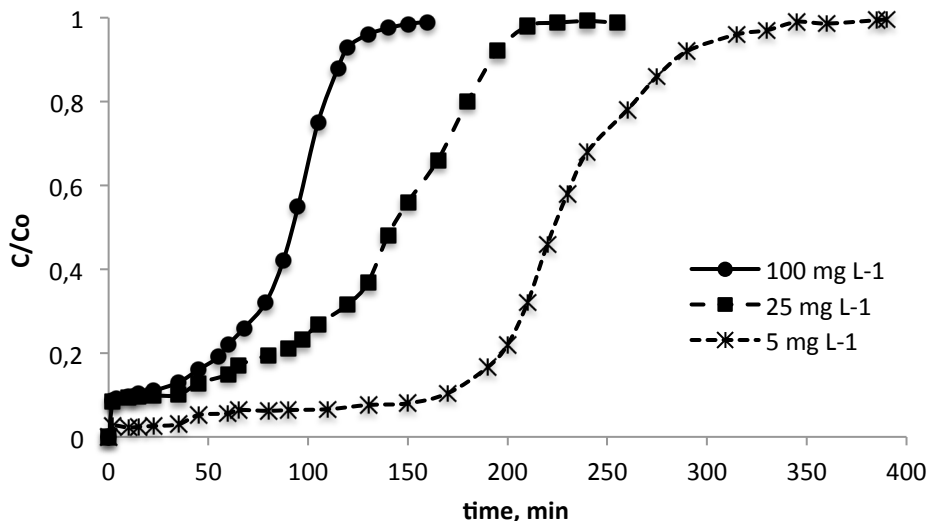


Figure 10.3b. Breakthrough curves for three different phenols concentrations in the influent: 5, 25 and 100 mg L⁻¹ inlet phenols concentrations. Common conditions: flow rate = 10 L h⁻¹, resin amount = 35 g and operating temperature = 298 K. Resin: Amberlite IRA-67

9.3.2.2 Analysis using Thomas model

Thomas model was applied to the experimental data for C/C_0 ratios ranging from 0.01 to 0.99 while varying the initial phenols concentration, for both resins. As listed in Table 9.4, when C_0 increased, the value of q_0 noticeably incremented, but the value of k_{Th} decreased. This fact, which occurred for both resins, is attributed to the difference in the driving force for adsorption as a result of the concentration difference (XiaoFeng et al., 2014). Thus, the higher driving force resulting from higher phenols concentration led to a higher q_0 value. Additionally, it was found that the values of q_0 estimated using Thomas model are closer to the q_e values obtained from the experimental results with varying C_0 conditions for Amberlyst A26 than for Amberlite IRA-67. In both cases, the high values of the non-linear regression coefficients demonstrated the adequacy of the linearized Thomas model equation to fit the experimental data along a non-linear regression (Table 9.4). Furthermore, comparing the R^2 and SSE values for the three studied models revealed that Thomas model suitably described the phenols IE/adsorption process in a fixed-bed column for the investigated resins.

Table 10.4. Thomas model parameters of phenols adsorption onto Amberlyst A26 and Amberlite IRA-67 resins at different inlet concentration using linear regression analysis.

Inlet phenols concentration (mg L ⁻¹)	Thomas model parameters			
	k_{Th} (ml min ⁻¹ mg ⁻¹)	q_0 (mg g ⁻¹)	R^2	SSE
Amberlyst A26				
5	0.17	13.6	0.9869	0.0329
25	0.0776	42.22	0.9807	0.0135
100	0.0231	121.75	0.9917	0.0444
Amberlite IRA-67				
5	0.724	1.9	0.9358	0.3292
25	0.0584	15.94	0.9221	0.0842
100	0.02365	35.5	0.9057	0.2100

10.3.2.3 Analysis using Yoon-Nelson model

Comparatively, Yoon-Nelson model was examined to investigate the breakthrough behavior of phenol adsorption onto both Amberlyst A26 and Amberlite IRA-67 resins. The values of K_{YN} , τ , and the rest of statistical parameters are listed in Table 9.5. As shown in this table, the value of

K_{YN} was found to decrease with increasing initial concentration for both resins. The values of τ were found to be significantly lower than the experimental t value at 50% breakthrough under all conditions, indicating that the Yoon- Nelson model is not very accurate in predicting the τ value in none of the investigated resins, which might be attributed to the relative simplicity of this model.

Table 10.5. Yoon-Nelson model parameters of phenols adsorption onto Amberlyst A26 and Amberlite IRA-67 resins at different inlet concentration using linear regression analysis.

Inlet phenols concentration (mg L ⁻¹)	Yoon and Nelson model parameters				
	K_{YN} (min ⁻¹)	τ (min)	q_0 (mg g ⁻¹)	R^2	SSE
Amberlyst A26					
5	0.0137	583.3	13.89	0.9768	0.0275
25	0.027	378.22	45	0.9465	0.2205
100	0.0395	254.5	121.2	0.9913	0.0447
Amberlite IRA-67					
5	0.025	202.7	4	0.9355	0.2848
25	0.0232	133.97	15.95	0.9167	0.094
100	0.0368	82.96	39.5	0.8873	0.1156

10.3.2.4 Analysis using Clark model

The values of Freundlich constant were found to be 1.8 and 1.4 for Amberlyst A26 and Amberlite IRA-67, respectively, from batch tests performed in our previous work. These values were used in the Clark model to calculate the other model parameters, A and r , which were, respectively, determined from Eq. (11). The observed increase in the rate of mass transfer (τ) with increasing flow rate was due to the higher flow rates shorten the distance for the molecular diffusion of adsorbates through the stationary layer of water that surrounds adsorbent particles.

The rate of mass transfer also increased with increasing inlet phenols concentration and with it, the driving force and mass transfer of the adsorbate to the adsorbent surface. As seen in Table 9.6, R^2 values were lower in comparison to the previous models and the corresponding SSE values were higher, indicating that Clark model predicts worst the breakthrough curve of phenols adsorption process among all tested models for both Amberlyst A26 and Amberlite IRA-67.

As it can be observed in Figure 10.4a-10.6b, Thomas model best described the experimental data for the three initial phenols concentrations in both cases. On the other hand, results from

Thomas model showed the behaviour of both systems was accurately simulated as a Langmuir adsorption, which matched our conclusion from previous batch study.

Table 10.6. Clark model parameters of phenols adsorption onto Amberlyst A26 and Amberlite IRA-67 resins at different inlet concentration using linear regression analysis.

Inlet phenols concentration (mg L ⁻¹)	Clark model parameters				
	r (min ⁻¹)	A	t _b (min)	R ²	SSE
Amberlyst A26					
5	0.0104	426.1	360.8	0.9672	0.1718
25	0.0235	7378.3	281	0.9949	0.474
100	0.0314	2480	175.59	0.9842	0.1724
Amberlite IRA-67					
5	0.0196	11.37	81.31	0.8945	0.6850
25	0.0215	5.27	38.36	0.8860	0.1190
100	0.0328	4.454	20.0	0.8569	0.1296

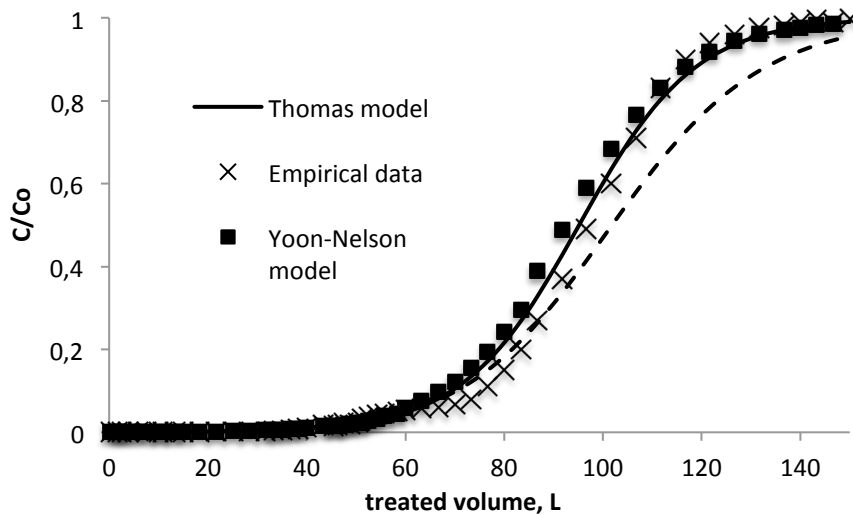


Figure 10.4a. Breakthrough curves comparison for experimental and predicted data for the three studied models. Common conditions: inlet phenols concentration: 5 mg L⁻¹, flow rate = 10 L h⁻¹, resin amount = 35 g and operating temperature = 298 K. Resin: Amberlyst A26

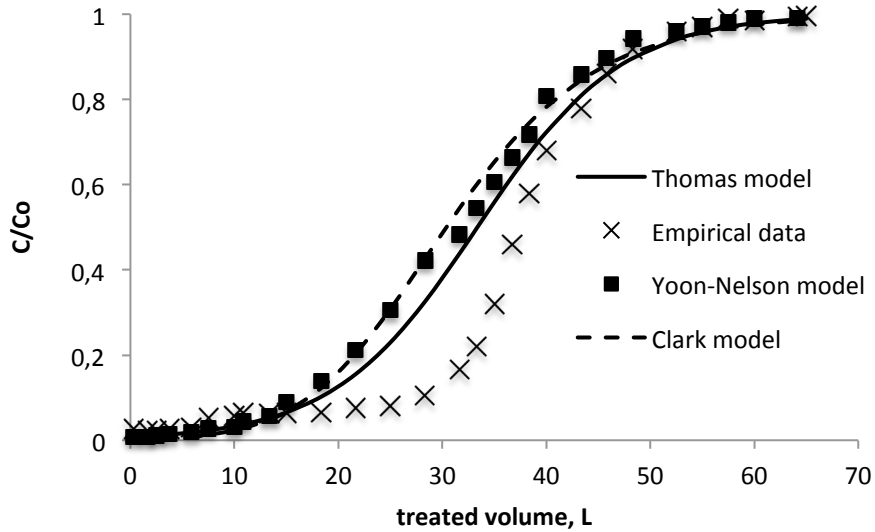


Figure 10.4b. Breakthrough curves comparison for experimental and predicted data for the three studied models. Common conditions: inlet phenols concentration: 5 mg L^{-1} , flow rate = 10 L h^{-1} , resin amount = 35 g and operating temperature = 298 K . Resin: Amberlite IRA-67

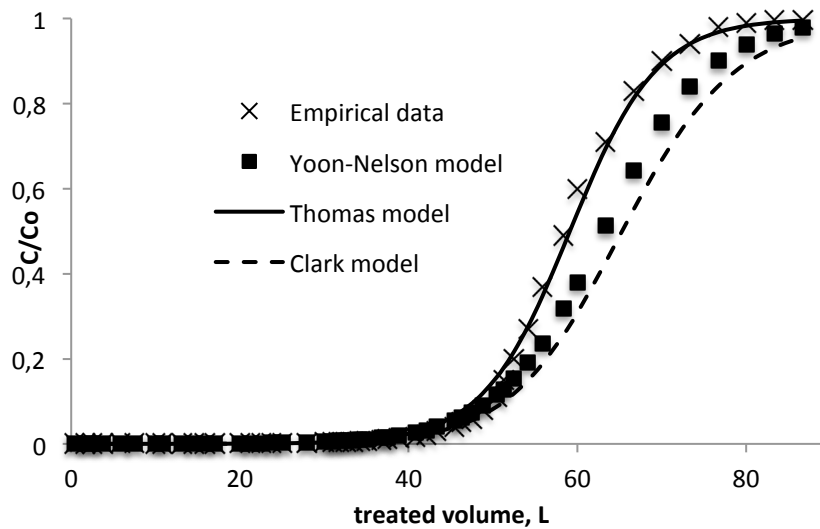


Figure 10.5a. Breakthrough curves comparison for experimental and predicted data for the three studied models. Common conditions: inlet phenols concentration: 25 mg L^{-1} , flow rate = 10 L h^{-1} , resin amount = 35 g and operating temperature = 298 K . Resin: Amberlyst A26

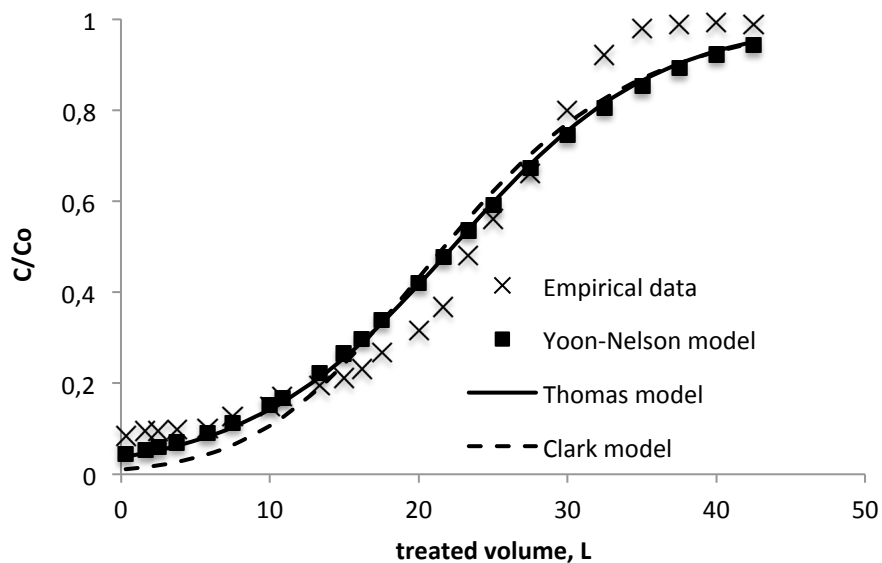


Figure 10.5b. Breakthrough curves comparison for experimental and predicted data for the three studied models. Common conditions: inlet phenols concentration: 25 mg L^{-1} , flow rate = 10 L h^{-1} , resin amount = 35 g and operating temperature = 298 K . Resin: Amberlite IRA-67

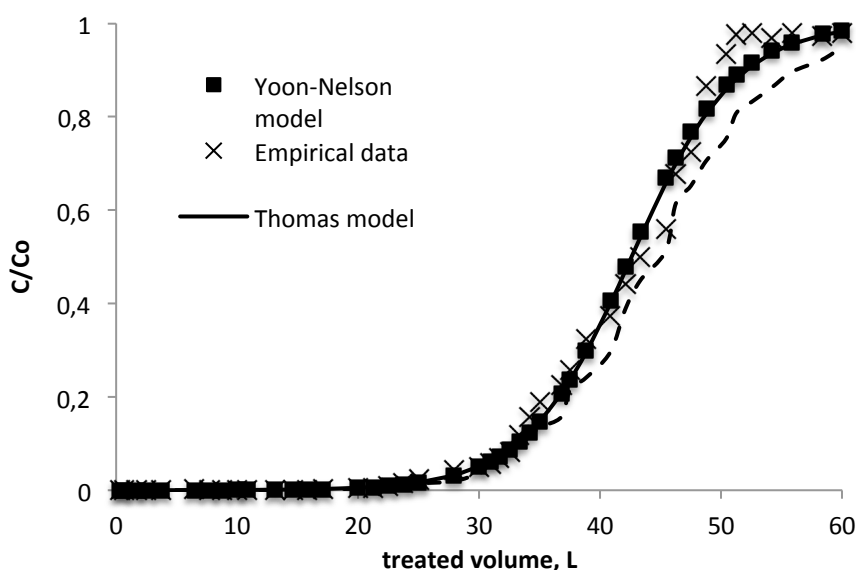


Figure 10.6a. Breakthrough curves comparison for experimental and predicted data for the three studied models. Common conditions: inlet phenols concentration: 100 mg L^{-1} , flow rate = 10 L h^{-1} , resin amount = 35 g and operating temperature = 298 K . Resin: Amberlyst A26

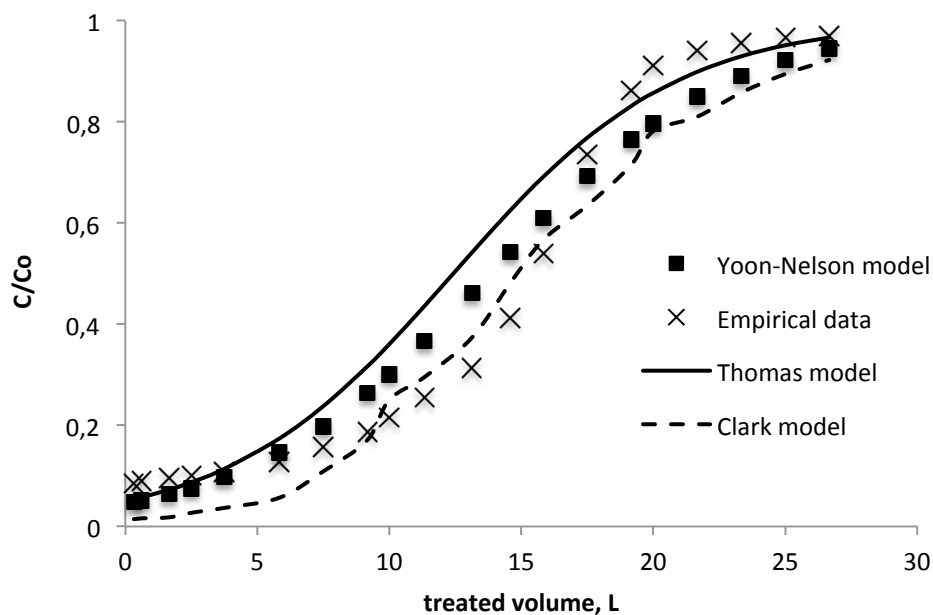


Figure 10.6b. Breakthrough curves comparison for experimental and predicted data for the three studied models. Common conditions: inlet phenols concentration: 100 mg L^{-1} , flow rate = 10 L h^{-1} , resin amount = 35 g and operating temperature = 298 K . Resin: Amberlite IRA-67

10.3.3 Phenols recovery

In each cycle, both resins were loaded with phenols until exhaustion, followed by elution by pumping 4% NaOH and 2% aqueous solutions for Amberlyst A26 strong-base and Amberlite IRA-67 weak-base anion exchange resins, respectively. In both cases, phenols recovery process was carried out at 2.5 L h^{-1} and room temperature. Finally, the eluted resins were washed with distilled water at 2.5 L h^{-1} during the 10 first minutes and subsequently increasing the flow rate until 20 L h^{-1} , following the manufacturer’s recommendations.

The desorption process indicated that phenols recovery efficiencies close to 100% were obtained for both resins. It may be stated that, in highly basic medium, hydroxide ions compete with phenolate ions and displace almost completely the adsorbed phenols. Caetano et al. used two different solutions for MN200 regeneration (Caetano et al., 2009). The first one was also NaOH solutions although the phenol recovery was poor. The second solution was a methanol/water solution ($50\% \text{ v/v}$), reaching a maximum recovery of 90% after 60 min regeneration process.

Finally, for 100 mg L^{-1} initial phenols concentration, a more concentrated solution, enriched in phenols, was obtained for Amberlyst A26 compared to Amberlite IRA-67 (8.5 g L^{-1} vs. 2.5 g L^{-1}), that is, more than threefold for the former, after 54 L and 27 L treated phenols-contaminated water, respectively.

10.4 Conclusions

OMW presents a wide range of phenolic compounds of high-added value, with concentrations above 80 mg L^{-1} . With the aims of phenols-contaminated water depuration and phenols recovery, two different IE resins were investigated in a fixed-bed column system.

The effect of initial pH on phenols removal showed that phenols removal efficiency increased, from 57 % to values above 94%, with an increase in the pH value up 7. Moreover, it can be observed that the IE efficiency remains virtually constant at higher pH values for Amberlyst A26 strong-base resin. On the other hand, phenols IE removal efficiency also increased with an increase in the pH value up 7, reaching phenols removal efficiencies close to 57 % for Amberlite IRA-67 weak-base resin. However, it can be observed that higher pH values led to lower IE efficiency. It can be assumed that the adsorption is the main responsible process for phenols removal through this latter resin.

The effect of inlet feed concentration on phenols adsorption/IE and the experimental breakthrough curves obtained revealed that that equilibrium phenols uptake (q_0) increased with the increment in the inlet concentration for both studied resins. Both breakthrough point and exhaustion time increased with increase in the inlet phenols concentration. Thomas, Yoon–Nelson, and Clark kinetic models were used to describe the column adsorption kinetics. The experimental breakthrough curves were compared satisfactorily with the breakthrough profile calculated by Thomas and Yoon–Nelson methods. However, Thomas model best described the experimental data for the three initial phenols concentrations in both resins.

The determination of the maximum loading capacities of phenols on Amberlyst A26 strong-base anion resin and Amberlite IRA-67 weak-base anion resin were found to be 148.6 and 76.3 mg L^{-1} , respectively. Therefore, it was concluded that Amberlyst A26 resin has higher potential for phenols removal than Amberlite IRA-67.

The desorption process indicated that phenols recovery efficiencies close to 100 % could be obtained for both resins.

Finally, for 100 mg L^{-1} initial phenols concentration, a more concentrated solution, enriched in phenols, was obtained for Amberlyst A26 compared to Amberlite IRA-67 (8.5 g L^{-1} vs. 2.5 g L^{-1}), that is, more than threefold for the former, after 54 L and 27 L treated phenols-contaminated water, respectively.

Column performance permits multiple service and regeneration cycles, thus enabling the treatment of considerably large volumes of wastewater. Regeneration of the saturated resins with sodium

hydroxide solutions was confirmed to be very effective since desorption results indicated close to 100 % phenols recovery efficiencies. IE process led to a solution of phenols susceptible to be concentrated and used in food, cosmetic or pharmaceutical sectors. For 100 mg L⁻¹ initial phenols concentration, a more concentrated solution, enriched in phenols, was obtained for Amberlyst A26 compared to Amberlite IRA-67 (8.5 g L⁻¹ vs. 2.5 g L⁻¹), after 54 L and 27 L treated phenols-contaminated water, respectively.

10.5 References

Akdemir, E.O., Ozer, A. (2009). Investigation of two ultrafiltration membranes for treatment of olive mill wastewaters. *Desalination*, 249:660-666.

Aksu, Z., Gönen, F. (2004). Biosorption of phenol by immobilized activated sludge in a continuous packed bed: prediction of breakthrough curves. *Process Biochemistry*, 39:599-613.

Azbar, N., Bayram, A., Filibeli, A., Muezzinoglu, A., Sengul, F., Ozer, A. (2004). A review of waste management options in olive oil production. *Critical Reviews in Environmental Science and Technology*, 34:209-247.

Bertin, L., Ferri, F., Scoma, A., Marchetti, L., Fava, F. (2011). Recovery of high added value natural polyphenols from actual olive mill wastewater through solid phase extraction. *Chem. Eng. J.*, 171:1287-1293.

Bouزيد, O., Navarro, D., Roche, M., Asther, M., Haon, M., Delattre, M., Lorquin, J., Labal, M., Asther, M., Lesage-Meessen, L. (2005). Fungal enzymes as a powerful tool to release simple phenolic compounds from olive oil byproducts. *Process Biochemistry*, 40:1855-1862.

Caetano, M., Valderrama, C., Farran, A., Cortina, J.L. (2009). Phenol removal from aqueous solution by adsorption and ion Exchange mechanisms onto polymeric resins. *J. Colloid. Interface Sci.*, 338:402-409.

Carmona, M., De Lucas, A., Valverde, J.L., Velasco, B., Rodríguez, J.F. (2006). Combined adsorption and ion exchange equilibrium of phenol on Amberlite IRA-420. *Chem. Eng. J.*, 117:55-160.

Chern, J.M., Chien, Y.W. (2002). Adsorption of nitrophenol onto activated carbon: isotherms and breakthrough curves. *Water Res.*, 36(3):647-655.

Clark, R.M. (1987). Evaluating the cost and performance of field-scale granular activated carbon systems. *Environ. Sci. Technol.*, 21:573-580.

- Conidi, C., Mazzei, R., Cassano, A., Giorno, L. (2014). Integrated membrane system for the production of phytotherapies from olive mill wastewaters. *J. Membr. Sci.*, 454:322-329.
- De Leonardis, A., Macciola, V., Lembo, G., Aretini, A., Nag, A. (2007). Studies on oxidative stabilization of lard by natural antioxidants recovered from olive oil mill wastewater. *Food Chem.*, 100:998-1004.
- De Marco, E., Savarese, M., Paduano, A., Sacchi, R. (2007). Characterization and fractionation of phenolic compounds extracted from olive mill wastewaters. *Food Chemistry*, 104:858-867.
- El-Abbassi, A., Kiai, H., Raiti, J., Hafidi, A. (2014). Application of ultrafiltration for olive processing wastewaters treatment. *J. Cleaner Prod.*, 65:432-438.
- Galanakis, C.M., Tornberg, E., Gekas, V. (2010). Recovery and preservation of phenols from olive waste in ethanolic extracts. *J. Chem. Technol. Biotechnol.*, 85:1148-1155.
- Garcia-Castello, E., Cassano, A., Criscuoli, A., Conidi, C., Drioli, E. (2010). Recovery and concentration of polyphenols from olive mill wastewaters by integrated membrane system. *Water Res.*, 44:3883-3892.
- Garcia Garcia, I., Jimenez Peña, P.R., Bonilla Venceslada, J.L., Martin Martin, A., Martin Santos, M.A., Ramos Gomez, E. (2000). Removal of phenol compounds from olive mill wastewater using *Phanerochaete chrysosporium*, *Aspergillus niger*, *Aspergillus terreus* and *Geotrichum candidum*. *Process Biochemistry*, 35:751-758.
- Greenberg, A.E., Clesceri, L.S., Eaton, A.D. (1992). Standard Methods for the Examination of Water and Wastewater, APHA/AWWA/WEF, 16th ed., Washington DC. Cabs.
- Hajji, F., Kunz, B., Weissbrodt J. (2014). Polymer incompatibility as a potential tool for polyphenol recovery from olive mill wastewater. *Food Chemistry*, 156:23-28.
- Jarboui, R., Chtourou, M., Azri, C., Gharsallah, N., Ammar, E. (2010). Time-dependent evolution of olive mill wastewater sludge organic and inorganic components and resident microbiota in multi-pond evaporation system. *Bioresource Technology*, 101:5749-5758.
- Kalogerakis, N., Politi, M., Foteinis, S., Chatzisyneon, E., Mantzavinou, D. (2013). Recovery of antioxidants from olive mill wastewaters: a viable solution that promotes their overall sustainable management. *J. Environ. Manage.*, 128:749-758.
- Lafka, T.A., Lazou, A.E., Sinanoglou, V.J., Lazos, E.S. (2011). Phenolic and antioxidant potential of olive oil mill wastes. *Food Chem.*, 125:92-98.

Ochando-Pulido, J.M., Hodaifa, G., Victor-Ortega, M.D., Martinez-Ferez, A. (2013). Effective treatment of olive mill effluents from two-phase and three-phase extraction processes by batch membranes in series operation upon threshold conditions. *Journal of Hazardous Materials.*, 263:168-176.

Ochando-Pulido, J.M., Victor-Ortega, M.D., Hodaifa, G., Martinez-Ferez, A. (2015). Physicochemical analysis and adequation of olive oil mill wastewater after advanced oxidation process for reclamation by pressure-driven membrane technology. *Science of the Total Environment*, 503-504:113-121.

Paraskeva, C.A., Papadakis, V.G., Kanellopoulou, D.G., Koutsoukos, P.G., Angelopoulos, K.C. (2007). Membrane filtration of olive mill wastewater (OMW) and OMW fractions exploitation. *Water Environment Research*, 79:421-429.

Roig, A., Cayuela, M.L., Sánchez-Monedero, M.A. (2006). An overview on olive mill wastes and their valorisation methods. *Waste Manage.*, 26:960–969.

Srivastava, V.C., Prasad, B., Mishra, I.M., Mall, I.D., Swamy, M.M. (2008). Prediction of Breakthrough Curves for Sorptive Removal of Phenol by Bagasse Fly Ash Packed Bed. *Ind. Eng. Chem. Res.*, 47:1603-1613.

Stoller, M., Bravi, M. (2010). Critical flux analyses on differently pretreated olive vegetation waste water streams: some case studies. *Desalination*, 250:578-582.

Thomas, H.C. (1944). Heterogeneous ion exchange in a flowing system. *J. Am. Chem. Soc.*, 66:1466–1664.

Tomati, U., Galli, E., Pasetti, L., Volterra, E. (1995). Bioremediation of olive mill wastewaters by composting. *Waste Management and Research*, 13:509-518.

Tsagaraki, E., Lazarides, H.N., Petrotos, K.B. (2007). Olive Mill Wastewater Treatment. In *Utilization of by-products and treatment of waste in the food Industry*. Springer Verlag 133–157.

Turano, E., Curcio, S., De Paola, M.G., Calabro, V., Iorio, G. (2002). An integrated centrifugation-ultrafiltration system in the treatment of olive mill wastewater. *Journal of Membrane Science*, 209:519-531.

Vázquez, G., Alonso, R., Freire, S., González-Álvarez, J., Antorrena, G. (2006). Uptake of phenol from aqueous solutions by adsorption in a Pinus pinaster bark packed bed. *J. Hazard. Mater.*, 133(1-3):61–67.

Víctor-Ortega, M.D., Ochando-Pulido, J.M., Godaifa, H., Martínez-Férez, A. (2014). Final purification of synthetic olive oil mill wastewater treated by chemical oxidation using ion exchange: Study of operating parameters. *Chem. Eng. Process.*, 85:241-247.

XiaoFeng, S., Tsuyoshi, I., Masahiko, S., Takaya, H., Koichi, Y., Ariyo, K., Shiori, N. (2014). Adsorption of phosphate using calcined Mg₃-Fe layered double hydroxides in a fixed-bed column study. *Journal of Industrial and Engineering Chemistry*, 20:3623-3630.

Yoon, Y.H., Nelson, J.H. (1984). Application of gas adsorption kinetics. I. A theoretical model for respirator cartridge service time. *Am. Ind. Hyg. Assoc. J.*, 45:509-516.

Zagklisa, D.P., Vavourakia, A.I., Kornarosa, M.E., Paraskeva, C.A. (2015). Purification of olive mill wastewater phenols through membrane filtration and resin adsorption/desorption. *J. Hazard. Mater.*, 285:69-76.

CHAPTER 11

ION EXCHANGE SYSTEM FOR THE FINAL PURIFICATION OF OLIVE MILL WASTEWATER: PERFORMANCE OF MODEL VS. REAL EFFLUENT TREATMENT

M.D. Víctor-Ortega^{1*}, J.M. Ochando-Pulido¹, A. Martínez-Ferez¹

¹ Chemical Engineering Department, University of Granada, 18071 Granada, Spain

*email: mdvictor@ugr.es

Submitted for publication. Current status: under review.

Science of the Total Environment

Publisher: ELSEVIER SCIENCE BV. PO BOX 211, 1000 AE AMSTERDAM, NETHERLANDS

Year: 2015

ISSN: 0048-9697

Impact factor: 4.099

Tertile: First



Abstract

Olive mill wastewater is a highly pollutant effluent which can be pretreated through an advanced oxidation process. After this, the effluent (OMW-2ST) presented high sodium and chloride concentrations, responsible for its high conductivity. In this context, two IE resins were examined (Dowex Marathon C and Amberlite IRA-67) for final OMW-2ST purification. As this effluent is extremely seasonal and deteriorates within few days, the main parameters affecting IE process were previously optimized with lab-made model OMW-2ST. Then the optimum operating conditions were tested with real OMW-2ST. Evolution of conductivity was evaluated as a function of recirculation time to study the effect of resins disposition and resins dosages and compared with both OMW-2ST. Equilibrium was reached in 10 and 20 min for model and real OMW-2ST, respectively. Furthermore, continuous mode experiments were carried out with the aim of investigating the evolution of conductivity as a function of operating time. Breakthrough time was lower for real versus model OMW-2ST (120 vs. 147.5 min). Minimum 10 g L⁻¹ resin dosage ensured 74% and 78% removal efficiencies, thus fulfilling irrigation water legal requirements and rendering the production system cost-effective and environmentally respectful. Finally, model OMW-2ST is confirmed as good simulating media to reproduce IE processes.

Keywords: ion exchange, olive mill effluent, purification, wastewater reclamation.

11.1 Introduction

Olive oil mill wastewater (OMW) generated by the olive oil production process is the main effluent of this industry, which derives from olives washing wastewater (OWW) and olive vegetation wastewater (OVW). The quantity and compositional characteristics of this effluent depend on several factors such as the variety of the olives, the meteorological conditions and the system of extraction used (Benítez et al., 1997; Raggi et al., 2000). In this work, the problem related to the reclamation of OMW from the two-phase-based system effluent (OMW-2) was investigated.

Regarding the physicochemical properties, what most characterizes this effluent is an acid pH value, black colour, very high chemical oxygen demand (COD) and high concentration of recalcitrant organic matter, such as phenolic compounds and tannins (Rozzi et al., 1998). On the other hand, inorganic compounds such as chloride, sulphate and phosphoric salts of potassium, calcium, iron, magnesium, sodium, copper and traces of other elements are usually present in OMW-2 (Garrido Hoyos et al., 2002). The low pH of this wastewater, as well as the presence of phytotoxic and antimicrobial compounds and toxic fatty acids, make it difficult to directly reuse

this wastewater. Therefore, the treatment of OMW-2 is a very crucial need for environmental protection and has been studied by several methods highlighting natural evaporation and thermal concentration (Paraskeva and Diamadopoulou, 2006; Annesini and Gironi, 1991), treatments with lime and clay (Aktas et al., 2001; Al-Malah et al., 2000), biological treatments (Ammary, 2005; Garrido Hoyos et al., 2002; Taccari and Ciani, 2011) composting (Cegarra et al., 1996; Papadimitriou et al., 1997; Bouranis et al., 1995) and physicochemical procedures such as coagulation–flocculation (Sarika et al., 2005; Martínez Nieto et al., 2011a; Stoller, 2009) and electrocoagulation (Inan et al., 2004; Tezcan Ün et al., 2008).

In our previous research works, OMW-2 was treated at a pilot scale by an advanced chemical oxidation process based on Fenton's reagent followed by a flocculation step and filtration in series through three different kinds of filtering materials (Martínez Nieto et al., 2010; Martínez Nieto et al., 2011b). This depuration sequence achieved a large reduction of phenolic compounds, COD and suspended solids. Nevertheless, after this secondary treatment the effluent stream presented concentration of dissolved monovalent and divalent ions, which cannot be removed by conventional physicochemical treatments.

Among physicochemical methods for water purification such as chemical reactions, electroflotation, reverse osmosis and adsorption, ion exchange (IE) technology is very attractive because of the relative simplicity of application and due to the low cost and the effectiveness to remove ions from wastewaters, particularly from diluted solutions (Pintar et al., 2001; Valverde et al., 2006). The use of IE technique depends on several factors such as contact time, operating temperature, pH, flow rate, initial pollutant concentration and resin characteristics (Caetano et al., 2009).

IE resins have also found an increasing application in the drinking water treatment sector over the last few decades, especially when there is a high concentration of natural organic matter (NOM) in contaminated water since high percentages on the removal efficiency of NOM by IE process are found (Eilers, 2008).

In this sense, selective resins can reduce the residual concentration of sodium, total iron chloride and phenols below the maximum standard limits established by the Drinking Water Directive. Council Directive 98/83/EC set the maximum concentration in drinking water at $200 \mu\text{g L}^{-1}$ for iron, 200mg L^{-1} for sodium and 250mg L^{-1} for chloride (European Commission, 1998). Phenols concentration is not established by the last European legislation. However, there is a previous directive in which maximum phenols level is set at $5 \mu\text{g L}^{-1}$ (European Commission, 1980).

In this research study, IE is presented as an efficient alternative for the purification of OMW-2ST, where iron, sodium, chloride and phenols are the major pollutants. With the goal of achieving the parametric requirements for reusing the final treated effluent in the process or at least for discharge in public waterways, a bench scale study was undertaken to evaluate the performance of a combination of two IE columns working in serial connection. With this regard, the performance of two IE resins, that is, Dowex Marathon C, a strong-acid cation exchange resin, and Amberlite IRA-67, a weak-base anion exchange resin, was examined. Moreover, as one of the main issues of this kind of wastewater stream is that it is extremely seasonal (olive oil campaign lasts 90 days/year) and deteriorates very quickly (within a few days) model OMW-2ST was prepared in the lab. The main parameters affecting the proposed IE process were formerly optimized with the lab-made model OMW-2ST stream, and subsequently the optimum operating conditions were tested and contrasted with real OMW-2ST. Evolution of conductivity and pollutants concentrations were followed as a function of recirculation time (in recirculation mode) and operating time (in continuous mode) and compared with both OMW-2ST, and the efficacy of the model OMW-2ST as simulating media of real OMW-2 prepared was also corroborated.

11.2 Experimental section

11.2.1 Model water solutions

Model water simulating pretreated OMW-2ST was prepared in the laboratory by dissolving reagent-grade sodium chloride, iron (III) chloride 30 % (w/w) aqueous solution and phenol (all of them provided by Panreac) in double distilled water. These water solutions were prepared prior to the start of the experiments, stored at 4 °C and brought to room temperature before being used.

The physicochemical composition of the OMW-2ST effluent is reported in Table 11.1 (Ochando-Pulido et al., 2012a; Ochando-Pulido et al., 2012b; Víctor-Ortega et al., 2014). The desired concentrations for chloride and sodium were fixed at the highest values registered on average at the outlet of the OMW-2 secondary treatment: approximately 1050 mg L⁻¹ and 750 mg L⁻¹, respectively, whereas about 1 mg L⁻¹ and 0.4 mg L⁻¹ for phenol and total iron concentrations.

11.2.2 Real OMW samples

Wastewater samples were collected from different olive oil mills in the South of Spain, operating with the two-phase centrifugation system (OMW-2).

OMW-2 samples were conducted to the aforementioned secondary treatment thoroughly described in former works by the Authors (Martínez Nieto et al.; 2011; Hodaifa et al., 2013a; Hodaifa et al., 2013b), before being subjected to the final IE purification process. Chemical oxygen demand (COD), total phenolic compounds (TPh), sodium, chloride, total iron, electroconductivity (EC) and pH were measured in the outlet stream samples of the secondary treatment as well as of the IE system, respectively.

Table 11.1. Physicochemical characteristics of OMW-2ST.

Factor	Value
pH	7.78 - 8.17
Conductivity, mS cm⁻¹	3.15 - 3.55
COD, mg L⁻¹	120.5 - 226.6
Total phenolic compounds, mg L⁻¹	0.39 - 0.98
[Cl⁻], mg L⁻¹	875.83 - 1045.03
[Na⁺], mg L⁻¹	534.01 - 728.71
Total [Fe], mg L⁻¹	0.04 - 0.4

11.2.3 Ion exchange process

Strong-acid cation exchange Dowex Marathon C resin and weak-base anion exchange Amberlite IRA-67 resin, both provided by Sigma Aldrich, were used in this study. Their properties and specifications are reported Table 11.2.

Table 11.2. Physicochemical characteristics of selected IE resins.

Properties	Dowex Marathon C	Amberlite IRA-67
Type	Strong-acid cation	Weak-base anion
Matrix	Styrene-DVB, gel	Tertiary amine
Ionic form as shipped	H ⁺	OH ⁻
Particle size, mm	0.55-0.65	0.5-0.75
Effective pH range	0-14	0-7
Total exchange capacity, eq L⁻¹	1.80	1.60
Shipping weight, g L⁻¹	800	700

Both resins present similar total exchange capacities. Dowex Marathon C presents styrene-DVB matrix whereas Amberlite IRA-67 matrix is based on a tertiary amine (see Table 11.2). On the other hand, it is worthy to point out that strong-acid cationic resin presents effective pH throughout the whole pH range (i.e. 0-14). However, effective pH range for the weak-base anionic resin is 0-7.

The bench-scale IE equipment, used in this research study, consisted on two IE columns operating in serial connection through recirculation mode or continuous mode (Figure 11.1). IE columns employed in this study were made of an acrylic tube of 540 mm height x 46 mm internal diameter. The columns are provided with a mobile upper retaining grid, which could be fixed in the column to adjust it as a fixed bed or a semi-fluidized bed. The IE device (MionTec) was equipped with a peristaltic pump (Ecoline VC-380) and a temperature-controlled thermostatic bath (Precistern JP Selecta).

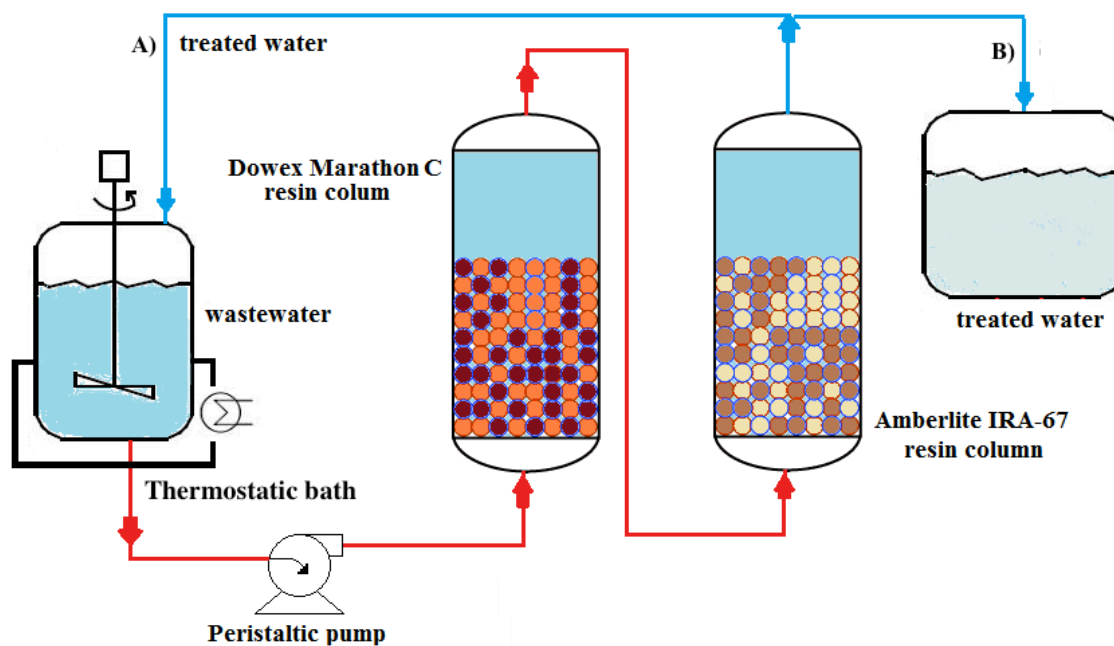


Figure 11.1. Flow-sheet scheme for IE operating cycle for final purification of OMW-2: A) recirculation mode and B) continuous operation mode.

11.2.4 Recirculation and continuous IE experiments

Recirculation experiments were carried out in semi-fluidized bed operating mode on a closed loop system. In these experiments, the total sample volume of simulating OMW-2ST solution was fixed at 2 L and the operation time varied up to 60 min, respectively. OMW-2ST solutions were put in contact with the studied IE resins until equilibrium was achieved. The flask containing the feed solution was stirred continuously during the whole experiments. The extent

of the IE equilibrium data of each species was determined by measuring the residual amount of these ions in the liquid phase as follows:

$$\% \text{ Sorption} = \frac{C_0 - C_e}{C_0} \times 100 \quad (1)$$

where C_0 and C_e are the initial and equilibrium iron concentration (mg L^{-1}), respectively.

Additionally, continuous IE process was examined for the final purification of OMW-2ST. During continuous IE experiments, model and real OMW-2ST feedstreams were introduced at the bottom of the first column in upflow mode, leaving this column by the top. Then, OMW-2ST passed through the second column also in upflow mode from the bottom to the top. The evolution of the concentration of ionic species as well as the conductivity values in the outlet stream were continuously measured during the operating time by removing 50 mL solution aliquots. EC was chosen as the key parameter to follow the performance of both continuous and recirculation mode IE experimental runs.

In both operating modes, temperature and flow rate were fixed at 298 K (ambient temperature) and 10 L h^{-1} (V́ctor-Ortega et al., 2014b). Besides, the initial pH of the solution was adjusted to the optimum pH value obtained in the former semi-batch IE experiments (V́ctor-Ortega et al., 2015).

After each operational cycle, the Dowex Marathon C cation exchange resin was fully washed with a 2 % HCl aqueous solution for 30 min at 298 K. In a similar way, Amberlite IRA-67 anion exchange resin was washed with a 4 % NaOH aqueous solution for 40 min. Then, the resins were rinsed with double distilled water to remove all excess of acid or base, respectively.

11.2.5 Analytical methods

Analytical grade reagents and chemicals with purity over 99 % were used for the analytical procedures, applied at least in triplicate.

Sodium concentration values were determined by using a Crison GLP 31 Sodium Ion-Selective Electrode 96 50, with autocorrection of temperature. To calibrate the electrode in the laboratory, 0.01, 0.1 and $1.0 \text{ g L}^{-1} \text{ Na}^+$ standard solutions were prepared.

For the measurement of the total iron concentration, all iron ions were reduced to iron ions (II) in a thioglycolate medium with a derivative of triazine, forming a reddish-purple complex that was determined photometrically at 565 nm (Standard German methods ISO 8466-1 and German DIN 38402 A51) (Greenberg et al., 1992).

Chloride concentration values were assessed by a Crison GLP 31 Chloride Ion-Selective Electrode 96 52 C, with autocorrection of temperature. To this end, 0.01, 0.1 and 1.0 g L⁻¹ Cl⁻ standard solutions required for the electrode calibration were also prepared in the laboratory.

Total phenols and phenol derivatives were analyzed by reaction with a derivative thiazol, giving a purple azo dye which was determined photometrically using a Helios Gamma UV-visible spectrophotometer (Thermo Fisher Scientific) at 475 nm (Standard German methods ISO 8466-1 and DIN 38402 A51) (Greenberg et al., 1992).

EC and pH measurements were evaluated with a Crison GLP31 conductivity-meter and a Crison GLP21 pH-meter, provided with autocorrection of temperature. Buffer standard solutions for EC (1,413 μS cm⁻¹ and 12.88 mS cm⁻¹) and pH (pH 4.01, 7.00 and 9.21) measurements respectively were supplied as well by Crison.

11.3 Results and discussion

In the present work, resins disposition and resins dosage, which are the two main parameters affecting the proposed IE process for the purification of the OMW-2ST stream, were optimized and contrasted with both model and real effluents in recirculation mode experiments. The operating temperature and flow rate, optimized with self lab-prepared model OMW-2ST in previous studies (V́ctor-Ortega et al., 2014b, V́ctor-Ortega et al., 2015), were fixed at the optimal operating conditions (298 K and 10 L h⁻¹) for experiments with real OMW-2ST in this study.

Finally, the proposed IE process performance was compared for model and real OMW-ST through continuous mode experiments in order to check the suitability of using model OMW-2ST as simulating media in IE processes.

11.3.1 Recirculation mode experiments

Firstly, recirculation mode experiments were carried out with both model and real OMW-2ST samples in order to evaluate the effect of resins disposition and resins dosages.

11.3.1.1 Effect of resins disposition

The effect of resins disposition on the IE performance was examined, represented as the EC value in the outlet stream, and reported in Figure 11.2 for both lab-made model and real OMW-2ST streams samples.

Throughout the whole experiments, relevant EC differences between the cationic + anionic (C + A) and anionic + cationic (A + C) resins disposition were registered for both model and real OMW-2T. These differences were even slightly more pronounced in case of model OMW-2ST, but the patterns between model or real effluents were practically replicated, as it can be observed in Figure 11.2.

Working with C + A resins configuration, equilibrium was reached in about 10 min and 20 min for model and real OMW-2ST, respectively. On the other hand, when operating with A + C resins configuration, equilibrium was achieved at higher recirculation times, namely 30 and 40 min for model and real OMW-2ST, respectively.

These results confirmed that setting the cation exchange resin followed by the anion exchange one provides better IE performances than in the opposite order for both model and real OMW-2ST.

A focus on this figure permits to notice that the results showed considerable reduction of the pollutants concentrations with increasing contact time, gathered in the EC value as key parameter (close to 100 % removal efficiencies). In addition, in C + A resins disposition, conductivity values were confirmed to be lower than 0.1 mS cm^{-1} in both OMW-2ST streams, which will allow to fulfil the drinking water quality standards for reuse in the production process or at least for discharge in public waterways (European Commission, 1980; European Commission, 1998).

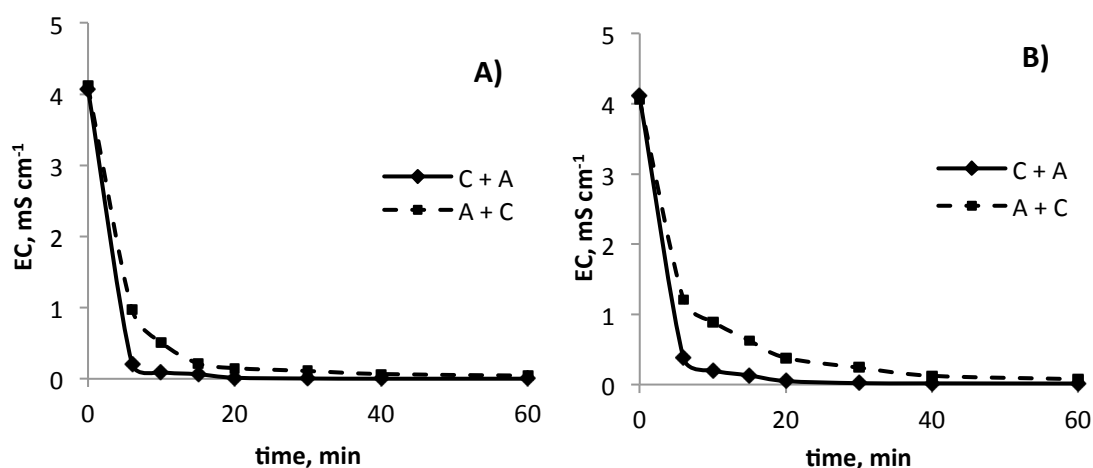


Figure 11.2. Effect of resins position (C-A: cation + anion, and A-C: anion + cation) on conductivity (EC). Recirculation mode experiments. A) Model OMW-2ST. B) Real OMW-2ST. Operating temperature: 298 K; Flow rate: 10 L h^{-1} .

11.3.1.2 Effect of resins dosage

Subsequently, the effect of Dowex Marathon C and Amberlite IRA-67 resin dosages on the IE removal of the cationic and anionic pollutants in the OMW-2ST stream was investigated in recirculation mode experiments.

Figure 11.3.a shows the IE removal of cations (mainly sodium and iron) as a function of the Dowex Marathon C resin dosage, which was varied from 5 to 40 g L⁻¹ and equilibrated for 60 min. The experimental results revealed that sodium removal efficiency increased up to an optimum dosage, beyond which the removal efficiency had no change with the resin dosage. In both cases (real and model OMW-2ST), a minimum resin dosage equal to 20 g L⁻¹ was confirmed in order to achieve sodium removal efficiency above 90 %.

Moreover, a deep analysis of Figure 11.3a reveals that this resin dosage provided around 90 % cations removal. Under these conditions, the achieved concentrations for both sodium and iron were lower than the established maximum limits.

Similarly, the removal of anions was evaluated as a function of Amberlite IRA-67 resin dosage, which was varied from 5 to 40 g L⁻¹ and equilibrated for 60 min (Figure 11.3b). The experimental results confirmed that anions removal efficiency increased up to an optimum dosage equal to 30 g L⁻¹, such that further incrementing the anionic resin dosage did not bring enhanced IE efficiency for real and model OMW-2ST.

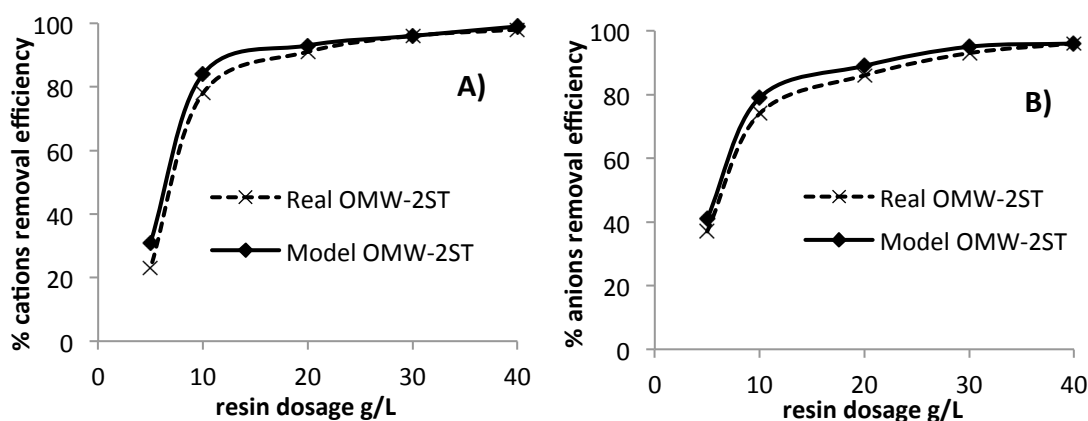


Figure 11.3. Effect of Dowex Marathon C resin dosage on cations IE removal (A caption) and Amberlite IRA-67 resin dosage on anions IE removal (B caption). Recirculation time: 30 min; Operating temperature: 298 K; Flow rate: 10 L h⁻¹.

For all the studied species, the IE uptake is highly dependent on the initial concentration of the sorbate and sorbent. The equilibrium concentrations of all the OMW-2ST pollutants

decreased with increasing the adsorbent doses for a given initial concentration. The increase in the removal percentage with the increase in the adsorbents dosage is due to the greater availability of the exchangeable sites or surface area at higher concentration of the adsorbent (Krishnan and Anirudhan, 2003; Rengaraj and Moon, 2002). The resin dosage is a key economical factor affecting the process performance, of utmost importance for the industrial scale-up of the proposed IE process (Yu et al., 2003). Therefore, on the basis of the compliance of water quality standards for irrigation reuse, a minimum resin dosage of 10 g L^{-1} would be enough for both Dowex Marathon C and Amberlite IRA-67, ensuring as high as 74% and 78% removal efficiencies for cations and anions, respectively. In the final effluent, concentrations of the studied target ions were lower than the maximum established levels (European Commission, 1980; European Commission, 1998).

11.3.2 Continuous mode experiments

Finally, the evolution of the conductivity in the IE outlet stream was monitored as a function of the operating time (continuous mode) for both model and real OMW-2ST (Figure 11.4a and Figure 11.4b, respectively). Results showed that breakthrough time (t_{Br}) was equal to 120 min and 147.5 min for real OMW-2ST and model OMW-2ST, respectively. In this t_{Br} point, sodium, chloride and total iron concentration were below the maximum levels established by legislation.

Otherwise, all pollutants concentrations were only found to be slightly higher in real OMW-2ST (see Table 11.3). It is important to highlight that when the t_{Br} was reached, the conductivity value was 0.792 for real OMW-2ST, that is, in the same range of the model OMW-2ST stream. To sum up, this final treated water would present good water quality standards for its reuse in irrigation taking into account the FAO recommendations, reported in Table 11.4.

On the other hand, the exhaustion time of the IE process (t_{Ex}) was registered at 220 min for model OMW-2ST. However, this time was observed to be 210 min for real OMW-2ST samples. As a result, up to 36.67 L model OMW-2ST could be treated before resins became exhausted, while 35.0 L real OMW-2ST were treated in the same conditions before exhaustion (Table 11.3). It is worth highlighting that these results support that there is no significant difference between the performances of the lab-made model OMW-2ST when compared to the raw effluent.

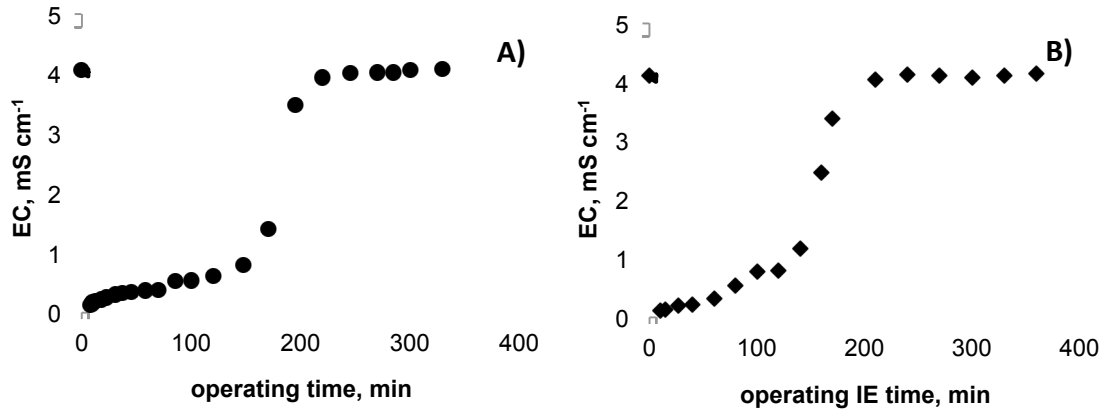


Figure 11.4. Evolution of conductivity in the outlet stream as a function of operating time during continuous IE experiments. A) Model OMW-2ST. B) Real OMW-2ST. Operating temperature: 298 K; Flow rate: 10 L h⁻¹.

Table 11.3. Comparison of different parameters between model OMW-2ST and real OMW-2ST. Continuous IE operation mode.

Parameters		Model	Real
		OMW-2ST	OMW-2ST
IE process	t_{Br}, min	147.5	120
	t_{Ex}, min	220	210
	treated volume, L	36.67	35.0
Treated water	EC, mS cm⁻¹	0.795	0.792
	[Na⁺]_{Br}, mg L⁻¹	125	194
	[Cl⁻]_{Br}, mg L⁻¹	233	272
	Total [Fe]_{Br}, mg L⁻¹	0.04	0.07
	Total [phenols]_{Br}, mg L⁻¹	0.4	0.52

Table 11.4. Water quality for irrigation according to Food and Agriculture Organization (FAO).

EC, mS cm ⁻¹	Water Quality	Hazardous due to salinity
0-1	Excellent - Good	Low - Medium
1-3	Good - Poor	High
> 3	Poor – Non acceptable	Very high

It is worth highlighting the high removal efficiency exhibited by the studied resins. These removal efficiencies were particularly high in the case of monovalent ions removal, such as sodium and chloride, especially during the first treatment hour (Figure 11.4). This may be owed to the high monovalent ions load ($[Cl^-] + [Na^+] + [Total\ phenols] + [Total\ Fe]$) in OMW-2ST. On the other hand, chloride ions have similar ionic charge as hydroxide ions, and the same occurs to sodium ions with respect to hydrogen ions. This also can give advantage to monovalent ions exchange, since ionic charge plays an important role in the IE process. Resins have preference for certain ionic species that have similar ionic charge characteristics. In general, the selectivity of the resins depends on the ionic charge and the ions size (Clifford et al.; 1983). Also, similar results were obtained by Apell and Boyer when magnetic cation exchange resin (MIEX-Na) and magnetic anion exchange resin (MIEX-Cl) were combined, hardness removal appeared to be cumulative, while dissolved organic matter (DOM) removal was not cumulative (Apell and Boyer, 2010). These results are explained by the fact that DOM-Ca⁺ complexes retain deprotonated carboxylic acid groups in the presence of calcium, so DOM-Ca⁺ can theoretically be removed by anion and cation exchange, depending on the ratio of calcium to carboxylic acid groups.

Finally, the treated OMW-2ST could be reused in the process, and thus rend the production system cost-effective and environmentally respectful. Moreover, model OMW-2ST is confirmed as good simulating media to reproduce IE processes.

11.4 Conclusions

In this work, an ion exchange (IE) process comprising two resins in serial connection (Dowex Marathon C and Amberlite IRA-67) was examined for the purification of secondary-treated olive mill wastewater (OMW-2ST), in order to obtain final water that fulfils the requirements for drinking water production for its reuse in the process. After this secondary treatment, an effluent with high concentration of sodium and chloride ions is obtained. Furthermore, phenols and iron are present in OMW-2ST.

Moreover, as one of the main issues of this kind of wastewater stream is that it is extremely seasonal and deteriorates very quickly model OMW-2ST was self-prepared in the lab. In this context, the main parameters affecting the proposed IE process were optimized previously with lab-made model OMW-2ST, and subsequently the optimum operating conditions were tested with real OMW-2ST. Evolution of conductivity was evaluated as a function of recirculation time to study the effect of resins disposition and resins dosages and compared with both OMW-2ST. In this sense, results showed that equilibrium was reached in about 10 min for model OMW-2ST and 20 min for real OMW-2ST, working with C + A resins configuration. However, when

operating with A + C resins configuration, equilibrium was achieved at higher recirculation times, namely 30 and 40 min for model and real OMW-2ST, respectively. Therefore, it was confirmed that setting the cation exchange resin followed by the anion exchange one offers better results than in the opposite order for model and real OMW-2ST. In addition, 20 g L⁻¹ and 30 g L⁻¹ for the cationic and anionic resins, respectively, were the minimum dosages to ensure removal efficiencies above 90 % for both model and real OMW-2ST. However, on the basis of the compliance of water quality standards for irrigation reuse and the cost-efficiency of the IE process, a resin dosage of 10 g L⁻¹ would be enough to ensure as high as 74% and 78% removal efficiencies for cations and anions, respectively.

Furthermore, continuous mode experiments were carried out with the aim of investigating the evolution of conductivity as a function of operating time. Breakthrough time was lower for real versus model OMW-2ST (120 vs. 147.5 min) whereas pollutants concentrations were slightly higher at this point.

Moreover, it is confirmed that the lab-made model OMW-2ST can be employed as a good simulating media to reproduce IE processes. Finally, it was found that OMW-2ST treated by the proposed methodology fulfils the legislated requirements for drinking water been therefore suitable to reuse it in the process. For this reason, final OMW-2ST can be reused in the process, which leads to economic and environmental benefits.

11.5 References

- Aktas, E.S., Imre, S., Esroy, L. (2001). Characterization and lime treatment of olive mill wastewater. *Water Res.*, 35:2336-2340.
- Al-Malah, K., Azzam, M.O.J., Abu-Lail, N.I. (2000). Olive mills effluent (OME) wastewater post-treatment using activated clay. *Sep. Purif. Technol.*, 20:225-234.
- Ammary, B.Y. (2005). Treatment of olive mill wastewater using an anaerobic sequencing batch reactor. *Desalination*, 177:157-165.
- Annesini, M., Gironi, F. (1991). Olive oil mill effluent: ageing effects on evaporation behavior. *Water Res.*, 25:1157-1960.
- Apell, J.N., Boyer, T.H. (2010). Combined ion exchange treatment for removal of dissolved organic matter and hardness. *Water Res.*, 44:2419-2430.
- Benitez, F.J., Beltran de Heredia, J., Torregrosa, J., Acero, J.L. (1997). Aerobic degradation of olive mill wastewater. *Appl. Microbiol. Biot.*, 47:185-188.

Bouranis, D.L., Vlyssides, A.G., Drossopoulos, J.B., Karvouni, G. (1995). Some characteristics of a new organic soil conditioner from the co-composting of olive oil processing wastewater and solid residue. *Commun. Soil Sci. Plant Anal.*, 26:2461-2472.

Caetano, M., Valderrama, C., Farran, A., Cortina, J.L. (2009). Phenol removal from aqueous solution by adsorption and ion exchange mechanisms onto polymeric resins. *J. Colloid Inter. Sci.*, 338:402-409.

Cegarra, J., Paredes, C., Roig, A., Bernal, M.P., García, D. (1996). Use of olive mill wastewater compost for crop production, *Int. Biodet. Biodegrad.*, 38(3-4):193-203.

Clifford, D., Weber, Jr., Walter, J. (1983). The determinants of divalent/monovalent selectivity in anion exchangers. *Reactive Polymers, Ion Exchangers, Sorbents*, 1:77-89.

Eilers, A.K. (2008). Ion exchange for NOM removal in drinking water treatment, Master of Science thesis in Civil engineering. Delft University of Technology.

European Commission. (1980). Council Directive 80/778/EEC of 15 July 1980 on the quality of water intended for human consumption.

European Commission. Council Directive 98/83/EC of 3 November 1998 on the quality of water intended for human consumption. 1998. Brussels, Belgium.

Garrido Hoyos, S.E., Martínez Nieto, L., Camacho Rubio, F., Ramos Cormenzana, A. (2002). Kinetics of aerobic treatment of olive-mill wastewater (OMW) with *Aspergillus terreus*. *Process Biochem.*, 37:1169-1176.

Greenberg, A.E., Clesceri, L.S., Eaton, A.D. (1992). Standard Methods for the Examination of Water and Wastewater, APHA/AWWA/WEF, 16th ed., Washington DC. Cabs.

Hodaifa, G., Ochando-Pulido, J.M., Rodriguez-Vives, S., Martinez-Ferez, A. (2013a). Optimization of continuous reactor at pilot scale for olive-oil mill wastewater treatment by Fenton-like process. *Chem. Eng. J.*, 220:117-124.

Hodaifa, G., Ochando-Pulido, J.M., Alami, S.B.D., Rodriguez-Vives, S., Martinez-Ferez, A. (2013b). Kinetic and thermodynamic parameters of iron adsorption onto olive stones. *Ind. Crops Prod.*, 49:526-534.

Inan, H., Dimoglo, A., Şimşek, H., Karpuzcu, M. (2004). Olive oil mill wastewater treatment by means of electro-coagulation. *Sep. Purif. Technol.*, 36(1):23-31.

Krishnan, K.A., Anirudhan, T.S. (2003). Removal of cadmium (II) from aqueous solutions by steamactivated sulphurised carbon prepared from sugar-cane bagasse pith: Kinetics and equilibrium studies. *Water SA*, 29(2):147-156.

Martínez Nieto, L., Hodaifa, G., Rodríguez Vives, S., Giménez Casares, J.A. (2010). Industrial plant for olive mill wastewater from two-phase treatment by chemical oxidation. *J. Environ. Eng.*, 136(11):1309-1313.

Martínez Nieto, L., Hodaifa, G., Rodríguez Vives, S., Giménez Casares, J.A., Ochando J. (2011a). Flocculation–sedimentation combined with chemical oxidation process, *Clean – Soil Air Water*, 39(10):949–955.

Martínez Nieto, L., Hodaifa, G., Rodríguez Vives, S., Giménez Casares, J.A., Ochando, J. (2011b). Degradation of organic matter in olive oil mill wastewater through homogeneous Fenton-like reaction, *Chem. Eng. Journal*, 173:503-510.

Ochando-Pulido, J.M., Hodaifa, G., Martínez-Férez, A. (2012a). Fouling inhibition upon Fenton-like oxidation pretreatment for olive mil wastewater reclamation by membrane process. *Chem. Eng. Process*, 62:89-98.

Ochando-Pulido, J.M., Hodaifa, G., Rodriguez-Vives, S., Martinez-Ferez, A. (2012b). Impacts of operating conditions on reverse osmosis performance of pretreated olive mill wastewater. *Water Res.*, 46(15):4621-4632.

Papadimitriou, E.K., Chatjipavlidis, I., Balis, C. (1997). Application of composting to olive mill wastewater treatment, *Environ. Technol.*, 18(1):10-107.

Paraskeva, P., Diamadopoulos, E. (2006). Technologies for olive mill wastewater (OMW) treatment: a review. *J. Chem. Technol. Biotechnol.*, 81:1475-1485.

Pintar, A., Batista, J., Levec, J. (2001). Integrated ion exchange/catalytic process for efficient removal of nitrates from drinking water. *Chem. Eng. Sci.*, 56:1551-1559.

Raggi, A., Cichelli, A., Pagliuca, G., Costantino, A. (2000). A screening LCA of olive husk combustion for residential heating. In: Proceedings of the First World Conference on Biomass Energy and Industry, pp 1001-1004.

Rengaraj, S., Moon, S.H. (2002). Kinetic of Adsorption of Co (II) Removal from Water and Wastewater by Ion Exchange Resins. *Water Res.*, 36(7):1783-1793.

- Rozzi, A., Limoni, N., Menegatti, S., Boari, G., Liberti, L., Passino, R. (1998). Influence of Na and Ca alkalinity on UASB treatment of olive mill effluents. *Part I. Preliminary results, Process Chem.*, 23:86-90.
- Sarika, R., Kalogerakis, N., Mantzavinos, D. (2005). Treatment of olive mill effluents. Part II. Complete removal of solids by direct flocculation with poly-electrolytes, *Environ. Int.*, 31:297-304.
- Stoller, M. (2009). On the effect of flocculation as pretreatment process and particle size distribution for membrane fouling reduction. *Desalination*, 240:209–217.
- Taccari, M., Ciani, M. (2011). Use of *Pichia fermentans* and *Candida* sp. Strains for the biological treatment of stored olive mill wastewater. *Biotechnol. Lett.*, 33:2385-2390.
- Tezcan Ün, Ü., Altay, U., Koparal, A.S., Ogutveren, U.B. 2008. Complete treatment of olive mill wastewaters by electrooxidation. *Chem. Eng. J.*, 139:445–452.
- Valverde, J.L., DeLucas, A., Carmona, M., Pérez, J.P., González, M., Rodríguez, J.F. (2006). Minimizing the environmental impact of the regeneration process of an ion exchange bed charged with transition metals. *Sep. Purif. Technol.*, 49:167-173.
- Víctor-Ortega, M.D., Ochando-Pulido, J.M., Hodaifa, G., Martínez-Ferez, A. (2014a). Ion exchange as an efficient pretreatment system for reduction of membrane fouling in the purification of model OMW. *Desalination*, 343:198-207.
- Víctor-Ortega, M.D., Ochando-Pulido, J.M., Martínez-Férez, A. (2015). Impacts of integrated strong-acid cation exchange and weak-base anion exchange process for successful removal of saline toxicity from model olive mill wastewater. *Ecol. Eng.*, 77:18-25.
- Víctor-Ortega, M.D., Ochando-Pulido, J.M., Godaifa, H., Martínez-Férez, A. (2014b). Final purification of synthetic olive oil mill wastewater treated by chemical oxidation using ion exchange: Study of operating parameters. *Chem. Eng. Process.*, 85:241-247.
- Yu, L.J., Shukla, S.S., Dorris, K.L., Shukla, A., Margrave, J.L. (2003). Adsorption of chromium from aqueous solutions by maple sawdust. *J. Hazard. Mater.* 100:53-63.

CHAPTER 12

EXPERIMENTAL DESIGN FOR OPTIMIZATION OF OLIVE MILL WASTEWATER FINAL PURIFICATION WITH DOWEX MARATHON C AND AMBERLITE IRA-67 ION EXCHANGE RESINS

María Dolores Víctor-Ortega^{1*}, Javier Miguel Ochando-Pulido¹, Diego Airado-Rodríguez², Antonio Martínez-Ferez¹

¹ Chemical Engineering Department, University of Granada, 18071 Granada, Spain

*email: mdvictor@ugr.es

² Nofima AS - the Norwegian Institute of Food, Fisheries and Aquaculture Research, Osloveien 1, 1430 Ås, Norway

Accepted for publication:

Journal of Industrial and Engineering Chemistry

Publisher: ELSEVIER SCIENCE INC. 360 PARK AVE SOUTH, NEW YORK, NY 10010-1710

Year: 2015

ISSN: 1226-086X

Impact factor: 3.50

Tertile: First



Abstract

The final purification of two-phase olive mill wastewater (OMW-2) by ion exchange (IE) was addressed. This pollutant effluent was previously subjected to Pseudo-Fenton secondary treatment. Consequently, OMW-2 presented high concentrations of chloride, sodium, phenols and iron, which hinder its discharge. Experimental design was used to optimize the IE process. Around 88 % removal efficiencies of these pollutants were achieved when initial pH, temperature and flow rate were 5.1, 26.8 °C and 12.1 L h⁻¹, respectively. Finally, 28 L treated water could be accomplished in continuous mode under optimal conditions, complying with standards for reuse in the olive oil production process.

Keywords: Central composite design; Ion exchange; Olive mill wastewater; Pollutants; Response surface.

12.1 Introduction

Around 3 million tons of olive oil are produced annually worldwide, being EU countries, principally Spain, Italy and Greece, the major manufacturers (Dhouib et al., 2006). However, the extraction process generates a highly pollutant effluent which carries a significant environmental problem. Olive mill wastewater (OMW) is a dark effluent characterized by high organic carbon content, particularly phenols and polyphenols, which are highly polluting. When disposed into the environment, OMW create severe deteriorations such as coloring of natural waters, serious threat to the aquatic life, pollution in surface and ground waters, alterations in soil quality, phytotoxicity and odor nuisance (Dhouib et al., 2006; Kestioğlu et al., 2005).

The two-phase continuous decanting system (OMW-2) is currently the main olive oil production procedure used in many countries, such as Spain, where the implementation of this technology has benefited from public funding. The two-phase centrifugation technology is commonly called “ecological” because of its minor water and energy requirements and reduced pollution load (Table 12.1) (FAIR, 2000). Although other olive oil producing countries are also slowly adopting the two phase technology, the three-phase extraction process (OMW-3) is still surviving in some areas where small olive oil enterprises resist switching due to the capital investment, especially where water economy is not a major consideration.

Industrial wastewater is subjected to strict environmental legislation, thus making its adequate management a key issue. Moreover, it is well known that the European Environmental Regulations will become more stringent in virtue of the ‘H2020 Horizon’. There is a plethora of technologies described in the scientific literature regarding wastewater treatments. Current methods for wastewater purification include precipitation, coagulation/flocculation,

sedimentation, flotation, filtration, membrane processes, electrochemical techniques, Ion Exchange (IE), biological processes and chemical reactions, among others (Demirbas et al., 2005). Nevertheless, most of these techniques imply some disadvantages and limitations such as secondary pollution, complicated treatment processes, high cost and energy consumption (Balcıoğlu and Gönder, 2014; Chen et al., 2010; Das, 2010; Fu and Wang, 2011; Li et al., 2011; Sen Gupta and Bhattacharyya, 2011).

Table 12.1. Approximate Input-Output data for two-phase and three-phase olive oil production systems (FAIR, 2000).

Production process	Input	Amount of input	Output	Amount of output (kg)
Three-phase process	Olives	1 ton	Oil	200
	Wash water	0.1-0.12 m ³	Solid waste	500-600
	Fresh water for decanter	0.5-1 m ³	Wastewater (94% water + 1% oil)	1000-1200
	Water to polish the impure oil	10 L		
Two-phase process	Olives	1 ton	Oil	200
	Washing water	0.1-0.12 m ³	Solid + water waste (60% water + 3% oil)	800-950

In the recent years, new treatment technologies have been developed to reduce the organic and phenolic contaminants load of OMW, e.g. lagooning and thermal concentration (Annesini and Gironi, 1991; Niaounakis and Halvadakis, 2006), composting (Cegarra et al., 1996; Papadimitriou et al., 1997), treatments with clay (Al-Malah et al., 2000) or with lime (Aktas et al., 2001), biosorption (Hodaifa et al., 2013a), coagulation-flocculation (Martínez Nieto et al., 2011a; Sarika et al., 2005), electrochemical treatments (Papastefanakis, 2010; Tezcan et al., 2008), ozonation (Beltrán de Heredia and Garcia, 2005), photocatalysis (Caprariis et al., 2012), biological (Al-Qodah et al., 2014a; Garrido Hoyos et al., 2002; Paraskeva and Diamadopoulos, 2006) and hybrid processes (Al-Qodah et al., 2014b; Lafi et al., 2009; Lafi et al., 2010; Rizzo et al., 2008). However, the majority of the processes proposed until today for the treatment of OMW are rather cost-ineffective, and olive oil industry in its current status, composed of little and dispersed factories, is not willing to bear such high costs.

Among them, advanced oxidation process based on Fenton's reaction is presented as an efficient secondary treatment (ST), able to remove the organic and phenolic pollutants of OMW-2 (Martínez Nieto et al., 2011b). However, high levels of monovalent ions, mainly sodium and chloride, as well as iron, are found in OMW-2ST, derived from the dosage of the catalyst and neutralizing agents during the secondary treatment (Martínez Nieto et al., 2011b; Hodaifa et al., 2013b). Furthermore, a significant phenols amount above maximum legislated standard level (0.005 mg L^{-1}) (European Commission, 1980) was present in this secondary-treated OMW-2ST effluent and iron concentration exceeded the maximum levels allowed by the European legislation for drinking water (0.2 mg L^{-1}) (European Commission, 1998).

In this scenario, conventional and advanced physicochemical treatments are not able to abate the high salinity of OMW-2ST, which exhibited electroconductivity (EC) values above the range $2\text{--}3 \text{ mS cm}^{-1}$, thus presenting hazardous salinity levels according to the standard limits established by the Food and Agricultural Association (FAO) with the goal of reusing the regenerated water for irrigation purposes.

Within this context, novel IE resins developed over the past few decades have promoted this technology as a suitable separation and purification process for wastewater treatment (Demirbas et al., 2005; Fu and Wang, 2011; Comstock and Boyer, 2014). Moreover, IE is considered a green and simple technology, capable of achieving high removal efficiencies and selectivity (Demirbas et al., 2005; Fu and Wang, 2011). There are various studies focused on the use of IE resins for the elimination of sodium and chloride ions in aqueous media (El-Naggar et al., 1996; Pivovarov, 2008; Víctor-Ortega, 2015). Also, several research works have been described in the literature for the removal of iron and phenolic species by means of IE technology (Abburi, 2003; Caetano et al., 2009; Carmona et al., 2006; Keller, 2004; Ku et al., 2004; Ostroski et al., 2009; Tahir and Rauf, 2004; Vaaramaa and Lehto, 2003).

In this research work, the final purification of OMW-2ST by IE is addressed. To the Authors' knowledge, no previous work can be found in the scientific literature on the application and optimization of IE technology for the purification of real two-phase olive mill wastewater streams. The main objective was the optimization of the final purification of OMW-2 by means of an IE system comprising two resins in serial connection: cation exchange Dowex Marathon C and anion exchange Amberlite IRA-67.

Recirculation mode experiments were carried out to examine the impacts of the main operating parameters on the IE process performance - operating temperature, initial pH and flow rate - as well as the interactions among them. For this purpose, the IE process was modeled by means of central composite design (CCD), statistically tested using analysis of variance (ANOVA).

Additionally, the optimal resins dosages were also investigated. Subsequently, continuous experiments were carried out under the optimum operating conditions found in order to evaluate the studied IE resins for their application in the purification of OMW-2ST at industrial scale. Finally, water quality standards for reusing the purified olive mill effluent in the olive oil production process and thus reducing the environmental impact were checked.

12.2 Experimental section

12.2.1 Materials

Wastewater (OMW-2) samples were collected from different olive oil mills in the South of Spain, operating with the two-phase centrifugation system. Firstly, OMW-2 samples were conducted to the secondary treatment thoroughly described in previous works by the Authors (Martínez Nieto et al., 2011b; Hodaifa et al., 2013b; Ochando-Pulido et al., 2012). The effluent after the secondary treatment, hereafter referred as OMW-2ST, was the feed stream to the final IE purification process. Chemical oxygen demand (COD), total phenolic compounds (TPh), sodium, chloride, total iron, electroconductivity (EC) and pH were measured in the outlet stream samples of the secondary treatment as well as of the IE system, following standard methods (Greenberg et al., 1992). The physicochemical composition of the OMW-2ST samples is reported in Table 12.2.

Strong-acid cation exchange Dowex Marathon C and weak-base anion exchange Amberlite IRA-67 resins, both provided by Sigma Aldrich, were used in this work. Dowex Marathon C was conditioned in hydrochloric acid solution and finally in water before being used in the IE experiments. On the other hand, Amberlite IRA-67 was treated with sodium hydroxide solution and then was washed with water following the advice of the resin manufacturer. Typical physical and chemical characteristics of the used resins are described in Table 12.3.

After each operational cycle, the Dowex Marathon C cation exchange resin was fully washed with 1L 4% HCl aqueous solution. In a similar way, Amberlite IRA-67 anion exchange resin was washed with 1L 2% NaOH aqueous solution. Finally, the resins were washed with double distilled water to remove all excess of acid or base, respectively.

Table 12.2. Physico-chemical characterization of OMW-2ST.

Factor	Value
pH	6.82 ± 0.55
Conductivity, mS cm⁻¹	4.35 ± 0.30
COD, mg L⁻¹	162.0 ± 1.2
Total phenolic compounds, mg L⁻¹	0.012 ± 0.001
[Cl⁻], mg L⁻¹	1250 ± 3
[Na⁺], mg L⁻¹	870 ± 5
[Total iron], mg L⁻¹	0.9 ± 0.1

Table 12.3. Properties of Dowex Marathon C and Amberlite IRA-67 IE resins.

Properties	Dowex Marathon C	Amberlite IRA-67
Type	Strong-acid cation	Weak-base anion
Matrix	Styrene-DVB, gel	Tertiary amine
Ionic form as shipped	H ⁺	OH ⁻
Particle size, mm	0.55-0.65	0.5-0.75
Effective pH range	0-14	0-7
Total exchange capacity, eq L⁻¹	1.80	1.60
Shipping weight, g L⁻¹	800	700

12.2.2 Ion exchange equipment

A bench-scale IE equipment was used to evaluate the performance of the combination of two IE columns operating in serial connection for the purification of OMW-2ST, as shown in Figure 12.1. The IE columns employed in this study were made of an acrylic tube with dimensions 540 mm height x 46 mm internal diameter. The columns are provided with a mobile upper retaining grid, which could be fixed in the column to adjust it as a fixed bed or a semi-fluidized bed. The IE device (MionTec) was equipped with a peristaltic pump (Ecoline VC-380) and a temperature-controlled thermostatic bath (Precisterm JP Selecta).

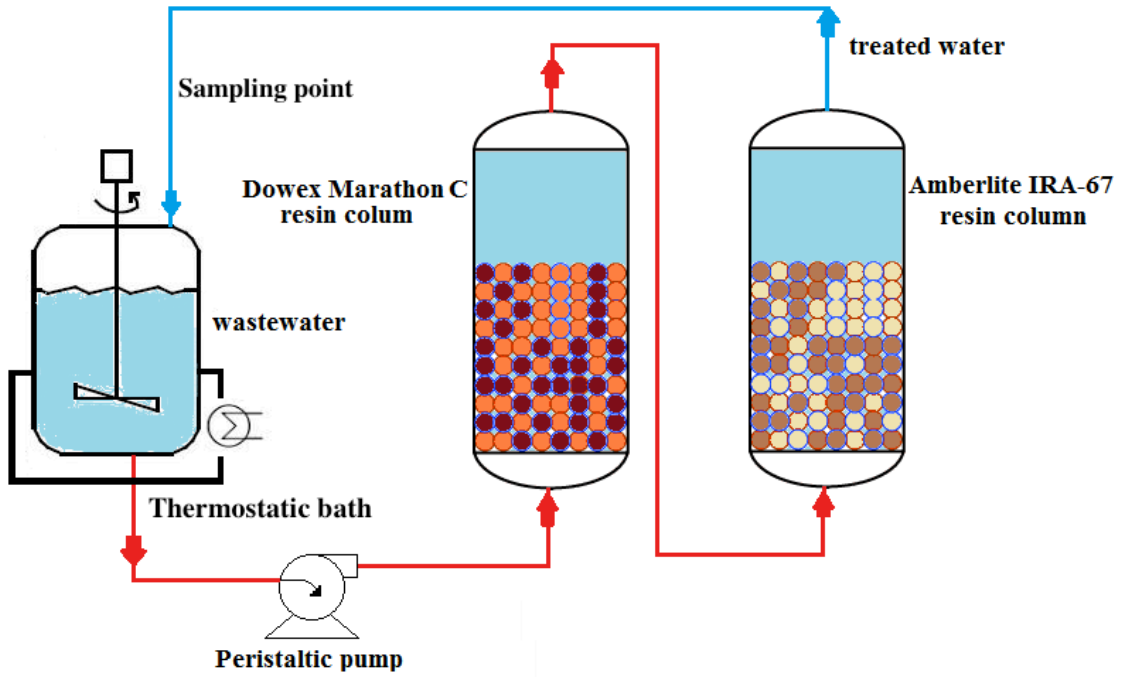


Figure 12.1. Flow-sheet scheme for IE recirculation operating experiments.

12.2.3 Recirculation IE experiments

The IE removal efficiencies of sodium, chloride, iron and phenolic compounds from OMW-2ST were addressed by performing IE experiments in recirculation mode. The flask containing the 2 L feed solution was magnetically stirred continuously during the whole course of the experiments. The recirculation time was varied from 0 to 60 minutes. The initial pH, operating temperature and flow rate ranges studied are reported in Table 12.4. Each experiment was carried out twice to check the reproducibility of the results.

The percent of removal efficiency of the contaminant species was defined as follows:

$$\% \text{ Removal efficiency} = \frac{C_i - C_f}{C_i} \times 100 \quad (1)$$

where C_i and C_f are the initial and final species' concentration (mg L^{-1}), respectively.

Table 12.4. Values range of the factors used in the experimental design.

Independent variable	Range
Initial pH	3 - 8
Operating temperature, °C	10 - 50
Flow rate, L h^{-1}	5 - 20

12.2.4 Experimental design and optimization of IE operating parameters

In this work, the impacts of the main operating variables on the IE removal of chloride, sodium, phenols and iron ions in OMW-2ST was examined by means of experimental design. The proposed IE process was modeled by means of CCD and statistically tested using ANOVA.

Traditional univariate optimization techniques imply the study of the effect of one factor at a time, maintaining constant the rest of involved variables. This methodology is time consuming and requires an excessive and unnecessary number of experiments for the determination of the optimum levels, which are usually unreliable. Moreover, the main drawback of those methods is that possible interactions among factors are not taken into account. These limitations can be eliminated by optimizing all the affecting variables collectively by means of experimental design in combination with Response Surface Methodology (RSM) (Elibol, 2002). RSM is a collection of mathematical and statistical techniques useful for development, improvement and optimization of processes and can be used to evaluate the relative significance of several affecting factors. This methodology is able to gather large amounts of information from a minimum number of data points. The main objective of RSM is to determine the optimum operational conditions for the system or to determine a region that satisfies the operating specifications (Ravikumar et al., 2005).

Under this methodology, the system is represented through an empirical equation, based on the experimental data obtained for the system under study for the adjustment of the corresponding coefficients. It is common practice the employment of second order polynomial models with crossed terms that enable the description of concavities or convexities in the surface. Thus, the surface represented by this polynomial model is called “Response Surface” (RF), which equation for the study of two variables is (Box and Wilson, 1951):

$$y = b_0 + b_1x_1 + b_2x_2 + b_{11}x_1^2 + b_{22}x_2^2 + b_{12}x_1x_2 \quad (2)$$

where y is the response function and x_1 and x_2 the studied variables.

The values for the variables x_1 and x_2 at the optimal point can be determined by solving the next first grade system:

$$\frac{\delta y}{\delta x_1} = b_1 + 2b_{11}x_1 + b_{12}x_2 = 0 \quad (3)$$

$$\frac{\delta y}{\delta x_2} = b_2 + 2b_{22}x_2 + b_{12}x_1 = 0 \quad (4)$$

The application of experimental design techniques in IE process development can result in improved product yields, reduced process variability, closer confirmation of the output response to the nominal and target requirements and reduced development time and overall costs

(Annadurai et al., 2002). The first step when performing experimental design involves the selection of the experimental outcome to be optimized. The experimental outcome is normally the value for a certain property or a mathematical combination of several of them that represents a realistic measure of the process performance.

The initial pH, operating temperature and flow rate were selected as independent variables and the global percentage of the pollutant species removed as RF. The assayed ranges for the selected variables were equal to 10-50 °C for temperature, 3.0-7.0 for initial pH and 5-20 L h⁻¹ for flow rate, on the basis of previous studies carried out by the Authors with synthetic OMW-2ST (V́ctor-Ortega et al., 2014a; V́ctor-Ortega et al.; 2014b). A CCD was used in order to calculate simultaneously the effect of the change in each one of these variables and also their possible interactions. Five levels were considered for each variable and three central samples were also included, which gives rise to a total of 17 experiments (Table 12.5). This design is rotatable, and therefore the precision in the calculation of the response is uniform over the whole experimental field. The optimization of the model was made with The Unscrambler software package (v. 9.8, Camo AS, Oslo, Norway), and the results were interpreted with the RSM.

12.2.5 Analytical methods

Sodium concentration values were determined by using a Crison GLP 31 Sodium Ion-Selective Electrode 96 50, with autocorrection of temperature. To this end, 0.01, 0.1 and 1.0 g L⁻¹ Na⁺ standard solutions were prepared in the laboratory to calibrate the electrode. Chloride concentration values were assessed by a Crison GLP 31 Chloride Ion-Selective Electrode 96 52 C, with autocorrection of temperature. For this purpose, 0.01, 0.1 and 1.0 g L⁻¹ Cl⁻ standard solutions required for the electrode calibration were also prepared in the laboratory.

For the measurement of the total iron concentration, all iron ions were reduced to iron ions (II) in a thioglycolate medium with a derivative of triazine, forming a reddish-purple complex that was determined photometrically at 565 nm (Standard German methods ISO 8466-1 and German DIN 38402 A51) (Greenberg et al., 1992).

Total phenols and phenol derivatives were analyzed by reaction with a derivative thiazol, giving a purple azo dye, which was determined photometrically using a Helios Gamma UV-visible spectrophotometer (Thermo Fisher Scientific) at 475 nm (Standard German methods ISO 8466-1 and DIN 38402 A51) (Greenberg et al., 1992).

EC and pH measurements were evaluated with a Crison GLP31 conductivity-meter and a Crison GLP21 pH-meter, provided with autocorrection of temperature. Buffer standard solutions for

EC ($1,413 \mu\text{S cm}^{-1}$ and 12.88 mS cm^{-1}) and pH (pH 4.01, 7.00 and 9.21) measurements respectively were supplied as well by Crison.

Analytical grade reagents and chemicals with purity over 99 % were used for the analytical procedures, applied at least in triplicate.

12.3 Results and discussion

12.3.1 Resins disposition study

Beforehand, the impacts of the disposition of both resins on the IE system performance were examined. Experiments were carried out in recirculation operation mode at fixed conditions equal to $25 \text{ }^\circ\text{C}$ and 10 L h^{-1} for 100 min, to ensure equilibrium was achieved (V́ctor-Ortega et al., 2014a; V́ctor-Ortega et al., 2014b). Results are reported in Figure 12.2.

The evolution of sodium IE removal as a function of the recirculation time for both resins configurations, shown in Figure 12.2a, reveals that equilibrium was achieved in a shorter time for the A-type resin disposition than for the B-type one (20 min for A configuration vs. 45 min for B configuration). Similarly, equilibrium for chloride IE removal was reached within 30 min for the A-type resins configuration, whereas equilibrium for the B-type configuration was not achieved until 60 min operation time (Figure 12.2b).

Otherwise, the measured total iron concentration in the outlet stream was below 0.2 mg L^{-1} throughout the entire experiments disregarding the chosen resins disposition (Figure 12.2c). This meant that removal efficiencies were higher than 80 % during the total operating time. There were no significant differences regarding total iron removal for both IE resins configurations. This fact may be explained by the low concentration level of this pollutant in the inlet stream.

On the other hand, considerably significant differences between the studied resin dispositions were found in case of phenols IE removal efficiency (Figure 12.2d). When experiments were carried out according to the B configuration, the highest phenols removal efficiency (at equilibrium point) was about 30 %, whereas in the case of the A configuration the highest phenols removal percentage was found to be above 50 %.

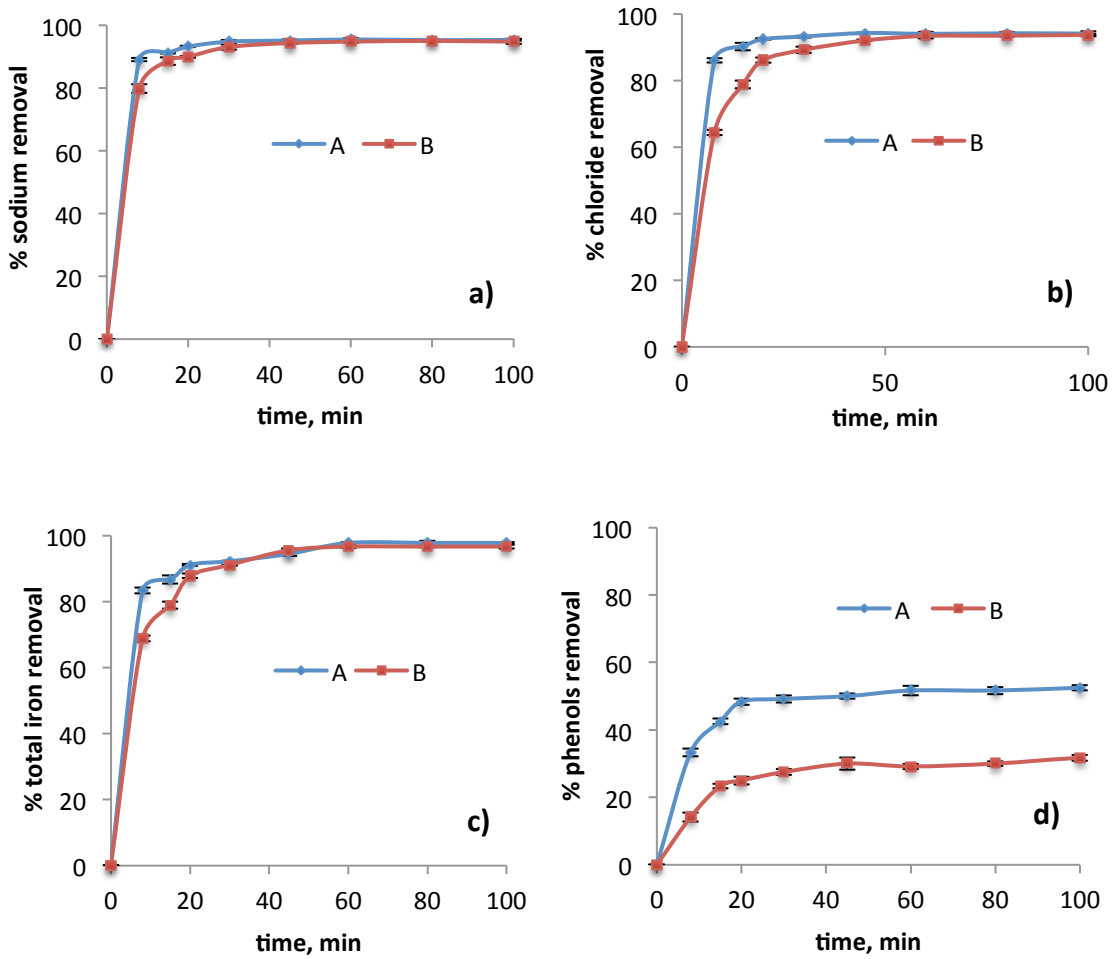


Figure 12.2. Effect of resins disposition (A: cation + anion, and B: anion + cation) on chloride, sodium, total iron, and phenols IE removal efficiencies as a function of recirculation time. Operating conditions: 25 °C and 10 L h⁻¹.

Monovalent ions (sodium and chloride) and iron in OMW-2ST are removed by means of IE. The total exchange capacities of the employed resins are high enough (1.8 and 1.6 eq L⁻¹, Table 12.3) to justify the IE mechanism. In case of phenols, the uptake in the resin is assumed to be accomplished by two ways: IE and molecular adsorption. Cations are exchanged in the first column (cation exchange resin), thus at the end of this column pH drops approximately to 1.5–2.5 because H⁺ species are released. In the second column (anion exchange resin), anions are exchanged and pH progressively increases, being in the range 7-8 at the end of the process. The phenol dissociation to phenol and phenolate can be considered as a function of the total concentration of phenol and the pH of the liquid solution (pH > 8). At acidic pH (pH < 8) the phenol dissociation is low and therefore the molecular adsorption process is predominant (cationic IE resin), whereas both adsorption and IE are important at alkaline pH (anionic IE resin) (Carmona et al., 2006).

These results confirm the cation exchange resin column followed by the anion exchange one as the optimal arrangement of the selected resins. This outcome is supported by the fact that the cationic resin is active in the whole pH range whereas the anionic one is only active in the range 0–7 (Table 12.2). In that way, as the OMW-2ST stream passed through the cation exchange resin, the pH decreased due to protons release (pH below 2) and thus the anions uptake is favoured in the anionic column. OH⁻ are liberated in this latter column, thus equilibrating the pH value of the IE system output. These results obtained in recirculation mode experiments verify the patterns observed in continuous IE operation mode experiments carried out by the Authors with synthetic OMW-2ST in former studies (V́ctor-Ortega, 2014a).

12.3.2 Optimization study

The study of the effect of the main operating parameters on the IE process efficiency as well as their possible interactions - initial pH, temperature and flow rate - was carried out by means of experimental design. The objective of this optimization was to investigate the set of values for the operating conditions that maximize the performance of the IE process for OMW-2ST purification. The initial pH (pH₀) range studied was varied between 3 and 8, whilst the temperature was fixed between 10 °C and 50 °C. On the other hand, the flow rate was varied from 5 to 20 L h⁻¹. Namely, a CCD, which involves a total of 17 experiments (see Table 12.4), was employed. The average value of the mean removal efficiencies for sodium, chloride, iron, phenols and organic pollutants (COD) was selected as RF, which represents the overall IE removal efficiency in a realistic way. The actual operating conditions and results obtained from the optimization study are given in Table 12.5.

The results derived from the optimization of the model were further interpreted by means of the RSM. In the corresponding ANOVA a second-grade quadratic model was assumed (model check quadratic, p-value (95%) = 0.0001) (see Table 12.6).

The operating temperature-flow rate, initial pH-temperature and flow rate-initial pH interactions were found non-significant to the model, since for these interactions it was confirmed that the p-value was above 0.05 (p-value > 0.05). However, it was confirmed that each factor considered individually, as well as its quadratic interactions, contributed significantly to the model for a 95% confidence level (p-values < 0.05). On the other hand, the p-value (95%) calculated for lack of fit was 0.1531, highlighting that the model describes properly the true shape of the response surface.

Table 12.5. CCD matrix for the IE process optimization.

Experiment	T (°C)	pH ₀	Q (L h ⁻¹)	% sodium removal	% chloride removal	iron% removal	phenols% removal	% COD removal	% global removal
Exp 1	9.8	5.5	12.6	81.0	77.0	88.0	55.0	80.0	76.2
Exp 2	50.2	5.5	12.6	68.0	72.0	80.0	38.0	70.0	65.6
Exp 3	30.0	3.0	12.6	88.0	81.0	79.0	61.0	78.0	77.4
Exp 4	30.0	8.0	5.1	87.0	74.0	71.0	54.0	71.0	71.4
Exp 5	30.0	5.5	5.1	77.0	74.0	82.0	44.0	74.0	70.2
Exp 6	30.0	5.5	20.0	83.0	79.0	72.0	47.0	70.0	70.2
Exp 7	18.0	4.0	8.1	89.0	80.0	89.0	63.0	82.0	80.6
Exp 8	42.0	4.0	8.1	82.0	78.0	85.0	43.0	72.0	72.0
Exp 9	18.0	7.0	8.1	86.0	75.0	73.0	55.0	74.0	72.6
Exp 10	42.0	7.0	8.1	83.0	75.0	72.0	41.0	75.0	69.2
Exp 11	18.0	4.0	17.0	85.0	80.0	75.0	56.0	73.0	73.8
Exp 12	42.0	4.0	17.0	80.0	73.0	87.0	41.0	70.0	70.2
Exp 13	18.0	7.0	17.0	85.0	77.0	72.0	51.0	75.0	72.0
Exp 14	42.0	4.0	17.0	81.0	71.0	70.0	39.0	73.0	66.8
Exp 15	30.0	5.5	12.6	94.0	92.0	91.0	64.0	92.0	86.6
Exp 16	30.0	5.5	12.6	96.0	95.0	90.0	66.0	94.0	88.2
Exp 17	30.0	5.5	12.6	96.0	94.0	91.0	65.0	92.0	87.6

* Average value of removal efficiencies of sodium, chloride, total iron, phenols and COD.

The estimated response surfaces for each pair of variables are represented in Figure 12.3. A focus on these figures permits noting that the IE global removal efficiency becomes incremented with an increase of the temperature, flow rate and initial pH values. However, there is an inflection point for each operating variable studied, such that further increasing their values does not yield higher IE removal. The maximum value of RF in the obtained surfaces and the optimum values of the process variables are reported in Table 12.7. These results closely agree with those obtained from the response surface analysis, confirming that the RSM could be effectively used to optimize the IE process parameters for the final purification of OMW-2ST.

It seems that the excessive protonation of the active sites of the Dowex Marathon C cation exchange resin at low pH values (below 5) hinders the formation of links between sodium ions

and the active sites of the cation exchange resin. Similar results were found by Senthil Kumar and Gayathri in their study on bael tree leaf powder as adsorbent to remove lead (Pb^{2+} ions) from aqueous solutions (Senthil Kumar and Gayathri, 2009). On the other hand, at moderate pH values (3-6) the linked H^+ is released from the active sites of the cation exchange resin and as a result the extent of IE of sodium ions is found to increase. Otherwise, with regard to chloride ions, the decrease of the IE efficiency by incrementing the pH value was attributed to the fact that Amberlite IRA-67 anion exchange resin exhibits weak-base properties, active in a pH range from 0 to 7. The pH of the solution becomes increased as chloride ions are exchanged and hydroxyl ions are released from the anion exchange resin, thus making the removal efficiency to decrease.

Otherwise, the required time to reach equilibrium decreased with increasing the flow rate. Chen et al. found that at higher flow rate fixed the stream does not have enough time to contact/react with the ion exchange resins because of too low residence times (Chen et al., 2002).

Finally, it was found that increasing the operating temperature above ambient conditions ($T > 26.8\text{ }^\circ\text{C}$) led to a progressive decrease of the global IE efficiency (Figure 12.3a,b). These results are supported by those found by Demirbas et al. (2005) in their study of the effect of temperature on the adsorption of metal ions onto Amberlite IR-120 resin (Demirbas et al., 2005). Moreover, phenols removal is major at lower operating temperature. Roostaei and Tezel (2004) proved that phenols adsorption capacity decreased with increasing temperature by using silica gel, HiSiv 3000, activated alumina, activated carbon, Filtrasorb-400 and HiSiv 1000 (Roostaei and Tezel, 2004). In other studies, adsorption of molecular phenol species on N-butylimidazolium functionalized strongly basic anion exchange resin with chloride anion (MCl) was found to be exothermic under acidic pH conditions. Similar results were observed by other authors on Purolite A-510, NDA103 and IRA96C resins (Ku et al., 2004; Erdem et al., 2005). Zhu et al. (2011) concluded that the molecular adsorption of phenols on MCl was exothermic (Zhu et al., 2011).

To sum up, global removal efficiencies higher than 80 % were obtained for temperatures ranging between 20-30 $^\circ\text{C}$ (Figure 12.3a and Figure 12.3b) and for pH values in the range 4.5-7 (Figure 12.3a and Figure 12.3c). This fact would permit the operation of the proposed IE process at ambient temperature conditions upon a pH of the feed stream in the range of that attained at the outlet of the secondary treatment (Martínez Nieto et al., 2011b; Hodaifa et al., 2013b), thus having important implications in the reduction of the IE operating costs.

Table 12.6. ANOVA for results of CCD.

Source	Sum of square (SS)	Degree of freedom (DF)	Mean square (MS)	F-ratio	p-value
Model	781.184	9	86.798	29.906	0.0001
Intercept	$3.240 \cdot 10^3$	1	$3.240 \cdot 10^3$	$1.116 \cdot 10^3$	0.0000
A: Temperature	109.253	1	109.253	37.642	0.0005
B: Initial pH	49.845	1	49.845	17.174	0.0043
C: Flow rate	9.853	1	9.853	3.395	0.1080
AB	1.620	1	1.620	0.558	0.4793
AC	1.280	1	1.280	0.441	0.5279
BC	3.920	1	3.920	1.351	0.2833
AA	350.557	1	350.557	120.782	0.0000
BB	212.237	1	212.237	73.125	0.0001
CC	382.364	1	382.364	131.741	0.0000
Lack of fit	19.010	5	3.802	5.819	0.1531
Pure error	1.307	2	0.653		
Total error	20.317	7	2.902		

Table 12.7. Optimum parameters values for maximum IE process efficiency.

Factor	T (°C)	pH ₀	Q (L h ⁻¹)	Predicted max. global removal	% Multiple Correlation (R)	R-Square (R ²)
Optimal value	26.80	5.14	12.12	88.03	0.987	0.975

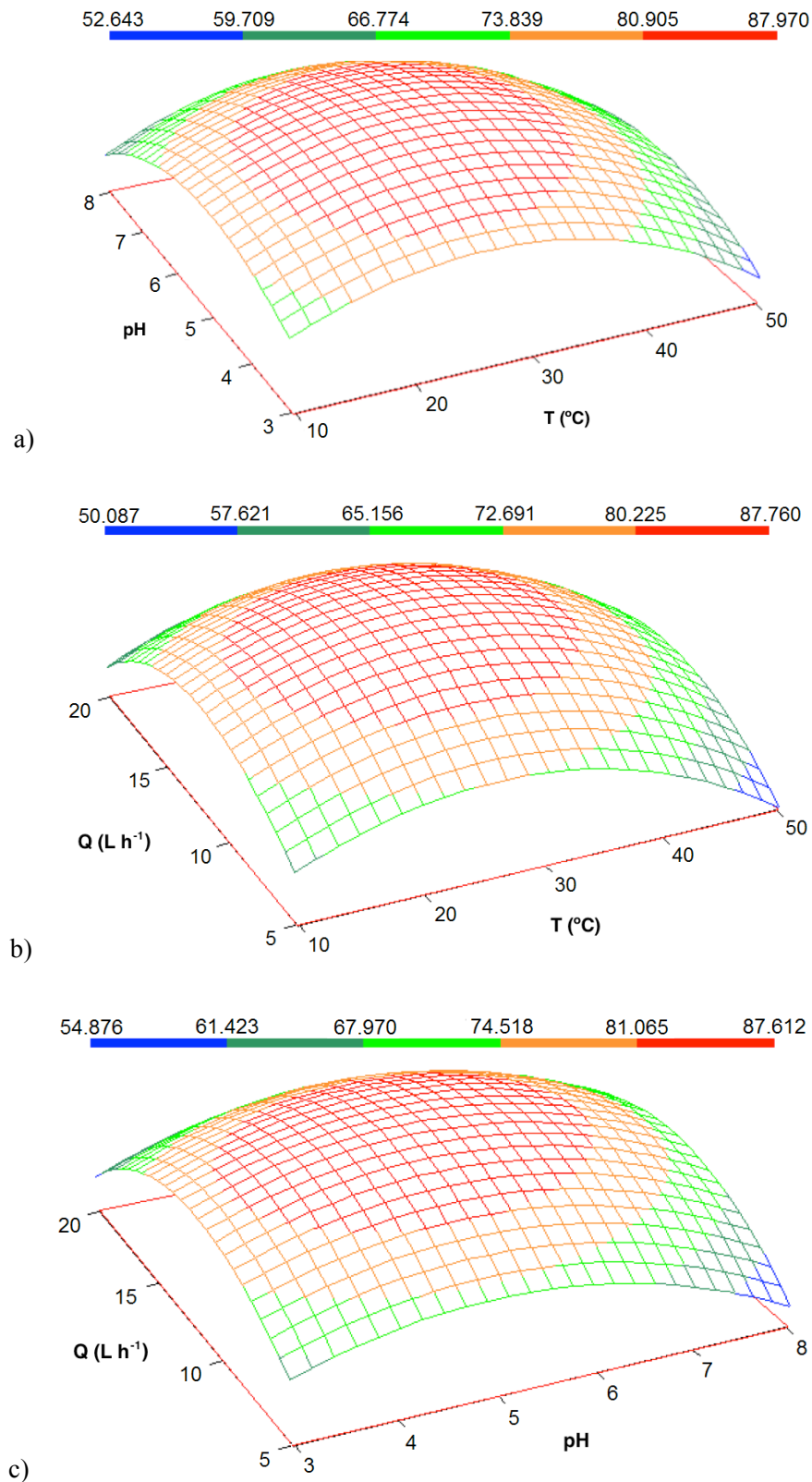


Figure 12.3. Response surface plots showing the effect of temperature, initial pH and flow rate and their interactions on global IE removal: a) temperature and initial pH ($Q = 12.55 \text{ L h}^{-1}$), b) flow rate and temperature ($\text{pH}_0 = 5.5$), c) initial pH and flow rate ($T = 30 \text{ }^\circ\text{C}$). Recirculation time: 60 min; resins dosage: 35 g L^{-1} .

12.3.3 Effect of IE resins dosages

Subsequently, the effect of Dowex Marathon C and Amberlite IRA-67 resin dosages on the IE removal of the pollutants in the OMW-2ST stream was investigated under the optimal operating conditions formerly obtained by means of the CCD optimization. Results are reported in Figure 12.4.

Figure 12.4.a shows the IE removal of sodium as a function of the Dowex Marathon C resin dosage, which was varied from 5 to 40 g L⁻¹ and equilibrated for 60 min. The experimental results revealed that sodium removal efficiency increased up to an optimum dosage, beyond which the removal efficiency had no change with the resin dosage. In this case, a minimum resin dosage equal to 20 g L⁻¹ was confirmed in order to achieve sodium removal efficiency above 90 %.

Moreover, a deep analysis of Figure 12.4.a reveals that 12 g L⁻¹ Dowex Marathon C cation exchange resin provided 80 % sodium removal as well as 90 % iron removal. Under these conditions, the achieved concentrations for both contaminants were lower than the established maximum limits (Habuda-Stanic et al., 2008). Otherwise, the maximum iron IE percentage (about 90 %), obtained for a minimum resin dosage of 10 g L⁻¹, was higher than that observed in case of sodium since the initial iron concentration is sensibly lower than the initial sodium level.

Similarly, the removal of chloride ions was evaluated as a function of Amberlite IRA-67 resin dosage, which was varied from 5 to 40 g L⁻¹ and equilibrated for 60 min (Figure 12.4.b). The experimental results confirmed that chloride removal efficiency increased up to an optimum dosage equal to 30 g L⁻¹, such that further incrementing the anionic resin dosage did not bring enhanced IE efficiency (up to 95 %).

On the other hand, the removal efficiency for COD with the increase of the anionic resin dosage was found to be lower than for chloride when the resin dosage ranged between 5-30 g L⁻¹, but similar removal efficiencies were found upon dosages higher than 30 g L⁻¹ for both resins. Otherwise, a maximum adsorption percentage for the phenolic compounds by Amberlite IRA-67 resin, close to 60 %, was attained at a minimum anion exchange resin dosage equal to 20 g L⁻¹, as reported in Figure 12.4.b.

For all the studied species, the IE uptake is highly dependent on the initial concentration of the sorbate and sorbent. The equilibrium concentrations of all the OMW-2ST pollutants decreased with increasing the adsorbent doses for a given initial concentration. The increase in the removal percentage with the increase in the adsorbents dosage is due to the greater availability of the exchangeable sites or surface area at higher concentration of the adsorbent (Krishnan and

Anirudhan, 2003; Rengaraj and Moon, 2002). The resin dosage is a key economical factor affecting the process performance, of utmost importance for the industrial scale-up of the proposed IE process (Yu et al., 2003).

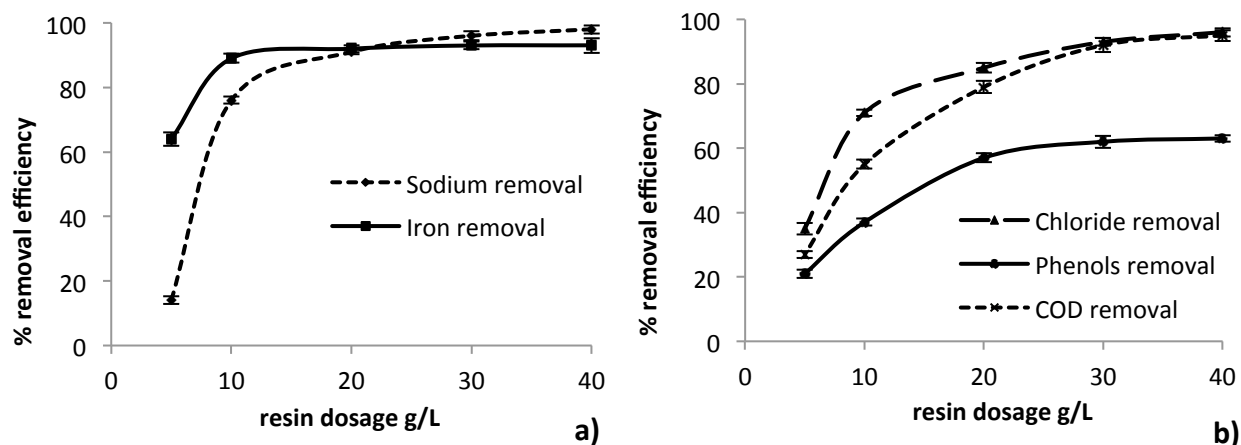


Figure 12.4. Effect of Dowex Marathon C resin dosage on sodium and total iron IE removal (a caption) and Amberlite IRA-67 resin dosage on chloride, phenols and COD IE removal (b caption). Recirculation time: 60 min; temperature: 27 °C; flow rate: 12 L h⁻¹.

It may be concluded that Amberlite IRA-67 provides very high IE capacity for the removal of chloride, organic pollutants and phenolic species in OMW-2ST for pH values below 2.0, in good line with the pH of the stream exiting the cationic column according to the optimum disposition arrangement formerly found (section 3.1.). Furthermore, a minimum dosage of Amberlite IRA-67 equal to 15 g L⁻¹ allowed achieving 80 % removal efficiency for chloride ions (Figure 12.4.b), which correspond to levels below the maximum acceptable concentrations legislated. Moreover, 50 % uptake efficiency for phenols and around 70 % removal percentage for COD were obtained for this low resin dosage.

12.3.4 Industrial application of continuous IE process

Finally, continuous experiments were carried out with the aim of evaluating the performance of the proposed IE process for the final purification of OMW-2ST at industrial scale.

Within this context, continuous IE experiments were performed at ambient operating temperature (25 °C), flow rate equal to 12 L h⁻¹ and initial feed stream pH fixed at 6.8 (pH value at the outlet of the secondary treatment). In this regard, it is important to highlight the possibility of working efficiently at low temperature conditions, which enhances the cost-efficiency of the IE process since those are the conditions usually attained during autumn-winter periods, when the olive oil production takes place and this effluent shall be managed. Furthermore, inlet stream

pH values in the range 4.5-7 provided global removal efficiencies higher than 80 %, thus raw OMW-2ST can be directly subjected to the proposed IE process (see section 13.3.2).

Continuous IE runs were performed for 180 min, corresponding to the exhaustion time of the selected resins regarding chloride and sodium, which are the limiting ions for Dowex Marathon C and Amberlite IRA-67, respectively.

A comparison between the maximum legislated standard values for drinking water production and the final treated effluent after the proposed integral process is reported in Table 12.8. The final treated OMW-2ST effluent by the IE process fulfills the legislated requirements for drinking water (European Commission, 1980; European Commission, 1998). A final OMW-2ST effluent treated volume up to 28 L could be achieved, for 140 min IE operating time. Chloride, sodium, total iron and phenols concentrations stood below the maximum levels established by the legislation in the IE outlet stream. This fact allows the successful reutilization of the final treated effluent in the olives washing machines and finally closing the loop, thus rendering the production process cost-effective and environmentally respectful.

Table 12.8. Comparison between the initial and final values of OMW-2ST and the legislated values of drinking water.

Stream	[Na ⁺] (mg L ⁻¹)	[Cl ⁻] (mg L ⁻¹)	[Fe _T] (mg L ⁻¹)	[Ph] (mg L ⁻¹)	COD (mg L ⁻¹)	volume (L)	time (min)
^a OMW-2ST ₀	870	1250	0.9	0.012	162	-	-
^b OMW-2ST _f	161.8	247.3	0.08	0.004	4.8	28	140
^c Drinking water	200	250	0.2	0.005	-	-	-

^aOMW-2ST₀: OMW-2ST before IE process; ^bOMW-2ST_f: OMW-2ST after IE process under optimal conditions; ^c Required values for Drinking Water (European Commission, 1980; European Commission 1998).

The obtained results are highly relevant since the operating temperature is a key variable from a technical–economical point of view. In this regard, the examined resins work highly efficiently at ambient temperature conditions, hence giving a sensible economical boost to the IE process. Furthermore, it is worth indicating that the volume produced by the regeneration of the resins is sensibly lower than volumes of final treated water and this regeneration volume can be reused for several operating cycles.

The optimized IE process proposed is presented as a cost-efficient alternative for the final purification of two-phase olive mill wastewater, in contrast with conventional separation processes which are not able to abate the dissolved pollutants concentration in OMW-2ST, or thermal

processes involving high energetic costs such as osmotic or vacuum distillation (Garcia-Castello et al., 2010). The proposed IE process may also replace membrane technology, which implies higher operating costs as high pressures are needed to achieve similar removal efficiencies (Ochando-Pulido et al., 2012; Cassano et al., 2011). Moreover, the output provided by membrane processes changes continuously during operation time due to fouling, in contrast with the results shown by the IE process reported in this work.

12.4 Conclusions

In this research work, the final purification of two-phase olive mill wastewater (OMW-2) by ion exchange (IE) is addressed. To the Authors' knowledge, no previous work can be found in the scientific literature on the use of IE technology for OMW-2 reclamation.

The IE process was optimized through a central composite design. Results reveal that setting the cation exchange resin followed by the anion exchange one provided the major IE efficiency. The proposed IE process yielded up to 88 % removal of these pollutants when the initial pH, operating temperature and flow rate were set to 5.1, 26.8 °C and 12.1 L h⁻¹, respectively. It was confirmed that each factor considered individually, as well as its quadratic interactions, contributed significantly to the model at 95% confidence level.

Moreover, it was found that 20 g L⁻¹ Dowex Marathon C resin and 30 g L⁻¹ Amberlite IRA-67 resin were the minimum dosages to ensure removal efficiencies above 90 %. However, minimum dosages equal to 12 g L⁻¹ for the cation exchange resin and 15 g L⁻¹ for the anion exchange one ensured up to 80 % sodium and chloride as well as 90 % iron removal, together with 50 % uptake efficiency for phenols and 70 % for COD.

Under optimal conditions, concentrations for all contaminants in the final stream were maintained below the maximum established limits. Finally, high treated effluent volume recovery (28 L) could be achieved in continuous mode under the optimal operating conditions found, complying with standards for reuse in the production process.

12.5 References

- Abhuri, K. (2003). Adsorption of phenol and p-chlorophenol from their single and bisolute aqueous solutions on Amberlite XAD-16 resin. *J. Hazard. Mater.*, 105:143-156.
- Aktas, E.S., Imre, S., Esroy, L. (2001). Characterization and lime treatment of olive mill wastewater. *Water Res.*, 35:2336-2340.

- Al-Qodah, Z., Al-Shannag, M., Bani-Melhem, K., Assirey, E., Alananbeh, K., Bouqellah, N. (2014b). Biodegradation of olive mills wastewater using thermophilic bacteria. *Desalination and Water Treatment*, In press (DOI: 10.1080/19443994.2014.954148).
- Al-Qodah, Z., Al-Bsoul, A., Assirey, E., Al-Shannag, M. (2014b). Combined ultrasonic irradiation and aerobic biodegradation treatment for olive mills wastewaters. *Environ. Eng. Manag. J.*, 8:2109-2118.
- Al-Malah, K., Azzam, M.O.J., Abu-Lail, N.I. (2000). Olive mills effluent (OME) wastewater post-treatment using activated clay. *Separ. Purif. Technol.*, 20:225-234.
- Annadurai, G., Juang, R.S., Lee, D.J. (2002). Factorial design analysis of adsorption of activated carbon on activated carbon incorporated with calcium alginate. *Adv. Environ. Res.*, 6:191-198.
- Annesini, M., Gironi, F. (1991). Olive oil mill effluent: ageing effects on evaporation behavior. *Water Res.*, 25:1157-1960.
- Balcioğlu, G., Gönder, Z.B. (2014). Recovery of baker's yeast wastewater with membrane processes for agricultural irrigation purpose: fouling characterization. *Chem. Eng. J.*, 255:630–640.
- Beltrán de Heredia, J., Garcia, J. (2005). Process integration: continuous anaerobic digestion - ozonation treatment of olive mill wastewater. *Ind. Eng. Chem. Res.*, 44:8750-8755.
- Box, G.E.P., Wilson, K.B.J. (1951). On the experimental attainment of optimum conditions. *J. R. Stat. Soc.*, B 13:1-45
- Caetano, M., Valderrama, C., Farran, A., Cortina, J.L. (2009). Phenol removal from aqueous solution by adsorption and ion exchange mechanisms onto polymeric resins. *J. Colloid Interface Sci.*, 338:402-409.
- Carmona, M., De Lucas, A., Valverde, J.L., Velasco, B., Rodriguez, J.F. (2006). Combined adsorption and ion exchange equilibrium of phenol on Amberlite IRA-420. *Chem. Eng. J.*, 117(2):155-160.
- Cassano, A., Conidi, C., Drioli, E. (2011). Comparison of the performance of UF membranes in olive mill wastewaters treatment. *Water Res.*, 45:3197-3204.
- Cegarra, J., Paredes, C., Roig, A., Bernal, M.P., García, D. (1996). Use of olive mill wastewater compost for crop production. *Int. Biodet. Biodegrad.*, 38(3-4):193-203.

Chen, J.P., Chua, M.L., Zhang, B. (2002). Effects of competitive ions, humic acid, and pH on removal of ammonium and phosphorous from the synthetic industrial effluent by ion exchange resins. *Waste Manag.*, 22:711–719.

Chen, H., Dai, G.L., Zhao, J., Zhong, A.G., Wu, J.Y., Yan, H. (2010). Removal of copper (II) ions by a biosorbent-Cinnamomum camphora leaves powder. *J. Hazard. Mater.* 177:228-236.

Comstock, S.E.H., Boyer, T.H. (2014). Combined magnetic ion exchange and cation exchange for removal of DOC and hardness. *Chem. Eng. J.*, 241:366-375.

Das, N. (2010). Recovery of precious metals through biosorption – a review. *Hydro-metallurgy*, 103:180-189.

De Caprariis, B., Di Rita, M., Stoller, M., Verdone, N., Chianese, A. (2012). Reaction-precipitation by a spinning disc reactor: Influence of hydrodynamics on nanoparticles production. *Chem. Eng. Sci.*, 76:73-80.

Demirbas, A., Pehlivan, E., Gode, F., Altun, T., Arslan, G. (2005). Adsorption of Cu(II), Zn(II), Ni(II), Pb(II) and Cd(II) from aqueous solution on Amberlite IR-120 synthetic resin. *J. Colloid and Interface Sci.*, 282:20-25.

Dhouib, A., Aloui, F., Hamad, N., Sayadi, S. (2006). Pilot-Plant treatment of olive mill wastewaters by phanerochaete chrysosporium coupled to anaerobic digestion and ultrafiltration. *Process Biochem.*, 41:159-167.

Elibol, M. (2002). Response surface methodological approach for inclusion of perfluorocarbon in actinorhodin fermentation medium. *Process Biochem.*, 38:667-673.

El-Naggar, I.M., El-Dessouky, M.E., Aly, H.F. (1996). Ion-exchange equilibrium of alkali metal/hydrogen ions on amorphous cerium (IV) antimonite. *React. Funct. Polym.*, 28:209-214.

Erdem, E., Colgecen, G., Donat, R. (2005). The removal of textile dyes by diatomite earth. *J. Colloid Interface Sci.*, 282:314–319.

European Commission. (1980). Council Directive 80/778/EEC of 15 July 1980 on the quality of water intended for human consumption.

European Commission. (1998). Council Directive 98/83/EC of 3 November 1998 on the quality of water intended for human consumption.

FAIR CT96–1420, Annex 2. Final report, Improlive, investments of treatment and validation of liquid–solid waste from the two phase olive oil extraction. www.nf2000.org/publications/q30011.pdf2000.

Fu, F., Wang, Q. (2011). Removal of heavy metal ions from wastewaters: a review. *J. Environ. Manage.*, 92:407-418.

Garcia-Castello, E., Cassano, A., Criscuoli, A., Conidi, C., Drioli, E. (2010). Recovery and concentration of polyphenols from olive mill wastewaters by integrated membrane system. *Water Res.*, 44:3883-3892.

Garrido Hoyos, S.E., Martínez Nieto, L., Camacho Rubio, F., Ramos Cormenzana, A. (2002). Kinetics of aerobic treatment of olive mill wastewater (OMW) with *Aspergillus terreus*. *Process Biochem.*, 37(10):1169-1176.

Greenberg, A.E., Clesceri, L.S., Eaton, A.D., 1992. Standard Methods for the Examination of Water and Wastewater, APHA/AWWA/WEF, 16th ed., Washington DC. Cabs.

Habuda-Stanic, M., Kalajdzic, B., Kuleš, M., Velic, N. (2008). Arsenite and arsenate sorption by hydrous ferric oxide/polymeric material. *Desalination*, 229:1–9.

Hodaifa, G., Ochando-Pulido, J.M., Ben-Driss-Alami, S., Rodriguez-Vives, S., Martinez-Ferez, A. (2013a). Kinetic and thermodynamic parameters of iron adsorption onto olive stones. *Ind. Crops Prod.*, 49:526-534.

Hodaifa, G., Ochando-Pulido, J.M., Rodriguez-Vives, S., Martinez-Ferez, A. (2013b) Optimization of continuous reactor at pilot scale for olive-oil mill wastewater treatment by Fenton-like process. *Chem. Eng. J.*, 220:117-124.

Keller, M. (2004). Iron removal by ion exchange: standing on solid ground. *Water Cond. Purif.*, 46(6):20-23.

Kestioğlu, K., Yonar, T., Azbar, N. (2005). Feasibility of physico-chemical treatment and advanced oxidation processes (AOPS) as a means of pre-treatment olive mill effluent (OME). *Process Biochem.* 40:2409-2416.

Krishnan, K.A., Anirudhan, T.S. (2003). Removal of cadmium (II) from aqueous solutions by steamactivated sulphurised carbon prepared from sugar-cane bagasse pith: Kinetics and equilibrium studies. *Water SA.*, 29(2):147-156.

Ku, Y., Lee, K., Wang, W. (2004). Removal of phenols form aqueous solutions by purolite A-

510 resin. *Sep. Sci. Technol.*, 39:911–923.

Lafi, W.K., Shannak, B., Al-Shannag, M., Al-Anber, Z., Al-Hasan, M. (2009). Treatment of olive mill wastewater by combined advanced oxidation and biodegradation. *Separ. Purif. Technol.*, 70(2):141-146.

Lafi, W.K., Al-Anber, M., Al-Anber, Z.A., Al-Shannag, M., Khalil, A. (2010). Coagulation and Advanced Oxidation Processes in the Treatment of Olive Mill Wastewater (OMW). *Desalin. Water Treat.*, 24:251-256.

Li, L., Liu, F., Jing, X., Ling, P., Li, A. (2011). Displacement mechanism of binary competitive adsorption for aqueous divalent metal ions onto a novel IDA-chelating resin: isotherm and kinetic modelling. *Water Res.* 45:1177-1188.

Martínez Nieto, L., Hodaifa, G., Rodríguez Vives, S., Giménez Casares, J.A., Ochando, J. (2011a). Flocculation–sedimentation combined with chemical oxidation process. *Clean - Soil, Air, Water*, 39(10):949-955.

Martínez Nieto, L., Hodaifa, G., Rodríguez, S., Giménez, J.A., Ochando, J. (2011b). Degradation of organic matter in olive oil mill wastewater through homogeneous Fenton-like reaction. *Chem. Eng. J.*, 173(2):503-510.

Niaounakis, M., Halvadakis, C.P. (2006). Olive processing waste management literature review and patent survey, 2nd ed., Elsevier: Waste Management Series 5:23-64.

Ochando-Pulido, J.M., Hodaifa, G., Rodríguez-Vives, S., Martínez-Ferez, A. (2012). Impacts of operating conditions on reverse osmosis performance of pretreated olive mill wastewater. *Water Res.*, 46(15):4621-4632.

Ostroski, I.C., Barros, M.A., Silva, E.A., Dantas, J.H., Arroyo, P.A., Lima, O.C. (2009). A comparative study for the ion exchange of Fe(III) and Zn(II) on zeolite NaY. *J. Hazard. Mater.*, 161:1404-1412.

Papadimitriou, E.K., Chatjipavlidis, I., Balis, C. (1997). Application of composting to olive mill wastewater treatment. *Environ. Technol.*, 18(1):10-107.

Papastefanakis, N., Mantzavinos, D., Katsaounis, A. (2010). DSA electrochemical treatment of olive mill wastewater on Ti/RuO₂ anode. *J. Appl. Electrochem.*, 40(4):729-737.

Paraskeva, P., Diamadopoulos, E. (2006). Technologies for olive mill wastewater (OMW) treatment: A review. *J. Chem. Technol. Biotechnol.*, 81:475-1485.

- Pivovarov, S. (2008) Adsorption of ions onto amorphous silica: Ion exchange model. *J. Colloid Interface Sci.*, 319:374-376.
- Ravikumar, K., Deebika, B., Balu, K. (2005). Decolourization of aqueous dye solutions by a novel adsorbent: Application of statistical designs and surface plots for the optimization and regression analysis. *J. Hazard. Mater.*, 122(1-2):75-83.
- Rengaraj, S., Moon, S.H. (2002). Kinetic of Adsorption of Co (II) Removal from Water and Wastewater by Ion Exchange Resins. *Water Res.*, 36(7):1783-1793.
- Rizzo, L., Lofrano, G., Grassi, M., Belgiorno, V. (2008). Pretreatment of olive mill wastewater by chitosan coagulation and advanced oxidation processes. *Separ. Purif. Technol.*, 63(3):648-653.
- Roostaei, N., Tezel, F.H. (2004). Removal of phenol from aqueous solutions by adsorption. *J. Environ. Manag.*, 70:157–164.
- Sarika, R., Kalogerakis, N., Mantzavinos, D. (2005). Treatment of olive mill effluents. Part II. Complete removal of solids by direct flocculation with poly-electrolytes. *Environ. Int.*, 31:297-304.
- Sen Gupta, S., Bhattacharyya, K.G. (2011). Kinetics of adsorption of metal ions on inorganic materials: a review. *Adv. Colloid Interface Sci.*, 162:39-58.
- Senthil Kumar, P., Gayathri, R. (2009). Adsorption of Pb²⁺ ions from aqueous solutions onto bael tree leaf powder: isotherms, kinetics and thermodynamics study. *J. Eng. Sci. Technol.*, 4(4):381–399.
- Tahir, S.S., Rauf, N. (2004). Removal of Fe²⁺ from the waste water of a galvanized pipe manufacturing industry by adsorption onto bentonite clay. *J. Environ. Manage.*, 73:285-292.
- Tezcan Ün, Ü., Altay, U., Koparal, A.S., Ogutveren, U.B. (2008). Complete treatment of olive mill wastewaters by electrooxidation. *Chem. Eng. J.*, 139:445-452.
- Vaaramaa, K., Lehto, J. (2003). Removal of metals and anions from drinking water by ion exchange. *Desalination*, 155:157-170.
- Victor-Ortega, M.D., Ochando-Pulido, J.M., Hodaifa, G., Martínez-Ferez, A. (2014a). Ion exchange as an efficient pretreatment system for reduction of membrane fouling in the purification of model OMW. *Desalination*, 343:198-207.

Víctor-Ortega, M.D., Ochando-Pulido, J.M., Hodaifa, G., Martínez-Férez, A. (2014b). Final purification of synthetic olive oil mill wastewater treated by chemical oxidation using ion exchange: Study of operating parameters. *Chem. Eng. Process.*, 85:241-247.

Víctor-Ortega, M.D., Ochando-Pulido, J.M., Martínez-Férez, A. (2015). Impacts of integrated strong-acid cation exchange and weak-base anion exchange process for successful removal of saline toxicity from model olive mill wastewater. *Ecol. Eng.*, 77:18-25.

Yu, L.J., Shukla, S.S., Dorris, K.L., Shukla, A., Margrave, J.L. (2003). Adsorption of chromium from aqueous solutions by maple sawdust. *J. Hazard. Mater.*, 100:53-63.

Zhu, L., Deng, Y., Zhang, J., Chen, J. (2011). Adsorption of phenol from water by N butylimidazolium functionalized strongly basic anion exchange resin. *J. Colloid. Interface Sci.*, 364:462-468.

CHAPTER 13

COMPARISON AND OPTIMIZATION OF DIFFERENT ION EXCHANGE RESINS COMBINATIONS FOR FINAL TREATMENT OF OLIVE MILL EFFLUENT

María Dolores Víctor-Ortega^{1*}, Javier Miguel Ochando-Pulido¹, Antonio Martínez-Ferez¹

¹ Chemical Engineering Department, University of Granada, 18071 Granada, Spain

*email: mdvictor@ugr.es

Submitted for publication:

Desalination

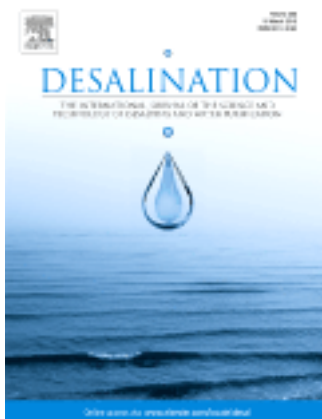
Publisher: ELSEVIER SCIENCE BV. PO BOX 211, 1000 AE AMSTERDAM, NETHERLANDS

Year: 2015

ISSN: 0011-9164

Impact factor: 3.756

Tertile: First



Abstract

The final purification of two-phase olive mill wastewater (OMW-2), a highly polluted effluent by-produced in olive oil factories, was investigated through four ion exchange resins (a weak-acid cation exchange resin, a strong-acid cation exchange resin, a weak-base anion exchange resin and a strong-base anion exchange resin). Central composite design was used for the optimization of the IE processes. Results revealed that the only final treated OMW-2ST effluent fulfilling the legislated requirements for drinking water was the one from the combination of the strong-acid cation exchange resin and the weak-base anion exchange resin. The proposed IE process yielded up to 88 % removal of these pollutants when the initial pH, operating temperature and flow rate were set to 5.1, 26.8 °C and 12.1 L h⁻¹, respectively. Under these conditions, the achieved concentrations for all contaminants in the final stream were maintained below the maximum established limits. Moreover, it is important to highlight the possibility of working efficiently at low temperature conditions, which enhances the cost-efficiency of the IE process. Finally, high treated effluent volume recovery (28 L) could be achieved in continuous mode under the optimal operating conditions found, complying with standards for reuse in the production process.

Keywords: Experimental design; Ion Exchange resins; Olive mill wastewater; Optimization; Pollutants.

13.1 Introduction

Nowadays, water resources are becoming insufficient in order to satisfy the increasing demand of water worldwide. Water scarcity specially concerns agricultural irrigation, which represents the largest demand of fresh water worldwide, that is, more than 70% of the total water consumption (FAO, 2003). However, the possibility of using regenerated wastewater for irrigation purposes would solve this problem and bring very positive environmental and economic impacts.

In this regard, olive oil industry, which is currently one of the main agro-industrial activities in the Mediterranean Basin countries, generates one of the most highly polluted agro-industrial effluents known nowadays: olive mill wastewater (OMW). This effluent is mainly characterized by high organic carbon content, particularly phenols and polyphenols, which are highly polluting. OMW disposal into the environment causes severe deteriorations such as colouring of natural waters, serious threat to the aquatic life, pollution in surface and ground waters, alterations in soil quality, phytotoxicity and odour nuisance (Dhouib et al., 2006; Kestioğlu et al., 2005).

An average-sized modern olive oil factory currently generates 10-15 m³ of OMW daily. Only in Spain, the main olive oil producer worldwide, with more than 1,700 olive oil factories, this raises a total volume of more than 9 million m³ of OMW per year, which represents a huge amount of this highly contaminant effluents. Furthermore, olive oil production is steadily growing worldwide and it is now an emergent agro-food industry in China and several other countries such as the USA, Australia and the Middle East. Hence, the treatment of OMW is becoming a task of global concern.

Chemical remediation strategies are thereafter required for the depuration of this wastewater (De Caprariis et al., 2012; Martínez Nieto et al., 2011a; Niaounakis and Halvadakis, 2006; Paraskeva and Diamadopoulos, 2006; Sacco et al., 2012). In former works, a treatment process based on Fenton's reaction was optimized with the aim of removing the organic and phenolic pollutants of OMW-2. The treatment process comprises natural precipitation to remove coarse particles followed by Fenton-like advanced oxidation, flocculation–sedimentation and filtration through olive stones in series (secondary treatment, ST) (Martínez Nieto et al., 2010, 2011a,b). However, high levels of monovalent ions, mainly sodium and chloride, as well as iron, are found in OMW-2ST, derived from the dosage of the catalyst and neutralizing agents during the secondary treatment (Martínez Nieto et al., 2011b; Hodaifa et al., 2013b). In addition, a significant phenols amount above maximum legislated standard level (0.005 mg L⁻¹) (European Commission, 1980) was present in this secondary-treated OMW-2ST effluent, and iron concentration exceeded the maximum standard levels allowed by the European legislation for drinking water (0.2 mg L⁻¹) (European Commission, 1998).

On the other hand, the measured electroconductivity (EC) values in the effluent at the outlet of the secondary treatment are well above the range 2–3mS cm⁻¹, thus presenting hazardous salinity levels according to the standards established by the Food and Agricultural Association (FAO) with the goal of reusing the regenerated water for irrigation purposes (Sancho Cierva, 2000).

Therefore, a tertiary treatment is necessary for final purification of OMW-2ST. With this regard, membrane technology has been employed in the last decades for final treatment of this effluent (Ochando-Pulido et al., 2012a; Ochando-Pulido et al., 2012b; Ochando-Pulido et al., 2013a; Ochando-Pulido et al., 2013b). However, membrane fouling plays an important role in the industrial scale-up of this broad applied technology, and this drawback is especially relevant in the case of wastewater purification processes (Ochando-Pulido et al., 2012a; Stoller et al., 2013a,b).

On the other side, novel IE resins developed over the past few decades have promoted this

technology as a suitable separation and purification process for wastewater treatment (Demirbas et al., 2005; Fu and Wang, 2011; Comstock and Boyer, 2014). In this sense, IE is considered a green and simple technology, capable of achieving high removal efficiencies and selectivity (Demirbas et al., 2005; Fu and Wang, 2011). There are various studies focused on the use of IE resins for the elimination of sodium and chloride ions in aqueous media (El-Naggar et al., 1996; Pivovarov, 2008; Víctor-Ortega, 2015a). Also, several research works have been described in the literature for the removal of iron and phenolic species by means of IE technology (Abhuri, 2003; Caetano et al., 2009; Carmona et al., 2006; Keller, 2004; Ku et al., 2004; Ostroski et al., 2009; Tahir and Rauf, 2004; Vaaramaa and Lehto, 2003).

In this research study, the final purification of OMW-2ST is addressed through different combinations of four IE resins selected on the basis of their different properties: a weak-acid cation exchange resin, a strong-acid cation exchange resin, a weak-base anion exchange resin and a strong-base anion exchange resin. The main objective was the optimization of the final purification of OMW-2 by means of the different IE systems comprising two of these resins in serial connection (one cationic and one anionic).

Firstly, recirculation mode experiments were carried out to examine the impacts of the main operating parameters on the IE process performance - operating temperature, initial pH and flow rate - as well as the interactions among them. For this purpose, the IE processes based on the different IE resins were modelled by means of central composite design (CCD).

Subsequently, continuous experiments were performed under the optimum operating conditions formerly found for each pair of resins in order to find the best IE resins combination for its application in the purification of OMW-2ST at industrial scale. Finally, water quality standards for reusing the purified olive mill effluent in the olive oil production process and thus reducing the environmental impact were checked.

13.2 Experimental section

13.2.1 Materials

In the present work, samples of OMW were taken from olive oil mills located in the South of Spain, which operate with the modern two-phase olive oil extraction procedure. Firstly, these samples were conducted to the secondary treatment thoroughly described in previous works by the Authors (Martínez Nieto et al., 2011b; Hodaifa et al., 2013b; Ochando-Pulido et al., 2012b). The effluent after the secondary treatment, hereafter referred as OMW-2ST, was the feed stream to the final IE purification process. Chemical oxygen demand (COD), total phenolic compounds (TPh), sodium, chloride, total iron, electroconductivity (EC) and pH were measured in the outlet

stream samples of the secondary treatment as well as of the IE system, following standard methods (Greenberg et al., 1992). The physicochemical composition of the OMW-2ST samples is reported in Table 13.1.

Weak-acid and strong-acid cationic resins as well as weak-base and strong-base anionic resins Amberlite IRA-67 resins (Dowex MAC 3, Dowex Marathon C, Amberlite IRA-67 and Amberlyst A26, respectively) all of them provided by Sigma Aldrich, were used in this work in order to cover all kinds of IE resins. Dowex MAC 3 was conditioned in sulfuric acid while Dowex Marathon C was conditioned in hydrochloric acid solution. Then, both resins were washed with water before being used in the IE experiments. On the other hand, Amberlite IRA-67 and Amberlyst A26 resins were treated with sodium hydroxide solution and then were washed with water following the advice of the resin manufacturer. Typical physical and chemical characteristics of the used resins are described in Table 13.2.

Table 13.1. Physicochemical characterization of OMW-2ST.

Factor	Value
pH	6.82 ± 0.55
Conductivity, mS cm⁻¹	4.35 ± 0.30
COD, mg L⁻¹	162.0 ± 1.2
Total phenolic compounds, mg L⁻¹	0.012 ± 0.001
[Cl⁻], mg L⁻¹	1250 ± 3
[Na⁺], mg L⁻¹	870 ± 5
[Total iron], mg L⁻¹	0.9 ± 0.1

Table 13.2. Physicochemical properties of selected IE resins (from manufacturer specifications).

IE Resin	DOWEX MAC 3	DOWEX MARATHON C	AMBERLITE IRA-67	AMBERLYST A 26
Resin type	Weak acid-cation	Strong-acid cation	Weak-base anion	Strong-base anion
Matrix	Polyacrylic, macroporous	Styrene-DVB, gel	Crosslinked acrylic gel	Styrene- divinylbenzene
Functional group	Carboxylic acid	Sulfonic acid	Tertiary amine	Quaternary ammonium
Ionic form as shipped	H ⁺ form	H ⁺ form	OH ⁻ form	OH ⁻ form
Ion Exchange capacity^a, eq L⁻¹	3.8	1.80	1.60	0.80
Water content, %	44-52	50-56	56-64	66-75
Shipping density, g L⁻¹	750	800	700	675

^a Ion exchange capacity is the minimum wet capacity as specified by the manufacturer.

13.2.2 Ion exchange equipment

Figure 13. 1 shows the flow diagram of the proposed IE process. A bench-scale IE equipment was used to evaluate the performance of the combination of two IE columns operating in serial connection for the purification of OMW-2ST. The IE columns employed in this study were made of an acrylic tube with dimensions 540 mm height x 46 mm internal diameter. The columns are provided with a mobile upper retaining grid, which could be fixed in the column to adjust it as a fixed bed or a semi-fluidized bed. The IE device (MionTec) was equipped with a peristaltic pump (Ecoline VC-380) and a temperature-controlled thermostatic bath (Precisterm JP Selecta).

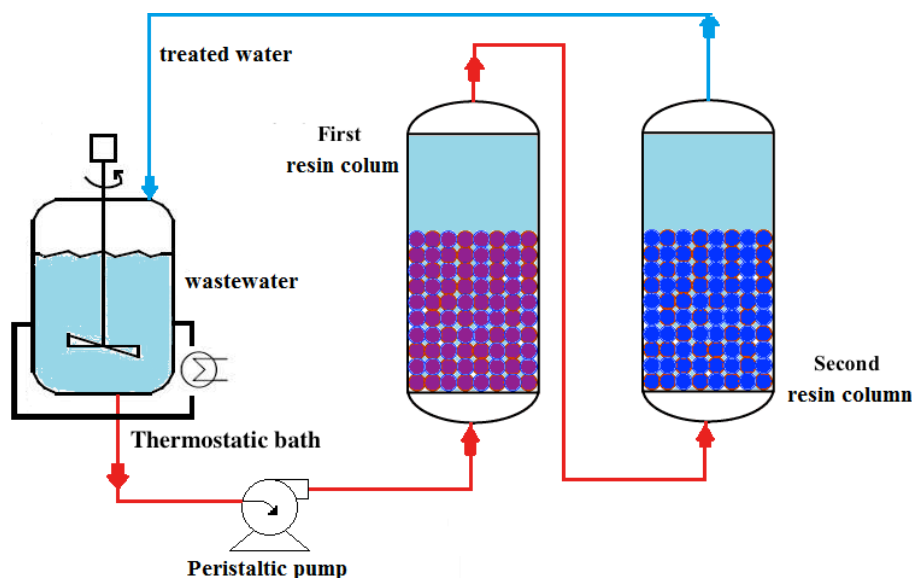


Figure 13.1. Flow-sheet scheme for IE recirculation operating experiments.

13.2.3 Recirculation IE experiments

In IE experiments in recirculation mode, the flask containing the 2 L feed solution was magnetically stirred continuously during the whole course of the experiments. The contact time was varied from 0 to 60 minutes. The initial pH, operating temperature and flow rate ranges studied are reported in Table 13.3. Each experiment was carried out twice to check the reproducibility of the results.

The IE removal efficiencies of sodium, chloride, iron and phenolic compounds from OMW-2ST were addressed during IE experiments in recirculation mode by calculating the percent of removal efficiency of the contaminant species was defined as follows:

$$\% \text{ Removal efficiency} = \frac{C_i - C_f}{C_i} \times 100 \quad (1)$$

where C_i and C_f are the initial and final species' concentration (mg L^{-1}), respectively.

Table 13.3. Values range of the factors used in the experimental design.

Independent variable	Range
Initial pH	3 - 8
Operating temperature, °C	10 - 50
Flow rate, L h^{-1}	5 - 20

13.2.4 Experimental design and optimization of IE operating parameters

In this work, the impacts of the main operating variables on the IE removal of chloride, sodium, phenols and iron ions in OMW-2ST was examined by means of experimental design for all the possible IE resins combinations. The proposed IE processes was modelled by means of CCD.

The application of experimental design techniques in IE process development can result in improved product yields, reduced process variability, closer confirmation of the output response to the nominal and target requirements and reduced development time and overall costs (Annadurai et al., 2002). The first step when performing experimental design involves the selection of the experimental outcome to be optimized. The experimental outcome is normally the value for a certain property or a mathematical combination of several of them that represents a realistic measure of the process performance; this is commonly referred to as the Response Function (RF).

The initial pH, operating temperature and flow rate were selected as independent variables, and the global percentage of the pollutant species removed as RF. The assayed ranges for the selected variables were equal to 10-50 °C for the operating temperature, 3.0-7.0 for the initial pH and 5-20 L h⁻¹ for the flow rate, on the basis of previous studies carried out by the Authors with synthetic OMW-2ST (V́ctor-Ortega et al., 2014a; V́ctor-Ortega et al.; 2014b). A CCD was used in order to calculate simultaneously the effect of the change in each one of these variables and also their possible interactions. Five levels were considered for each variable and three central samples were also included, which gives rise to a total of 17 experiments. The actual operating conditions for each experiment of the four optimization studies (one per each pair of resins) are given in Table 13.5.

The average value of the mean removal efficiencies for sodium, chloride, iron, phenols and organic pollutants (COD) was selected as RF, which represents the overall IE removal efficiency in a realistic way.

This design is rotatable, and therefore the precision in the calculation of the response is uniform over the whole experimental field. The optimization of the model was made with The Unscrambler software package (v. 9.8, Camo AS, Oslo, Norway), and the results were interpreted with the RSM.

Table 13.5. CCD matrix for the IE process optimization.

Experiment	T (°C)	pH₀	Q (L h⁻¹)
Exp 1	9.8	5.5	12.6
Exp 2	50.2	5.5	12.6
Exp 3	30.0	3.0	12.6
Exp 4	30.0	8.0	5.1
Exp 5	30.0	5.5	5.1
Exp 6	30.0	5.5	20.0
Exp 7	18.0	4.0	8.1
Exp 8	42.0	4.0	8.1
Exp 9	18.0	7.0	8.1
Exp 10	42.0	7.0	8.1
Exp 11	18.0	4.0	17.0
Exp 12	42.0	4.0	17.0
Exp 13	18.0	7.0	17.0
Exp 14	42.0	4.0	17.0
Exp 15	30.0	5.5	12.6
Exp 16	30.0	5.5	12.6
Exp 17	30.0	5.5	12.6

13.2.5 Analytical procedures

Sodium concentration values were determined by using a Crison GLP 31 Sodium Ion-Selective Electrode 96 50, with autocorrection of temperature. To this end, 0.01, 0.1 and 1.0 g L⁻¹ Na⁺

standard solutions were prepared in the laboratory to calibrate the electrode. Chloride concentration values were assessed by a Crison GLP 31 Chloride Ion-Selective Electrode 96 52 C, with autocorrection of temperature. For this purpose, 0.01, 0.1 and 1.0 g L⁻¹ Cl⁻ standard solutions required for the electrode calibration were also prepared in the laboratory.

For the measurement of the total iron concentration, all iron ions were reduced to iron ions (II) in a thioglycolate medium with a derivative of triazine, forming a reddish-purple complex that was determined photometrically at 565 nm (Standard German methods ISO 8466-1 and German DIN 38402 A51) (Greenberg et al., 1992).

Total phenols and phenol derivatives were analyzed by reaction with a derivative thiazol, giving a purple azo dye, which was determined photometrically using a Helios Gamma UV-visible spectrophotometer (Thermo Fisher Scientific) at 475 nm (Standard German methods ISO 8466-1 and DIN 38402 A51) (Greenberg et al., 1992).

EC and pH measurements were evaluated with a Crison GLP31 conductivity-meter and a Crison GLP21 pH-meter, provided with autocorrection of temperature. Buffer standard solutions for EC (1,413 μ S cm⁻¹ and 12.88 mS cm⁻¹) and pH (pH 4.01, 7.00 and 9.21) measurements respectively were supplied as well by Crison.

Analytical grade reagents and chemicals with purity over 99 % were used for the analytical procedures, applied at least in triplicate.

13.3 Results and discussion

13.3.1 Resins disposition studies

First of all, the effect of resins disposition on the performance of the proposed IE process was investigated for each pair of resins (sections from 13.3.1.1 to 13.3.1.4). The possible resins combinations are reported in Table 13.4.

Table 13.4. Different combinations of the studied IE resins.

Resins	Strong acid cationic (Dowex Marathon C)	Weak acid cationic (Dowex MAC 3)
Weak base anionic (Amberlite IRA-67)	Combination 1	Combination 4
Strong base anionic (Amberlyst A26)	Combination 2	Combination 3

13.3.1.1 Resins combination 1: Strong-acid cation exchange resin and weak-base anion exchange resin

Figure 13.2 shows the pollutants removal efficiencies as a function of contact time and for both cation exchange resin and weak-base anion exchange resin dispositions.

The impact of the resins disposition on the IE system performance was studied by carrying out recirculation mode experiments at fixed operating conditions (25 °C and 10 L h⁻¹ for 60 min) to ensure equilibrium was achieved (V́ctor-Ortega et al., 2014a; V́ctor-Ortega et al., 2014b).

These results confirm the cation exchange resin column followed by the anion exchange one as the optimal arrangement of the selected resins. This outcome is supported by the fact that the cationic resin is active in the whole pH range whereas the anionic one is only active in the range 0–7 (Table 13.1). In that way, as the OMW-2ST stream passed through the cation exchange resin, the pH decreased due to protons release (pH below 2) and thus the anions uptake is favoured in the anionic column. OH⁻ are liberated in this latter column, thus equilibrating the pH value of the IE system output.

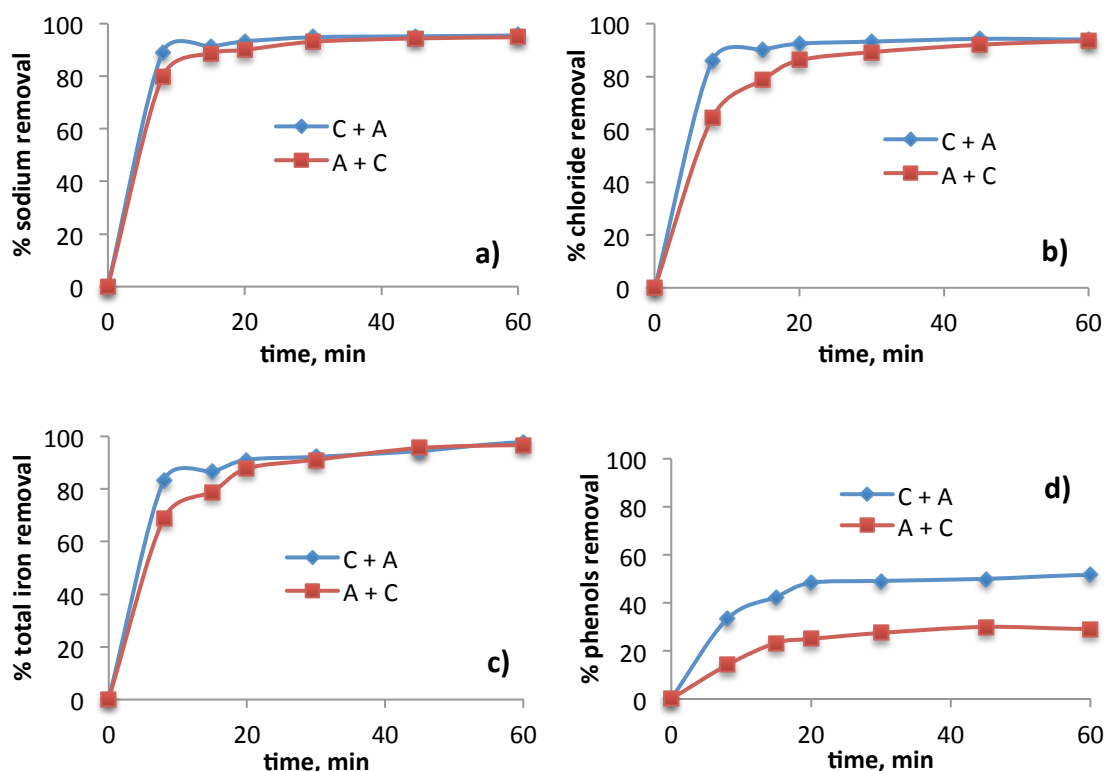


Figure 13.2. Effect of resins disposition (A + C: cationic resin + anionic resin; A + C: anionic resin + cationic resin) on a) sodium, b) chloride, c) total iron, and d) phenols IE removal efficiencies as a function of recirculation time. Operating conditions: 25 °C and 10 L h⁻¹.

Cationic resin: Dowex Marathon C; Anionic resin: Amberlite IRA-67.

13.3.1.2 Resins combination 2: Strong-acid cation exchange resin and strong-base anion exchange resin

Secondly, it was investigated the effect of resins disposition on sodium, chloride, total iron and phenols removal efficiencies through the strong-acid cationic and the strong-base anionic resins.

As it can be observed in Figure 13.3, there were no differences between using the cationic resin followed by the anionic one and the opposite order for sodium and chloride removal efficiencies. In this case, removal efficiencies were higher than 90 % since the first operating minutes.

However, it is important to highlight that in case of total iron removal, equilibrium was achieved in a shorter time when using the cationic resin followed by the anionic one. This fact can be explained taking into account the optimum pH value for total iron removal by means of Dowex Marathon C, which was found to be 4 in previous studies (V́ctor-Ortega et al., 2015b). In this sense, when OMW-2ST is driven firstly through the anionic resin, the pH increases due to chloride and phenols uptake and OH⁻ release (pH above 10) during the first minutes, which hinders total iron removal. Then, the pH value decreases as the solution passes through the cationic resin. However, if OMW-2ST passes firstly through the cationic resin, the pH solution decreases as the sodium ions are replaced by H⁺ which facilitates total iron removal at the same time.

The opposite trend was observed for phenols removal efficiency. In this case, when using the cationic resin in first place pH value decreases (pH values below 2). However, phenols removal through Amberlyst A26 resin is favoured at pH values higher than 7 (V́ctor-Ortega et al., 2015c), thus phenol removal efficiencies would be extremely low during the first operating minutes. On the contrary, if OMW-2ST passes firstly through the anionic resin, the pH value increases as chloride ions are replaced by OH⁻ and, as a result, phenols removal efficiency is highly enhanced since the first operating minutes.

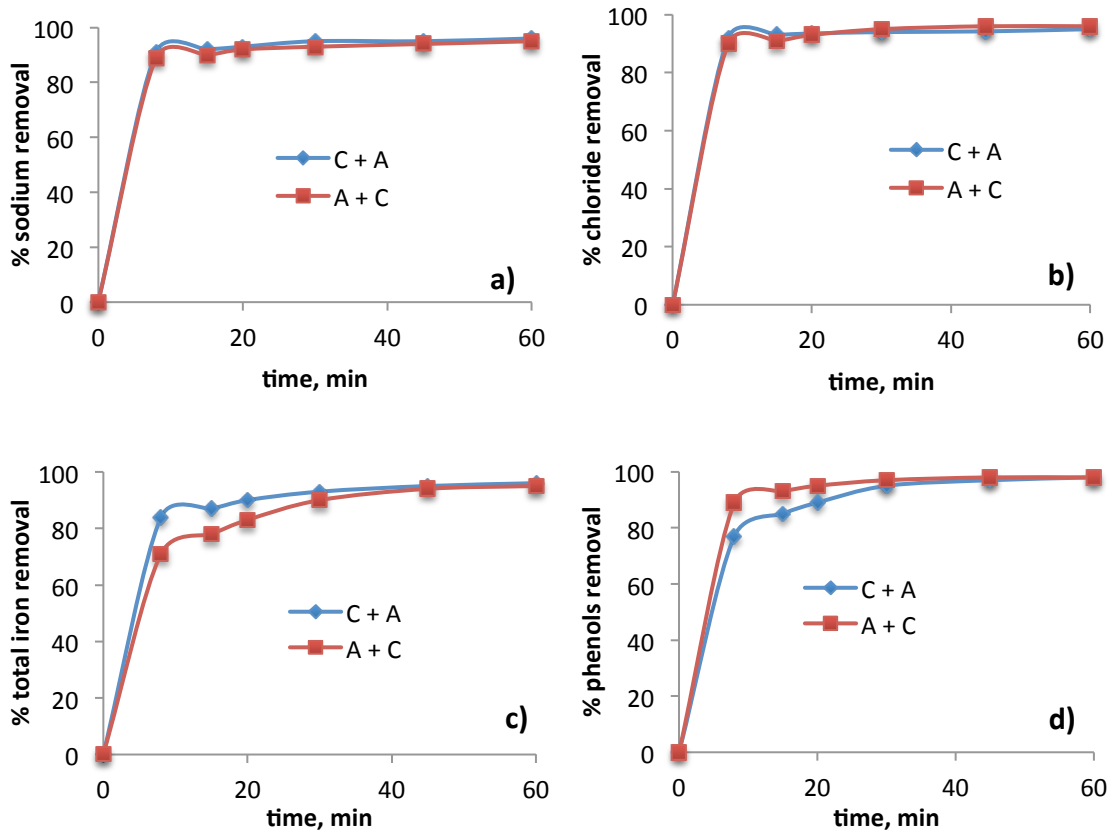


Figure 13.3. Effect of resins disposition (A + C: cationic resin + anionic resin; A + C: anionic resin + cationic resin) on a) sodium, b) chloride, c) total iron, and d) phenols IE removal efficiencies as a function of recirculation time. Operating conditions: 25 °C and 10 L h⁻¹.

Cationic resin: Dowex Marathon C; Anionic resin: Amberlyst A26.

To sum up, as the mentioned effect was more pronounced in the case of total iron removal, using the cationic resin followed by the anionic one was selected as the best resins disposition for these resins.

13.3.1.3 Resins combination 3: Weak-acid cation exchange resin and strong-base anion exchange resin

In this case, the highest sodium removal efficiencies were obtained setting the anionic resin followed by the cationic one (see Figure 13.4). This can be explained since the weak-acid cation exchange resin used in this study (Dowex MAC 3) is active in the range 5-14. Therefore, as the solution passes through the anionic resin, the effluent pH increases due to OH⁻ ions release, reaching optimal pH conditions for sodium removal.

On the other hand, the opposite trend was observed for total iron removal through weak-acid Dowex MAC 3 resin, but this effect was less pronounced than for sodium removal.

Regarding chloride and phenols removal efficiencies, there were no significant differences between using the cationic resin or the anionic one in first place.

Therefore, considering all these above results, using the strong-base anionic resin followed by the weak-acid cationic one was selected as the most suitable resins disposition, given that the removal of sodium, which is present in the OMW-2ST effluent in very high concentration, was enhanced with this IE process configuration.

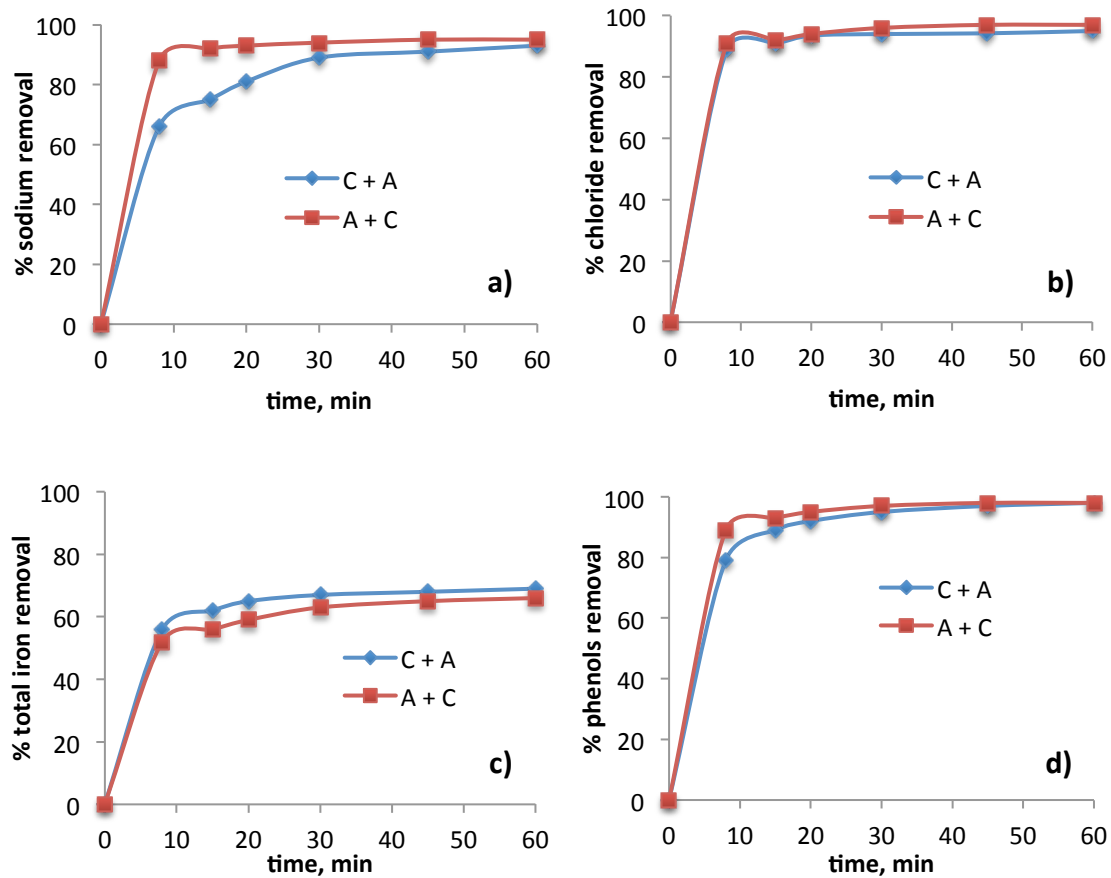


Figure 13.4. Effect of resins disposition (A + C: cationic resin + anionic resin; A + C: anionic resin + cationic resin) on a) sodium, b) chloride, c) total iron, and d) phenols IE removal efficiencies as a function of recirculation time. Operating conditions: 25 °C and 10 L h⁻¹.

Cationic resin: Dowex MAC 3; Anionic resin: Amberlyst A26.

13.3.1.4 Resins combination 4: Weak-acid cation exchange resin and weak-base anion exchange resin

Finally, the effect of resins disposition on sodium, chloride, total iron and phenols removal efficiencies by using the weak-acid cationic and the weak-base anionic resins was addressed.

Results from Figure 13.5a confirmed that higher sodium removal efficiencies were obtained

when the anionic resin was employed before the cationic one during the whole recirculation time. Although this effect was sharper during the first operating minutes, sodium removal efficiencies were still higher for the first resin disposition when the IE equilibrium was reached (80 % vs. 76 %).

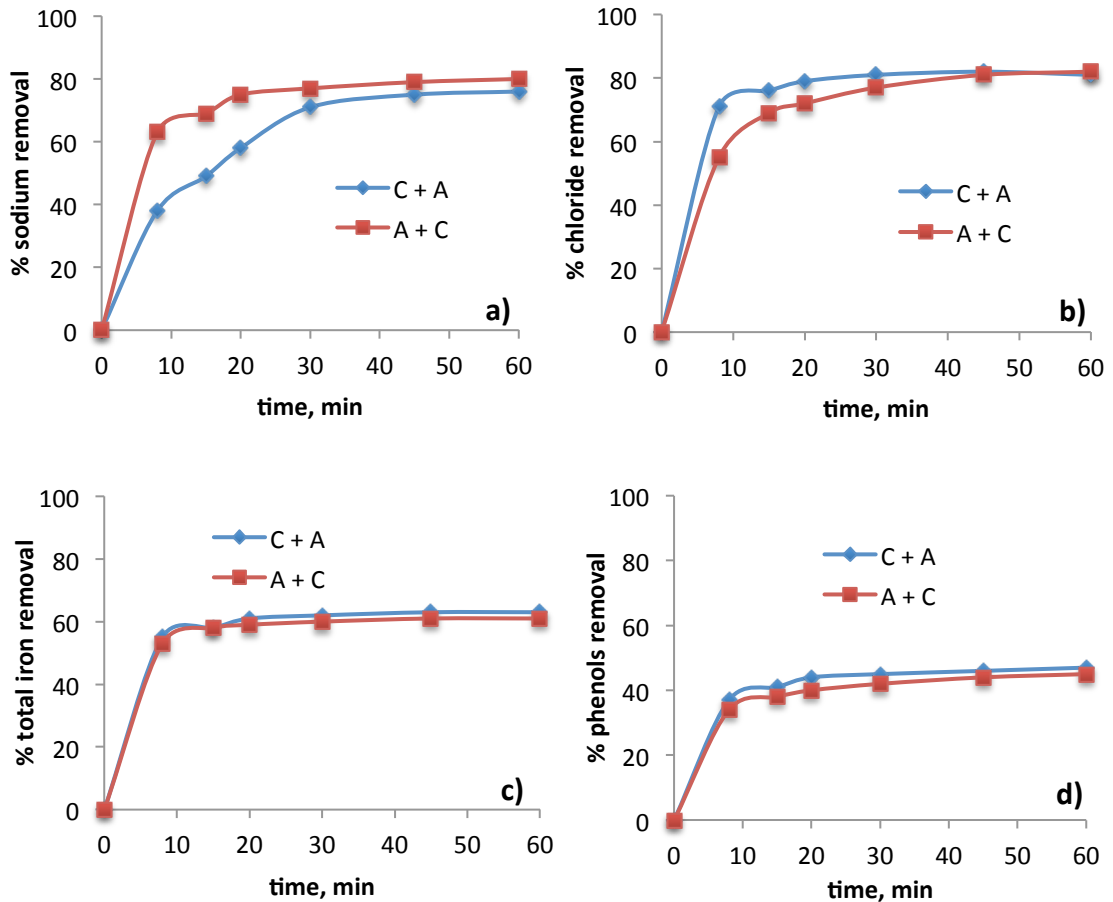


Figure 13.5. Effect of resins disposition (A + C: cationic resin + anionic resin; A + C: anionic resin + cationic resin) on a) sodium, b) chloride, c) total iron, and d) phenols IE removal efficiencies as a function of recirculation time. Operating conditions: 25 °C and 10 L h⁻¹.

Cationic resin: Dowex MAC 3; Anionic resin: Amberlite IRA-67.

On the other side, Figure 13.5b shows that even though chloride removal efficiencies were the highest when using the cationic resin followed by the anionic one during the first operating minutes, they were similar at the equilibrium point (around 80 %).

Otherwise, there were no significant differences between using both resins disposition for total iron and phenols removal efficiencies (Figure 13.5c and Figure 13.5d, respectively). In this sense, maximum total iron removal efficiencies were about 60 % while phenols removal efficiencies were lower than 45 %, disregarding the configuration set. It is worth highlighting that the removal efficiencies attained for total iron and phenols were the lowest achieved in

comparison with the rest of resins combinations.

Based on these results, using the weak-base anionic resin followed by the weak-acid cationic one was chosen as the best resins configuration.

To sum up, it is worthy to underline that the use of the strong-acid cationic and the strong-base anionic resins allowed achieving the highest removal efficiencies for all the studied pollutants for both possible resins disposition, whereas the lowest removal efficiencies were yielded by the weak-acid cationic and the weak-base anionic resin configuration.

13.3.2 IE process optimization

The study of the effect of the main operating parameters - initial pH, temperature and flow rate - on the IE processes efficiency with the different resins selected was carried out by means of experimental design. The objective of this optimization was to investigate the set of values for the operating conditions that maximize the performance of each IE process for OMW-2ST final purification. The initial pH (pH_0) range studied was varied between 3 and 8, whilst the temperature was fixed between 10 °C and 50 °C. On the other hand, the flow rate was varied from 5 to 20 L h⁻¹. Namely, a CCD, which involves a total of 17 experiments for each couple of resins was employed (see Table 13.5).

The maximum value of RF (% global removal) in the obtained surfaces and the optimum values of the process variables are reported in Table 13.6. Results from the optimization studies confirmed that the highest global removal efficiencies (close to 90 %) were obtained for Combination 1 and Combination 2, that is, strong-acid cation exchange resin and weak-base anion exchange resin or strong-acid cation exchange resin and strong-base anion exchange resin.

On the other hand, the resins combination which achieved the lowest global removal efficiencies was found to be the one consisting of the weak-base anionic and the weak-acid cationic resins (Combination 4). In this case, global removal efficiency was below 60 %, which would lead to pollutants concentrations higher than the maximum established limits for its reuse in the process. Therefore, this resins combination was completely discarded.

Table 13.6. Optimum parameters values for maximum IE process efficiency.

Factor	T (°C)	pH ₀	Q (L h ⁻¹)	Predicted max. % global removal	Multiple Correlation (R)	R-Square (R ²)
Combination 1	26.80	5.14	12.12	88.03	0.987	0.975
Combination 2	20.6	4.15	13.83	89.1	0.971	0.943
Combination 3	31.2	4.1	7.6	75.3	0.977	0.955
Combination 4	28.8	6.6	5.9	57.2	0.954	0.910

* Combination 1: Dowex Marathon C + Amberlite IRA-67; Combination 2: Dowex Marathon C + Amberlyst A 26; Amberlyst A-26 + Dowex MAC 3; Dowex MAC 3 + Amberlite IRA-67.

Furthermore, although Combination 3 (strong-base anionic and weak-acid cationic resins) allowed fulfilling legislated standards levels for all the studied contaminants, this option was finally discarded on the basis that the optimal operating temperature was found to be 31.2 °C. Therefore, it would be necessary to heat during IE process in order to achieve optimal pollutants removal efficiencies, which would mean energy consumption and hence an increase of the operating costs.

Otherwise, optimal flow rates lower than 15 L h⁻¹ were found for all the resins combinations. It is known that the required time to reach equilibrium decreased with increasing the flow rate. Chen et al. found that at higher flow rate fixed the stream does not have enough time to contact/react with the ion exchange resins because of too low residence times (Chen et al., 2002). It is worthy to point out that as the strength of the acid or base of the resins increased, the optimal flow rate increased too.

13.3.3 Continuous IE processes

Finally, continuous IE experiments were carried out under the optimal operating conditions for each resins combination. The main objective was to evaluate the performance of the proposed IE processes for the final purification of OMW-2ST at industrial scale.

A comparison between the maximum legislated standard values for drinking water production and the final treated effluents after the proposed integral processes is reported in Table 13.7.

The only final treated OMW-2ST effluent fulfilling the legislated requirements for drinking water (European Commission, 1980; European Commission, 1998) was found to be the one exiting the combination of the strong-acid cation exchange resin (Dowex Marathon C) and the weak-base anion exchange resin (Amberlite IRA-67). In this case, a final OMW-2ST effluent treated volume up to 28 L could be achieved, for 140 min IE operating time. Chloride, sodium, total iron and phenols concentrations stood below the maximum levels established by the legislation in the IE outlet stream. This fact allows the successful reutilization of the final treated effluent in the olives washing machines and finally closing the loop, thus rendering the production process cost-effective and environmentally respectful.

Moreover, these resins work highly efficiently at ambient temperature conditions, hence giving a sensible economical boost to the IE process, since the operating temperature is a key variable from a technical–economical point of view.

It is important to underline that resins combination number 2 (strong-acid cationic resin and strong-base anionic resin) allows treating the highest OMW-2ST volume before overcoming standard limits for all the studied pollutants. However, in this case conductivity was above the maximum levels due to the high OH^- ions release. Moreover, although pollutants concentrations were lower than maximum limits, $\text{EC} > 1 \text{ mS cm}^{-1}$ and pH higher than maximum and lower than minimum values were found for combination 3 and combination 4, respectively.

Finally, results suggest that the proposed IE process (resins combination 1) may replace membrane technology for the final purification of two-phase olive mill wastewater, which implies higher operating costs as high pressures are needed to achieve similar removal efficiencies (Ochando-Pulido et al., 2012b; Cassano et al., 2011).

Table 13.7. Comparison between the initial and final values of OMW-2ST and the legislated values of drinking water.

Stream	[Na ⁺] (mg L ⁻¹)	[Cl ⁻] (mg L ⁻¹)	[Fe _T] (mg L ⁻¹)	[Ph] (mg L ⁻¹)	COD (mg L ⁻¹)	EC, mS cm ⁻¹ ,	pH	volume (L)	time (min)
^a OMW-2ST ₀	870	1250	0.9	0.012	162			-	-
^b OMW-2ST _{f,1}	161.8	247.3	0.08	0.004	4.8	0.792	7.68	28	140
^b OMW-2ST _{f,2}	183.2	232.3	0.03	0.001	2.2	1.975	8.47	31	135
^b OMW-2ST _{f,3}	195.1	230.1	0.09	0.003	3.8	2.122	9.13	22	174
^b OMW-2ST _{f,4}	171.3	248.6	0.15	0.008	11.9	3.56	4.33	16	163
^c Drinking water	200	250	0.2	0.005	-	< 1.000	6.0-9.0	-	-

^aOMW-2ST₀: OMW-2ST before IE process; ^bOMW-2ST_f: OMW-2ST after IE process under optimal conditions; ^c Required values for Drinking Water (European Commission, 1980; European Commission, 1998).

13.4 Conclusions

In this research work, the final purification of two-phase olive mill wastewater (OMW-2), previously subjected to a secondary treatment, through different combination of four ion exchange (IE) resins is addressed. The IE resins used in the optimization studies were: a weak-acid cation exchange resin, a strong-acid cation exchange resin, a weak-base anion exchange resin and a strong-base anion exchange resin.

Central composite design was used for the optimization of the IE processes. Results reveal that the only final treated OMW-2ST effluent fulfilling the legislated requirements for drinking water was the one from the combination of the strong-acid cation exchange resin (Dowex Marathon C) and the weak-base anion exchange resin (Amberlite IRA-67). In this case, the best resins disposition was the strong-acid cation exchange resin followed by the weak-base anion exchange resin. The proposed IE process yielded up to 88 % removal of these pollutants when the initial pH, operating temperature and flow rate were set to 5.1, 26.8 ° C and 12.1 L h⁻¹, respectively. Under these conditions, the achieved concentrations for all contaminants in the final stream were maintained below the maximum established limits. Moreover, high treated

effluent volume recovery (28 L) could be achieved in continuous mode under the optimal operating conditions found, complying with standards for reuse in the production process.

The resins combination consisting of the strong-acid cationic resin followed by the strong-base anionic resin allowed treating the highest OMW-2ST volume before overcoming standard limits for all the studied pollutants. However, in this case conductivity was above the maximum levels due to the high OH⁻ ions release.

On the other hand, although the pollutants concentrations were lower than maximum limits, EC > 1 mS cm⁻¹ and pH higher than maximum and lower than minimum values were found for combination 3 (strong-base anion exchange resin and weak-acid cation exchange resin) and combination 4 (weak-base anion exchange resin and weak-acid cation exchange resin), respectively.

Finally, results suggest that the proposed IE process (resins combination 1) may replace membrane technology for the final purification of two-phase olive mill wastewater, which implies higher operating costs as high pressures are needed to achieve similar removal efficiencies.

13.5 References

Abhuri, K. (2003). Adsorption of phenol and p-chlorophenol from their single and bisolute aqueous solutions on Amberlite XAD-16 resin. *J. Hazard. Mater.*, 105:143-156.

Annadurai, G., Juang, R.S., Lee, D.J. (2002). Factorial design analysis of adsorption of activated carbon on activated carbon incorporated with calcium alginate. *Adv. Environ. Res.*, 6:191-198.

Caetano, M., Valderrama, C., Farran, A., Cortina, J.L. (2009). Phenol removal from aqueous solution by adsorption and ion exchange mechanisms onto polymeric resins. *J. Colloid Interface Sci.*, 338:402-409.

Carmona, M., De Lucas, A., Valverde, J.L., Velasco, B., Rodriguez, J.F. (2006). Combined adsorption and ion exchange equilibrium of phenol on Amberlite IRA-420. *Chem. Eng. J.*, 117(2):155-160.

Cassano, A., Conidi, C., Drioli, E. (2011). Comparison of the performance of UF membranes in olive mill wastewaters treatment. *Water Res.*, 45:3197-3204.

Chen, J.P., Chua, M.L., Zhang, B. (2002). Effects of competitive ions, humic acid, and pH on removal of ammonium and phosphorous from the synthetic industrial effluent by ion exchange

resins. *Waste Manag.*, 22:711–719.

Comstock, S.E.H., Boyer, T.H. (2014). Combined magnetic ion exchange and cation exchange for removal of DOC and hardness. *Chem. Eng. J.*, 241:366-375.

De Caprariis, B., Di Rita, M., Stoller, M., Verdone, N., Chianese, A. (2012). Reaction-precipitation by a spinning disc reactor: Influence of hydrodynamics on nanoparticles production. *Chem. Eng. Sci.*, 76:73-80.

Demirbas, A., Pehlivan, E., Gode, F., Altun, T., Arslan, G. (2005). Adsorption of Cu(II), Zn(II), Ni(II), Pb(II) and Cd(II) from aqueous solution on Amberlite IR-120 synthetic resin. *J. Colloid and Interface Sci.*, 282:20-25.

Dhouib, A., Aloui, F., Hamad, N., Sayadi, S. (2006). Pilot-Plant treatment of olive mill wastewaters by phanerochaete chrysosporium coupled to anaerobic digestion and ultrafiltration. *Process Biochem.*, 41:159-167.

El-Naggar, I.M., El-Dessouky, M.E., Aly, H.F. (1996). Ion-exchange equilibrium of alkali metal/hydrogen ions on amorphous cerium (IV) antimonite. *React. Funct. Polym.*, 28:209-214.

European Commission. (1980). Council Directive 80/778/EEC of 15 July 1980 on the quality of water intended for human consumption.

European Commission. (1998). Council Directive 98/83/EC of 3 November 1998 on the quality of water intended for human consumption.

Food and Agricultural Organization (FAO). (2003). Review of world water resources by country. Water Reports 23, Rome, Italy.

Fu, F., Wang, Q. (2011). Removal of heavy metal ions from wastewaters: a review. *J. Environ. Manage.*, 92:407-418.

Greenberg, A.E., Clesceri, L.S., Eaton, A.D., (1992). Standard Methods for the Examination of Water and Wastewater, APHA/AWWA/WEF, 16th ed., Washington DC. Cabs.

Hodaifa, G., Ochando-Pulido, J.M., Ben-Driss-Alami, S., Rodriguez-Vives, S., Martinez-Ferez, A. (2013a). Kinetic and thermodynamic parameters of iron adsorption onto olive stones. *Ind. Crops Prod.*, 49:526-534.

Hodaifa, G., Ochando-Pulido, J.M., Rodriguez-Vives, S., Martinez-Ferez, A. (2013b) Optimization of continuous reactor at pilot scale for olive-oil mill wastewater treatment by Fenton-like process. *Chem. Eng. J.*, 220:117-124.

Keller, M. (2004). Iron removal by ion exchange: standing on solid ground. *Water Cond. Purif.*, 46(6):20-23.

Kestioğlu, K., Yonar, T., Azbar, N. (2005). Feasibility of physico-chemical treatment and advanced oxidation processes (AOPS) as a means of pre-treatment olive mill effluent (OME). *Process Biochem.* 40:2409-2416.

Ku, Y., Lee, K., Wang, W. (2004). Removal of phenols form aqueous solutions by purolite A-510 resin. *Sep. Sci. Technol.*, 39:911–923.

Martínez Nieto, L., Hodaifa, G., Rodríguez Vives, S., Giménez Casares, J.A. (2010). Industrial plant for olive mill wastewater from two-phase treatment by chemical oxidation. *J. Environ. Eng.*, 136 (11):1309–1313.

Martínez Nieto, L., Hodaifa, G., Rodríguez Vives, S., Giménez Casares, J.A., Ochando, J. (2011a). Flocculation–sedimentation combined with chemical oxidation process. *Clean - Soil, Air, Water*, 39(10):949-955.

Martínez Nieto, L., Hodaifa, G., Rodríguez, S., Giménez, J.A., Ochando, J. (2011b). Degradation of organic matter in olive oil mill wastewater through homogeneous Fenton-like reaction. *Chem. Eng. J.*, 173(2):503-510.

Niaounakis, M., Halvadakis, C.P. (2006). Olive processing waste management literature review and patent survey, 2nd ed., Elsevier: Waste Management Series 5:23-64.

Ochando-Pulido, J.M., Stoller, M., Bravi, M., Martinez-Ferez, A., Chianese, A. (2012a.) Batch membrane treatment of olive vegetation wastewater from two-phase olive oil production process by threshold flux based methods. *Sep. Purif. Technol.*, 101:34–41.

Ochando-Pulido, J.M., Hodaifa, G., Rodriguez-Vives, S., Martinez-Ferez, A. (2012b). Impacts of operating conditions on reverse osmosis performance of pretreated olive mill wastewater. *Water Res.*, 46(15):4621-4632.

Ochando-Pulido, J.M., Hodaifa, G., Víctor-Ortega, M.D., Rodriguez-Vives, S., Martinez-Ferez, A. (2013a). Effective treatment of olive mill effluents from two-phase and three-phase

extraction processes by batch membranes in series operation upon threshold conditions. *J. Hazard Mater.*, 263:168-176.

Ochando-Pulido, J.M., Hodaifa, G., Víctor-Ortega, M.D., Rodríguez-Vives, S., Martínez-Ferez, A. (2013b). Reuse of olive mill effluents from two-phase extraction process by integrated advanced oxidation and reverse osmosis treatment. *J. Hazard Mater.*, 263:158-167.

Ostroski, I.C., Barros, M.A., Silva, E.A., Dantas, J.H., Arroyo, P.A., Lima, O.C. (2009). A comparative study for the ion exchange of Fe(III) and Zn(II) on zeolite NaY. *J. Hazard. Mater.*, 161:1404-1412.

Paraskeva, P., Diamadopoulos, E. (2006). Technologies for olive mill wastewater (OMW) treatment: A review. *J. Chem. Technol. Biotechnol.*, 81:475-485.

Pivovarov, S. (2008) Adsorption of ions onto amorphous silica: Ion exchange model. *J. Colloid Interface Sci.*, 319:374-376.

Sancho Cierva JIn: Giner JF, editor. (2000). Water Quality for irrigation use. Valencia: Universida Politécnic de Valencia-Generalitat Valenciana—Phytoma.

Stoller, M., Bravi, M., Chianese A. (2013a). Threshold flux measurements of a nanofiltration membrane module by critical flux data conversion. *Desalination*, 315:142–8.

Stoller, M., De Caprariis, B., Cicci, A., Verdone, N., Bravi, M., Chianese, A. (2013b). About proper membrane process design affected by fouling by means of the analysis of measured threshold flux data. *Sep. Purif. Technol.*, 114:83–9.

Tahir, S.S., Rauf, N. (2004). Removal of Fe²⁺ from the waste water of a galvanized pipe manufacturing industry by adsorption onto bentonite clay. *J. Environ. Manage.*, 73:285-292.

Vaaramaa, K., Lehto, J. (2003). Removal of metals and anions from drinking water by ion exchange. *Desalination*, 155:157-170.

Víctor-Ortega, M.D., Ochando-Pulido, J.M., Hodaifa, G., Martínez-Ferez, A. (2014a). Ion exchange as an efficient pretreatment system for reduction of membrane fouling in the purification of model OMW. *Desalination*, 343:198-207.

Víctor-Ortega, M.D., Ochando-Pulido, J.M., Hodaifa, G., Martínez-Férez, A. (2014b). Final purification of synthetic olive oil mill wastewater treated by chemical oxidation using ion exchange: Study of operating parameters. *Chem. Eng. Process.*, 85:241-247.

Víctor-Ortega, M.D., Ochando-Pulido, J.M., Martínez-Férez, A. (2015a). Impacts of integrated strong-acid cation exchange and weak-base anion exchange process for successful removal of saline toxicity from model olive mill wastewater. *Ecol. Eng.*, 77:18-25.

Víctor-Ortega, M.D., Ochando-Pulido, J.M., Martínez-Férez, A. (2015b). Iron removal and reuse from Fenton-like pretreated olive mill wastewater with novel strong-acid cation exchange resin fixed-bed column. *J. Ind. Eng. Chem.*, Submitted.

Víctor-Ortega, M.D., Ochando-Pulido, J.M., Martínez-Férez, A. (2015c). Performance and modelling of continuous ion exchange processes for phenols recovery from olive mill wastewater. *Sep. Purif. Technol.*, Submitted.

Zhu, L., Deng, Y., Zhang, J., Chen, J. (2011). Adsorption of phenol from water by N butylimidazolium functionalized strongly basic anion exchange resin. *J. Colloid. Interface Sci.*, 364:462-468.

CHAPTER 14

**IMPACTS OF MAIN PARAMETERS ON THE REGENERATION PROCESS
EFFICIENCY OF SEVERAL ION EXCHANGE RESINS AFTER FINAL
PURIFICATION OF OLIVE MILL EFFLUENT**

María Dolores Víctor-Ortega^{1*}, Javier Miguel Ochando-Pulido¹, Antonio Martínez-Ferez¹

¹ Chemical Engineering Department, University of Granada, 18071 Granada, Spain

*email: mdvictor@ugr.es

Submitted for publication:

Ecological Engineering

Publisher: ELSEVIER SCIENCE BV. PO BOX 211, 1000 AE AMSTERDAM,
NETHERLANDS

Year: 2015

ISSN: 0925-8574

Impact factor: 2.580

Tertile: First



Abstract

The key for the cost-efficient application of ion exchange (IE) processes relies on the fact that resins should be effectively regenerated to ensure their operation for the maximum possible working cycles. The main objective of this research work was to examine the effect of the main parameters affecting the regeneration process of several IE resins previously used for the purification of secondary-treated olive mill wastewater (OMW-2ST), comprising the regenerant concentration and type, the operating temperature and the flow rate. For this purpose, the impacts on the regeneration and rinse times as well as the regeneration efficiency were addressed. Results show regeneration time decreased but rinse time increased with regenerant concentration increment for all resins. As a general rule, minor flowrate (2.5 L h^{-1}) provided the highest possible regeneration, whereas efficiencies above 96 % were noted upon the lowest temperature examined (298 K), which have both important implications on the cost-efficiency of the regeneration and integral effluent treatment process. Finally, 0.6 L HCl 4% and 0.8 L H_2SO_4 2% solutions achieved complete regeneration of Dowex Marathon C and Dowex MAC 3 resins, whereas 0.7 L and 1 L NaOH 4% ensured complete regeneration of Amberlyst A26 and Amberlite IRA-67 resins, respectively.

Keywords: ion exchange, olive mill effluent, regeneration efficiency, synthetic resins

14.1 Introduction

Industrial wastewater is subjected to strict environmental legislation, thus making its adequate management a key issue. In this regard, there is a plethora of technologies described in the scientific literature regarding wastewater treatments. Within this context, novel IE resins developed over the past few decades have promoted this technology as a suitable separation and purification process for wastewater treatment (Demirbas et al., 2005; Fu and Wang, 2011; Comstock and Boyer, 2014).

Ion exchange (IE) is an adsorption process whereby a target ion in the aqueous phase is transferred to a solid phase, mainly synthetic resin, and exchanged with a like-charged presaturant ion that diffuses into solution (Frederick, 1996). Because many aqueous contaminants are charged, IE is used to remove numerous contaminants from water and wastewater including several heavy metals and anionic pollutants (Clifford et al., 2011). In this context, IE resins are classified as strong or weak acid cation exchange resins and strong or weak base anion exchange resins.

During IE processes the liquid or effluent to be purified passes through a fixed bed filled with IE resin. The key for the cost-efficient implementation of an IE process is to ensure that the IE

resins can be easily and effectively regenerated, in order to guarantee their operation for the maximum possible working cycles (Simon, 1991). For that purpose, IE processes must be stopped periodically and the IE resin regenerated. In the regeneration step the resin is returned to its original state and the ions that had been substituted on the resin go back into solution. Cationic resins are usually regenerated by using a concentrated acid solutions, and anionic resins by means of a concentrated base. The net result is a solution that is much more concentrated than the feed to the system (Balchen and Mummè, 1988). For many substances, such as heavy metals, this is usually the first step in a recovery process. For others, it is merely a mean of concentration before ultimate disposal occurs.

Hydroxide (OH^-) and chloride (Cl^-) as well as hydrogen ion (H^+) and sodium (Na^+) are the most commonly used presaturant ions in anion exchange and cation exchange processes, respectively, because they readily exchange with contaminant ions (Balchen and Mummè, 1988; Pakzadeh, 2010). As a result, highly concentrated base or acid solutions in one hand or sodium chloride (NaCl) solution in the other hand are required to regenerate contaminant-saturated (i.e., exhausted) IE resin. In combined systems comprising cationic resins and anionic resins in series, using acid such as HCl and base like NaOH as regenerants would give as a result the formation of H_2O in the regenerant outlet stream, thereby facilitating the disposal of final regenerant waste. This fact presents many benefits from an environmental point of view. In this case, both acid and base are used in excess quantities. Meanwhile, the advantages of NaCl as a regenerant include high aqueous solubility, low human toxicity, and low cost when compared to the alternate regeneration chemicals considered in this study. There are, however, recognized disadvantages associated with the disposal of waste streams high in NaCl . For instance, high strength NaCl solution that is sent to a wastewater treatment plant inhibit biological processes (Panswad and Anan, 1999) and increase the NaCl content of receiving waters, which in turn have adverse impacts on aquatic organisms and ecosystems (Canedo-Arguelles et al., 2013).

Different regenerant solutions have been used for cation and anion exchangers. For instance, Millar et al. used hydrochloric acid solutions to regenerate strong-acid cation exchange resins (Millar et al., 2015). Also, Marañón et al. regenerated a series of cation and chelating resins using hydrochloric acid solutions (Marañón et al., 1999).

On the other hand, Caetano et al. used NaOH and methanol/water solutions for MN200 anion exchange resin regeneration (Caetano et al., 2009). In addition, Sowmya and Meenakshi (2014) studied the regeneration of a novel quaternized anionic resin, by using NaCl solution (Sowmya and Meenakshi, 2014).

In previous research works, the final purification of olive mil wastewater coming from the two-

phase continuous decanting process (OMW-2) was carried out through IE system comprising several combinations of two resins in serial connection: one cationic resin and the other one anionic resin (Victor-Ortega et al., 2015). This effluent is a hardly treated by-product generated during olive oil production which constitutes an important environmental problem, since its disposal into watercourses leads to deterioration of natural water bodies, pollution and environmental degradation (Danellakisa et al., 2011). Previous to this final treatment by means of IE technology, OMW-2 was conducted to a secondary treatment based on Fenton reaction-advanced oxidation process followed by a flocculation–sedimentation step and filtration-in-series through different filtration medium (Martínez Nieto et al., 2011a; Hodaifa et al., 2013; Martínez Nieto et al., 2011b).

The goal of this research study was to examine the effect of the main parameters affecting the regeneration process of several IE resins - Dowex Marathon C strong-acid cation exchange resin, MAC 3 weak-acid cation exchange resin, Amberlyst A26 strong-base anion exchange resin and Amberlite IRA-67 weak-base anion exchange resin - previously used for the purification of the secondary-treated olive mill wastewater stream (OMW-2ST). For this purpose, the impacts on the regeneration and rinse times as well as the overall regeneration efficiency of the IE resins were addressed as a function of the regeneration operation variables, comprising the regenerant concentration and type, the operating temperature and the flow rate.

The regeneration of the selected IE resins with a minimum amount of residual pollutant ions and the subsequent reuse are of paramount importance for cost-effective implementation of the integral OMW-2 treatment process. To the Authors' knowledge, no previous work can be found in the scientific literature on the regeneration procedure of IE resins saturated after the treatment of these heavily-polluted effluents.

14.2 Methods and Materials

14.2.1 Ion exchange resins and equipment

Four IE resins (all of them provided by Sigma Aldrich), previously employed for final purification of OMW-2ST, were used for the regeneration experiments based on differences in functional group, polymer composition, and ion exchange capacity. These resins were Dowex Marathon C strong-acid cation exchange resin, MAC 3 weak-acid cation exchange resin, Amberlyst A26 strong-base anion exchange resin and Amberlite IRA-67 weak-base anion exchange resin. Their main physicochemical characteristics are shown in Table 14.1.

It is important to highlight the different matrix each resin presents as well as the total exchange capacity exhibited by the different resins. Furthermore, it is worthy to point out that strong-acid

cationic resin and strong-base anionic resin present effective pH throughout the whole pH range (i.e. 0-14), whereas effective pH ranges are 5-14 and 0-7 for the weak-acid cationic resin and for the weak-base anionic resin, respectively.

Table 14.1. Physicochemical properties of selected IE resins (from manufacturer specifications).

IE Resin	DOWEX MAC 3	DOWEX MARATHON C	AMBERLITE IRA-67	AMBERLYST A26
Resin type	Weak acid-cation	Strong-acid cation	Weak-base anion	Strong-base anion
Matrix	Polyacrylic, macroporous	Styrene-DVB, gel	Crosslinked acrylic gel	Styrene-divinylbenzene
Functional group	Carboxylic acid	Sulfonic acid	Tertiary amine	Quaternary ammonium
Ionic form as shipped	H ⁺ form	H ⁺ form	OH ⁻ form	OH ⁻ form
Ion Exchange capacity^a, eq/L	3.8	1.80	1.60	0.80
Water content, %	44-52	50-56	56-64	66-75
Shipping density, g/L	750	800	700	675

^a Ion exchange capacity is the minimum wet capacity as specified by the manufacturer.

The IE device (MionTec) was equipped with a peristaltic pump (Ecoline VC-380) and a temperature-controlled thermostatic bath (Precistern JP Selecta). Figure 14.1 shows the scheme of the IE equipment used for regeneration experiments.

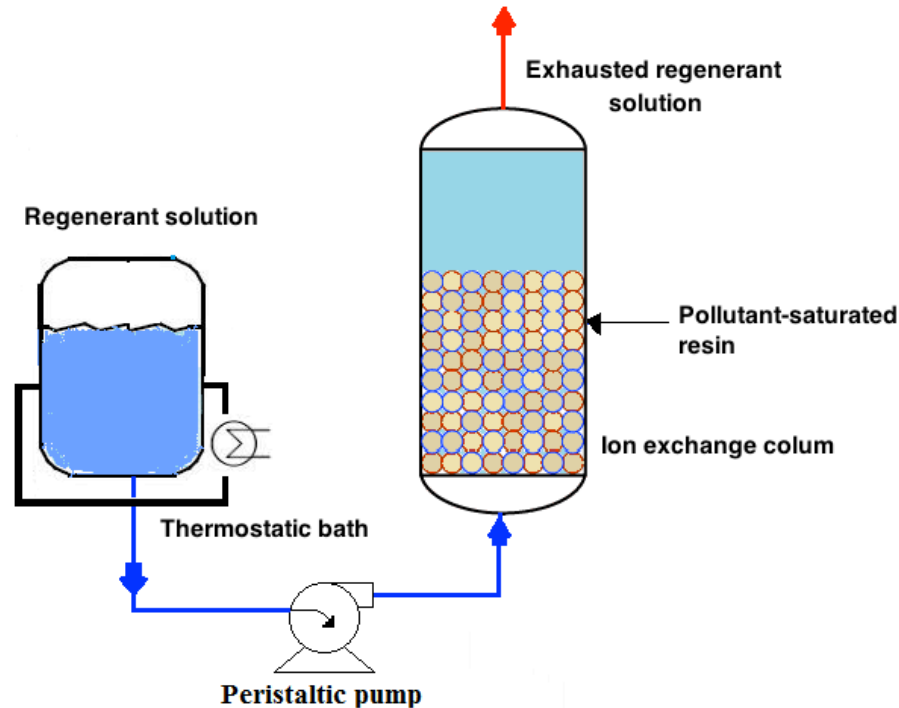


Figure 14.1. Scheme of the IE equipment used for regeneration experiments.

14.2.2 Chemicals

OMW-2 samples were collected during the olive oil production campaign from different olive oil mills in the South of Spain, operating with the two-phase centrifugation system.

All solutions were prepared from ACS reagent grade purity chemicals in deionized water. The following regenerants were used: hydrochloric acid 37 % (Panreac), sulfuric acid 98% (Sigma-Aldrich), sodium hydroxide (Panreac) and ammonia 30% (Panreac).

14.2.3 Regeneration experiments

Firstly, OMW-2 samples were conducted to the secondary treatment full described in previous works by the Authors (Martínez Nieto et al., 2011a; Hodaifa et al., 2013; Martínez Nieto et al., 2011b). The effluent after the secondary treatment (OMW-2ST) presented the physicochemical characteristics reported in Table 14.2. As it can be seen, the OMW-2ST exhibited considerable COD, EC, sodium, chloride, iron and phenols concentration values. Subsequently, the OMW-2ST stream was subjected to the proposed IE purification process fully described in previous work by the Authors (V́ctor-Ortega et al., 2015).

After these steps, resins become saturated, ready for regeneration experiments, which were undertaken in triplicate. Fix-bed regeneration experiments were performed for the different resins using the different acid and base regenerant solutions with regeneration concentration

varying from 1 to 10 % (v.v). Furthermore, temperature was studied in the range 288 K – 318 K. Finally, the impact of flow rate in the regeneration process was examined at different values: 2.5 L h⁻¹, 5 L h⁻¹, 10 L h⁻¹ and 15 L h⁻¹.

Table 14.2. Physicochemical characterization of OMW-2ST.

Factor	Value
pH	6.82
Conductivity, mS cm⁻¹	4.35
COD, mg L⁻¹	162.0
Total phenolic compounds, mg L⁻¹	1.2
[Cl⁻], mg L⁻¹	1250
[Na⁺], mg L⁻¹	870
[Total iron], mg L⁻¹	0.9

During continuous regeneration experiments, regenerant solution feedstream was introduced at the bottom of each column (cationic or anionic, as appropriate) in upflow mode, leaving this column by the top. Then, exhausted regenerant solution was collected and analyzed.

The regeneration efficiency (expressed as a percent) was quantified according to the following equation (Eq. 1):

$$\% \text{ Regeneration efficiency} = \frac{M_r}{M_a} \times 100 \quad (1)$$

where M_a and M_r are the adsorbed and released ion amount from the resin (mg), respectively.

13.2.4 Analytical methods

Sodium concentration values were determined by using a Crison GLP 31 Sodium Ion-Selective Electrode 96 50, with autocorrection of temperature. To this end, 0.01, 0.1 and 1.0 g L⁻¹ Na⁺ standard solutions were prepared in the laboratory to calibrate the electrode. Chloride concentration values were assessed by a Crison GLP 31 Chloride Ion-Selective Electrode 96 52 C, with autocorrection of temperature. For this purpose, 0.01, 0.1 and 1.0 g L⁻¹ Cl⁻ standard solutions required for the electrode calibration were also prepared in the laboratory.

For the measurement of the total iron concentration, all iron ions were reduced to iron ions (II) in a thioglycolate medium with a derivative of triazine, forming a reddish-purple complex that was

determined photometrically at 565 nm (Standard German methods ISO 8466-1 and German DIN 38402 A51) (Greenberg et al., 1992).

Total phenols and phenol derivatives were analyzed by reaction with a derivative thiazol, giving a purple azo dye, which was determined photometrically using a Helios Gamma UV-visible spectrophotometer (Thermo Fisher Scientific) at 475 nm (Standard German methods ISO 8466-1 and DIN 38402 A51) (Greenberg et al., 1992).

EC and pH measurements were evaluated with a Crison GLP31 conductivity-meter and a Crison GLP21 pH-meter, provided with autocorrection of temperature. Buffer standard solutions for EC ($1,413 \mu\text{S cm}^{-1}$ and 12.88 mS cm^{-1}) and pH (pH 4.01, 7.00 and 9.21) measurements respectively were supplied as well by Crison.

Analytical grade reagents and chemicals with purity over 99 % were used for the analytical procedures, applied at least in triplicate.

14.3 Results and discussion

In this research work, regeneration process of Dowex Marathon C, Dowex MAC 3, Amberlite IRA-67 and Amberlyst A26 resins was studied through the impact of several parameters, such as regenerant type and concentration, temperature and flow rate, on regeneration and rinse times as well as regeneration process efficiency.

14.3.1 Nature of regenerant solutions

In first place, the impacts of the type of regenerant solution used on the effective regeneration of the used resins were studied upon fixing the regeneration operating variables at 298 K and 2.5 L h^{-1} and regenerant concentration: 6% (v:v) regenerants for Amberlyst A26 and Dowex Marathon C and 4 % (v:v) regenerants for Amberlite IRA-67 and Dowex MAC 3. For this goal, the influence of different regenerant solutions on regeneration and rinse times was investigated. On the one hand, hydrochloric acid and sulfuric acid solutions were examined for cation exchange resins regeneration while, on the other hand, sodium hydroxide and ammonia solutions were employed for anion exchange resins regeneration.

In general, it is recommended to use a strong acid or base at high concentrations with the aim of replacing any ion which is attached to the active sites of the resin, following the “Le Chatelier’s principle”.

14.3.1.1 Cationic IE resins

For each regenerant solution, the regeneration time together with the rinsing time was examined for all the tested resins. Two different regenerant solutions were tested for cation exchange resins regeneration. Figure 14.2.a shows the influence of both acid solutions on regeneration and rinse times for Dowex Marathon C. In this case, the highest regeneration time was obtained for HCl while rinse time was higher for H₂SO₄. It can be seen that for this strong-acid cation exchange resin the lowest total regeneration cycle time comprising regeneration and rinsing periods was attained with the HCl solution in contrast with H₂SO₄ regenerant, that is, 45.5 min for the former in contrast with up to 57 min for the latter, respectively. Therefore, this last solution was chosen for Dowex Marathon C resin regeneration. On the other hand, for weak-acid cation exchange Dowex MAC 3 resin the lowest regeneration and rinse times were found to be attained by using H₂SO₄ regenerant solution (12 and 60 min, respectively) (Figure 14.2b).

On the other hand, in case of Dowex Marathon C resin, 98 % and 95 % removal efficiencies were achieved with 6 % HCl and 6 % H₂SO₄ solutions, respectively. However, around 95 % removal efficiencies of Dowex MAC 3 were obtained for 4 % HCl and 4 % H₂SO₄ solutions, respectively.

According to all these results, HCl aqueous solution was chosen for Dowex Marathon C resin regeneration whereas H₂SO₄ solution was found to give the best regeneration conditions for Dowex MAC 3.

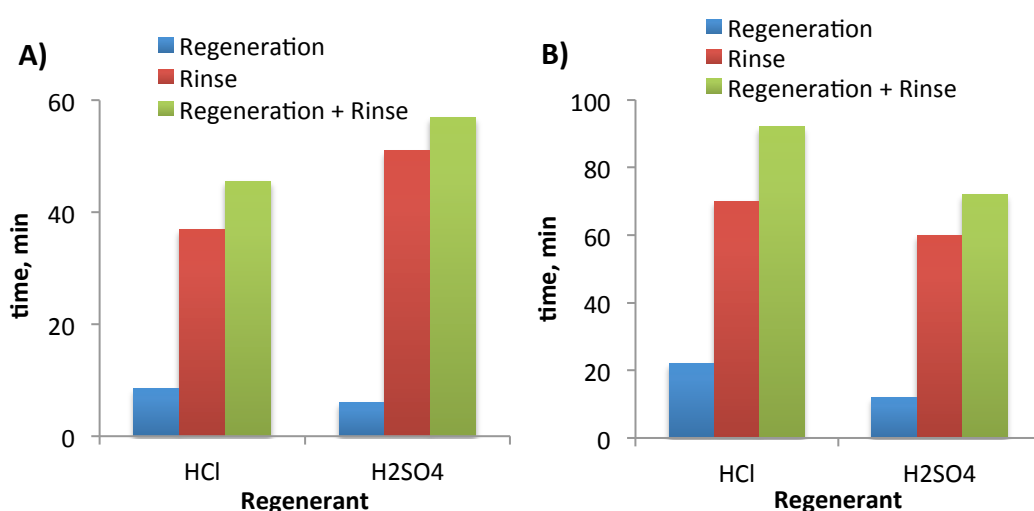


Figure 14.2. Impact of nature of regenerant solution on regeneration and rinse time of a) Dowex Marathon C strong-acid cation exchange resin and b) Dowex MAC 3 weak-acid cation exchange resin. Common conditions: Regenerant concentration: 6 % (v:v) for Dowex Marathon C and 4 % (v:v) for Dowex MAC 3; Temperature: 298 K; Flow rate: 2.5 L h⁻¹.

Similarly, Millar et al. used hydrochloric acid solutions to regenerate strong-acid cation exchange resins. They obtained regeneration efficiencies higher than 90% using 10 % HCl (Millar et al., 2015). Also, Marañón et al. regenerated a series of cation and chelating resins using hydrochloric acid solutions. In general, the regeneration efficiency was considerably higher with strong-acid cation resins (70–90%) compared to chelating resins (20–40%) (Marañón et al., 1999).

14.3.1.2 Anionic IE resins

Anion exchange resins regeneration was performed through NaOH and NH₄OH solutions. In this case, regeneration and rinse times were higher for NH₄OH than for NaOH for both Amberlite IRA-67 and Amberlyst A26 resins. This fact can be explained taking into account that NaOH is a strong base whereas NH₄OH is a weak base. Thus, the stronger is the base, the more effective is as regenerant.

Concretely, the required times for Amberlyst A26 were 10 min and 12 min using NaOH and NH₄OH solutions, respectively. On the other hand, 15 min vs. 24 min were necessary with NaOH and NH₄OH solutions, respectively, for regeneration of Amberlite IRA-67. A similar trend was found for rinse times: 45 vs. 50 minutes for NaOH and NH₄OH solutions, respectively (Amberlyst A26 resin) and 65 vs. 67 min for NaOH and NH₄OH solutions, respectively (Amberlite IRA-67). Thus, NH₄OH solution was selected for further regeneration experiments (see Figure 14.3a,b).

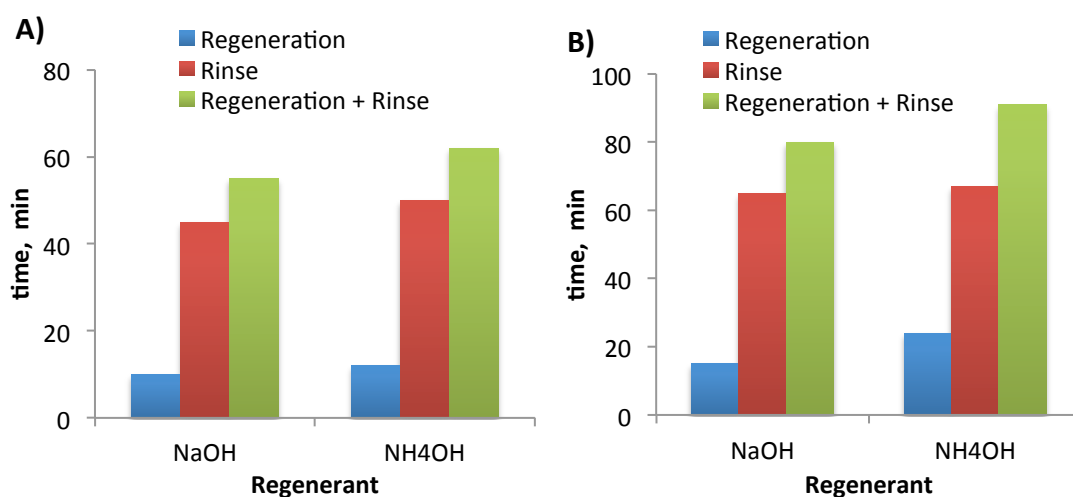


Figure 14.3. Impact of nature of regenerant solution on regeneration and rinse time of a) Amberlyst A26 strong-base anion exchange resin and b) Amberlite IRA-67 weak-base anion exchange resin. Common conditions: regenerant concentration: 6 % (v:v) for Amberlyst A26 and 4 % (v:v) for Amberlite IRA-67; Temperature: 298 K; Flow rate: 2.5 L h⁻¹.

In this sense, Caetano et al. used two different solutions for MN200 anion exchange resin regeneration (Caetano et al., 2009). The first one was NaOH solution although the regeneration efficiency was poor. The second solution was a methanol/water one (50% v/v), reaching a maximum regeneration efficiency of 90 % after 60 min regeneration process. Sowmya and Meenakshi (2014) studied the regeneration of saturated ADVEGR, a novel quaternized anionic resin, by using 0.025 M NaCl solution (Sowmya and Meenakshi, 2014).

14.3.2 Regenerant solutions concentration

Following the study of the appropriate regenerant solution type, the impact of the regenerant solutions concentration on resins regeneration and rinse times was examined. Results are shown in Figure 14.4.a,b and Figure 14.5.a,b. The results show that regeneration time decreased and rinse time increased with increasing regenerant concentration for all the selected resins.

14.3.2.1 Cationic IE resins

The impact of the different regenerant solutions concentrations on the performance of the regeneration procedure of the selected cationic IE resins is reported in Figure 14.4. As it can be noted, the regeneration time decreased and the rinse time increased with increasing acid concentration for both Dowex Marathon C and Dowex MAC 3 cationic resins. Moreover, it is worth highlighting that both effects were more pronounced for the strong-acid cation exchange resin than for the weak-acid cationic resin.

Taking into account the counterbalance of the regeneration and rinse total time, it can be pointed out that the optimal regenerant concentrations were equal to 4 % and 2% for Dowex Marathon C and Dowex MAC 3, respectively. This is highlighted by the minimum inflection point shown in both figures (Figure 14.4a,b). In this sense, 0.6 L HCl 4% solution and 0.8 L H₂SO₄ 2% solution were successfully used for complete regeneration of Dowex Marathon C and Dowex MAC 3 resin, respectively.

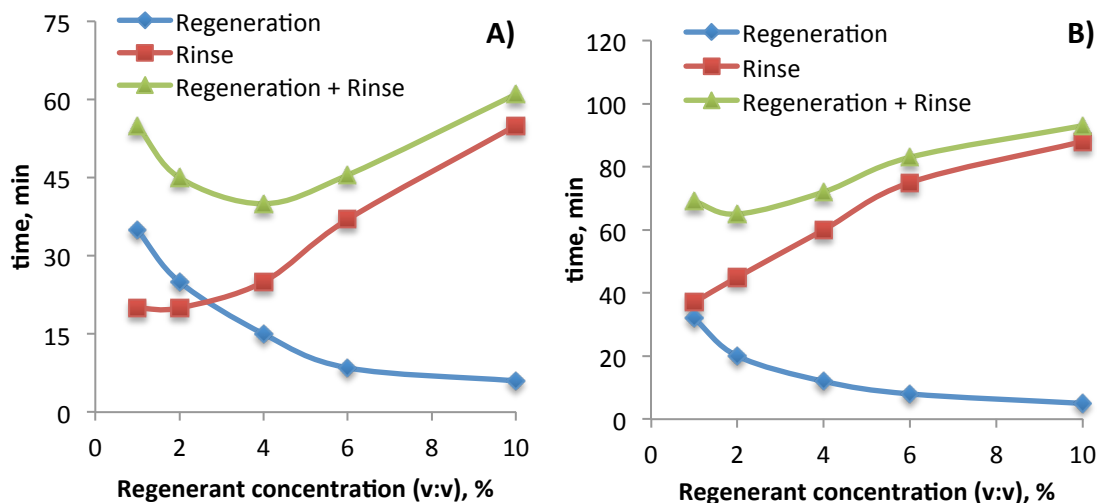


Figure 14.4. Impact of nature of regenerant solution on regeneration and rinse time of a) Dowex Marathon C strong-acid cation exchange resin and b) Dowex MAC 3 weak-acid cation exchange resin. Common conditions: regenerant: HCl for Dowex Marathon C and H₂SO₄ for Dowex MAC 3; Temperature: 298 K; Flow rate: 2.5 L h⁻¹.

14.3.2.2 Anionic IE resins

Similarly, the results obtained from the experimental runs on the effect of the concentration of the different regenerant solutions on the performance of the anionic resins regeneration process is given in Figure 14.5.

In this case, the increase of rinse time and decrease of regeneration time with increasing base concentration is also sharper for the strong-base anionic resin than for the weak-base anion exchange resin.

The trends shown in Figure 14.5a,b indicate that the optimal regenerant concentration were found to be 4 % and 2 % NaOH solution for Amberlyst A26 and Amberlite IRA-67 resins, respectively. Again, this is indicated by the minimum inflection point noted in this figures, counterbalancing the regeneration and rinse total time. On the other hand, 0.7 L and 1 L NaOH 4% were employed for complete regeneration of Amberlyst A26 and Amberlite IRA-67 resins, respectively.

It is worthy to highlight that higher regenerant solution concentrations were necessary for complete regeneration of strong-acid cation and strong-base anion exchange resins in comparison with weak-acid cation and weak-base anion exchange resins.

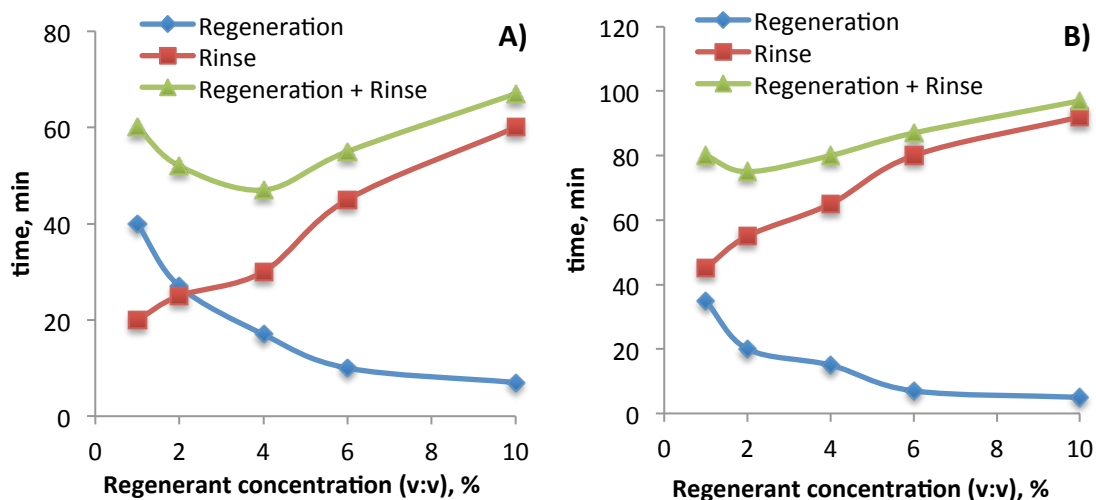


Figure 14.5. Impact of regenerant solution concentration on regeneration and rinse time of a) Amberlyst A26 strong-base anion exchange resin and b) Ambelite IRA-67 weak-base anion exchange resin. Common conditions: Regenerant: NaOH; Temperature: 298 K; Flow rate: 2.5 L h⁻¹.

14.3.3 Effect of temperature

The influence of the temperature on IE resins regeneration performance is reported in Figure 14.6. The regeneration process was studied at 288 K, 298 K, 308 K and 318 K. As shown in Figure 14.6, for Dowex Marathon C strong-acid cation exchange resin there were no significant differences between regeneration efficiencies at 298 K and 308 K (both close to 100 %). However, the first temperature was chosen as the optimum since it would not be necessary to heat in this case. Moreover, temperatures above 308 K yielded lower regeneration efficiencies of the resin. On the contrary, for Dowex MAC 3 weak-acid cation exchange resin the regeneration efficiency increased with an increase in the temperature up 308 K (97% regeneration efficiency), but it can be observed that higher temperature led to lower IE regeneration efficiency.

On the other hand, results showed that the optimum temperature for Amberlyst A26 strong-base anionic resin regeneration was found to be 298 K (almost 100 % regeneration efficiency). Regeneration efficiency in the same range was attained at 308 K for this resin, but discardable from the energy costs point of view. Finally, as it can be observed in Figure 14.6, the set temperature has lower impact on the regeneration efficiency of Amberlite IRA-67 weak-base anionic resin. For this resin, regeneration efficiencies higher than 96% were obtained for all the studied temperatures, although slightly higher regeneration efficiency was observed upon the lower temperature assayed (298 K).

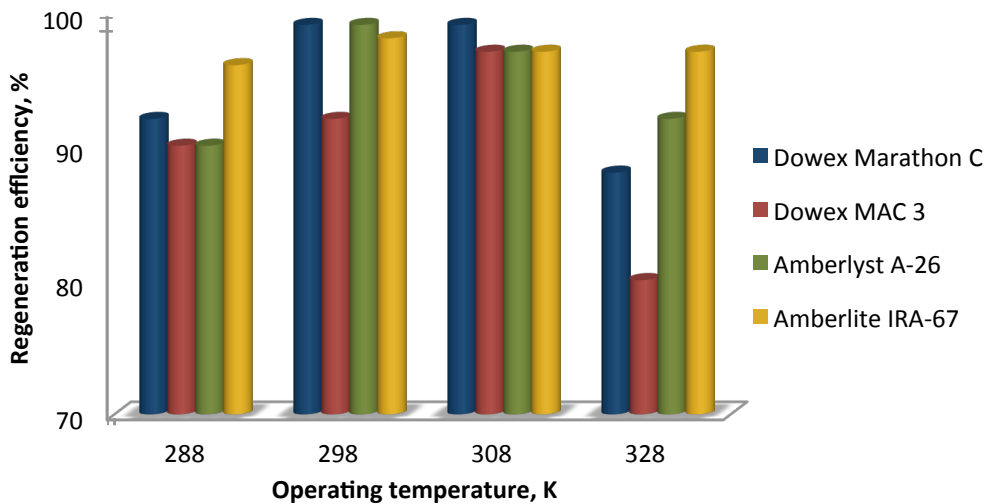


Figure 14.6. Impact of temperature on regeneration efficiency of the selected resins. Common conditions: Regenerant: 4% HCl for Dowex Marathon C, 2% H₂SO₄ for Dowex MAC 3, 4% NaOH for Amberlyst A26 and 2% NaOH for Amberlite IRA-67; Flow rate: 2.5 L h⁻¹.

To sum up, major regeneration efficiencies were confirmed for all the tested resins upon the lowest temperature examined (in the range 298 K), implying no heating expenses, which has important positive implications on the cost-efficiency of the resins regeneration process.

14.3.4 Effect of flow rate

The impact of flow rate on the selected IE resins regeneration process efficiency is reported in Figure 14.7. In this case, flow rates lower than 2.5 L h⁻¹ were not studied according to the minimum flow rate recommended by the IE equipment manufacturer.

For all the investigated resins, regeneration efficiencies decreased with increasing flow rates. In this sense, optimum flow rate was found to be 2.5 L h⁻¹, which yielded regeneration efficiencies close to 100 % for the selected IE resins. This decrease was highly pronounced for Dowex MAC 3 weak-acid cation exchange resin (from 97 % to 55 % regeneration efficiencies), whereas it exhibited less impact for Amberlite IRA-67 weak-base anion exchange resin (from 98 % to 80 %). For this resin, the effect of the decrease of the regeneration efficiency upon increasing the regenerant flow rate was observed to be more gradual. This tendency is in agreement with results obtained by Chen et al., who found that at higher flow rate, thus low residence times, the solution does not have enough time to contact and react with the IE resins (Chen et al., 2002). On the other hand, too low flow rate is also not necessary due to the excessively long regeneration times required, that would not be cost-efficient for the continuous operation of the OMW-2ST purification IE process. Furthermore, for this resin weak-base anionic resin, regeneration

efficiencies within the same range (aprox. 98 %) were confirmed upon both 2.5-5 L h⁻¹ flow rates, thus it may be similarly efficient to operate the regeneration process at this higher flow rate to attain minor regeneration cycle times.

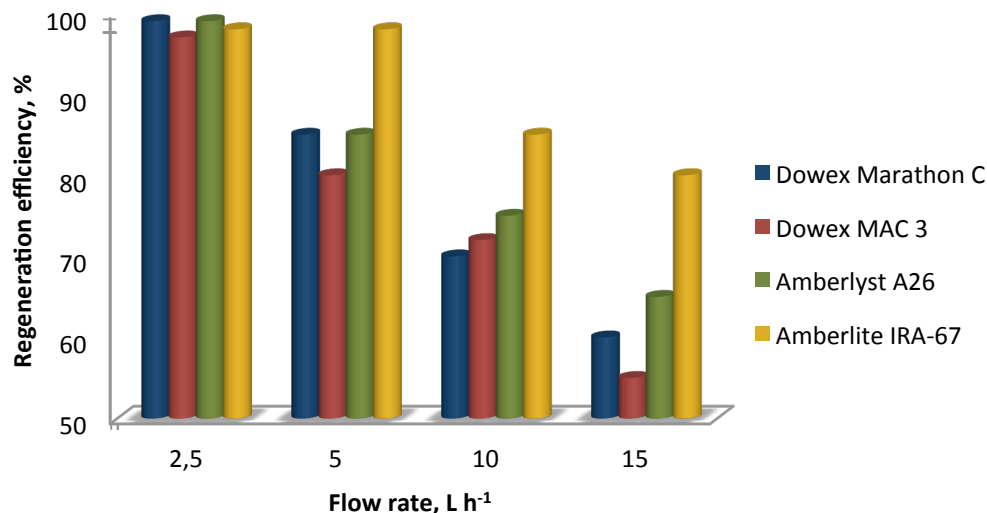


Figure 14.7. Impact of flow rate on regeneration efficiency of the selected resins. Common conditions: Regenerant: 4% HCl for Dowex Marathon C, 2% H₂SO₄ for Dowex MAC 3, 4% NaOH for Amberlyst A26 and 2% NaOH for Amberlite IRA-67; Temperature: 298 K.

Finally, the optimal parameters values obtained for regeneration of each IE resin are summarized in Table 14.3.

Table 14.3. Optimal parameters values for regeneration of the selected IE resins

	DOWEX MAC 3	DOWEX MARATHON C	AMBERLITE IRA-67	AMBERLYST A26
Nature of regenerant	H ₂ SO ₄	HCl	NaOH	NaOH
Concentration	2 % (v:v)	4 % (v:v)	2 % (v:v)	4 % (v:v)
Regenerant volume	0.8 L	0.6 L	1 L	0.7 L
Rinse volume	0.8 L	1 L	0.8 L	1.3 L
Temperature	308 K	298 K	298 K	298 K
Flow rate	2.5 L h ⁻¹	2.5 L h ⁻¹	2.5 L h ⁻¹	2.5 L h ⁻¹

14.4 Conclusions

In this research work, the effect of the main parameters affecting the regeneration process of several cationic and anionic resins (Dowex Marathon C, Dowex MAC 3, Amberlite IRA-67 and Amberlyst A26), previously used for the purification of secondary-treated olive mill wastewater (OMW-2ST), were examined comprising the regenerant concentration and type, the operating temperature and the flow rate. For this purpose, the impacts on the regeneration and rinse times as well as the regeneration efficiency were addressed.

The results show that regeneration time decreased and rinse time increased with increasing regenerant concentration for all the selected resins. In this sense, 0.6 L HCl 4% solution and 0.8 L H₂SO₄ 2% solution were used for complete regeneration of Dowex Marathon C and Dowex MAC 3 resins, respectively. On the other hand, 0.7 L and 1 L NaOH 4% and 2 % were employed for complete regeneration of Amberlyst A26 and Amberlite IRA-67 resins, respectively.

Furthermore, the optimal temperature for regeneration of Dowex Marathon C, Amberlyst A26 and Amberlite IRA-67 was found to be 298 K (regeneration efficiencies higher than 96 % in all cases). However, results indicate that 308 K was the optimal temperature for regeneration of Dowex MAC 3. This would imply no heating expenses, thus having important positive implications on the cost-efficiency of the resins regeneration process.

The impact of flow rate on the selected IE resins regeneration process efficiency revealed that, for all the investigated resins, regeneration efficiencies decreased with increasing flow rates. In this sense, optimum flow rate was found to be 2.5 L h⁻¹, which yielded regeneration efficiencies close to 100 % for the selected IE resins. Higher flow rates were not found to be necessary to attain complete regeneration of the IE resins, also having both important implications on the cost-efficiency of the regeneration and integral effluent treatment process.

14.5 References

Balchen, J.G., Mummè K.I., (1988). *Process Control Structures and Applications*. New York: Van Nostrand Reinhold.

Caetano, M., Valderrama, C., Farran, A., Cortina, J.L. (2009). Phenol removal from aqueous solution by adsorption and ion Exchange mechanisms onto polymeric resins. *J. Colloid. Interface Sci.*, 338:402-409.

Canedo-Arguelles, M., Kefford, B.J., Piscart, C., Prat, N., Schafer, R.B., Schulz, C.J. (2013).

Salinisation of rivers: an urgent ecological issue. *Environ. Pollut.*, 173:157–167.

Chen, J.P., Chua, M.L., Zhang, B. (2002). Effects of competitive ions, humic acid, and pH on removal of ammonium and phosphorous from the synthetic industrial effluent by ion exchange resins, *Waste Manage.*, 22:711–719.

Clifford, D., Sorg, T.J., Ghurye, G.L. (2011). Ion exchange and adsorption of inorganic contaminants, in: J.K. Edzwald (Ed.), *Water Quality & Treatment: A Handbook on Drinking Water*, McGraw-Hill Inc., New York.

Comstock, S.E.H., Boyer, T.H. (2014). Combined magnetic ion exchange and cation exchange for removal of DOC and hardness. *Chem. Eng. J.*, 241:366–375.

Danellakisa, D., Ntaikoub, I., Kornarosb, M., Dailianis, S. (2011). Olive oil mill wastewater toxicity in the marine environment: Alterations of stress indices in tissues of mussel *Mytilus galloprovincialis*. *Aquatic Toxicology*, 101:358-366.

Demirbas, A., Pehlivan, E., Gode, F., Altun, T., Arslan, G. (2005). Adsorption of Cu(II), Zn(II), Ni(II), Pb (II) and Cd(II) from aqueous solution on Amberlite IR-120 synthetic resin. *J. of Colloid and Interface Science*, 282:20-25.

Frederick, K. (1996). Countercurrent regeneration: principles and applications. *Ultrapure Water*, 53–56.

Fu, F., Wang, Q., Removal of heavy metal ions from wastewaters: a review, *J. Environ. Manage.* 92 (2011) 407-418.

Greenberg, A.E., Clesceri, L.S., Eaton, A.D. (1992). *Standard Methods for the Examination of Water and Wastewater*, APHA/AWWA/WEF, 16th ed., Washington DC. Cabs.

Hodaifa, G., Ochando-Pulido, J.M., Rodriguez-Vives, S., Martinez-Ferez, A. (2013). Optimization of continuous reactor at pilot scale for olive-oil mill wastewater treatment by Fenton-like process. *Chem. Eng. J.*, 220:117-124.

Marañón, E., Suárez, F., Alonso, F., Fernández, Y., Sastre, H. (1999). Preliminary study of iron removal from hydrochloric pickling liquor by ion exchange. *Ind. Eng. Chem. Res.*, 38(7):2782–2786.

Martínez Nieto, L., Hodaifa, G., Rodríguez Vives, S., Giménez Casares, J.A., Ochando, J. (2011a). Degradation of organic matter in olive oil mill wastewater through homogeneous Fenton-like reaction. *Chem. Eng. J.*, 173:503-510.

Martínez Nieto, L., Hodaifa, G., Rodríguez Vives, S., Giménez Casares, J.A., Ochando, J. (2011b). Flocculation–sedimentation combined with chemical oxidation process. *Clean - Soil, Air and Water*, 39(10):949–955.

Millar, G.J., Schot, A., Couperthwaite, S.J., Shilling, A., Nuttall, K., de Bruyn, M. (2015). Equilibrium and column studies of iron exchange with strong acid cation resin. *J. Environ. Chem. Eng.*, 3:373-385.

Pakzadeh, B. (2010). Ion-exchange (IX): arsenic and chromium removal from brines and removal of inorganic contaminants by specialty resins. Doctoral thesis. University of Nevada Las Vegas.

Panswad, T., Anan, C. (1999). Impact of high chloride wastewater on an anaerobic/anoxic/aerobic process with and without inoculation of chloride acclimated seeds. *Water Res.*, 33:1165–1172.

Simon, G.P. (1991). Ion Exchange Training Manual. Chapter 6. Springer Science. New York.

Sowmya, A., Meenakshi, S. (2014). A novel quaternized resin with acrylonitrile/divinylbenzene/vinylbenzyl chloride skeleton for the removal of nitrate and phosphate. *Chem. Eng. J.*, 257:45–55.

Víctor-Ortega, M.D., Ochando-Pulido, J.M., Airado-Rodríguez, D., Antonio Martínez-Ferez, A. (2015). Experimental design for optimization of olive mill wastewater final purification with Dowex Marathon C and Amberlite IRA-67 ion exchange resins. *Journal of Industrial and Engineering Chemistry*, Accepted for publication.

PART III

SUMMARY AND CONCLUSIONS

CHAPTER 15

CONCLUSIONS

Based on the research carried out, the following conclusions were drawn:

1. To the author's knowledge, no former studies focusing on IE treatment of two-phase olive mill wastewater (OMW-2) are available in the scientific literature.
2. Simulating media: The lab-made model OMW-2ST can be employed as a good simulating media to reproduce IE processes.
3. Settling of the resins: Dowex Marathon C strong-acid cation exchange resin followed by Amberlite IRA-67 weak-base anion exchange resin offered better results than in the opposite order for model and real OMW-2ST. In this sense, remediation of sodium, total iron, chloride and phenols ions from synthetic and real OMW-2 was successfully achieved using these IE resins.
4. Recirculation operation mode: In general, removal percentages of sodium, total iron, chloride and phenols increased considerably with increasing contact time. Using Dowex Marathon C strong-acid cation exchange resin and Amberlite IRA-67 weak-base anion exchange resin, the equilibrium was obtained in about 30 min for sodium, chloride and total iron, whereas that the highest percentage of phenols removal was obtained for the first minutes of IE treatment.
5. Continuous operation mode: For all the studied ionic species (sodium, chloride, total iron and phenols), both the breakthrough point and the exhaustion time decreased with an increase of the inlet ion concentration. In addition, the breakthrough time has been lower for real versus model OMW-2ST (120 vs. 147.5 min) whereas pollutants concentrations have resulted slightly higher at this point for the strong-acid cation exchange resin (Dowex Marathon C) and the weak-base anion exchange resin (Amberlite IRA-67).
6. With the aim of decreasing membrane fouling in the purification of OMW, Dowex Marathon C (strong-acid cation exchange resin) and Amberlite IRA-67 (weak-base anion exchange resin) reduced the residual concentration of chloride, sodium, total iron and phenols, which are the main pollutants in OMW-2ST, to limits which are not harmful for the performance of an ulterior membrane system.
7. Sodium, total iron and chloride adsorption efficiencies seemed not to be affected by operating temperature, while the best results were obtained at 298 K for phenols

removal for Dowex Marathon C strong-acid cation exchange resin and Amberlite IRA-67 weak-base anion exchange resin.

8. Flow rates of 10 and 15 L h⁻¹ did not affect importantly to sodium, total iron and chloride adsorption on Dowex Marathon C strong-acid cation exchange resin and weak-base anion exchange resin, respectively, after equilibrium was achieved, in which removal efficiency percentages around 90-100 % were ensured for these ions. However, the best results for adsorption of phenols onto Amberlite IRA-67 weak-base anion exchange resin were obtained at 10 L h⁻¹, achieving removal efficiency higher than 70 % at the end of the test.
9. For all the studied pollutants the removal efficiencies decreased as the concentration in the feedstream increased through all the investigated IE resins (Dowex Marathon C strong-acid cation exchange resin, Dowex MAC 3 weak-acid cation exchange resin, Amberlite IRA-67 weak-base anion exchange resin and Amberlyst A26 strong-base anion exchange resin).
10. Sodium removal efficiency was found to increase with an increase in the pH value up 5 through Dowex Marathon C (strong-acid cation exchange resin), whereas the optimum pH value for IE of chloride ions resulted to be the lowest pH value studied (about 1) by means of Amberlite IRA-67 (weak-base anion exchange resin).
11. Iron IE efficiency increased with an increase in the pH value up 4, but lower IE efficiency was observed upon higher pH due to formation of iron hydroxide causing hindrance of the cation exchange capacity. On the other hand, phenols removal efficiency increased with an increase in the pH value up 7 and the IE efficiency remains virtually constant at higher pH values for Amberlyst A26 strong-base resin but higher pH values led to lower IE efficiency for Amberlite IRA-67 weak-base resin.
12. The Langmuir isotherm provided the most accurate prediction (in comparison with Freundlich and Temkin isotherms) of the equilibrium results for all the studied pollutants ($R^2 > 0.99$).
13. Maximum IE capacities were found to be: 22.94, 25.06 28.0 and 22 mg g⁻¹ for sodium (by Dowex Marathon C strong-acid cation exchange resin), chloride (through weak-base anion exchange resin), total iron (onto Dowex Marathon C strong-acid cation exchange resin) and phenols (through Amberlyst A26 strong-base anion exchange resin), respectively.
14. The second-order model described with utmost accuracy the adsorption kinetics of iron onto Dowex Marathon C strong-acid cation exchange resin and the phenols uptake through both Amberlyst A26 strong-base anion exchange resin and Amberlite IRA-67

weak-base anion exchange resin. Furthermore, the kinetics of phenols uptake on the selected strong-base and weak-base anion exchange resins could be also satisfactorily described by intraparticle diffusion model.

15. Dowex Marathon C strong-acid cation exchange resin was confirmed to be considerably more efficient than natural adsorbents such as olive stones (maximum IE capacities: 28.0 mg g⁻¹ vs. 2.12 mg g⁻¹) for the removal of iron from industrial effluents.
16. Up to 100 % iron recovery efficiencies were maintained even after 10 complete-exhaustion IE cycles, which facilitates the effective iron load recovery through the proposed IE process to permit its reuse in the Fenton reactor as catalyst and thus would sensibly boost the cost-efficiency of the integral process for OMW reclamation.
17. For Amberlyst A26 strong-base anion exchange resin, it can be ensured that IE was the predominant process responsible of phenols removal but adsorption is the main responsible process for phenols removal through this Amberlite IRA-67 weak-base anion exchange resin. Moreover, Amberlyst A26 strong-base anion exchange resin was confirmed to be considerably more efficient than Amberlite IRA-67 weak-base anion exchange resin (maximum IE capacities: 22.0 mg g⁻¹ vs. 7.5 mg g⁻¹) for the potential removal of phenols from industrial effluents.
18. IE process led to a solution of phenols susceptible to be concentrated and used in food, cosmetic or pharmaceutical sectors. In this sense, for 100 mg L⁻¹ initial phenols concentration, a more concentrated solution, enriched in phenols, was obtained for Amberlyst A26 strong-base anion exchange resin compared to Amberlite IRA-67 weak-base anion exchange resin (8.5 g L⁻¹ vs. 2.5 g L⁻¹), after 54 L and 27 L treated phenols-contaminated water, respectively.
19. Results from optimization studies with real OMW-2ST revealed that the only final treated effluent fulfilling the maximum standard limits established by the Drinking Water Directive was the one from the combination of the strong-acid cation exchange resin (Dowex Marathon C) and the weak-base anion exchange resin (Amberlite IRA-67), being the best resins disposition: Dowex Marathon C resin followed by Amberlite IRA-67.
20. The IE process consisting of Dowex Marathon C strong-acid cation exchange resin and Amberlite IRA-67 weak-base anion exchange resin yielded up to 88 % removal of these pollutants when the initial pH, operating temperature and flow rate were set to 5.1, 26.8 °C and 12.1 L h⁻¹, respectively.
21. Minimum dosages equal to 12 g L⁻¹ for Dowex Marathon C strong-acid cation exchange resin and 15 g L⁻¹ for Amberlite IRA-67 weak-base anion exchange resin ensured up to

80 % sodium and chloride as well as 90 % iron removal, together with 50 % uptake efficiency for phenols and 70 % for COD.

22. High treated effluent volume recovery (28 L) could be achieved in continuous mode under the optimal operating conditions (pH 5.1, 26.8 ° C and 12.1 L h⁻¹) for Dowex Marathon C strong-acid cation exchange resin and Amberlite IRA-67 weak-base anion exchange resin system, complying with standards for reuse in the production process. Moreover, final effluent accomplished good quality standards according to the recommendations of the Food and Agricultural Association (FAO) with the goal of reusing the regenerated water for irrigation purposes, and also complied with the water quality standard values established by the Guadalquivir Hydrographical Confederation (Spain) for discharge into public waterways, thus permitting reducing the environmental impact of the industrial olive oil production process.
23. The resins combination consisting of the strong-acid cationic resin (Dowex Marathon C) followed by the strong-base anionic resin (Amberlyst A26) allowed treating the highest OMW-2ST volume before overcoming standard limits for all the studied pollutants but conductivity was above the maximum levels due to the high OH⁻ ions release.
24. Although pollutants concentrations were lower than maximum limits, EC > 1 mS cm⁻¹ and pH higher than maximum and lower than minimum values were found for combination 3 (Amberlyst A26 strong-base anion exchange resin and Dowex MAC 3 weak-acid cation exchange resin) and combination 4 (Amberlite IRA-67 weak-base anion exchange resin and Dowex MAC 3 weak-acid cation exchange resin), respectively.
25. The proposed IE process (resins combination 1: Dowex Marathon C strong-acid cation exchange resin and Amberlite IRA-67 weak-base anion exchange resin) might replace membrane technology for the final purification of OMW-2, which implies higher operating costs as high pressures are needed to achieve similar removal efficiencies.
26. Regeneration time decreased and rinse time increased with increasing regenerant concentration for all the selected resins (Dowex Marathon C strong-acid cation exchange resin, Dowex MAC 3 weak-acid cation exchange resin, Amberlite IRA-67 weak-base anion exchange resin and Amberlyst A26 strong-base anion exchange resin).
27. About 0.6 L HCl 4% solution and 0.8 L H₂SO₄ 2% solution were used for complete regeneration of Dowex Marathon C strong-acid cation exchange resin and Dowex MAC 3 weak-acid cation exchange resin, respectively. On the other hand, about 0.7 L and 1 L NaOH 4% and 2 % were employed for complete regeneration of Amberlyst A26 strong-base anion exchange and Amberlite IRA-67 weak-base anion exchange resin, respectively.

-
28. The optimal temperature for regeneration of Dowex Marathon C strong-acid cation exchange resin, Amberlyst A26 strong-base anion exchange resin and Amberlite IRA-67 weak-base anion exchange resin was found to be 298 K (regeneration efficiencies higher than 96 % in all cases) while the optimal temperature for regeneration of Dowex MAC 3 weak-acid cation exchange resin was found to be 308 K. The optimal regeneration temperatures would imply no heating expenses, thus having important positive implications on the cost-efficiency of the resins regeneration process.
 29. For all the investigated resins (Dowex Marathon C strong-acid cation exchange resin, Dowex MAC 3 weak-acid cation exchange resin, Amberlite IRA-67 weak-base anion exchange resin and Amberlyst A26 strong-base anion exchange resin), regeneration efficiencies decreased with increasing flow rates and thus optimum flow rate was found to be 2.5 L h^{-1} , which yielded regeneration efficiencies close to 100 % for the selected IE resins.

CHAPTER 16

RESUMEN

En este capítulo se resumirán los resultados más importantes de esta tesis así como las conclusiones que se han derivado de la misma.

16.1 Antecedentes

En los últimos años, la industria del aceite de oliva se ha convertido en uno de los principales motores de la economía de los países de la cuenca mediterránea, de los cuales España, Italia y Grecia hacen frente a la mayoría de la producción mundial. Otros países con una importante productividad anual son Siria y los países del norte de África - Argelia, Turquía, Marruecos, Tunisia, Libia, Líbano – así como Portugal, Francia, Serbia y Montenegro, Macedonia, Chipre, Egipto, Israel y Jordania.

El aceite de oliva puede ser obtenido principalmente mediante dos vías en las almazaras, dependiendo de la tecnología utilizada: mediante el sistema tradicional, cuyo uso es muy limitado en algunas almazaras protegidas como patrimonio, o mediante sistemas modernos nacidos en virtud de la evolución del sector haciendo posible la producción continua del aceite de oliva. En este caso, podemos distinguir entre el proceso de extracción en tres fases y en dos fases, de los cuales el primero ha sido sustituido por el segundo con el paso del tiempo en algunos países debido a problemas medioambientales.

La experiencia con los dos procesos de extracción modernos muestra que el sistema de dos fases tiene algunas ventajas, como son una mejor retención de polifenoles ya que no se añade agua durante el proceso y, por otro lado, presenta menos pérdida de aceite si el sistema opera correctamente.

El sistema de dos fases produce la mayor cantidad de residuo sólido porque éste tiene el contenido más alto de humedad. Además también produce la menor cantidad de agua residual con el valor de Demanda Biológica de Oxígeno (DBO) más baja. El contenido en polifenoles del aceite es más bajo en el sistema de tres fases debido a la adición de agua durante el proceso de centrifugación.

La calidad del aceite producido mediante el sistema de dos fases es más alta que la calidad del aceite producido en el de tres fases. Esto es debido a la alta concentración de polifenoles y o-

difenoles los cuales aparecen en el nuevo sistema, lo cual otorga más estabilidad durante el almacenamiento, de modo que la calidad del aceite es similar a la obtenida mediante el sistema clásico de prensado por la presencia de polifenoles.

El sistema de obtención de aceite por presión ha sido sustituido progresivamente por procesos basados en la centrifugación de la pasta de aceituna, cuyo uso se ha extendido durante las últimas décadas. Estos procesos incluyen los sistemas de centrifugación de dos fases y de tres fases. Como consecuencia, la cantidad de efluentes derivados de la industria del aceite de oliva ha aumentado rápidamente. Estos efluentes consisten en agua residual de vegetación de las aceitunas (ARVA) y agua residual del lavado de las aceitunas (ARLA), juntos llamados agua residual de almazara (ARA).

Este problema medioambiental concierne especialmente a los países mediterráneos, que representan el 97 % de la producción mundial del aceite de oliva, mientras que los países de la Unión Europea producen el 84 %. Sin embargo, las aceitunas se cultivan también fuera de la cuenca mediterránea, en el Medio Este, los EEUU, Argentina y Australia. En España, el principal productor mundial de aceite de oliva, hay más de 1700 fábricas de aceite de oliva que produjeron más de 1,700,000 toneladas de aceite durante la campaña de 2013/2014. La producción de aceitunas y de aceite de oliva crece año tras año y, de este modo, el ARA. Una fábrica de aceite de oliva puede producir entre 10 y 15 m³/día de ARA. Esta agua residual altamente contaminante se caracteriza por un valor de pH bajo, de color negro, con una demanda química de oxígeno (DQO) y alta concentración de compuestos inhibidores del crecimiento microbiano como compuestos fenólicos y taninos. Además, compuestos inorgánicos como cloruro, sulfato y sales fosfóricas de potasio, calcio, hierro, magnesio, sodio, cobre y trazas de otros elementos están presentes en ARA. En este sentido, aparecen problemas medioambientales relacionados con la disposición de ARA tales como la contaminación del suelo y de las aguas, infiltraciones subterráneas y malos olores.

Por todo ello, ARA debe ser tratada previamente a su disposición de acuerdo a la actual legislación medioambiental europea. Esto supone un coste elevado para los productores de aceite de oliva.

Además, la descentralización y el pequeño tamaño de la mayoría de las fábricas productoras de aceite de oliva impiden un tratamiento centralizado de ARA y hace necesario encontrar una solución viable y flexible para las pequeñas plantas.

Por otro lado, la composición de ARA no es constante y varía considerablemente dependiendo de varios factores tales como parámetros climáticos y de cultivo y el método de molienda aplicado

para la producción de aceite de oliva. Esto da lugar a un alto costo para su disposición y una gran cantidad de consumo de agua potable.

Hasta la actualidad se han propuesto numerosas técnicas de tratamiento de las aguas residuales de almazara, después de haber dado lugar a resultados diferentes. Los tratamientos convencionales incluyen lagunas o evaporación natural, la concentración térmica, compost, tratamientos con la cal, los tratamientos con arcilla, los procedimientos físico-químicos, tales como la coagulación-floculación y la electrocoagulación, y los tratamientos biológicos. El tratamiento biológico de ARA es una tarea difícil y ahora mismo no se aplica a gran escala debido a la estacionalidad y la resistencia de ARA a la degradación biológica.

Por otro lado, el ARA presenta niveles de toxicidad significativos solución salina, exhibiendo altos valores de conductividad eléctrica (EC). Los tratamientos fisicoquímicos convencionales no pueden disminuir la alta concentración de iones monovalentes y divalentes disueltos presentes en estos efluentes y, por lo tanto, es necesario recurrir a tecnologías de separación avanzadas con el fin de tratar de depuración completa de alpechín.

Como el proceso de producción de aceite de oliva de dos fases es el más utilizado actualmente, nos centraremos en el tratamiento de las aguas residuales procedentes de este sistema de producción (ARA-2).

El tratamiento secundario propuesto comprendía secuencialmente la oxidación química avanzada basada en la reacción de Fenton, la etapa de floculación/sedimentación y finalmente la filtración en serie a través de arena y hueso de aceituna.

Este tratamiento aseguró una importante reducción de la materia orgánica, confirmada por las elevadas eficiencias de eliminación de DQO y compuestos fenólicos. Por último, el efluente tratado podría ser reutilizado para fines de riego. El tratamiento secundario propuesto ya ha sido patentado y transferido a escala industrial por el Grupo de investigación 'Tecnología de Procesos Químicos y Bioquímicos' de la Universidad de Granada (Martínez-Nieto et al., 2008).

A pesar de la considerable eliminación de contaminantes orgánicos obtenida por el tratamiento secundario descrito, éste no fue capaz de reducir la alta concentración de iones monovalentes y divalentes disueltos, que no se pueden eliminar por tratamientos físico-químicos convencionales. Además, se observaron valores de EC más altos en comparación con ARA-2 sin tratar. Esto se debe principalmente al incremento en el contenido de sodio y cloruro derivado de la adición del agente neutralizante y el catalizador en los tanques de floculación y oxidación, respectivamente.

El tratamiento secundario propuesto garantiza el cumplimiento del efluente tratado con los estándares paramétricos delimitados en España por la Confederación Hidrográfica del Guadalquivir (C.H.G.), que en el momento actual establece límites con respecto al pH y los parámetros DQO y DBO₅. Sin embargo, las recomendaciones señaladas por la F.A.O. advierten del riesgo de emplear aguas regeneradas que presentan valores altos de salinidad para el riego. Además, de acuerdo con la Directiva 2000/60/CE, que tiene por objeto conferir la máxima protección al agua y las aguas residuales regeneradas, se deben respetar las normas de calidad para descargar el efluente tratado en cauces públicos o en los sistemas de tratamiento de alcantarillado municipales o incluso para su reutilización en el propio proceso de producción de aceite de oliva. Con este objetivo, se llevó a cabo una etapa posterior de separación por membranas a escala de laboratorio.

En este escenario y teniendo en cuenta que la legislación es cada vez más restrictiva, la tecnología de intercambio iónico ofrece muchos beneficios en contraste con otros procesos de separación. Como ventajas más relevantes podemos señalar el hecho de que esta técnica es tecnológicamente simple y permite la eliminación eficaz de incluso trazas de impurezas presentes en disoluciones. Los costes de operación y de instalación de los procesos de intercambio iónico son notablemente inferiores en comparación con otros procesos de tratamiento de aguas residuales como la filtración por membrana o el proceso de filtración mediante carbón activado granular. En este sentido, este proceso se considera muy atractivo debido a su relativa simplicidad y, en muchos casos, ha demostrado ser una técnica económica y eficaz para eliminar los iones de las aguas residuales, en particular a de disoluciones diluidas.

Teniendo en cuenta lo anterior, las resinas selectivas podrían reducir la concentración residual de sodio, hierro total, cloruro y fenoles, que son los principales contaminantes presentes en ARA después del tratamiento secundario de oxidación avanzada (ARA-TS), por debajo de los límites normales máximos establecidos por la Directiva sobre agua potable. La Directiva 98/83 / CE del Consejo establece la concentración máxima en el agua potable a 200 mg L⁻¹ para el hierro, 200 mg L⁻¹ para el sodio y 250 mg L⁻¹ para el cloruro. Por otro lado, una legislación europea anterior estableció un nivel de tolerancia legal de 5 mg L⁻¹ de fenoles totales en las aguas destinadas al consumo humano. Por lo tanto, la consecución de los estándares mencionados anteriormente, permitiría reutilizar el efluente tratado final en las máquinas de lavado de las aceitunas y finalmente cerrar el ciclo, haciendo así el proceso de producción rentable y respetuoso con el medio ambiente.

16.2 Justificación y objetivos

La presente Tesis Doctoral está enmarcada dentro de la línea de investigación principal del Grupo de investigación “Tecnología de Procesos Químicos y Bioquímicos” (TEP025), del Departamento de Ingeniería Química de la Universidad de Granada.

La disposición inadecuada de ARA hacia el medio ambiente o plantas de tratamiento de aguas residuales domésticas está prohibida debido a su toxicidad para los microorganismos, y también debido a la consecuente potencial contaminación de aguas superficiales y subterráneas. Por otra parte, existe una legislación que obliga a la reducción de la concentración global de indicadores - DQO y sólidos en suspensión – para que estos efluentes puedan ser reutilizados o ser descargados. Por otro lado, estas aguas residuales también presentan una elevada concentración de compuestos inorgánicos, especialmente altos niveles de sales de potasio (60-70%) y sulfatos, fosfatos y cloruros de hierro y calcio.

En trabajos de investigación anteriores, el Grupo de investigación "Tecnología de Procesos Químicos y Bioquímicos" (TEP025), del Departamento de Ingeniería Química de la Universidad de Granada, ha desarrollado un proceso físico-químico para el tratamiento continuo de ARA, que consiste en las siguientes etapas: (I) etapa de coagulación-floculación previa, (II) proceso de oxidación química avanzada basado en la reacción de Fenton, (III) etapa de neutralización / floculación, (IV) proceso de decantación y finalmente (V) filtración en serie a través de diferentes tipos de materiales filtrantes (arena y huesos de aceituna).

En este contexto, los objetivos planteados para esta tesis pueden ser resumidos en los siguientes puntos:

- Estudio de la purificación final del agua residual sintética que simula el efluente de almazara a la salida del tratamiento secundario mencionado anteriormente.
- Selección y caracterización de cuatro resinas de intercambio iónico (resina catiónica de ácido fuerte, resina catiónica de ácido débil, resina aniónica de base fuerte y resina aniónica de base débil) para la purificación final de ARA:
- ✓ Estudios en modo de operación de recirculación
 - Estudios termodinámicos (Modelos de isotermas de Langmuir, Freundlich y Temkin).
 - Estudios cinéticos (Modelos de Pseudo-primer orden, Pseudo-segundo orden y Difusión intrapartícula).
- ✓ Estudios en modo continuo

- Estudios en columna de curva de ruptura (aplicación de los modelos de Thomas, Yoon-Nelson y Clark). Determinación del tiempo de ruptura y de la capacidad máxima de adsorción.
- Optimización de las variables de operación que afectan la purificación final de los ARA mediante el proceso de intercambio iónico: pH inicial, temperatura, caudal, disposición de las resinas y cantidad de cada resina, con el fin de cumplir con los estándares legales para la descarga del agua final tratada a los cauces públicos e incluso para su reutilización en el propio proceso de producción - por ejemplo, en las máquinas de lavado de las aceitunas o durante el proceso de centrifugación del aceite de oliva - cerrando así el ciclo.
- Caracterización físico-química del agua tratada a la salida del tratamiento terciario una vez optimizado, mediante los siguientes indicadores:
 - ✓ Contenido en materia orgánica, DQO y fenoles totales.
 - ✓ Valores de electroconductividad y pH.
 - ✓ Análisis del contenido de los principales iones inorgánicos, incluyendo las concentraciones de sodio, hierro y cloruro.
- Estudio de la influencia de los principales factores que afectan el proceso de regeneración de las resinas estudiadas: temperatura, caudal, concentración y naturaleza de las disoluciones regenerantes.

La tesis está dividida en dos partes, cubriendo ambas la totalidad de los temas descritos anteriormente. La primera parte trata del estudio de la influencia de las principales variables de operación en la purificación final del agua residual sintética que simula ARA a la salida del tratamiento secundario, mediante el proceso de intercambio iónico. Además en esta sección también se desarrollan los estudios teóricos relativos a la termodinámica, cinética y curvas de ruptura para las resinas seleccionadas.

La segunda sección abarca por un lado la optimización de los factores de operación involucrados en la purificación final de ARA real procedente de diferentes provincias de Andalucía mediante intercambio iónico y, por otro lado, el estudio del efecto de los parámetros que principalmente influyen en el proceso de regeneración de todas las resinas estudiadas.

En este sentido, la primera parte incluye los capítulos del 3 al 9, mientras que los capítulos del 10 al 13 están incluidos en la segunda.

En los siguiente puntos se describen brevemente los capítulos que componen esta tesis:

- El capítulo 4 consiste en un estudio preliminar en el cual la tecnología del intercambio iónico es presentada como un pretratamiento eficiente para reducir el ensuciamiento de las membranas utilizadas para la purificación final de ARA. En este capítulo, se estudió la eliminación simultánea de los principales iones contaminantes presentes en el agua sintética que simula ARA a la salida del tratamiento secundario mediante las resinas Dowex Marathon C y Amberlite IRA-67. En este sentido, el orden de la disposición de las resinas y el efecto de la temperatura de operación fueron investigados tanto en modo continuo como en recirculación.
- En el capítulo 5, se propone el proceso de intercambio iónico como una opción adecuada para la purificación de ARA sintética tratada previamente mediante el tratamiento secundario mencionado. Los requisitos paramétricos para la producción de agua potable o al menos para la descarga en los cauces públicos fueron logrados mediante una combinación de dos columnas de intercambio iónico que trabajaban en serie a escala de laboratorio. Las resinas de intercambio iónico utilizadas en este estudio fueron también Dowex Marathon C y Amberlite IRA-67. El efecto del tiempo de contacto, la temperatura de operación y la velocidad de flujo en la eliminación simultánea de sodio, hierro total, cloruro y fenoles (las principales especies contaminantes en esta agua residual pretratada) fueron investigados.
- El capítulo 6 describe el funcionamiento de un sistema de intercambio iónico de lecho fijo, compuesto por una resina catiónica de ácido fuerte y una aniónica de base débil, el cual fue totalmente examinado con el objetivo de eliminar las especies iónicas responsables de la alta salinidad (iones sodio y cloruro) de ARA, procedente de almazaras que trabajan con la tecnología de extracción de dos fases, a la salida del tratamiento secundario descrito. En este capítulo, se estudió el efecto del pH, el tiempo de contacto y la concentración inicial de estas especies iónicas contaminantes en el rendimiento del proceso de intercambio iónico. Por otra parte, se obtuvieron las isothermas de equilibrio con el fin de recopilar información del sistema de equilibrio de intercambio iónico para la eliminación de sodio y cloruro de este efluente. Por último, se abordó la operación en continuo del proceso de intercambio iónico propuesto.
- En el capítulo 7, se estudió en profundidad la resina Dowex Marathon C para la eliminación de hierro de ARA después del tratamiento secundario. El efecto de la concentración inicial de hierro en la corriente efluente pretratado se investigó en el intervalo de 0,5 a 100 mg L⁻¹. Por otra parte, el comportamiento en el equilibrio de este contaminante fue predicho por las isothermas de Langmuir, Freundlich y Temkin.

Además, la cinética de adsorción de hierro en esta resina se investigó, haciendo uso para ello de los modelos de pseudo-primero orden, pseudo-segundo orden y el modelo de difusión intrapartícula. Por último, se analizó la conveniencia del proceso de intercambio iónico propuesto y las características del efluente final.

- En el capítulo 8, se estudió la influencia de la concentración de entrada de hierro y el pH del sistema con el fin de obtener la información de equilibrio relacionada con el comportamiento de saturación en columna de una resina de intercambio iónico. Más específicamente, el proceso de intercambio iónico fue modelado mediante el ajuste de los datos experimentales a diversos modelos de adsorción. Además, el efecto de las condiciones de regeneración sobre la capacidad de reutilización de la resina y en la eficiencia de intercambio iónico a largo plazo también fueron determinadas llevando a cabo múltiples ciclos de adsorción-desorción, para investigar el posible escalado industrial del proceso propuesto. Finalmente, se comprobó que el efluente final tratado cumplía con los estándares establecidos para su uso en riego.
- El capítulo 9 trata de la eliminación de fenoles presentes en disolución acuosa mediante Amberlyst A26, una resina de intercambio aniónico de base fuerte, y Amberlite IRA-67, una resina de intercambio aniónico de base débil. La influencia de la concentración de fenoles en la corriente de alimentación fue investigada así como el efecto del tiempo de recirculación. Los datos de equilibrio se ajustaron a las isothermas de Langmuir, Freundlich y Temkin. En este capítulo, se llevaron a cabo también estudios de cinética de adsorción de fenoles basados en los modelos de pseudo-primero orden, pseudo-segundo orden y el modelo de difusión intrapartícula. Los resultados confirmaron que Amberlyst A26 era más eficiente que Amberlite IRA-67 para la eliminación potencial de fenoles de efluentes industriales.
- El capítulo 10 describe el proceso de intercambio iónico en flujo continuo para la recuperación de los fenoles de ARA. Los experimentos se llevaron a cabo en una columna de relleno por un lado de una resina aniónica de base fuerte y por otro lado de una resina aniónica de base débil. El efecto del pH inicial en la eliminación de fenoles fue estudiado en el intervalo de pH 3-11. Por otro lado, se aplicaron los modelos de Thomas, Yoon-Nelson y Clark a los datos experimentales para predecir las curvas de ruptura y los parámetros del modelo como las constantes de velocidad y tiempos de ruptura para tres concentraciones de entrada diferentes y para las dos resinas. Los estudios de regeneración en columna demostraron que se podían alcanzar eficiencias de recuperación de fenoles cercanas al 100%. Por último, se comprobó que el proceso de intercambio iónico permitía obtener una disolución de fenoles susceptible a ser

concentrada para su utilización en la industria alimentaria, farmacéutica y cosmética.

- El capítulo 11 consiste en un estudio experimental, cuyo objetivo era probar las mejores condiciones de funcionamiento de intercambio iónico (previamente optimizadas con agua modelo que simula ARA a la salida del tratamiento secundario) con ARA real después del pretratamiento y comparar los resultados experimentales en términos de conductividad, así como de concentración de iones.
- En el capítulo 12, se llevó a cabo la optimización de la purificación final de ARA real mediante una resina catiónica de ácido fuerte y una resina aniónica de base débil. Se utilizó un diseño compuesto central para la optimización de las principales variables que afectan el proceso de intercambio iónico (temperatura de operación, caudal y pH inicial del sistema). El modelo obtenido fue probado estadísticamente utilizando el análisis de la varianza. Además, la cantidad de ambas resinas fue también optimizada. En condiciones óptimas, las concentraciones de todos los contaminantes en la corriente de salida se mantuvieron por debajo de los límites máximos establecidos, cumpliendo con los estándares legales para su reutilización en el proceso de producción.
- El capítulo 13 trata de la optimización de la purificación final de ARA mediante diferentes combinaciones de las siguientes resinas de intercambio iónico: la resina catiónica de ácido débil Dowex MAC, la resina catiónica de ácido fuerte Dowex Marathon C, la resina aniónica de base débil Amberlite IRA-67 ya la resina aniónica de base fuerte Amberlyst A26. En este capítulo, se llevó a cabo la comparación de todas las posibles combinaciones de resinas con el fin de dilucidar la mejor opción para la purificación de ARA en términos de concentración de iones, DQO y valores de pH y electroconductividad. Los resultados mostraron que la mejor opción era usar la resina catiónica de ácido fuerte, Dowex Marathon C, seguida de la resina aniónica de base débil Amberlite IRA-67.
- El último capítulo de esta tesis, el capítulo 14, comprende el estudio de los principales factores que afectan el proceso de regeneración de todas las resinas que han sido empleadas en los trabajos descritos el capítulo 3 al 12. En este capítulo, se investigó el efecto de la temperatura, caudal y concentración y naturaleza de regenerantes en la regeneración de cada resina de intercambio iónico.
- Finalmente, el capítulo 15 está dedicado a las principales conclusiones derivadas de nuestro trabajo y el capítulo 16 es un resumen en español de los principales resultados de la tesis.

16.3 Conclusiones

Las principales conclusiones derivadas de la investigación llevada a cabo en esta tesis pueden resumirse en las siguientes:

- No hay constancia en la bibliografía de la existencia de estudios anteriores centrados en el tratamiento de aguas residuales procedentes dealmazaras que trabajan con el sistema de dos fases (ARA-2) mediante la tecnología de intercambio iónico (IO).
- El agua modelo que simula ARA-2 a la salida del tratamiento secundario (ARA-2ST) puede ser empleada como un buen medio para simular los procesos de IO.
- La disposición de resinas en la que la resina catiónica de ácido fuerte Dowex Marathon C se colocaba antes que la resina aniónica de base débil Amberlite IRA-67 ofrecía mejores resultados que en orden contrario tanto para ARA-2ST modelo como real.
- En general, las eficiencias de eliminación de sodio, hierro total, cloruro y fenoles aumentaban considerablemente al aumentar el tiempo de contacto.
- El IO demostró ser un pretratamiento eficiente anterior a la tecnología de membranas con el fin de reducir el ensuciamiento (fouling) de las mismas durante la depuración de ARA-2. En este sentido, las resina catiónica de ácido fuerte Dowex Marathon C y la aniónica de base débil Amberlite IRA-67 reducían la concentración residual de cloruro, sodio, hierro total y fenoles, principales contaminantes en esta agua, hasta concentraciones que no eran perjudiciales para el funcionamiento del posterior sistema de membranas.
- Las eficiencias de eliminación de sodio, hierro total y cloruro no eran afectadas por la temperatura de operación, mientras que los mejores resultados para la eliminación de fenoles fueron obtenidos a la temperatura 298 K para Dowex Marathon C (resina catiónica de ácido fuerte) y Amberlite IRA-67 (resina aniónica de base débil).
- Los caudales de 10 y 15 L h⁻¹ no influyeron considerablemente en la adsorción de sodio, hierro total y cloruro en la resina catiónica de ácido fuerte (Dowex Marathon C) y la resina aniónica de base débil (Amberlite IRA-67). Una vez alcanzado el equilibrio, los porcentajes de eliminación de estos iones estaban entre el 90 y el 100 %. Sin embargo, los mejores resultados para la adsorción de fenoles en la resina aniónica de base débil se obtuvieron al caudal de 10 L h⁻¹, alcanzándose eficiencias de eliminación superiores al 70 %.

- Se obtuvieron porcentajes de recuperación de hierro del 100 % incluso tras 10 ciclos de agotamiento-regeneración de la resina catiónica de ácido fuerte (Dowex Marathon C).
- La eficiencia de eliminación disminuía al aumentar la concentración inicial para todos los contaminantes estudiados (sodio, cloruro, hierro total y fenoles).
- La eficiencia de eliminación de sodio aumentaba al aumentar el pH hasta un valor de 5 para Dowex Marathon C (resina catiónica de ácido fuerte), mientras que el valor óptimo de pH para la eliminación de cloruro se obtuvo al menor pH estudiado ($\text{pH} = 1$) para Amberlite IRA-67 (resina aniónica de base débil). Por otro lado, la eficiencia de eliminación de hierro aumentaba al aumentar el pH hasta un valor de 4 (para Dowex Marathon C). Para la eliminación de fenoles se encontró un pH óptimo igual 7 tanto para Amberlyst A26 como para Amberlite IRA-67.
- La isoterma de Langmuir predijo con mayor exactitud los datos de equilibrio para todos los contaminantes ($R^2 > 0.99$). Las capacidades máximas de IO obtenidas fueron: 22.94, 25.06 28.0 y 22 mg g^{-1} para sodio, cloruro, hierro total y fenoles, respectivamente.
- El modelo de Segundo Orden describía con mayor precisión la cinética de adsorción de hierro en Dowex Marathon C (resina catiónica de ácido fuerte) y de fenoles en tanto en Amberlyst A26 (resina aniónica de base fuerte) como en Amberlite IRA-67 (resina aniónica de base débil).
- Las curvas de ruptura experimentales fueron comparadas satisfactoriamente con los perfiles calculados por los modelos de Thomas y Yoon–Nelson, aunque el primero fue el que mejor describía los datos experimentales para todas las resinas estudiadas. Por otro lado, los puntos de ruptura y de agotamiento de las resinas aumentaban a la vez que lo hacía la concentración de entrada de los iones.
- El proceso de IO fue predominante en la eliminación de fenoles mediante Amberlyst A26, mientras que la adsorción fue la principal responsable en la eliminación de este contaminante utilizando Amberlite IRA-67.
- La resina Amberlyst A26 (aniónica de base fuerte) resultó ser considerablemente más eficiente que la resina Amberlite IRA-67 (aniónica de base débil) para la eliminación de fenoles de aguas industriales (capacidad máxima de IO: 22.0 mg g^{-1} frente a 7.5 mg g^{-1}).
- Los resultados de los estudios de optimización con ARA-2 real indicaron que solamente el efluente tratado mediante la combinación de la resina catiónica de ácido fuerte (Dowex Marathon C) y la aniónica de base débil (Amberlite IRA-67) cumplía

los requerimientos establecidos para agua potable. En este caso, la mejor disposición de resinas fue: Dowex Marathon C resina seguida de Amberlite IRA-67. Con esta combinación, se alcanzó un porcentaje de eliminación global de todos los contaminantes del 88 % cuando el pH inicial, la temperatura de operación y el caudal eran fijados a 5.1, 26.8 °C y 12.1 L h⁻¹, respectivamente. Además, la dosis de resina de 12 g L⁻¹ para la resina catiónica y la de 15 g L⁻¹ para la aniónica aseguraban hasta el 80 % de eliminación de sodio y cloruro y 90 % de hierro, junto con el 50 % de eliminación de fenoles y 70 % de COD.

- Utilizando la resina catiónica de ácido fuerte (Dowex Marathon C) seguida de la aniónica de base débil (Amberlite IRA-67), se podía tratar un elevado volumen de efluente (28 L) en modo continuo bajo estas condiciones, cumpliendo con los estándares establecidos para su reutilización en el proceso de producción.
- La combinación de resinas que consiste en la resina catiónica de ácido fuerte (Dowex Marathon C) seguida por la resina aniónica de base fuerte (Amberlyst A26) permitió tratar el mayor volumen de ARA-2TS antes de superar los límites estándar para todos los contaminantes estudiados. Sin embargo, la conductividad estaba por encima de los niveles máximos legislados debido a la alta liberación de iones OH⁻ por parte de la resina aniónica de base fuerte.
- Aunque las concentraciones de contaminantes eran inferiores a los límites máximos legislados, la conductividad era superior a 1 mS cm⁻¹ y el pH superior al máximo establecido para la combinación 3 (resina aniónica de base fuerte Amberlyst A26 y resina catiónica de ácido débil Dowex MAC 3) e inferior al mínimo para la combinación 4 (resina aniónica de base débil Amberlite IRA-67 y resina catiónica de base débil Dowex MAC 3).
- El proceso de IO propuesto (combinación de resinas 1: resina catiónica de ácido fuerte Dowex Marathon C y resina aniónica de base débil Amberlite IRA-67) podría sustituir a la tecnología de membranas para la depuración completa de ARA-2, la cual implica mayores costes de operación debido a las altas presiones necesarias para conseguir eficiencias de eliminación similares.
- El tiempo de regeneración disminuía al aumentar la concentración de regenerante para todas resinas previamente utilizadas en la depuración de ARA-2 (resina catiónica de ácido fuerte Dowex Marathon C, resina catiónica de ácido débil Dowex MAC 3, resina aniónica de base débil Amberlite IRA-67 y resina aniónica de base fuerte Amberlyst A26). En este sentido, 0.6 L de HCl al 4 % y 0.8 L de H₂SO₄ al 2 % se utilizaron para la regeneración completa de las resinas Dowex Marathon C y

Dowex MAC 3, respectivamente. Por otro lado, 0.7 L y 1 L de NaOH al 4% y al 2 % fueron necesarios para la regeneración de las resinas Amberlyst A26 y Amberlite IRA-67, respectivamente.

- La temperatura óptima de regeneración para Dowex Marathon C (resina catiónica de ácido fuerte), Amberlyst A26 (resina aniónica de base fuerte) y Amberlite IRA-67 (resina aniónica de base débil) era 298 K, alcanzándose eficiencias de regeneración superiores al 96 % en todos los casos. Sin embargo, la temperatura óptima para Dowex MAC 3 (resina catiónica de ácido débil) era 308 K.
- Para todas las resinas investigadas (resina catiónica de ácido fuerte Dowex Marathon C, resina catiónica de ácido débil Dowex MAC 3, resina aniónica de base débil Amberlite IRA-67 y resina aniónica de base fuerte Amberlyst A26), las eficiencias de regeneración disminuían al aumentar el caudal de regenerante. Por lo tanto, el valor óptimo de caudal era 2.5 L h^{-1} , que permitía alcanzar eficiencias de regeneración cercanas al 100 % para todas las resinas de IO seleccionadas.